2015

Phytochemical and biological studies on selected Stemona and Stichoneuron species (Stemonaceae)

Rosdayati Alino Ramli
University of Wollongong

Phytochemical and Biological studies on selected *Stemona* and S*tichoneuron* species (Stemonaceae)

A thesis submitted in fulfilment of the requirements

for the award of the degree of

Doctor of Philosophy

From

University of Wollongong

Rosdayati Alino Ramli

M.Sc. Chemistry

Supervisor: Professor Stephen G. Pyne

School of Chemistry

Febuary 2015

DECLARATION

I, Rosdayati Alino Ramli, declare all the materials in this thesis, submitted in partial fulfillment of requirement for the award of Doctor of Philosophy, conducted in the Department of Chemistry at the University of Wollongong, is my own work except when mentioned in this thesis. This document has not been submitted for qualification at any academic institution.

Rosdayati Alino Ramli

May, 2015

ACKNOWLEDGEMENTS

Firstly, I would like to sincerely thank my supervisor, Prof. Stephen Pyne, for his wisdom, kindness and patience throughout the whole period of my PhD project. I am so thankful for the opportunity he offered me to learn natural products chemistry and to attend some conferences and have a fun life in Wollongong. Secondly, I would like to record my thanks to all the technical support in the School of Chemistry particularly Dr. Wildford Lie for helping with my NMR experiments. Special thanks to Dr. Roonglawan Rattanajak from Medical Molecular Biology Research Unit, National Center for Genetic Engineering and Biotechnology, National Science and Technology Development Agency, Thailand for helping me with the antiplasmodial assays. I also thank to Ministry of Education Malaysia and University Sains Islam Malaysia (USIM) for the PhD scholarship. I would like to thank the Pyne group, especially Phurpa, Kung, Dr. Arife and Duc for their kind help, instructions in the lab and teaching me experimental skills, and for their friendship. I would like to give my special thanks to my husband, Md. Zubaidillah for his care and company, and also his never ending support. Special thanks to my family, my parents and my sibling, for their love, care and support. Without them, I can't image how I could complete my PhD. Finally, I would like to thank all my friends especially Prof. Emr. Dato' Noramly Muslim, Prof. Dr. Musa Ahmad, Azean Tajuddin, Najatulmuna Hamdan, Lili Hannah, Lydia Yusrina, Nur Indah and Madihah for their support, help and love.

ABSTRACT

Chapter 1 of this thesis is a review of the literature on the structure, biological activities and isolation of *Stemona* alkaloids from the Stemonaceae family of plants. This chapter also outlines the aims of this project, which were to isolated and determine the structures of the *Stemona* alkaloids and other chemical constituents in four species of Stemonaceae; three of them collected in peninsular Malaysia and another one in Indonesia. Another aim of this project was to determine the biological activities of these alkaloids.

Chapter 2 reviews and describes the genus of *Stemona* and *Stichoneuron* including their distribution and morphologies, and also the field work undertaken to collect the plants for this study. *Stemona curtisii* Hook F., *Stichoneuron halabalensis* Hook F. and *Stichoneuron caudatum* Ridley were collected from different sites in Malaysia by Ramli, R. A., while *Stemona javanica* (Kunth) Engl. was collected in Indonesia by our collaborator, Pudjiastuti, P.

Chapter 3 reviews the earlier studies on *S. curtisii* from Thailand. This chapter also describes the results of the isolation of the chemical constituents from the roots extract of *S. curtisii* from Malaysia using chromatographic techniques, including column chromatography and preparative thin layer chromatography. Six known alkaloids were successfully isolated and their structures were confirmed by NMR and ESI-MS analysis and from camparisons made with the spectroscopic data from the literature. The isolated compounds were (2'*S*)-hydroxystemofoline, stemocochinine, 1-hydroxyprotostemonine, oxystemokerrin-*N*-oxide, isostemofoline and stemofoline. Eleven *Stemona* alkaloids were reported from *S. curtisii* in Thailand; five of them, were

pyrrolo[1,2-*a*]azepine alkaloids while the others were pyrido[1,2-*a*]azepine alkaloids. In contrast, in this study only one pyrido[1,2-*a*]azepine alkaloid, oxystemokerrin-*N*-oxide, was isolated from *S. curtisii* from Malaysia. Stemofoline was the major alkaloid found in the roots of *S. curtisii* from Thailand while (2'*S*)-hydroxystemofoline was the major alkaloid from the roots of the plant material collected in Malaysia.

Chapter 4 describes the isolation of *Stemona* alkaloids from the root extracts of *Stemona javanica* using chromatograpic techniques. Two new protostemonine-type alkaloids, javastemonine A and B were isolated together with four known *Stemona* alkaloids, 13-demethoxy-11(S^*),12(R^*)-dihydroprotostemonine, isoprotostemonine, protostemonine and isomaistemonine. The structures and relative configurations of the new alkaloids were determined by spectroscopic analysis and molecular modeling studies.

Chapter 5 describes the isolation of the chemical components from the roots and leaf extracts of the hitherto unreported *Stichoneuron halabalensis*. This study led to the characterization of the known compounds (+)-α-tocopherol, (*R*)-(+)-goniothalamin, four known *Stemona* alkaloids, bisdehydrostemoninine A, stemoninine, sessilistemoamine C, sessilistemoamine A; and three new *Stemona* alkaloids, stichoneurines C, D and E. The structures and relative configurations of the new alkaloids were determined by spectroscopic analysis, and from comparisons made with published spectroscopic data and molecular modeling studies.

Chapter 6 provides a discussion of the isolation of four novel stichoneurine-type alkaloids, stichoneurines F and G and sessilistemonamines E and F, *Stemona* alkaloids, from the root extracts of *Stichoneuron caudatum*. The isolation and purification of these chemical constituents were achieved using various chromatographic techniques. The

structures and relative configurations of the new alkaloids have been determined by spectroscopic methods and molecular modeling experiments. A possible biosynthesis of these new alkaloids from stichoneurine B involving an intramolecular Mannich reaction to form the cyclopentane ring of these alkaloids was proposed.

Chapter 7 provides an introduction and discussion of the biological assays and the biological activities of the isolated chemical components. The results of the AChE inhibition studies showed that stemoninine and bisdehydoxystemoninine A had the highest inhibitory activities against human acetylcholinestrase (hAChE), with IC_{50} values of 3.74 $\pm$ 0.09 μM and 5.52 $\pm$ 0.13 μM, respectively. Both were far less active againt electric eel AChE (eeAChE). In contrast, stichoneurine E showed the highest activity against eeAChE (IC_{50} = 5.90 $\pm$ 0.08 μM) when compared to hAChE (IC_{50} = 34.63 $\pm$ 0.81 μM). The crude extracts of *S. curtisii*, *St. halabalensis* and *St. caudatum* showed significant inhibitory activities against hAChE (IC_{50} values of 41.8 $\pm$ 0.05, 32.94 $\pm$ 0.88 and 41.8 $\pm$ 0.05 μg/mL, respectively).

The MDR-reversing properties of eight selected *Stemona* alkaloids on the cytotoxicities of two cancer drugs, doxorubicin and paclitaxel, were performed by our collaborator, Assoc. Prof. Pornngarm Limtrakul from the Departement of Biochemistry, Faculty of Medicine, Chiang Mai University, Thailand. Among the tested compounds, isostemofoline showed the highest modulating effect on drug resistant K562-Adr cells by decreasing the IC_{50} of doxorubicin from 22.33 ± 2.08 μM to 2.52 ± 0.03 μM and decreasing the IC_{50} of paclitaxel from 1.48 ± 0.01 μM to 0.23 ± 0.01 μM. The other compounds that showed MDR-reversing properties were (11*Z*)-1′,2′-didehydrostemofoline, and (11*E*)-didehydrostemofoline. In the presence of these compounds, doxorubicin had IC_{50} values of 6.00 ± 0.00 and 4.83 ± 0.29 μM,

respectively, while for paclitaxel, the IC_{50} values decreased to 0.47 ± 0.01 and 0.38 ± 0.01 μM, respectively.

Thirteen isolated *Stemona* alkaloids were examined for their antiplasmodial activities. Compounds 13-demethoxy-11(S^*),12(R^*)-dihydroprotostemonine, isoprotostemonine, protostemonine, sessilistemoamine F, stichoneurine F, and 1-hydroxyprotostemonine demonstrated moderate *in vitro* antiplasmodial activity against the *P. falciparum* strains, TM4 (a wild type chloroquine and antifolate sensitive strain) with IC_{50} values of 17.7μg/mL, 16.8 μg/mL, 16.0 μg/mL, 18.5 μg/mL, 20.2 μg/mL, and 27.1 μg/mL, respectively, and K1 (multidrug resistant strain) with IC_{50} values of 16.8 μg/mL, 14.1 μg/mL, 11.9 μg/mL, 17.7 μg/mL, 16.5 μg/mL, 20.6 μg/mL, respectively. Stichoneurine G showed only moderate antiplasmodial activity against TM4 with an IC_{50} value of 26.8 μg/mL. The other compounds did not show antiplasmodial activity, even at the highest tested concentration of 38.9-42.3 μg/mL.

Thirteen isolated *Stemona* alkaloids were also examined for their cytotoxicities. None of the tested alkaloids showed toxicity against mammalian cell lines, KB (human mouth epidermal carcinoma cells) and Vero (kidney epithelial cells from an African green monkey) cells, even at the highest tested concentration of 38.9-42.3 μg/mL.

The conclusions arising from this study are described in Chapter 8. In addition, all the results and methodology of this study are presented in Chapter 9.

PUBLICATIONS ARISING FROM THIS THESIS

1. Ramli, A. R; Pudjiastuti, P.; Tjahjandaric, T.; Lie, W.; Rattanajak, R.; Kamchonwongapaisan, S.; Pyne, S. G. Alkaloids from the roots of *Stemona javanica* (Kunth) Engl. (Stemonaceae) and their anti-malarial, acetylcholinesterase inhibitory and cytotoxic activities. *Phytochem. Lett.* **2015**, *11*, 157–162.
2. Ramli, R. A.; Lie, W.; Pyne, S. G. Alkaloids from the roots of *Stichoneuron caudatum* and their acetylcholinesterase inhibitory activities. *J. Nat. Prod.* **2014**, *77*, 894–901.
3. Ramli, R. A.; Lie, W.; Pyne, S. G. Alkaloids from the roots and leaves of *Stichoneuron halabalensis* and their acetylcholinesterase inhibitory activities. *Nat. Prod. Commun.* **2013**, *8*, 695−698.

TABLE OF CONTENTS

LIST OF FIGURES

LIST OF TABLES

LIST OF SCHEMES

LIST OF ABBREVIATIONS

δ	Chemical shift
λ	Wavelength
$[\alpha]_D$	Specific rotation
Ar	Aromatic
ACh	Acetylcholine
AChE	Acetylcholinesterase
AD	Alzheimer's desease
ATCh	Acetylthiocholine
ATChI	Acetylthiocholine iodide
APT	Attached proton test
App	Apparent
calcd	Calculated
CC	Column chromatography
Methanol-d_4	Deuterated methanol
COSY	Correlation spectroscopy
DCM	Dichloromethane
DEPT	Distortionless enhancement by polarization transfer
DMSO	Dimethyl sulfoxide
DTNB	Dithiobisnitrobenzoate
d	Doublet
dd	Double of doublets (NMR)
ddd	double of doublet of doublets (NMR)

dddd	Double of doublet of doublet of doublets (NMR)
dq	Double of quartets (NMR)
dt	Double of triplets (NMR)
eeAChE	Electric eel acetylcholinestrase
EA	Ethyl acetate
EI	Electron impact
ESI	Electrospray ionization
ESIMS	Electrospray ionization mass spectrum
FR	Fold-revesal resistance
g	Gram
gCOSY	Correlated spectroscopy
gHMBC	Heteronuclear multiple bond correlation
gHSQC	Heteronuclear single quantum correlation
hAChE	Human acetylcholinestrase
Hz	Hertz
HRESIMS	High resolution electrospray ionization mass spectrum
IC_{50}	The half maximal inhibitory concentration
IR	Infrared
lit.	Literature
m	Multiplet
m/z	Mass/charge ratio
MDR	Multidrug resistance
mg	Milligram
mL	Mililitre

$[M+H]^+$	Protonated molecular ion
Me	Methyl
NMR	Nuclear Magnetic Resonance
NOESY	Nuclear Overhauser Effect Spectroscopy
P-gp	Permeability glycoprotein
ppm	Parts per million
PTLC	Preparative thin-layer chromatography
q	Quartet
R_f	Relative mobility
RR	Relative resistance
R^2	Coefficient of determination
rt	Room temperature
s	Singlet
SD	Standard deviation
S.	*Stemona*
St.	*Stichoneuron*
sp.	Species
t	Triplet
TLC	Thin layer chromatography
TMS	Tetramethylsilane
µL	Microlitre
µM	Micromolar

CHAPTER 1

INTRODUCTION

1.1 The Stemonaceae family

Stemonaceae is a small family of monocotyledonous perennial herbs.[1] The plants are found with or without a rhizome with 4-merous flowers, with superior or half-inferior, unilocular unicarpellate ovary. The Stemonaceae family consists of three genera (Figure 1.1: (i) *Stemona* (abbreviated *S.*), widespread in tropical South-East Asia; (ii) *Stichoneuron* (abbreviated *St.*) found in South East Asia; and (iii) *Croomia* found in Japan and North America.[2]

Stemona tuberosa

Stichoneuron membranaceum

Croomia heterosepala

Figure 1.1 Representative plants from the Stemonaceae family (Pictures taken from Majumdar & Datta).[3]

Although the Stemonaceae family comprises more than 30 species, the phytochemical investigations of this family has been mainly restricted to the most abundant genus *Stemona*. Prior to this study, only two species from the genus *Stichoneuron*, *Stichoneuron caudatum*[4] and *Stichoneuron calcicola*[5] had been studied

for their phytochemicals. Xu and coworkers[6] initiated an extensive investigation of some *Stemona* species in the early 1980s leading to the isolation and structural elucidation of many of the currently known *Stemona* alkaloids.[7] Most of the phytochemical studies of this family were restricted to the roots of *Stemona* plants although a few studies of the leaves and stems have been also reported.[8] Several reviews of the *Stemona* alkaloids, their structures, biological activities and the plant species and parts from which they have been isolated from have been published.[2,4–5] The chemical interest in Stemonaceae extracts was stimulated by their popular use in South-East Asia as insecticides and vermifuges, as well as their use against respiratory diseases.[9–13]

1.2 Biological activities of the *Stemona* alkaloids

Extracts of Stemonaceae have found popular use as insecticides, vermifuges, antihelmitics and in the treatment of respiratory diseases in China and Japan.[2,14–16] The water extracts obtained from the roots of some Stemonaceae species were widely used in China against human and cattle parasites, agricultural pests and as domestic insecticides.[14] The methanolic extracts obtained from the fresh leaves of *S. japonica* showed strong insecticidal activity against silk worm larvae.[14] The crude extracts of Stemonaceae species have also shown antitubercular and antitussive activities.[16] Previous chemical and pharmacological investigations have revealed that alkaloids might represent the main bioactive constituents in these plants. A further study on the isolated individual alkaloids revealed that isostenine (**3**) (Figure 1.5), neotuberostemonine (**11**) (Figure 1.5), bisdehydrostemoninine (**62**), stemoninine (**49**) and stemoamide (**36**) (Figure 1.6) were potent antitussive agents.[9,17–18]

Stemona tuberosa, *S. japonica*, and *S. sessilifolia* have been used in China and Japan for various medicinal and biological properties, especially the extracts from the fleshy tuberous roots which are still used to treat respiratory disorders, including pulmonary tuberculosis and bronchitis, but are also recommended against different insect pests.[8] Furthermore, stemonine (**37**) (Figure 1.6), stemospironine (**75**) (Figure 1.7) and stemofoline (**111**) (Figure 1.10) have been reported as active against the fourth instar *Bombyx mori* (silkworm larvae).[19] Tuberostemonine (**5**) (Figure 1.5) was the first *Stemona* alkaloid to have its biological activity tested. Although the initial results did not show activity against *Hymenolepis nana* and *Nematospiroides dubius*,[2] its anthelminthic activity was detected when tested against *Angiostrongylus cantonensis*, *Dipylidium caninum* and *Fasciola hepatica* with an effect on the motility of these helminthic worms. These results motivated Shinozaki and Ishida[20] to test the action of this alkaloid on the neuromuscular transmission in crayfish which is considered a model for studying the mechanism of drug action in the mammalian central nervous system. These tests demonstrated that tuberostemonine (**5**) (Figure 1.5) depressed glutamate-induced responses at similar concentrations to those of the established glutamate inhibitors.[16]

Examination of the insecticidal and antifeedant activities of the alkaloid 16,17-didehydro-16-(*E*)-stemofoline (**118**) and stemofoline (**111**) (Figure 1.10) were undertaken using the third instar larvae of the pyrethroid-resitance diamondback moth. Alkaloid **118** showed very potent activity, much more than its less unsaturated analogue, the alkaloid **111**.[15] In 1978, Sakata and co-workers reported the insecticidal activity of stemofoline (**111**), stemonine (**37**) and stemospironine (**75**) against the fourth instar silkworm larvae. The activity of stemofoline (**111**) was 10^4-fold higher than that

of the alkaloids **37** and **75**.[8] From these observations, the insecticidal activity of 16,17-didehydro-16-(*E*)-stemofoline (**118**) was evaluated to be strongest among the stemofoline-related alkaloids, so far isolated, from plants of the genus *Stemona*.[15]

The activities of these alkaloids were also studied on the nicotinic acetylcholine receptors (nAChRs) of insects. These receptors are cholinergic receptors which are triggered by the binding of the neurotransmitter acetylcholine (ACh).[21] This study indicated that 6β-hydroxystemofoline (**127**), 16-hydroxystemofoline (**128**) and neostemofoline (**58**) showed agonist effects on insect nAChR while protostemodiol (**110**) and 13-demethoxy-11(*S**),12(*R**)-dihydroprotostemonine (**55**) acted as an antagonist.[22]

Acetylcholine (ACh) receptors in humans are located at the top end of dendrites and are mainly present in the central nervous system. The acetylcholinestrase (AChE) enzyme controls the level and duration of action of ACh. This enzyme catalyses the hydrolysis of ACh to inactive choline and acetate (Scheme 1.1).[23] The inhibition of AChE prolongs the duration of action of ACh which is useful for the treatment of the symptoms of Alzheimer disease (AD). The cholinergic hypothesis states that AD patients have an abnormal low level of ACh. Many alkaloids have been reported to be AChE inhibitors. The well-known AD drugs are galanthamine, rivastigmine, donepezil and memantine (Figure 1.2).[24] However, a few *Stemona* alkaloids such as sessilistemonamine A (**96**) and B (**97**) were reported to act as AChE inhibitors but with less activity compared with the current clinical drug, galanthamine. These and other *Stemona* alkaloids may also have therapeutic applications in the treatment of AD.[25]

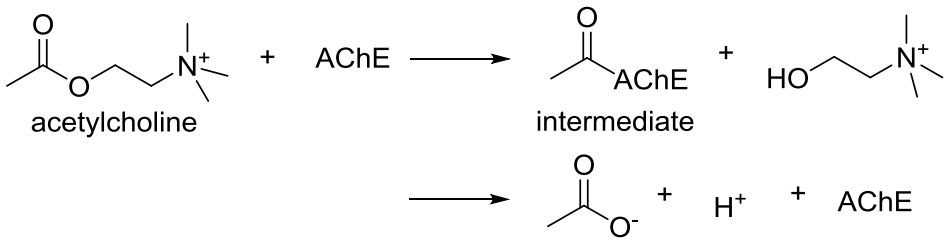

Scheme 1.1 Hydrolysis of acetylcholine (ACh).[23]

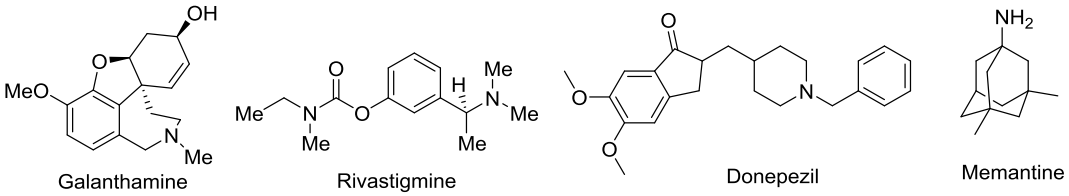

Figure 1.2 Common medicinal drugs for treatment of Alzheimer's disease.[24]

Another and interesting development with *Stemona* alkaloids is the finding that some of these alkaloids are P-glycoprotein (P-gp) modulators *in vitro* and may be effective in the treatment of multidrug resistant (MDR) cancers. P-gp belongs to the superfamily of transporter proteins containing an ATP-binding cassette. It is thought to function as a broad substrate, ATP-dependent, pump to reduce intracellular drug concentration below a cell-killing threshold.[26–28] Overexpression of P-gp causes cancer cells to be resistant to a variety of structurally and functionally dissimilar anticancer drugs, such as vinblastine, doxorubicin and paclitaxel. A study of *Stemona* alkaloids as P-gp inhibitors was carried out in 2011 by Chanmahasathien and co-workers. They found that the *Stemona* alkaloid, stemofoline (**111**) inhibited P-glycoprotein-mediated drug efflux and increased the efficiency of selected chemotherapeutic drugs.[29]

The worldwide spread of the H5N1 avian influenza virus has raised concerns that this virus might acquire the ability to be passed readily among humans, and cause a

pandemic. More recently, Manohar[30] screened various validated compounds from *S. tuberosa* as inhibitors against N1 neuraminidase of the H5N1 avian virus. Neuraminidase is one of the glycoproteins in the influenza virus membrane. They found that croomine (**74**) and stemonine (**37**) were better than the currently used anti-influenza drugs, zanamivir and oseltamivir (Figure 1.3). Hence, *S. tuberosa* could be a silver lining to the latest threat to mankind, the H5N1 pandemic.[30]

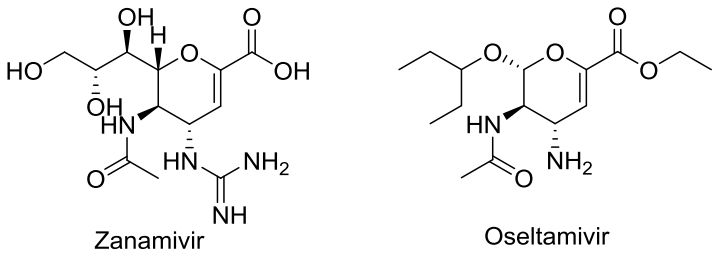

Figure 1.3 Anti-influenza drugs.[30]

1.3 The *Stemona* alkaloids

The *Stemona* alkaloids represent a typical and characteristic phytochemical feature of the family Stemonaceae.[4] In a previous review more than 170 *Stemona* alkaloids were reported and were mostly isolated from the roots of the largest genus *Stemona*.[14] Only two derivatives were characterized from both *Croomia heterosepala* [croomine (**74**) and didehydrocroomine (**79**)] (Figure 1.7) and *Stichoneuron caudatum* [stichoneurine A and B (**108**-**109**)] (Figure 1.9).[4–5,31]

1.4 Structural classification of the *Stemona* alkaloids

The *Stemona* alkaloids have been classified by Pili into eight groups, according to their different characteristic structures.[2,14] Six groups, stenine, stemoamide,

tuberostemospironine, stemonamine, parvistemofoline and stemofoline contain the pyrrolo[1,2-*a*]azepine nucleus (Figure 1.4) as their core structure. Another group with a pyrido[1,2-*a*]azepine nucleus (Figure 1.4) was named as the stemocurtisine group after its first member, stemocurtisine.[13] The eighth group comprises *Stemona* alkaloids that either lack the pyrrolo[1,2-*a*]azepine or the pyrido[1,2-*a*]azepine base structure and do not fit into the above mentioned seven groups. Thus, this group has been classified as the miscellaneous group. However, many alkaloids in this group are derived from a pyrrolo[1,2-*a*]azepine alkaloid precursor by a ring-opening or ring-cleavage process. After these classification, two other structural types were found, one based on a pyrido[1,2-*a*]azonine and another one based on an indolizidine core structure.

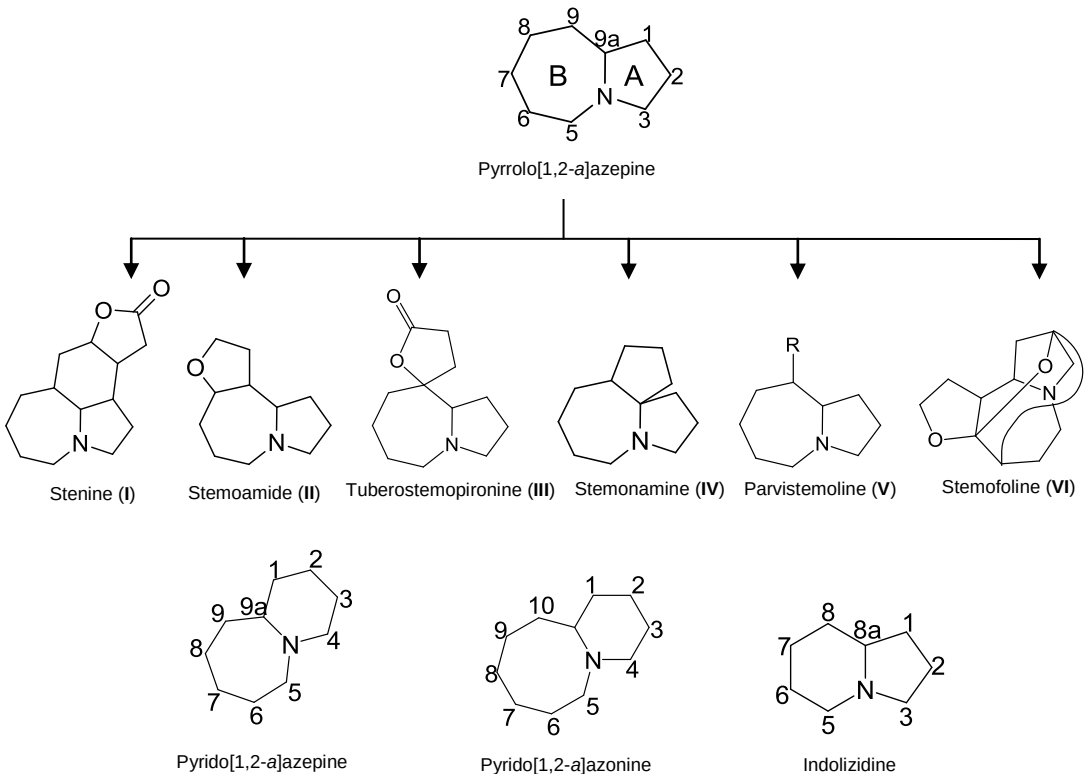

Figure 1.4 The heterocyclic base structures of the *Stemona* alkaloids group.[13–14,32]

1.4.1 Stenine group

The alkaloids in the stenine group (Figure 1.5) display the tetracyclic furo[2,3-*h*]pyrrolo[3,2,1-*jk*][1]benzazepin-10(2*H*)-one nucleus (**I**, Figure 1.4). This group is named after the first alkaloid in this group, stenine (**1**) which was first isolated from the roots of *Stemona tuberosa*.[33] The stenine group currently comprises 35 members consisting of the alkaloids **1**-**35** as shown in Figure 1.5. Many of the stenine alkaloids have the basic stenine structure with an appended γ-lactone ring at C-3, however several diastereoisomers of these compounds have been isolated. This may suggest that plants from the same species but growing in different locations have slightly different enzymes to biosynthesize these alkaloids. In several examples, the A-ring has been further oxidized to a pyrrole (e.g. **16**-**20**, **22**, **34** and **35**), a dihydro pyrrolidine (e.g. **14**, **15** and **28**) or by the addition of an oxygen substituent (e.g. **21**, **23**, **24**-**29**, **32** and **33**).

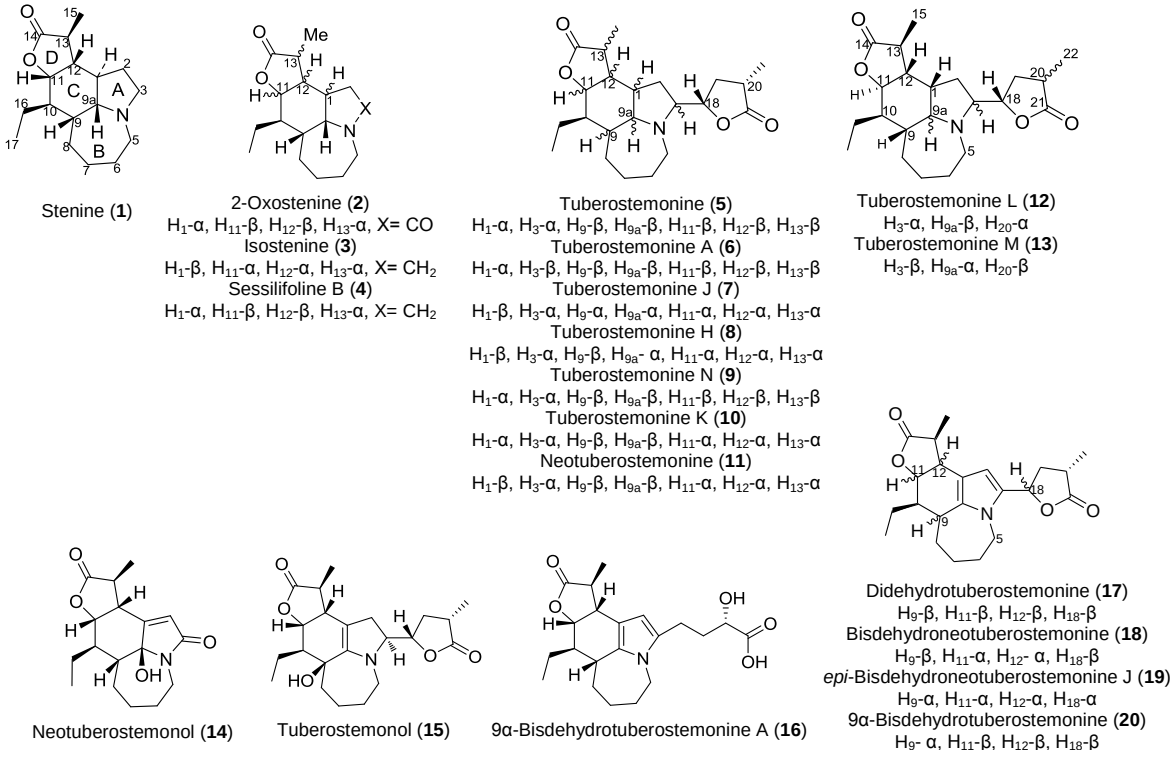

Figure 1.5 *Stemona* alkaloids of the stenine group.[13–14,32–38]

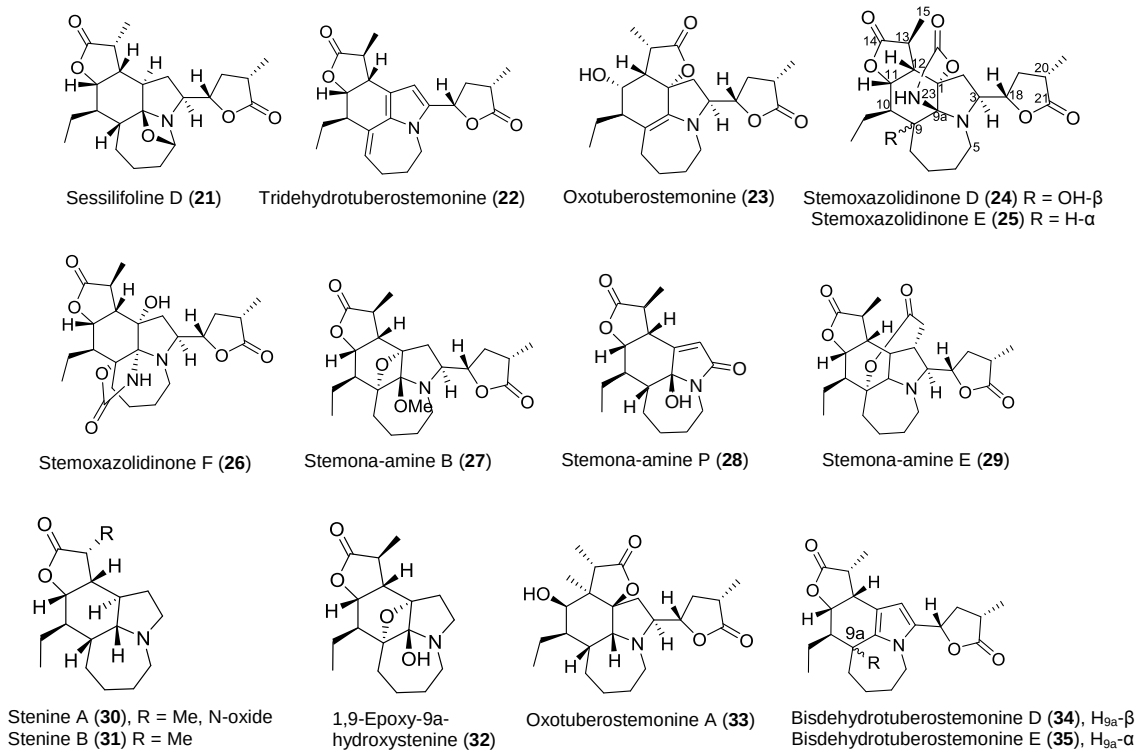

Figure 1.5 *Stemona* alkaloids of the stenine group (continued).[13–14,32–38]

1.4.2 Stemoamide group

The stemoamide group of alkaloids (Figure 1.6) display the tricyclic 2*H*-furo[3,2-*c*]pyrrolo[1,2-*a*]azepine nucleus (**II**, Figure 1.4). This group is currently represented by 35 alkaloids as shown in Figure 1.6. Stemoamide is the simplest member with the others having one or two additional γ-lactone rings. In addition, several alkaloids have a γ-lactone fused to a furan ring in a spirocyclic fashion (e.g. **47**-**49** and **59**-**72**). Several examples are known in which the ring has been oxidized to a pyrrole (e.g. **39**, **44**, **52**, **59** and **60**-**65**). Other examples have clearly arisen from the reduction of other alkaloids, for examples **46** from **40** and **53** and **54** from **38**.

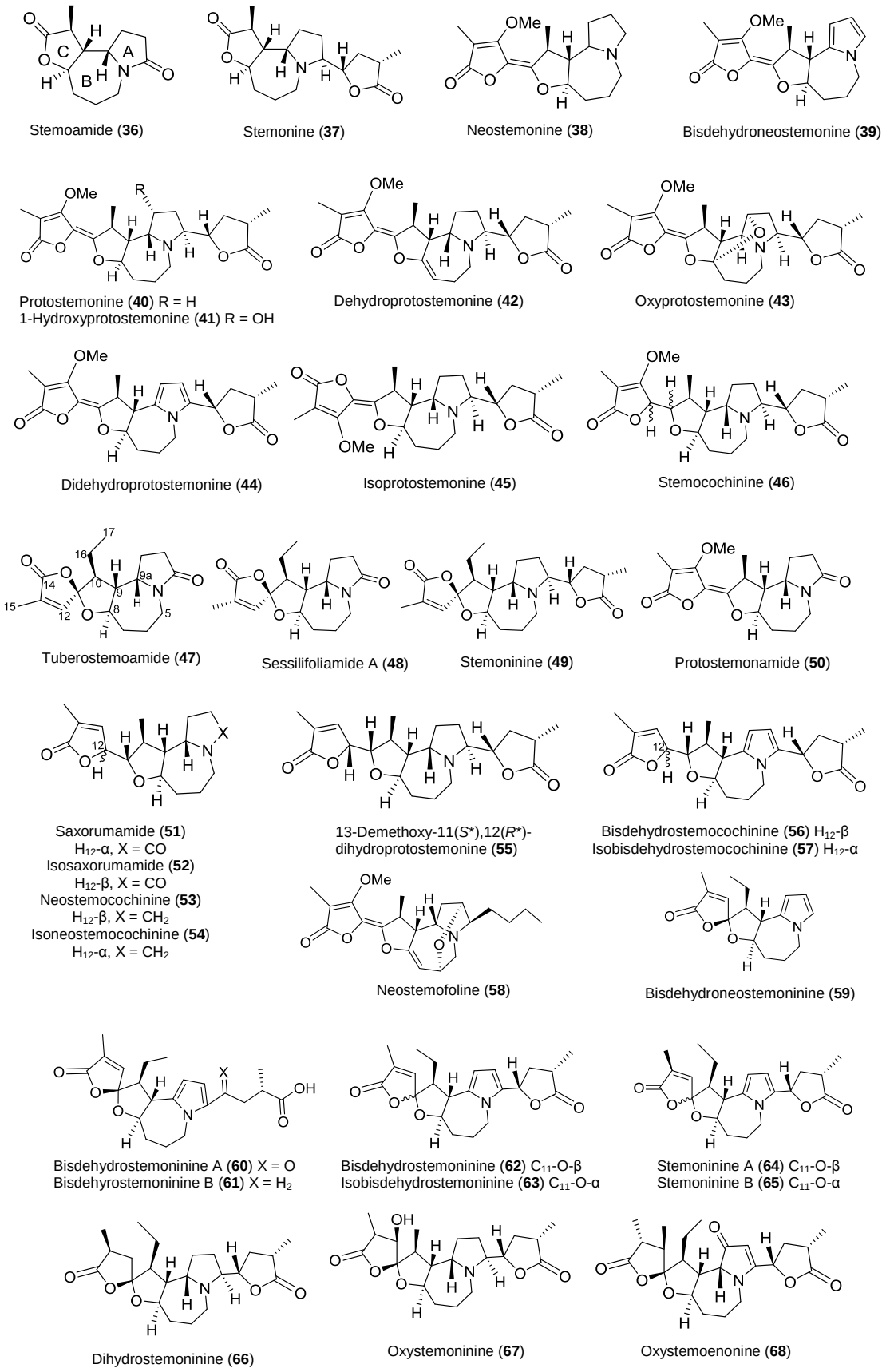

Figure 1.6 *Stemona* alkaloids of the stemoamide group. [2,14,35,39]

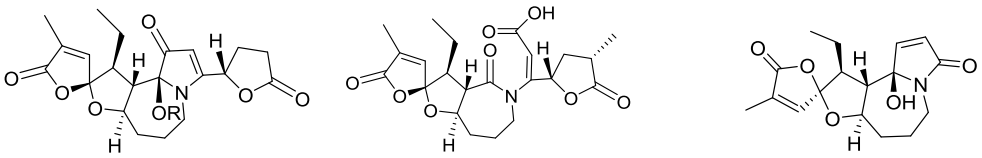

Stemoenonine (**69**) R = H
Methylstemoenonine (**70**) R = CH_3

1,9a-Seco-stemoninine (**71**)

Stemona-lactam O (**72**)

Figure 1.6 *Stemona* alkaloids of the stemoamide group (continued).[2,14,35,39]

1.4.3 Tuberostemospironine group

Alkaloids in the tuberostemospironine group (Figure 1.7) are characterized by the presence of a spiro[furan-2-(5*H*),9'[9*H*]pyrrolo[1,2-*a*]azepin]-5-one nucleus (**III**, Figure 1.4). There are 15 alkaloids included in this group as shown in Figure 1.7. These alkaloids are based around the simplest member, tuberostemospironine (**73**) and feature a spiro γ-lactone at C-9. Interestingly, stemona-lactam R (**86**), the C-9 epimer of **73**, has also been isolated suggesting different enzymes are involved in their biosynthesis. The most complex alkaloid in this group is sessilifoliamine A (**84**) which has a pentacyclic structure.

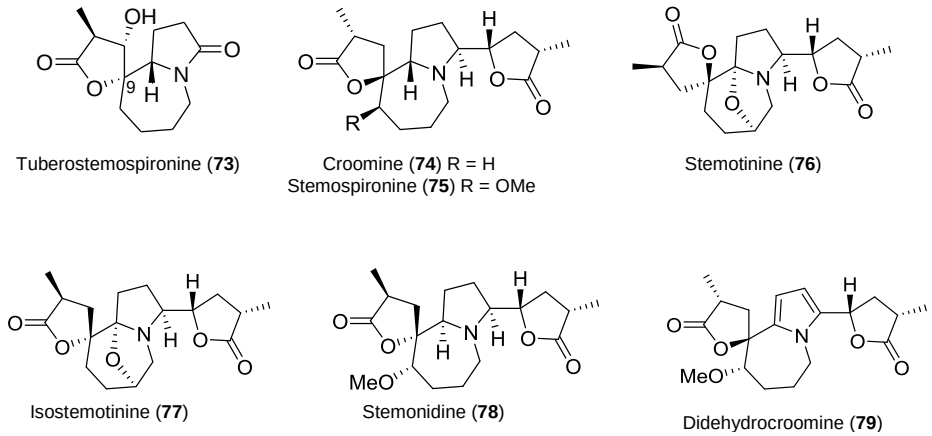

Tuberostemospironine (**73**)

Croomine (**74**) R = H
Stemospironine (**75**) R = OMe

Stemotinine (**76**)

Isostemotinine (**77**)

Stemonidine (**78**)

Didehydrocroomine (**79**)

Figure 1.7 *Stemona* alkaloids of the tuberostemospironine group.[2,5,14,31,35,40–41]

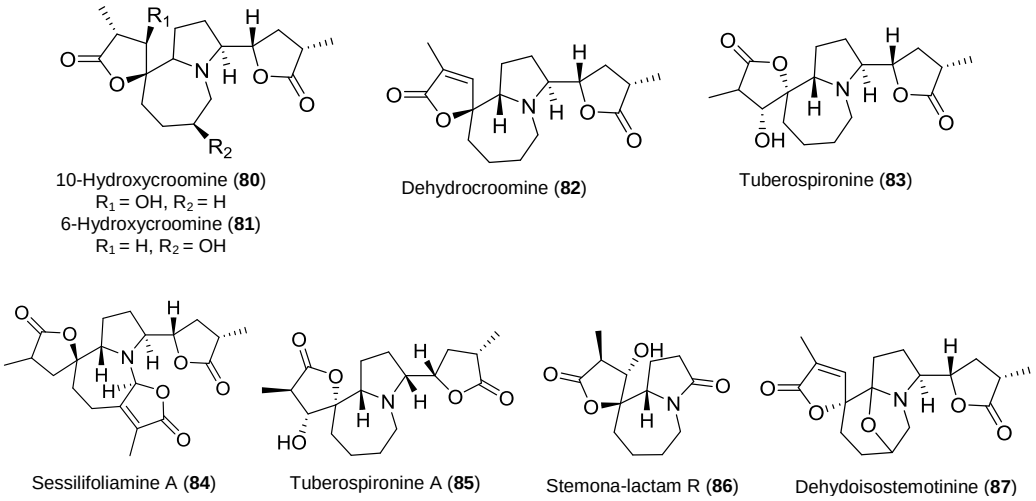

Figure 1.7 *Stemona* alkaloids of the tuberostemospironine group (continued).[2,5,14,31,35,40–41]

1.4.4 Stemoamine group

This group (Figure 1.8) is characterized by the presence of the tetracyclic spiro[1*H*-cyclopenta[*b*]pyrrolo[1,2-*a*]azepine-11(10*H*),2′(5′*H*)-furan]-5′,10-dione skeleton (**IV**, Figure 1.4) and comprises 11 alkaloids.

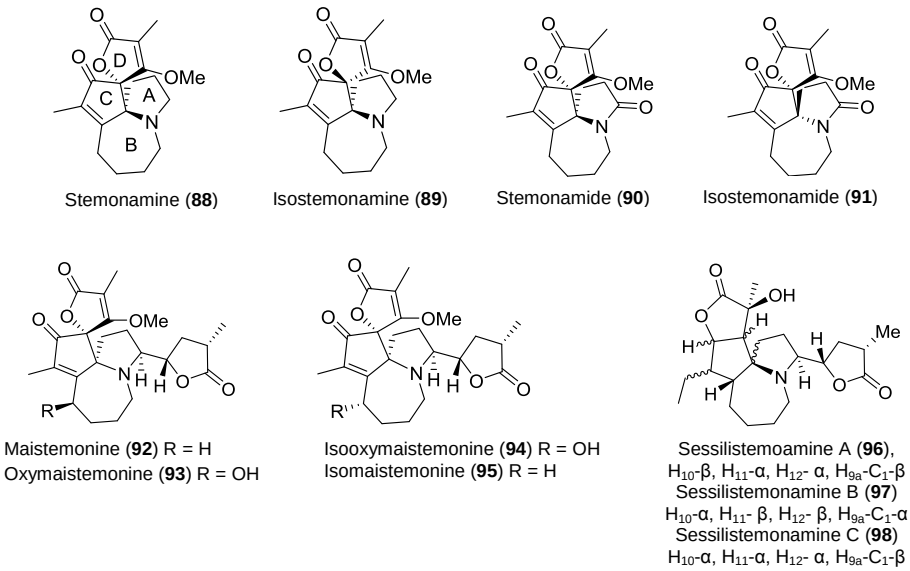

Figure 1.8 *Stemona* alkaloids of the stemonamine group.[2,14,25]

These alkaloids feature a cyclopentane C-ring and, in the case of alkaloids **85**-**95**, a γ-lactone ring attached in a spiro fashion to C-12 of the C-ring. In alkaloids **96**-**98**, a γ-lactone is attached to the C-ring in a fused fashion at C-11 and C-12.

1.4.5 Parvistemoline group

The parvistemoline group of alkaloids (Figure 1.9) are characterized by the lack of the B–C ring fusion and the presence of a substituent attached to C-9 in the pyrrolo[1,2-*a*]azepine nucleus. This group comprises 12 alkaloids as shown in Figure 1.9.

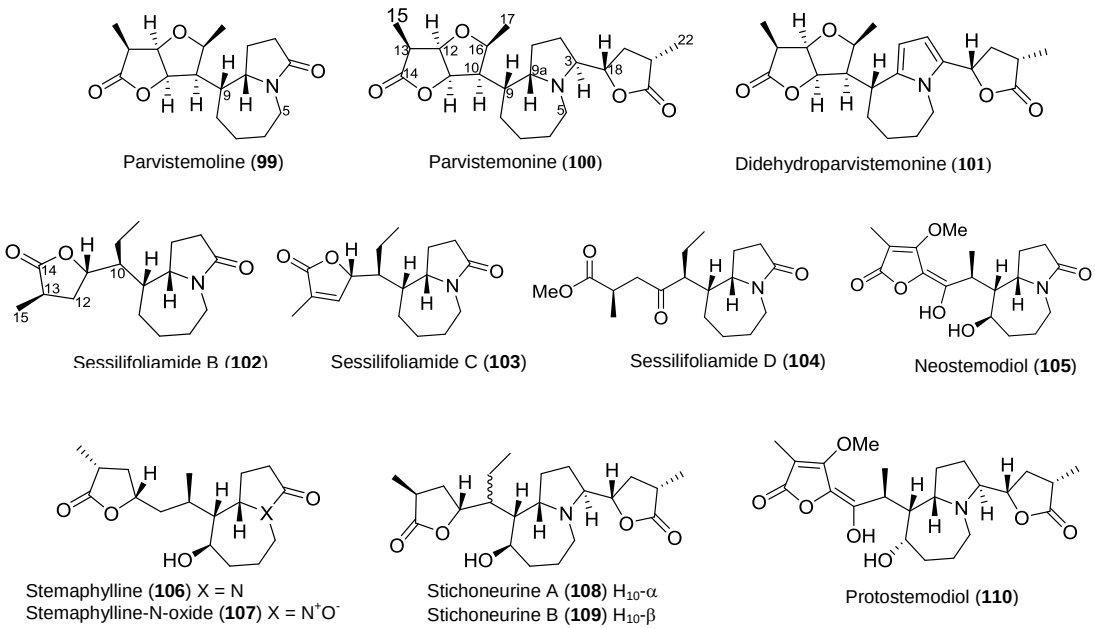

Figure 1.9 *Stemona* alkaloids of the parvistemoline group.[2,4,14]

1.4.6 Stemofoline group

The alkaloids from this group (Figure 1.10) typically have a complex caged structure which has an oxygen bridge between C-2 and C-8 and a carbon-carbon bond between C-3 and C-7. Twenty two alkaloids comprise this group with stemofoline (**111**)

being the most commonly found (Figure 1.10). Several alkaloids seem to have been derived from stemofoline (**111**) by oxidation of the C-3 butyl side chain (e.g. **112**, **119**, **124-126**, **129**, **130** and **132**). The derivatives **115** and **116** are interesting since both isomers were isolated from the same plant suggesting two different enzymes are present for this oxidation or they arise from oxidation of **118**.

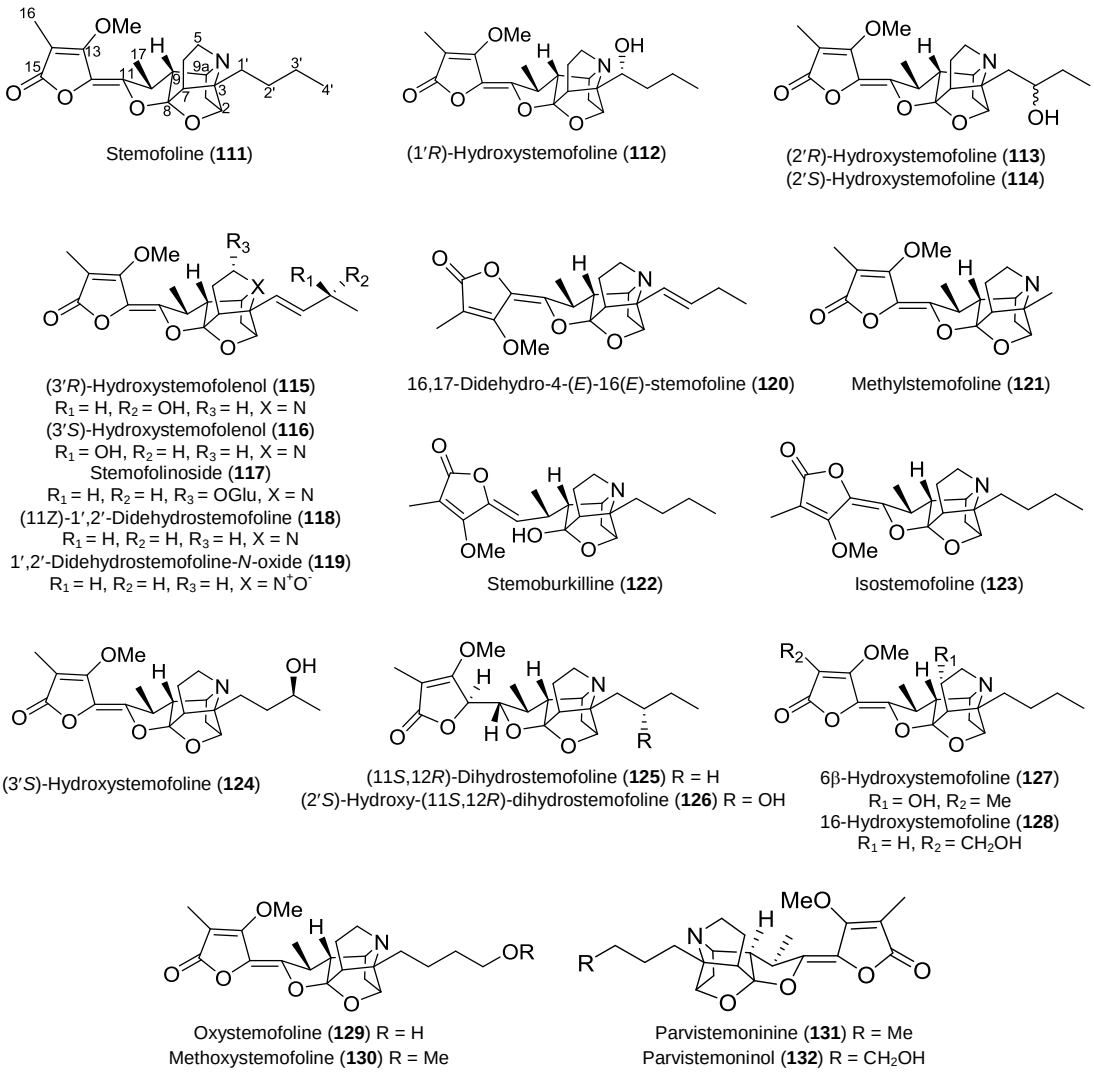

Figure 1.10 *Stemona* alkaloids of the stemofoline group.[2,14,42–43]

1.4.7 Stemocurtisine group

This group (Figure 1.11) is characterized by the presence of a pyrido[1,2-*a*]azepine base structure instead of a pyrrolo[1,2-*a*]azepine nucleus as featured in the previous groups. The first *Stemona* alkaloid isolated in this group was stemocurtisine (**133**) from the roots of *Stemona curtisii* in 2003 which led to this group's name.[13] Currently, this group includes 19 alkaloids as shown in Figure 1.11. The majority of these alkaloids have a (1′*R*)-hydroxypropyl side chain at C-4, stemocurtisinol (**142**) is an exception having a different configuration at C-4 and C-1′. The most recent member is the 5,6-seco-derivative (**148**) of stemocurtisine (**133**).

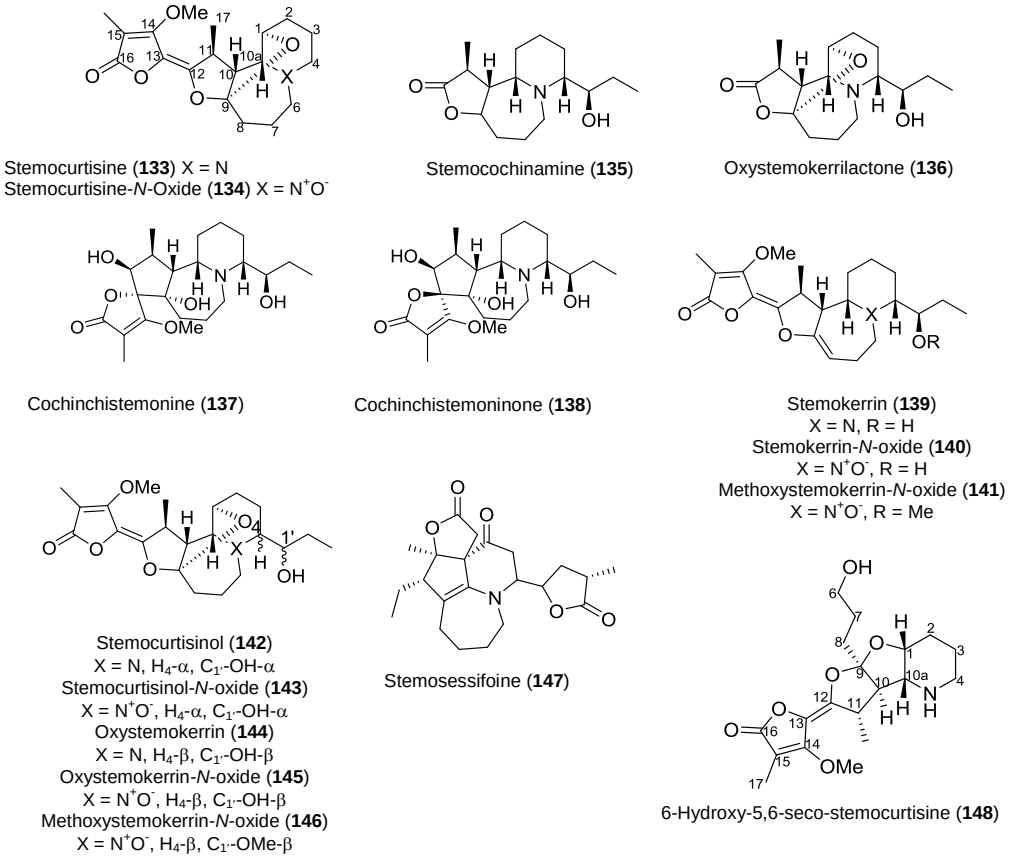

Figure 1.11 *Stemona* alkaloids of the stemocurtisine group.[2,13–14,39,44]

1.4.8 Miscellaneous group

The miscellaneous group (Figure 1.12) comprises alkaloids that do not fit in any of the general classifications as shown in Figure 1.12. Members of this group exhibit a polycyclic skeleton but neither a pyrrolo[1,2-*a*]azepine nor a pyrido[1,2-*a*]azepine system, except for tuberostemoenone (**162**), sessilistemonamine D (**164**) and stemoxazolidinone A-C (**170-172**). Many of these compounds arise from oxidative cleavage of the pyrido[1,2-*a*]azepine skeleton and further rearrangement, including the recently isolated alkaloids stemona-lactam M (**173**) and stemona-lactam N (**174**). Members of this group are parvistemoamide (**149**), tuberostemoninol (**150**), neotuberostemoninol (**151**), maireistemoninol (**152**), sessilifoliamide E (1**53**), sessilifoliamide F (**154**), tuberostemoline (**155**), sessilifoliamide I (**156**), sessilifoliamide G (**157**), sessilifoliamide H (**158**), tuberostemonone (**159**), neotuberostemonone (**160**), epoxytuberostemonone (**161**), tuberocrooline (**163**), 1,9a-seco-stemoenonine (**165**), parvineostemonine (**166**) and stemona-lactam Q (**175**) (Figure 1.12). However, other bicyclic systems were also found for example, the pyrido[1,2-*a*]azonine nucleus (Figure 1.12) is found in sessilifoliamide K (**167**) and sessilifoliamide L (**168**) and an indolizidine nucleus (Figure 1.12) in sessilifoliamide J (**169**). More recently, Hitotsuyanagi[36] reported another two *Stemona* alkaloids from *S. tuberosa* with a new skeleton. They are stemona-amines C and D (**176-177**) and in this thesis, we put them in this group as the authors claimed that these alkaloids have a novel skeleton.[36] Another three new *Stemona* alkaloids have been reported, tuberostemoline A and B (**178-179**) and tuberostemoninol C (**180**).[38] The total members of this group are 32 (Figure 1.12).

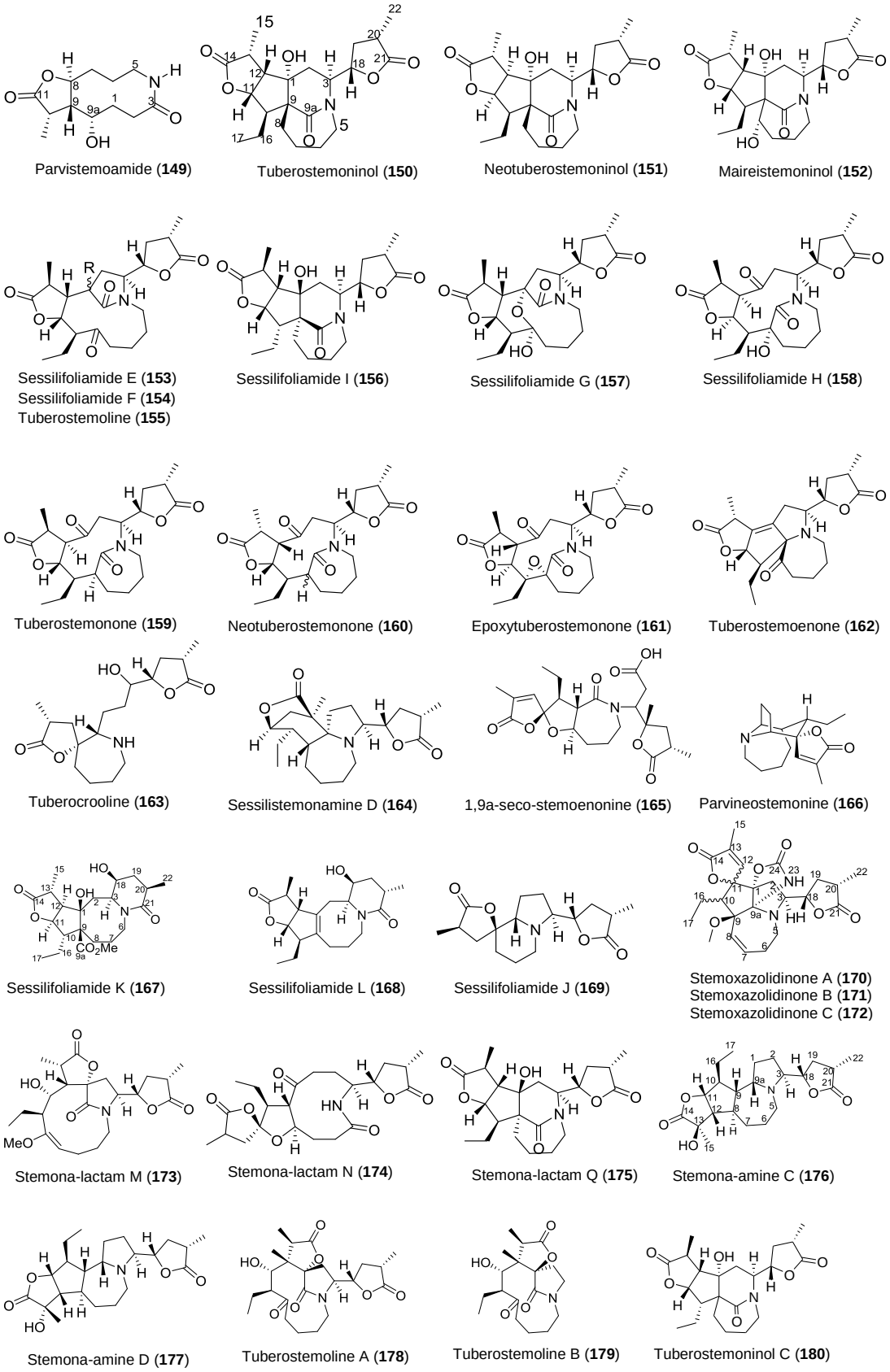

Figure 1.12 *Stemona* alkaloids of the miscellaneous group.[2,14,32,34,35,36,38,45]

1.5 Biosynthetic pathways of the *Stemona* alkaloids

To date no biosynthethic studies have been reported on the *Stemona* alkaloids. A possible biosynthetic connection between the pyrrolo- and pyrido[1,2-*a*]azepine alkaloids has been proposed by Kaltenegger in 2003.[10] He reported the investigation of the co-occurrence of alkaloids of both skeleton types from the root extracts of the same plant species. In this study, he proposed that hydrolysis of the lactone ring of protostemonine (**40**) followed by decarboxylation might result in the C-3 1′-hydroxybutyl side chain, which has been found in some stemofoline alkaloids (Scheme 1.2). Furthermore, it was proposed that ring expansion of the pyrrolidine A ring occurred to form the six member pyridine ring of the pyrido[1,2-*a*]azepines (Scheme 1.2). While this biosynthetic path is possible it does not explain the configuration of the pyrido[1,2-*a*]azepine alkaloids at C-4 and C-1′.

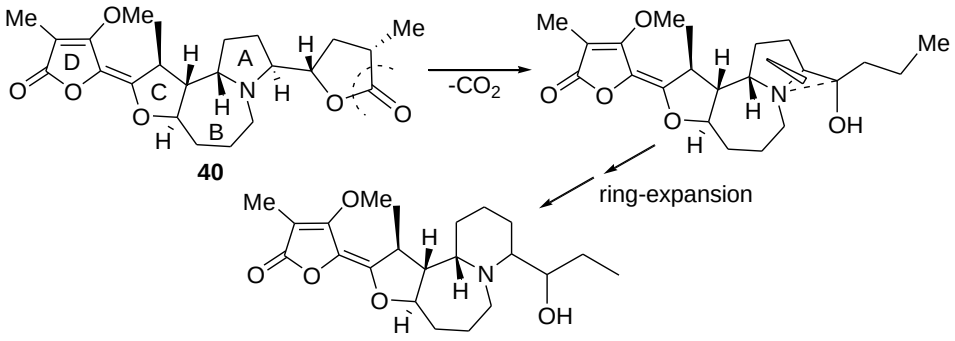

Scheme 1.2 Proposed biosynthetic connections between pyrrolo- and pyrido-azepines.[10]

Another possible biosynthetic pathway for the pyrrolo[1,2-*a*]azepines nucleus was suggested by Seger (2004)[46] and Greger (2006).[12] A number of *Stemona* alkaloids with a pyrrolo[1,2-*a*]azepines core were analysed (Figure 1.13). The C- and D-ring carbons were proposed to be of terpenoid origin while the A-ring of these alkaloids was suggested to arise from spermidine and the iminium ion intermediate **A** (Schemes 1.3

and 1.4). The proposed biosynthesis of stemofoline is shown in Scheme 1.4. Coupling of the pyrrolidine iminium ion intermediate **A** with the geranyl and prenyl units, **B** and **C**, respectively gives rise to the pyrrido-[1,2-*a*]azepines **D**. While this pathway seems possible no details were advanced to explain how the protostemonine intermediate in Scheme 1.4 could be activated to give the complex cage structure of stemofoline.

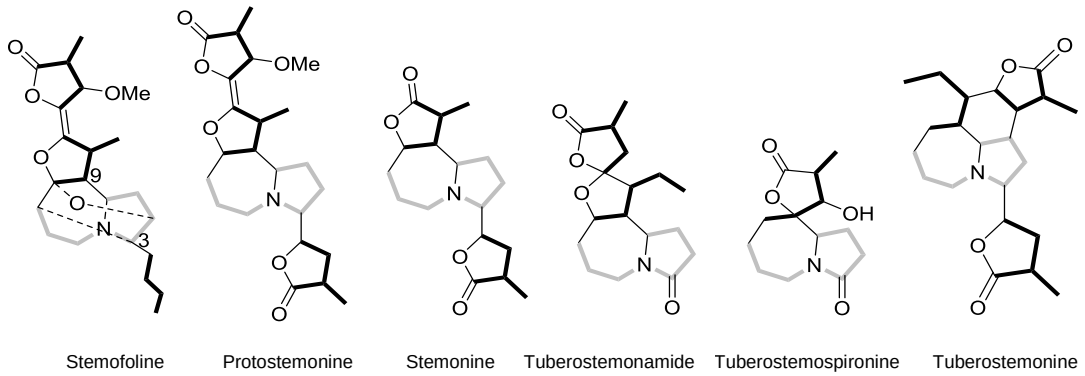

Figure 1.13 Structural comparisons of different *Stemona* alkaloids. The spermidine part of the pyrrolo[1,2-*a*] core is depicted with grey bold bonds and the terpenoids units with black bold bonds.[46]

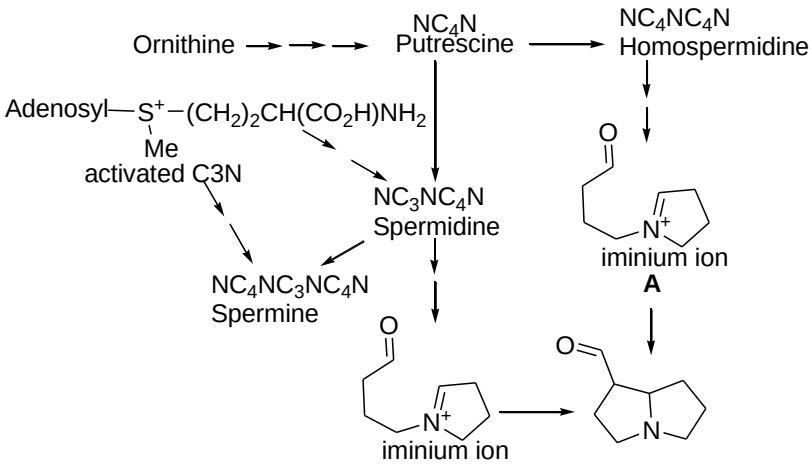

Scheme 1.3 Biosynthesis of spermidine and the iminium ion intermediate **A**.[46]

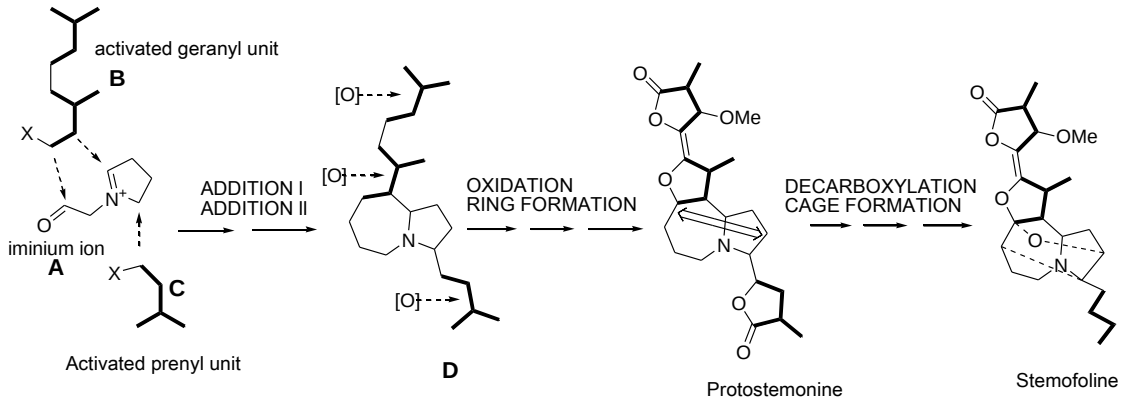

Scheme 1.4 Proposed biosynthetic pathway of stemofoline.[46]

In 2005, an alternative biosynthesis of the pyrido[1,2-*a*]azepine alkaloids was proposed by Mungkornawakul.[47] The proposed biosynthesis of the A-ring of oxystemokerrin (**144**) and stemocurtisinol (**142**) is based on the known biosynthesis of the hemlock alkaloid (+)-conhydrine (Scheme 1.5). They proposed that the piperidine iminium ion **E** was coupled to a geranyl intermediate to give the pyrido[1,2-*a*]azepine skeleton of these alkaloids.

In the case of the spirocyclic ring structures found in cochinchistemonine (**137**) and cochinchistemoninone (**138**), Lin has proposed that these alkaloids are derived biosynthetically from stemokerrin (**139**).[48] Hydrolysis of the enol ether group of stemokerrin (**139**) would be expected to give the diketone (**181**) which could undergo an intramolecular aldol reaction to give cochinchistemoninone (**138**). A diastreoselective reduction of the ketone group of cochinchistemoninone (**138**) would then give cochinchistemonine (**137**) (Scheme 1.6). This is the first biosynthetic proposal that provides a sound mechanistic possibility for a proposed biosynthetic pathway.

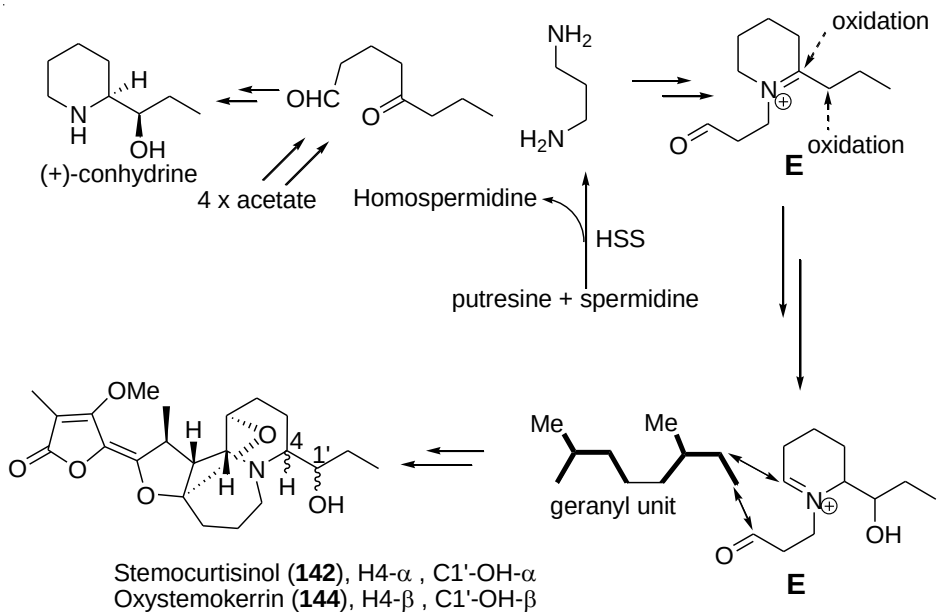

Scheme 1.5 Proposed biosynthesis pathway of pyrido[1,2-*a*]-azepines alkaloids.[47]

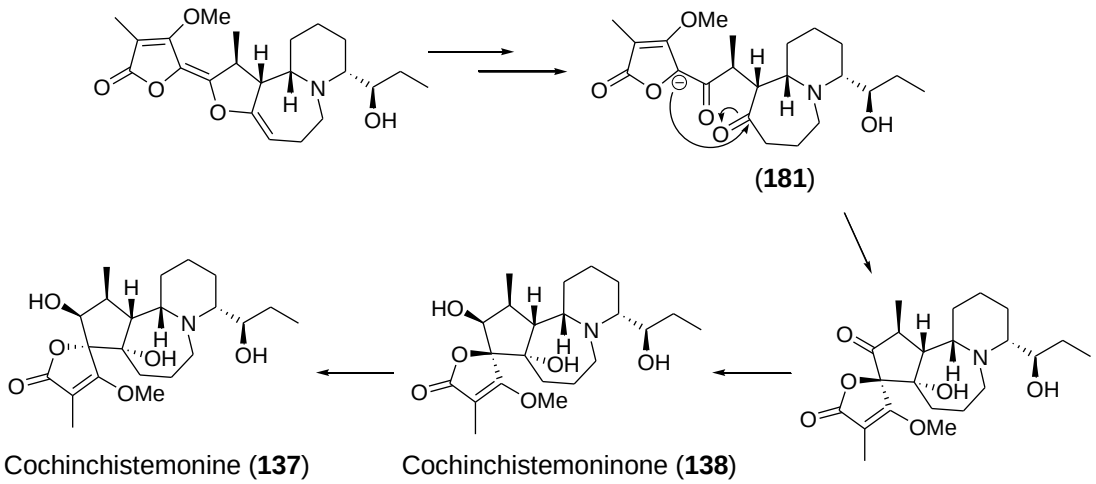

Scheme 1.6 Proposed biosynthesis of cochinchistemoninone (**138**) and cochinchistemonine (**137**).[48]

Based on his proposed biosyntheses, Greger has suggested a new classification of *Stemona* alkaloids into three skeleton types: stichoneurine-, protostemonine- and croomine-types (Scheme 1.7).[12] These three types skeleton can be distinguished by the different carbon chain attached to C-9 of the pyrrolo[1,2-*a*]azepine nucleus. In the stichoneurine- and protosemonine-types, these chains usually contain eight carbon atoms forming a terminal lactone ring, but differ among each other in the branching pattern. In the croomine-type, by contrast, the chain consists only of four carbon atoms forming a lactone ring directly attached to C-9 in a spiro system.

However in 2009, Greger and co-workers suggested a possible biosynthetic pathway to the *Stemona* alkaloids based on earlier published phytochemical studies on Stemonaceae and Pandanaceae plants.[5] The occurrence of pandamine (**183**) from Stemonaceae plants convinced Greger of the biosynthetic relationship between the *Pandanus* and *Stemona* alkaloids. Pandamine (**183**) was known to be a precursor of the pyrrolidine-type alkaloids, pandamarilactonine (**184**) and the spiro-piperidine alkaloids **185** isolated from *Pandanus amaryllifolius* Roxb.[49] The co-occurrence of pandamine (**183**) from *Stichoneuron calcicola* convinced Greger to propose pandamine (**183**) as a biogenetic precursor of the *Stemona* alkaloids, including croomine (**74**) (Scheme 1.8). Pandamine (**183**) was proposed to form through a decarboxylation, cyclization, reduction and dehydration process from the intermediate **182** which was produced by condensation of two units 4-hydroxy-4-methylglutamic acid and a C-4-N-C-4 dicarboxylic acid.[50] While this is a reasonable proposal further experimental studies using isotopically labeled precursors would be required to verify these mechanisms.

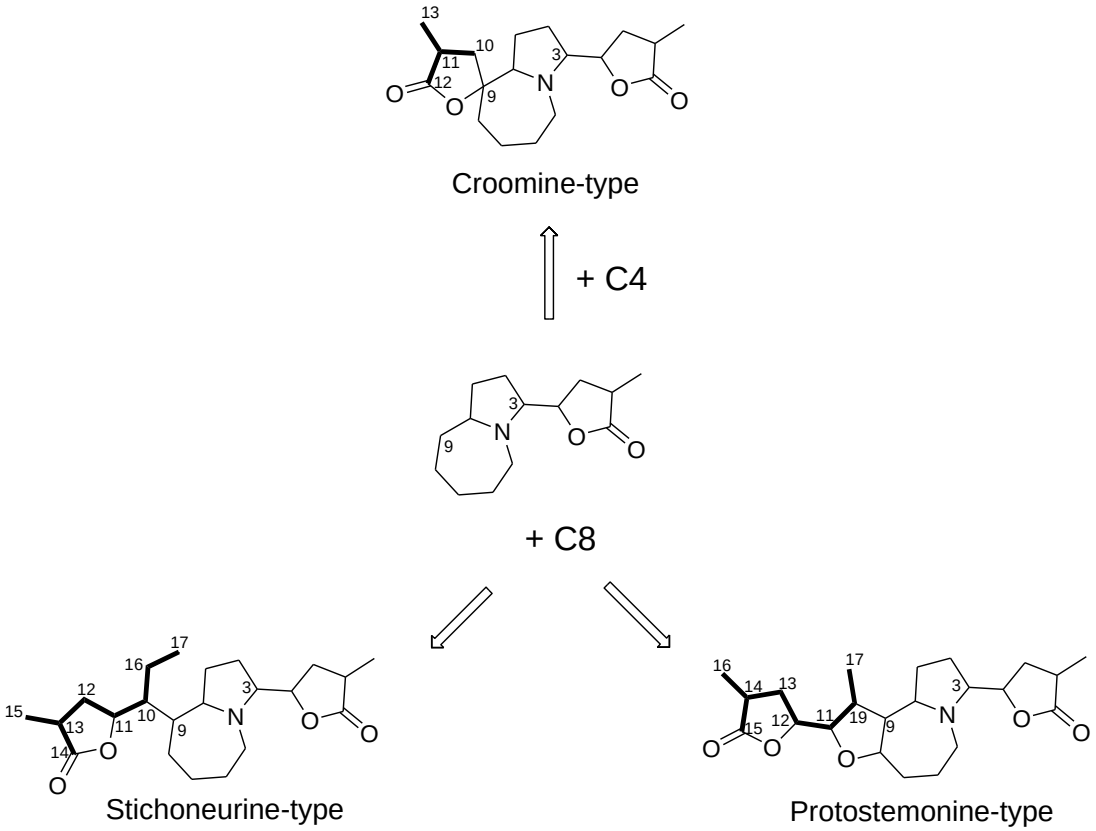

Scheme 1.7 Classification of *Stemona* alkaloids into three skeleton types based on different carbon chains attached to C-9 of the pyrroloazepine core.[12]

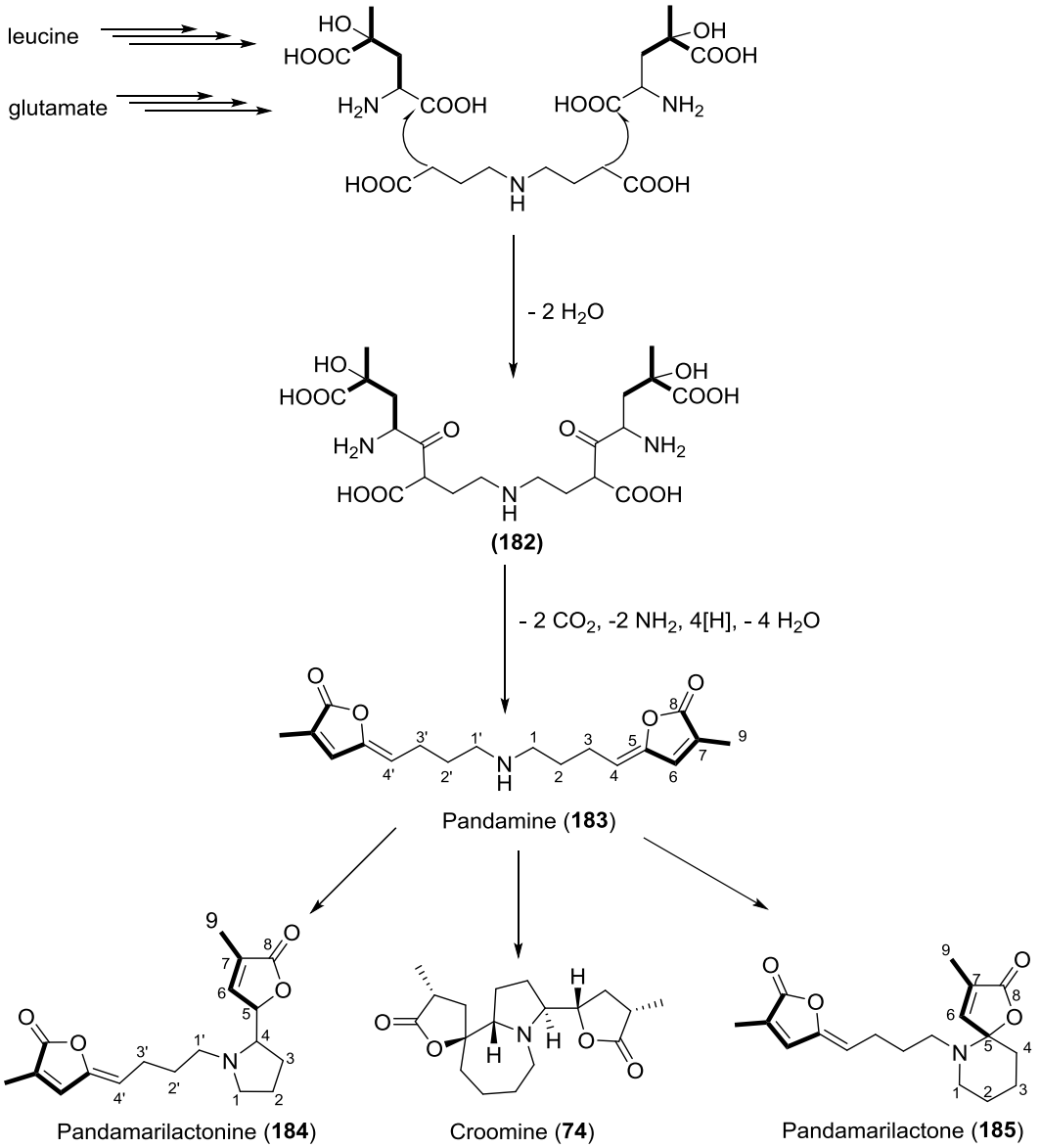

Scheme 1.8 Hypothetical biosynthetic pathway of pandanamide and its possible cyclization products **74**, **184** and **185**.[5]

1.6 Aims of this project

Despite *Stemona* plants and their component alkaloids having a wide range of biological activities that are useful, with potential applications in medicine and agriculture, only a few investigations have been carried out to determine the structures of the active compounds. Unfortunately, the limited supply of many of these alkaloids has prevented further biological investigations and developments. It is important that this family be studied further and their active principles be identified. The isolation of compounds from *Stichoneuron* and *Stemona* sp. were the particular interest for this study as well as the AChE inhibition activities of these alkaloids which may allow us to discover new derivatives that can be used as a treatment for Alzheimer's disease. The study of *Stichoneuron* sp was particular importance to establish if *Stemona*-alkaloids were also present in these plants. Such a study would also provide taxonomic support for this species being classified under the Stemonaceae family. In collaboration with the Department of Biochemistry, Faculty of Medicine, Chiang Mai University, we also planned to test some of the isolated *Stemona* alkaloids as P-glycoprotein (P-gp) inhibitors. With collaborators in Thailand (Dr. Sumalee Kamchonwongpaisan from the National Center for Genetic Engineering and Biotechnology, Thailand), we also planned to test the *Stemona* alkaloids for their antimalarial activities against wildtype and multidrug resistant *P. falciparum* strains and for their cytotoxicity activities against VERO cells (kidney epithelial cells from an African green monkey) and KB cells (human mouth epidermal carcinoma cells).

The aims of this project are:

1. To collect *S. curtisii* and *Stichoneuron* plants from peninsular Malaysia, document their locations and have them identified by a botanist.
2. Make ethanol or methanol extracts of the roots and leaves of these plants and then to isolate the chemical components, especially the *Stemona* alkaloids, from *St. halabalensis*, *St. caudatum*, *S. curtisii* and *S. javanica*. It should be noted in previous studies the majority of the *Stemona* alkaloids are found in the roots rather than the leaves.
3. To determine the structures of the isolated chemical components from these plants.
4. To determine the AChE inhibitory activity of the isolated chemical components.
5. To determine the P-gp inhibitory activity in the modulation of drug resistance of the isolated chemical components in cancer cell lines.
6. To determine the antimalarial activity of these alkaloids against wild type and multidrug resistant *P. falciparum* strains and cytotoxicity activities against Vero and KB cells.

CHAPTER 2

FIELD WORK

2.1 The *Stemona* genus

The *Stemona* plants are called by different names depending upon the regions that they are found, for example ‘Bai bu’ in China, ‘Bach bo’ in Vietnam and ‘Non-Tai-Yak’ in Thailand.[2] *Stemona* comprises about 25 species and represents the largest genus of the small monocotyledonous family Stemonaceae.[10] Many occur as perennial climbers or low lying plants with tufted tuberous roots in rather dry vegetation ranging from continental Asia and Japan through South East Asia to tropical Australia. Figure 2.1 shows the flowers of some *Stemona* species. In spite of the good delineation of *Stemona* from the nearest related genera *Croomia* and *Stichoneuron*, there are still many taxonomic problems at the species level that remain to be solved.[51–52]

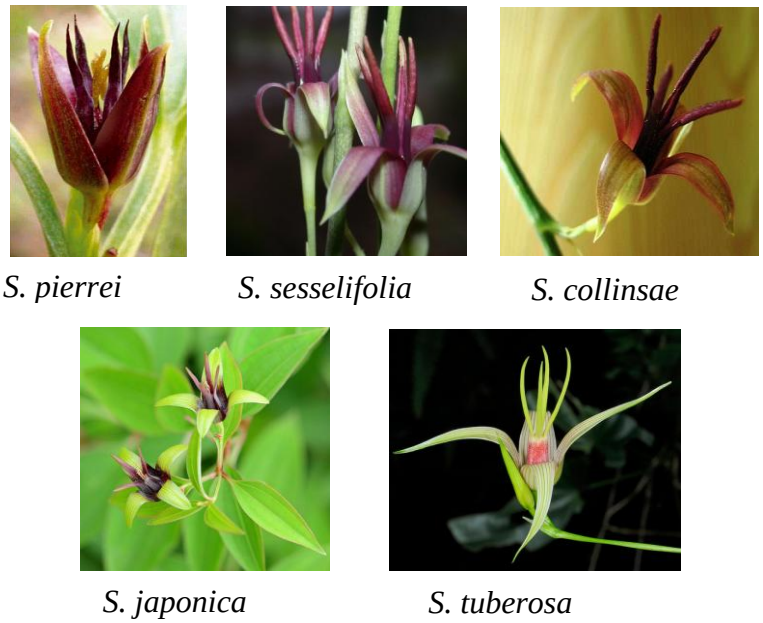

S. pierrei *S. sesselifolia* *S. collinsae*

S. japonica *S. tuberosa*

Figure 2.1 Shows the flowers of some *Stemona* species.[53–57]

2.1.1 Collection of *S. curtisii* from Dungun, Terengganu, Malaysia

Stemona curtisii was collected by R. A. Ramli in May 2011. The location of this plant material is shown in Figure 2.2. *Stemona curtisii* was found growing downstream of the Sura gate on the riverbank, in an area of sandy soil, which made it relatively easy to pull out the roots.

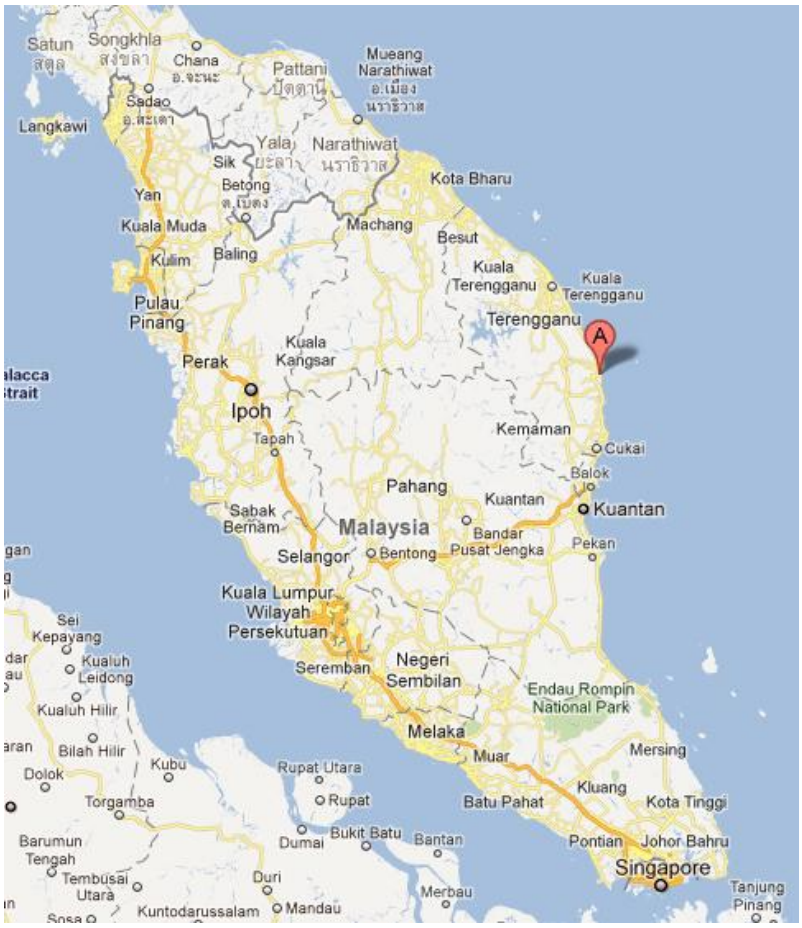

Figure 2.2 Map indicating the collection location of *S. curtisii*.[58]

Plant material

A voucher specimen for *S. curtisii* (Figure 2.3), (UKMB29952) was deposited at the Department of Biology, National University of Malaysia. The plant material was

identified by Mr. Sani from the same department. Figure 2.4 shows the drawings of *S. curtisii* by Murugan.[59]

Stemona curtisii is found in Sri Lanka (rare), Thailand and Malaysia. It is a glabrous twiner and has 150 cm long tuberous roots which form a bundle. It has alternate, seldom opposite leaves. Flowers are tepars pink, brown pink and brownish red. The species can be found near waterfalls, the seashore and on the riverbanks.[51] A few biological activities have been reported. The effect of the crude roots extract on the action potential of the frog sciatic nerve and its toxicity on house fly larvae (*Culex p. fatigans* and *Aedes aegypti*) have been reported.[60]

(A) (B)

(C) (D) (E)

Figure 2.3 *Stemona curtisii* Hook. f (A) habit, (B) roots, (D) leaf, (D) flower and (E) fruit (Photos taken by R. A. Ramli, 2 May 2011).

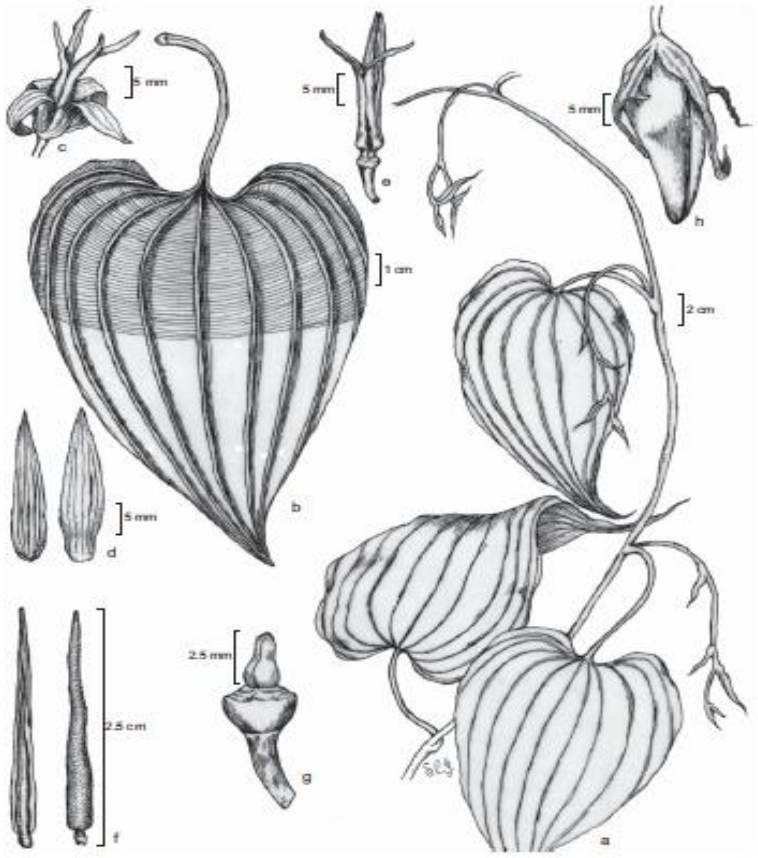

Figure 2.4 *Stemona curtisii* Hook. f.: (a) twig; (b) leaf; (c) flower; (d) tepals; (e). androecium; (f) stamens; (g) ovary with pedicel; (h) Capsule with persistent tepals [Taken from Murugan].[59]

2.1.2 Collection of *S. javanica* from Moluccas Island, Indonesia

The *Stemona javanica* (Figure 2.5) was collected from Purwo, East Java, Indonesia in June and December 2012 by our collaborator, Assoc. Prof. Pratiwi Pudjiastuti from the Department of Chemistry, Faculty of Science and Technology, University Airlangga, Surabaya, Indonesia.

Plant material

A voucher specimen of collected *S. javanica* (Figure 2.5), (No. IV.D.IV.7) was deposited at the Conservation Institute of Purwodadi Botanical Garden, Pasuruan, East Java, Indonesia. Figure 2.5 shows the specimen of *S. javanica*[61] and the drawings of *S. javanica* by Telford.[62] The synonym names of *S. javanica*: *Stemona australiana*, *Stemona sulensis* J.J.Sm, *Stemona papuana* Schltr, *Stemona asperula* J.J.Sm. *Roxburghia javanica* Kunth and *Roxburghia gloriosoides* Zoll. ex Kunth.[51,62]

Figure 2.5 Roots of *S. javanica* (Photo taken by P. Pudjiastuti, June 2012)

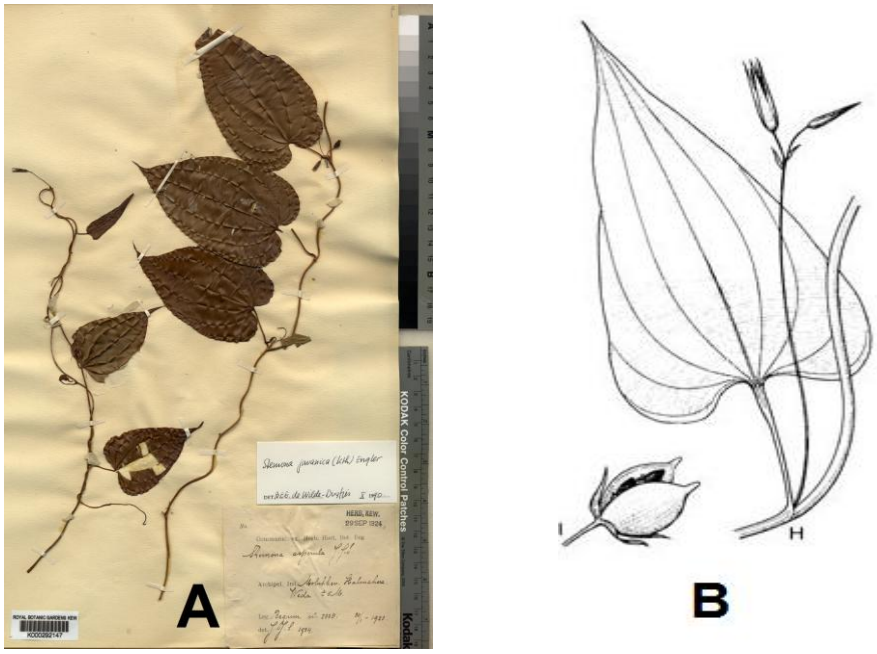

Figure 2.6 (A) Herbarium specimen of *S. javanica*[61] and (B) Drawing of picture of *S. javanica* by Telford.[62]

2.2 The *Stichoneuron* genus

In 2009, Inthachub and co-workers reported the descriptions and distribution of five *Stichoneuron* species of plants (Figure 2.7).[1] These five species were *Stichoneuron bognerianum* Duyfjes, *Stichoneuron calcicola* Inthachub, *Stichoneuron caudatum* Ridl., *Stichoneuron halabalensis* Inthachub and *Stichoneuron membranaceum* Hook. F. Three of them (*St. caudatum*, *St. halabalensis* and *St. bognerianum*) were found in the peninsular of Malaysia, while *St. calcicola* is found in southern Thailand and *St. membranaceum* was found in India (Meghalaya: Khasia Hills) and Burma.[1] The flowers of the five species are shown in Figure 2.8.

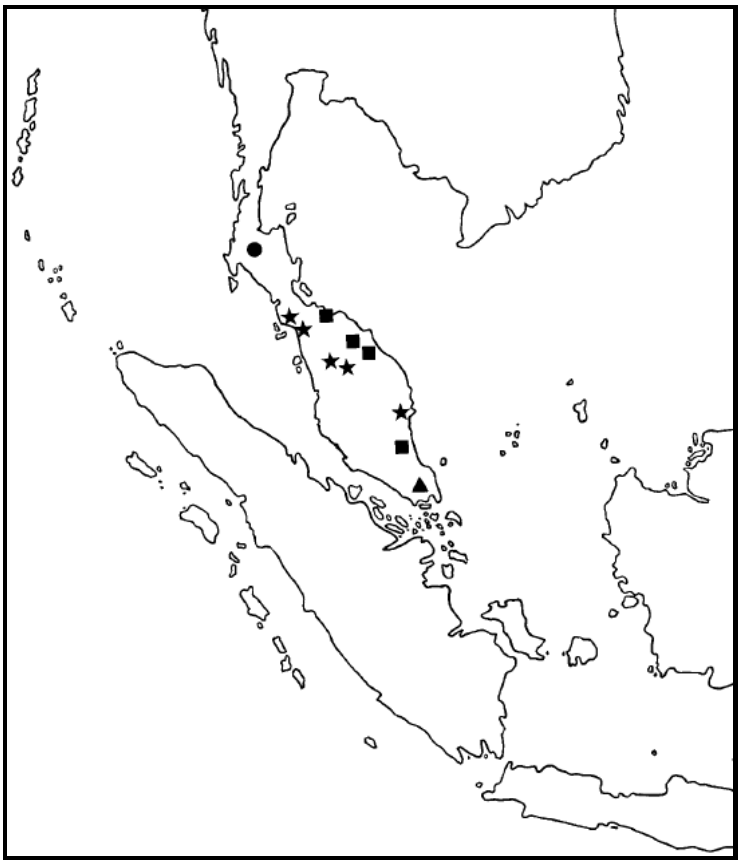

Figure 2.7 Distribution of four *Stichoneuron* species in Peninsular Thailand and Peninsular Malaysia: *St. bognerianum* (▲); *St. calcicola* (●); *St. caudatum* (★); *St. halabalensis* (■).[1]

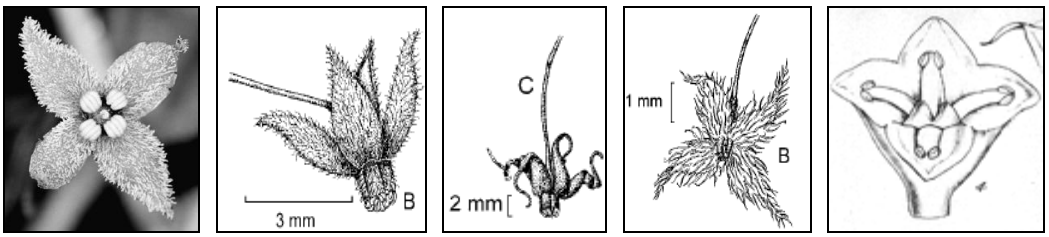

(A) **(B)** **(C)** **(D)** **(E)**

Figure 2.8 The flower of (A) *St. bognerianum*, (B) *St. calcicola*, (C) *St. caudatum*, (D) *St. halabalensis* and (E) *St. membranaceum.*[1,63]

Only two species of *Stichoneuron* have been studied for their phytochemicals; these are *St. caudatum* and *St. calcicola*.[4,5] Due to the limited research on this plant species, it is important to carry out more research on this genus which we believed may contain new alkaloid structures with novel biological activities.

2.2.1 Collection of *St. halabalensis* from Endau-Rompin National Park, Pahang, Malaysia

The field trip by R. A. Ramli to collect *St. halabalensis* was carried out in April 2010. The location is shown in Figure 2.9. This plant grows near to the Sungai Anak Endau riverbank. The area of sample collection in Endau-Rompin State is shown in Figure 2.10. In contrast, the soil of the collected area is clay and it was difficult to pull.

St. halabalensis is an erect herb 30-60 cm tall, with few branches; stem petiole and leaves sparsely hairy. Leaves: petiole (5-7) mm long, inconspicuously sheathing at the base, blade narrowly ovate-oblong or elliptic-oblong, glabrous, except veins on lower surface sparsely hairy. *St. halabalensis* can be found in the rain forest along streams (30-160 m). According to Inthachub, the distribution of *St. halabalensis* is in Peninsular Thailand (Narathiwat), and Peninsular Malaysia (Terengganu, Pahang).[1]

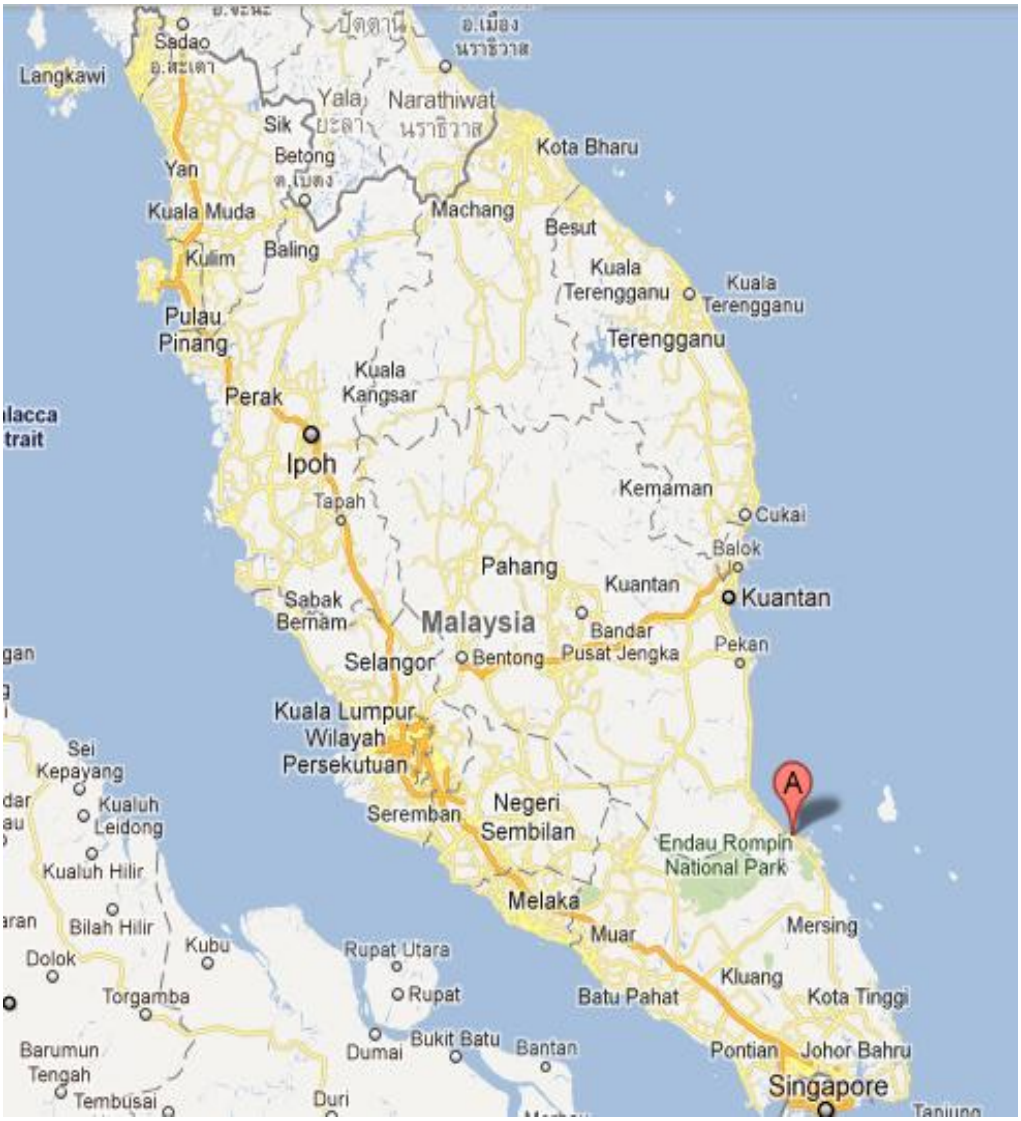

Figure 2.9 Location where *St. halabalensis* was collected in Peninsular of Malaysia.[64]

Figure 2.10 The area of sample collection in Endau-Rompin State Park (photographs taken by R. A. Ramli, 24 April 2010)

Plant material

A voucher specimen of *St. halabalensis* (Figure 2.11), UKM29953 was deposited at the Department of Biology, National University of Malaysia. The plant material was identified by Prof. Latiff Mohammad from the Department of Biology, National University of Malaysia. Figure 2.12 shows the drawings of *St. halabalensis* by Inthachub.[1]

(A)

(B)

(C)

(D)

Figure 2.11 *St. halabalensis* (A) young plants, (B) roots, (C) fruits and (D) flower (photographs taken by R. A. Ramli, 24 April 2010).

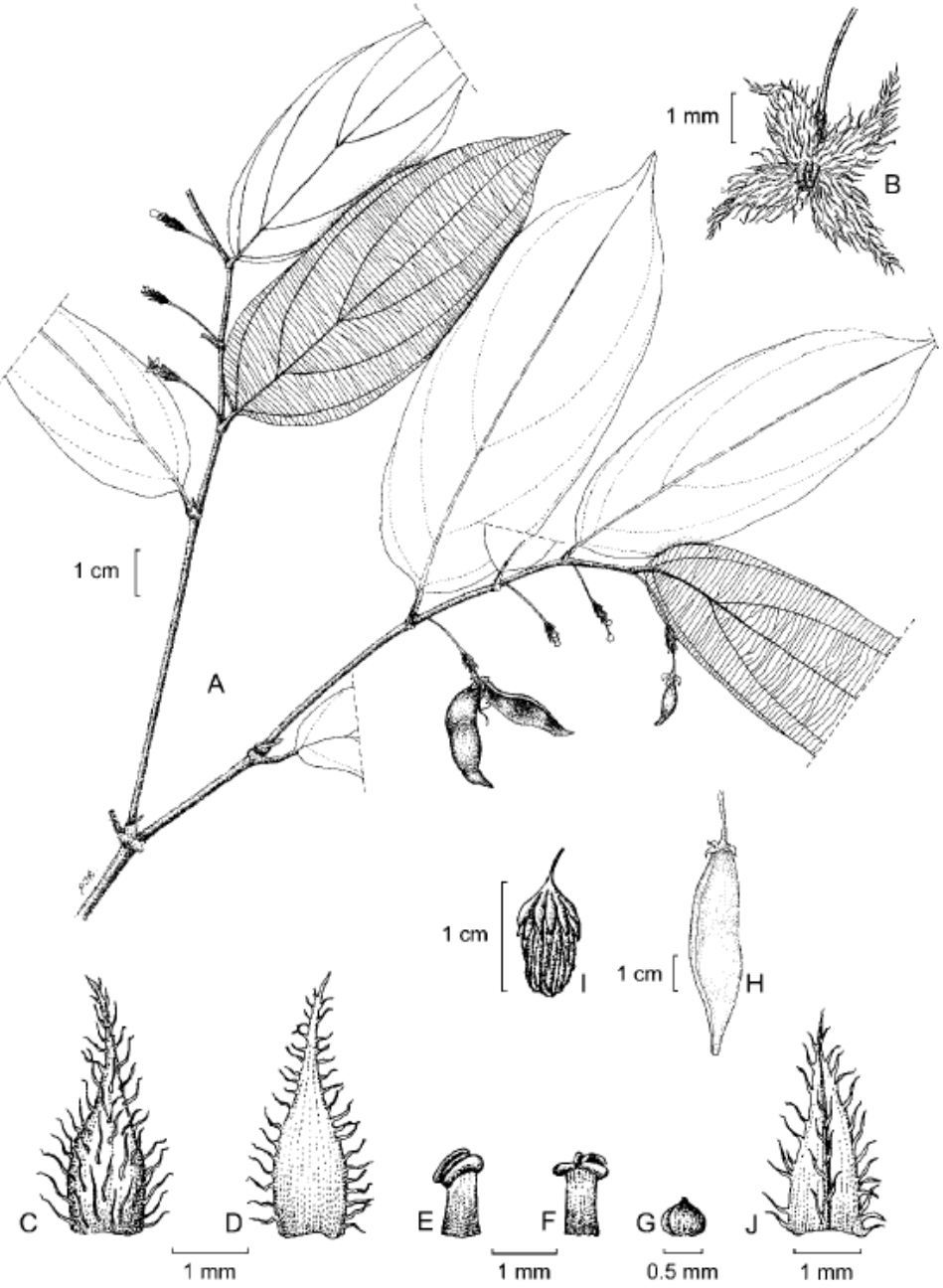

Figure 2.12 *St. halabalensis* Inthachub. (A) flowering and fruiting stem; (B) flower; (C-D) tepal, seen from inside and outside respectively; (E-F) stamens; (G) ovary; (H) fruit; (I) seed with finger-like aril lobes; (J) bract.[1]

2.2.2 Collection of *St. caudatum* from Lojing, Gua Musang, Kelantan, Malaysia

Stichoneuron caudatum (Figure 2.13) was collected by R. A. Ramli near the Lojing River, Gua Musang, Kelantan, Malaysia (Figure 2.14), in Dec 2011. Scenes from the area of sample collection in Endau-Rompin State are shown in Figure 2.15.

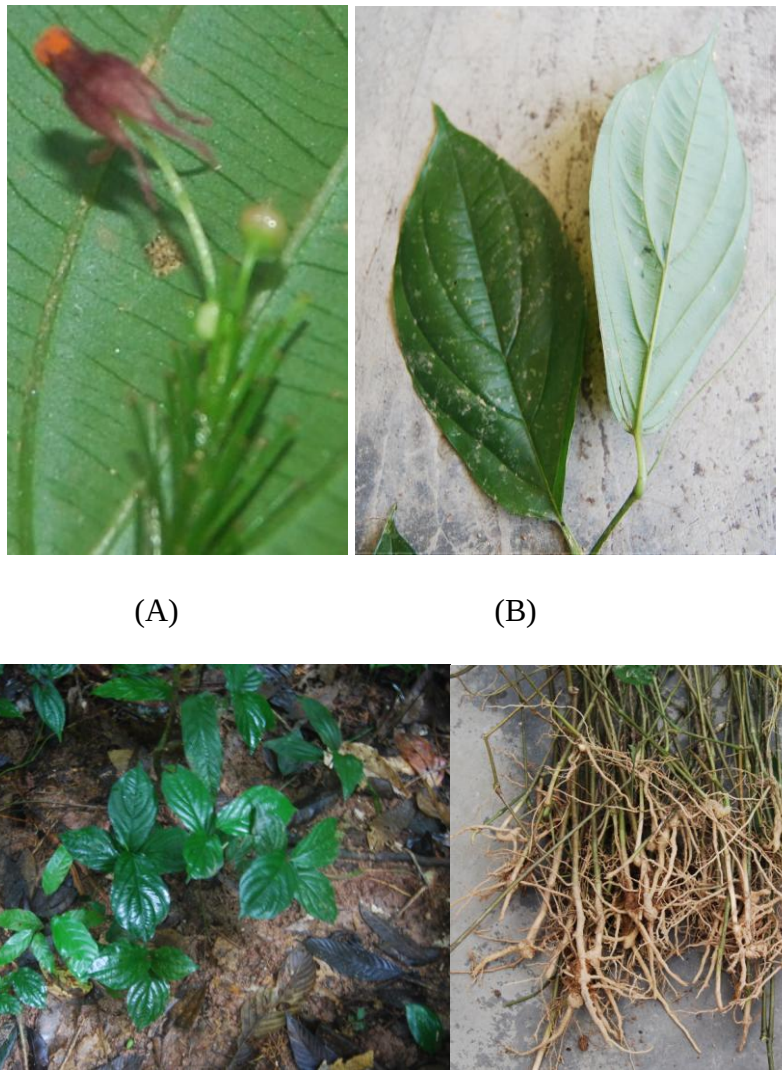

(A) (B)

(C) (D)

Figure 2.13 *St. caudatum* (A) flower, (B) leaves, (C) young plants and (D) roots (photographs taken by R. A. Ramli, 24 April 2010)

St. candatum Ridley is an erect herb plant, 20–40 cm tall and with short-hairy leaves. The leaves are petiole and 5 mm long, non-sheathing to barely sheathing, blade narrowly elliptic, 5–7 3 2.5–4 cm, base short-cuneate, lateral veins 3 (or 4) pairs and 3–4 mm long of prophyll. The inflorescences are glabrous; with 5 mm of peduncle; long, straight, 1–5-flowered, bracts 1–2 mm long and 6 fringed. The flowers are corolla pale greenish, 10–12 mm diameter, pedicel 10–15 mm long, persistent part 5–10 mm long, tepals spreading or faintly recurved, elliptic, margin 6 recurved, apex acute, lacking appendix, abaxially greenish and glabrous, adaxially pale green and densely somewhat papillose white-hairy, hairs c.0.5 mm long; stamens c.1.5 mm long, filaments purple-red, white-hairy; anthers curved over apex of filaments, (1–1.5) mm long, yellow; ovules 3 or 4. Fruit 15–20 mm long, 6–8 mm diameter and shortly beaked. Moreover, the seeds are 1 or 2, ellipsoid, 5–6 mm long, ridges sinuate, aril irregularly lobed; funicle short; pseudo-funicle not seen.[66]

In Malaysia, *St. candatum* is found in the southern peninsular Malaysia (Johor) and the Cha and Musang Caves in Kelantan.[67] Ecologically, *St. candatum* grows in or near swamp forests from sea level up to 30 m with wet habitats in lowland dipterocarp forests and rain forests, mostly near streams, granite bedrock, and sandy places around 30–600 m.[1, 67] *St. candatum* is known as “pokok segugut” or “Batek” by the local people. *St. caudatum* is taken with betel nut and or leaves as a tonic for convalescence and is used as an abortifacient.[68]

Plant material

A voucher specimen (UKM29978) was deposited at the herbarium of the Department of Biology, National University of Malaysia. Plant material was identified by Prof. Latiff Mohammad from the Department of Biology, National University of Malaysia. Figure 2.16 shows photos of *St. caudatum* taken by Inthachub in 2008[69] while Figure 2.17 shows the drawings of *St. caudatum* by Inthachub.[1]

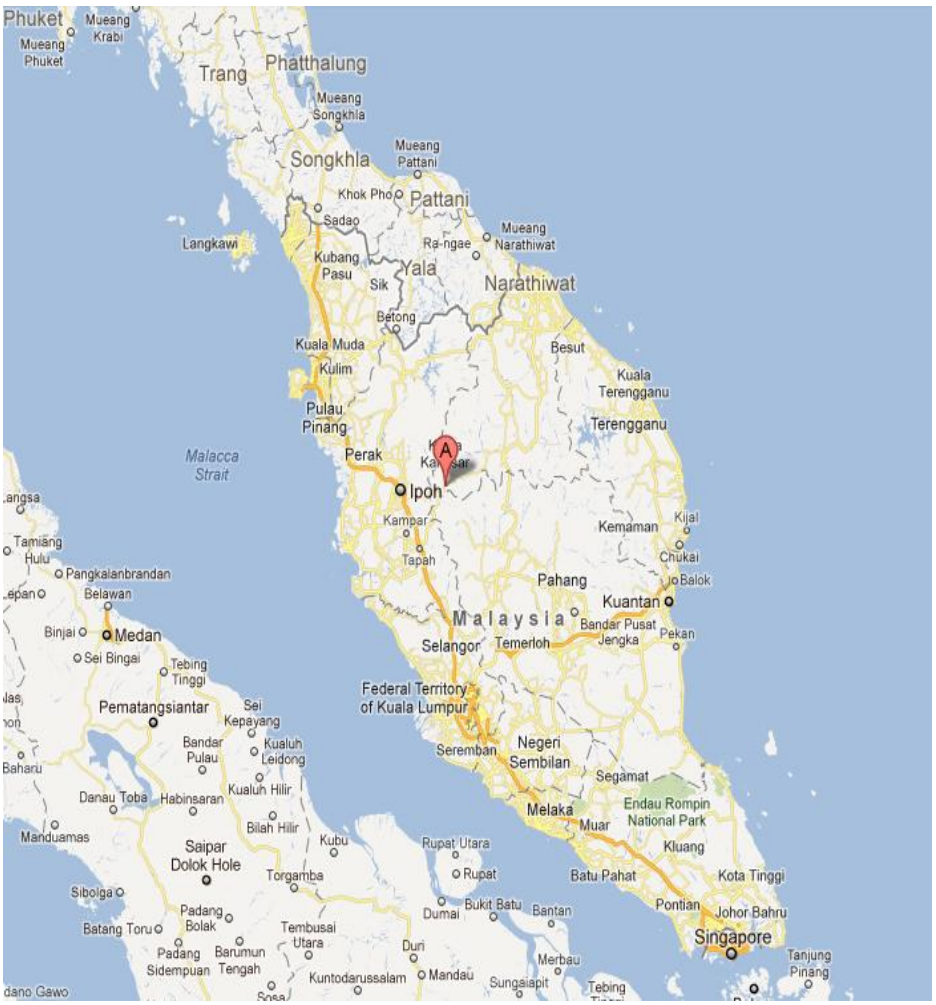

Figure 2.14 Location where *St. caudatum* was collected in Peninsular of Malaysia.[70]

Figure 2.15 The area of sample collection in Lojing, Gua Musang, Kelantan, Malaysia (photographs taken by R. A. Ramli, 10 December 2011).

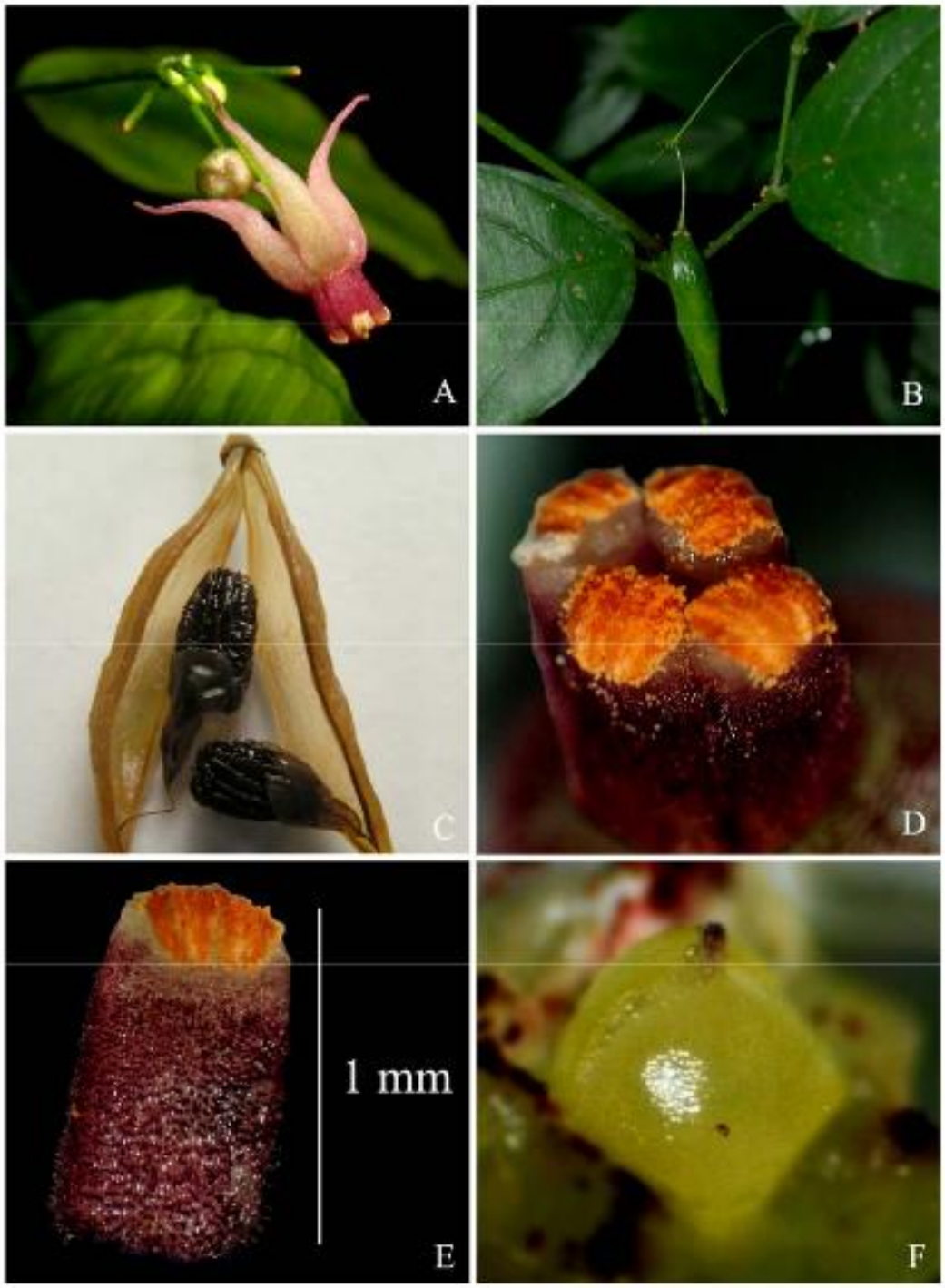

Figure 2.16 *St. caudatum*: (A) inflorescence; (B) fruit; (C) seed; (D) androcium; (E) stamen; (F) Ovary [Photographed by Inthachub, 2008).[69]

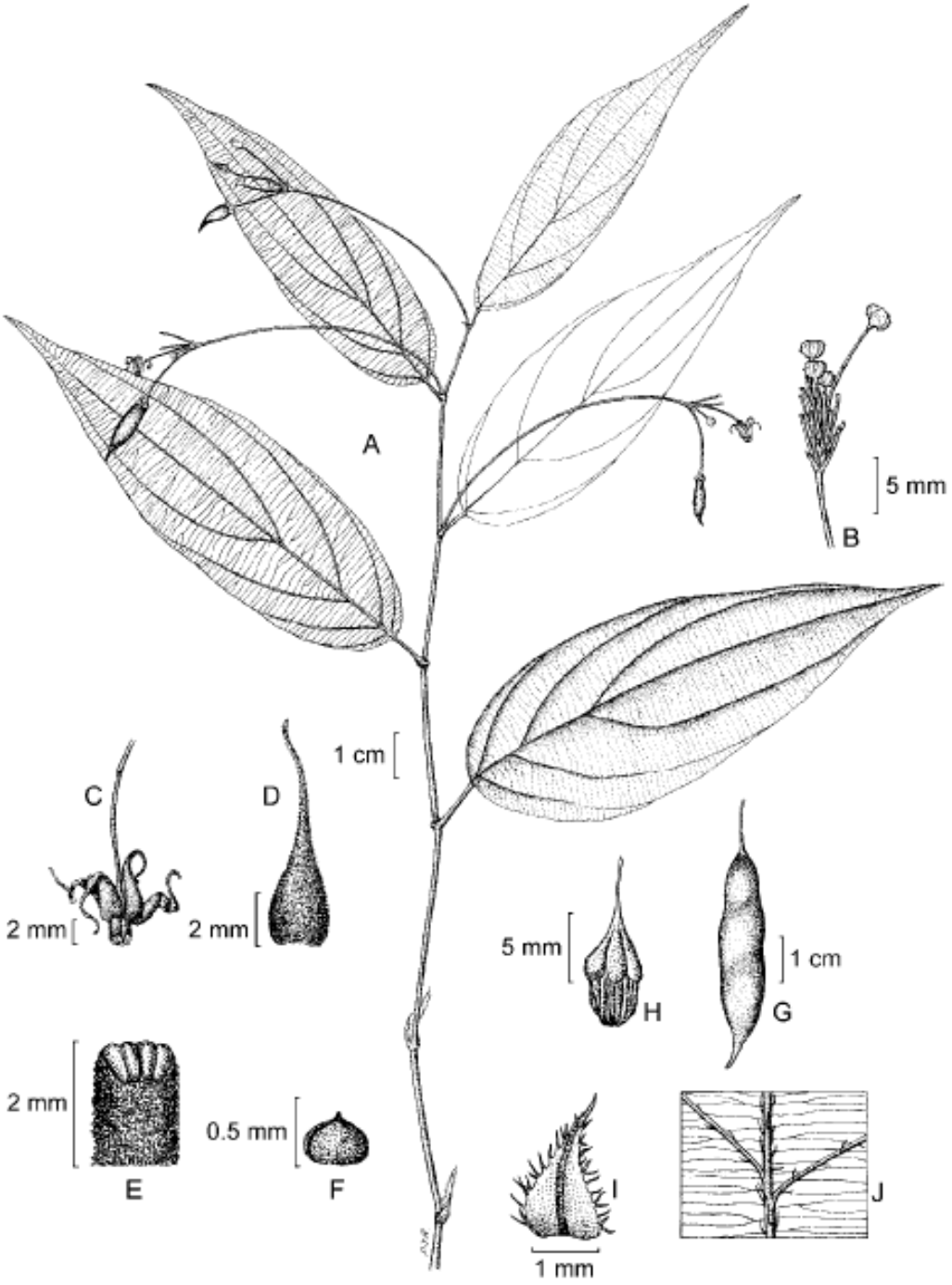

Figure 2.17 *St. caudatum* Ridl. (A) flowering and fruiting stem; (B) inflorescence with buds, (C) flower; (D) tepal, seen from inside; (E) stamen; (F) (ovary; (G) fruit; (H) seed with finger like aril lobes; (I) bract; (J) detail of lower leaf surface.[1]

2.2.3 Field Trip to Kota Tinggi, Johor, Malaysia

According to Inthachub, *St. bognerianum* Duyfjes, were located near to the Kaya River, near Mawai, beside the Kota Tinggi Road.[1] In December 2011, we went to this area to collect this species. However, we could not locate any specimens of this plant. We believe that this species is no longer growing in this area due to the floods that have happened regularly over the last 10 years. Figure 2.18 shows the flower of *St. bognerianum* and Figure 2.19 shows the area of Kaya River.[1]

Figure 2.18 Flower of *St. bognerianum* [Photographed by Bogner, 1789)].[1]

Figure 2.19 The area of Kaya River, Mawai, Kota Tinggi Johor, Malaysia (photographs taken by R. A. Ramli, 10 December 2011).

CHAPTER 3

ALKALOIDS FROM THE ROOTS OF *Stemona curtisii* HOOK F.

This chapter reports on a phytochemical study of the roots extracts of *Stemona curtisii* collected from Dungun, Terengganu in Malaysia.

3.1 Previous phytochemical studies on *S. curtisii*

A few phytochemical studies on *S. curtisii* have been reported. The earliest study was made in 2003 by Kaltenegger and co-workers.[10] *S. curtisii* was collected from South Thailand, Ko Lipe near Ko Adang in 2003. Six *Stemona* alkaloids were isolated from the roots, oxystemokerrin (**144**), dehydroprotostemonine (**42**), oxyprotostemonine (**43**), stemocochinine (**46**), (2′*S*)-hydroxystemofoline (**114**) and stemofoline (**111**), which was the major alkaloid.

In 2003, a phytochemical investigation on roots of *S. curtisii*, collected from Tumbol Kaunmao, Amphor Rasda, in the North of Trang Province, Thailand by Mungkornasawakul and co-workers.[13] This study led to the isolation of a new pentacyclic *Stemona* alkaloid, stemocurtisine (**133**), with a novel pyrido[1,2-*a*]azapine A,B-ring system. A year later, they reported another new *Stemona* alkaloid, stemocurtisinol (**142**), together with oxyprotostemonine (**43**) from the roots of *S. curtissi* from the same location.[11]

Further investigations on the roots of *S.curtisii* collected from Trang Province, Thailand were carried out in 2010. Two new *Stemona* alkaloids, 1-hydroxyprotostemonine (**41**) and stemocurtisine-*N*-oxide (**134**) were reported.[39]

In 2013, the aerial parts of *S. curtisii* were collected at Tambol Kaunmo, Amphor Rasda, in the North of Trang Province, Thailand again by Mungkornasawakul and co-workers. They reported a novel seco-stemocurtisine-type alkaloid, 6-hydroxy-5,6-seco-stemocurtisine (**148**).[44]

3.2 Isolation and purification of *Stemona* alkaloids from the ethanol extract of the roots of *S. curtisii*

In this current study, the roots of *S. curtisii* collected from the eastern part of Peninsular Malaysia were carried out. The roots (2205 g) were dried in an oven at 40 ^{o}C until the dry weight became constant. The air-dried roots of *S. curtisii* (558 g) were ground into a powder and extracted with 95% ethanol. The ethanolic extracts were evaporated to give a dark brown gum (7.2 g). The root extract was chromatographed by column chromatography (CC) on a silica gel using gradient elution CH_2Cl_2/EtOAc (3:7 to 0:10) to EtOAc/MeOH (10:0 to 8:2). A total of 2.5 L of eluent was collected in test tubes of 20 mL. These fractions were pooled on the basis of TLC analysis to give fractions A (97.4 mg), B (40.3 mg), C (50 mg) and D (5.7 g). Further separation of these fractions gave (2'*S*)-hydroxystemofoline (**114**, 21.1 mg; this was the major component by TLC analysis), stemocochinine (**46**, 5.9 mg), 1-hydroxyprotostemonine (**41**, 7.6 mg), oxystemokerrin-*N*-oxide (**145**, 2.9 mg), isostemofoline (**123**, 27.4 mg) and stemofoline (**111**, 6.9 mg). Figure 3.1 shows the structures of the isolated *Stemona* alkaloids from the roots of *S. curtisii*.

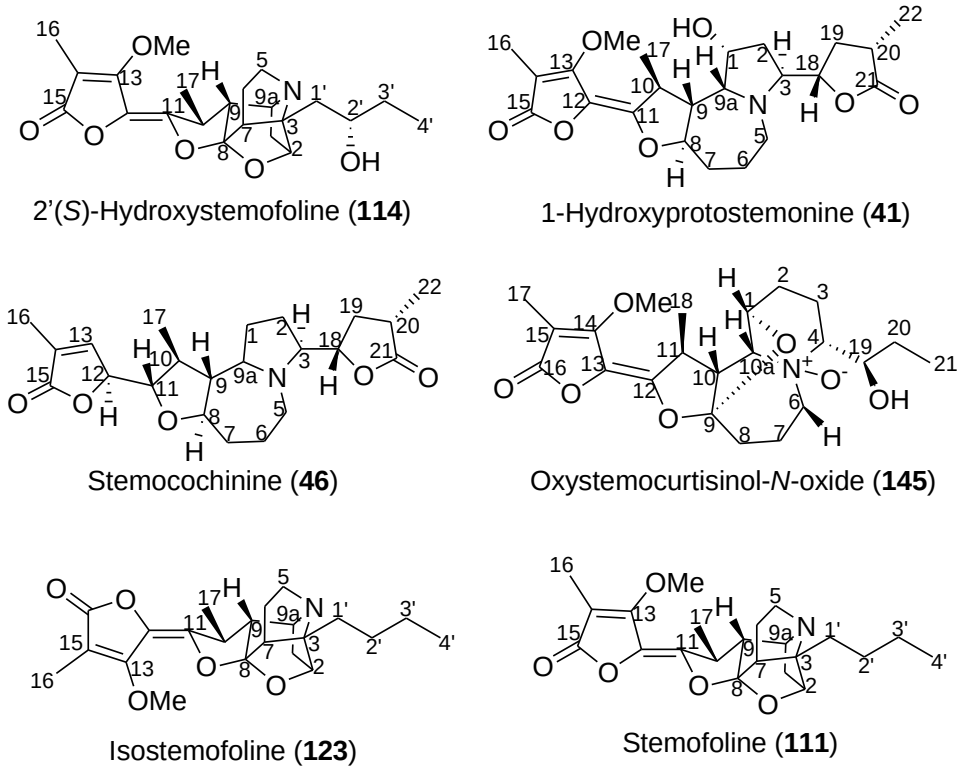

Figure 3.1 Isolated *Stemona* alkaloids from the roots of Malaysia *S. curtisii*.

3.3 Structure elucidation of isolated *Stemona* alkaloids from the roots of *S. curtisii*

3.3.1 1-Hydroxyprotostemonine (41)

1-Hydroxyprotostemonine (**41**) was isolated as a yellow gum; ESI-MS *m/z* 408 $[M+H]^+$, consistent with molecular $C_{22}H_{31}NO_7$ (MW 407) . The ^{1}H NMR spectrum of 1-hydroxyprotostemonine is shown in Figure 3.2. This compo98d was identified from a comparison of its NMR spectroscopic data with those in the literature.[39] The chemical shifts are in close agreement with those previously reported as summarized in Table 3.1.

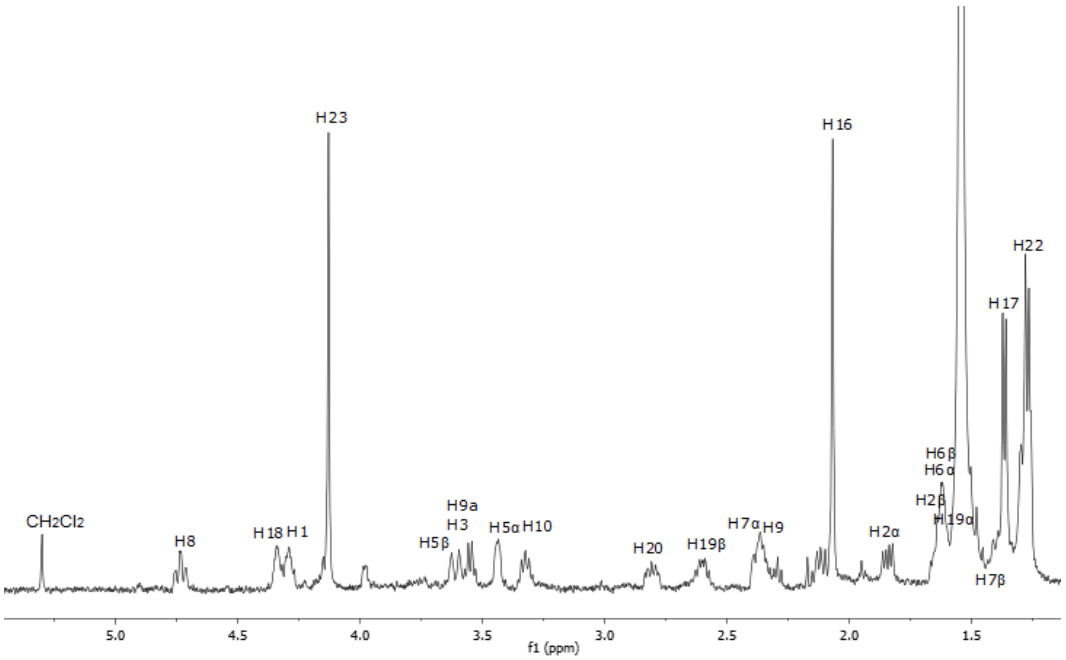

Figure 3.2 ^{1}H NMR spectrum (methanol-d_4, 500 MHz) of 1-hydroxyprotostemonine (**41**).

Table 3.1 ^{1}H NMR (500 MHz) spectroscopic data of 1-hydroxyprotostemonine (this work) and 1-hydroxyprotostemonine (**41**)[39] in methanol-d_4 solution (δ in ppm).

Data	**Experimental**	**Literature**[39]
Position	**δ_H (mult., *J* (Hz), assign.)**	**δ_H (mult., *J* (Hz), assign.)**
1	4.32-4.25 (overlap)	4.32 (t, *J* 3.9)
2α	1.84 (dd, *J* 13.5, 6.0)	1.85 (dd, *J* 13.0, 6.0)
β	1.70-1.65 (m)	1.71-1.67 (m)
3	3.58-3.61 (overlap)	3.55-3.60 (m)
5α	3.43 (dd, *J* 9.0, 6.5)	3.41 (dd, *J* 9.0, 6.5)
β	3.65-3.58 (m)	3.65-3.58 (m)
6α	1.63-1.58 (m)	1.63-1.58 (m)
β	1.63-1.58 (m)	1.63-1.58 (m)
7α	2.40-2.35 (m)	2.39-2.34 (m)
β	1.44-138 (m)	1.42 (m)
8	4.74 (dt, *J* 10.5, 3.8)	4.75 (dt, *J* 10.5, 3.8)
9	2.36-2.30 (m)	2.35-2.30 (m)
9a	3.60-3.54 (overlap)	3.61-3.56 (m)
10	3.31 (m)	3.30 (m)
16 (Me)	2.06 (s)	2.05 (s)
17 (Me)	1.36 (d, *J* 6.5)	1.35 (d, *J* 7.0)
18	4.34-4.32 (overlap)	4.33-4.30 (m)
19α	1.61-1.51 (m)	1.61-1.51 (m)
β	2.62-258 (m)	2.61 (m)
20	2.82-279 (m)	2.82 (m)
22 (Me)	1.27 (d, *J* 7.5)	1.27 (d, *J* 7.0)
OMe	4.12 (br s)	4.12 (br s)

3.3.2 (2′*S*)-Hydroxystemofoline (114)

(2′*S*)-Hydroxystemofoline (**114**) was isolated as a yellow gum; ESIMS *m/z* 404 $[M+H]^+$, consistent with molecular $C_{22}H_{29}NO_6$ (MW 403). The ^{1}H NMR spectrum of (2′*S*)-hydroxystemofoline is shown in Figure 3.3. This compound was identified by a comparison of its NMR spectroscopic data with those in the literature.[46] The ^{1}H NMR chemical shifts are in close agreement with those previously reported, as summarized in Table 3.2.

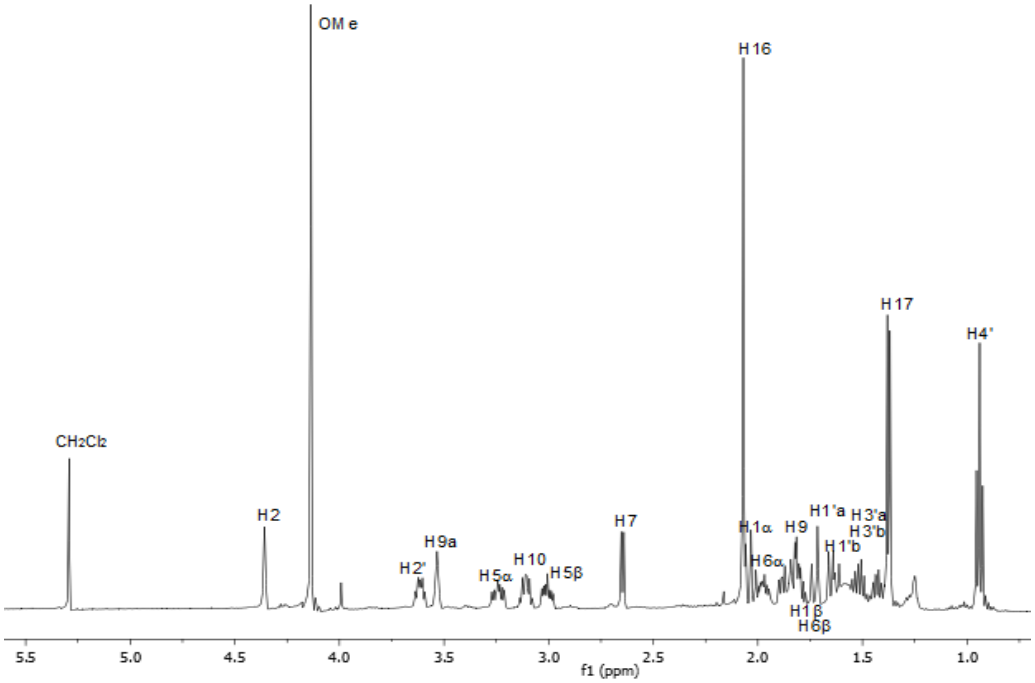

Figure 3.3 ^{1}H NMR spectrum ($CDCl_3$, 500 MHz) of (2′*S*)-hydroxystemofoline (**114**).

Table 3.2 ^{13}C (125 MHz) and ^{1}H (500 MHz) NMR spectroscopic data of (2′*S*)-hydroxystemofoline (this work) and (2′*S*)-hydroxystemofoline (**114**)[46] in $CDCl_3$ solution (δ in ppm).

Data	**Experimental**		**Literature**[46]	
Position	**δ_C**	**δ_H (mult., *J* (Hz), assign.)**	**δ_C**	**δ_H (mult., *J* (Hz), assign.)**
1α	33.7	2.06-2.03 (m)	33.7	2.06 (m)
β		1.91-1.88 (m)		1.89 (m)
2	78.7	4.37 (br s)	78.7	4.36 (br s)
3	82.7	-	82.9	-
5α	47.1	3.26-3.23 (m)	47.1	3.25 (m)
β		3.05-3.02 (m)		3.03 (m)
6α	26.6	2.06-2.03 (m)	26.6	2.04 (m)
β		1.90-1.87 (m)		1.88 (m)
7	52.7	2.65 (d, *J* 6.0)	51.7	2.65 (d, *J* 6)
8	112.0	-	112.0	-
9	47.6	1.84-1.81 (m)	47.6	1.82 (m)
9a	60.8	3.55 (br s)	60.8	3.55 (br s)
10	34.4	3.12 (dq, *J* 13.0, 6.5)	34.4	3.12 (dq, *J* 13.0, 6.5)
11	147.8	-	147.8	-
12	128.0	-	128.1	-
13	162.7	-	162.7	-
14	98.8	-	98.8	-
15	169.6	-	169.7	-
16 (Me)	9.2	2.08 (br s)	9.2	2.07 (br s)
17 (Me)	18.3	1.38 (d, *J* 6.5)	18.3	1.38 (d, *J* 6.5)
1′a	36.1	a: 1.82-1.79 (m)	36.2	1.81 (m)
b		b: 1.68-1.65 (m)		1.67 (m)
2′	71.2	3.62 (ddd, *J* 10.5, 5.5, 5.0)	71.2	3.62 (ddd, *J* 10.5, 5.5, 5.0)
3′a	30.6	a: 1.53-1.50 (m)	30.6	1.52 (m)
b		b: 1.46-1.43 (m)		1.44 (m)
4′ (Me)	9.7	0.95 (t, *J* 7.0)	9.8	0.94 (t, *J* 7.0)
OMe	58.8	4.15 (s)	58.9	4.14 (s)

3.3.3 Stemocochinine (46)

Stemocochinine (**46**) was isolated as a yellow gum; ESIMS *m/z* 390 $[M+H]^+$, consistent with molecular $C_{22}H_{31}NO_5$ (MW 389). The ^{1}H and ^{13}C NMR spectra of stemocochinine are shown in Figures 3.4 and 3.4, respectively. This compound was identified by a comparison of its NMR spectroscopic data with those in the literature.[10]

The chemical shifts are in close agreement with those previously reported, as summarized in Table 3.3.

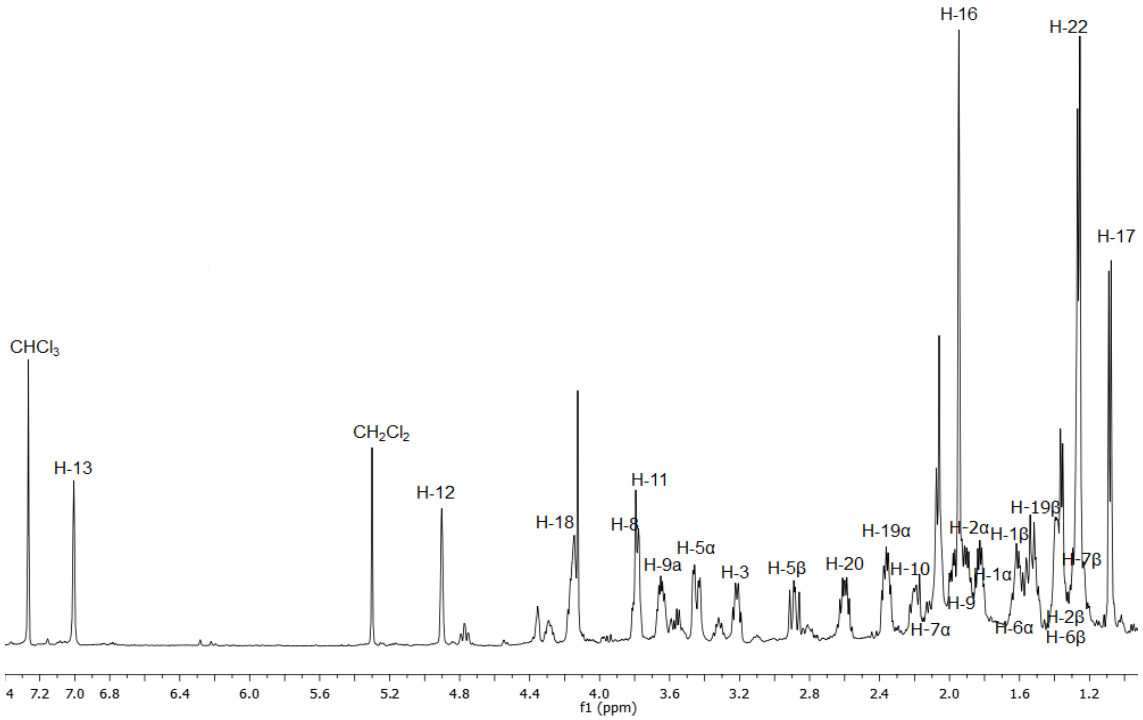

Figure 3.4 ^{1}H NMR spectrum ($CDCl_3$, 500 MHz) of stemocochinine (**46**).

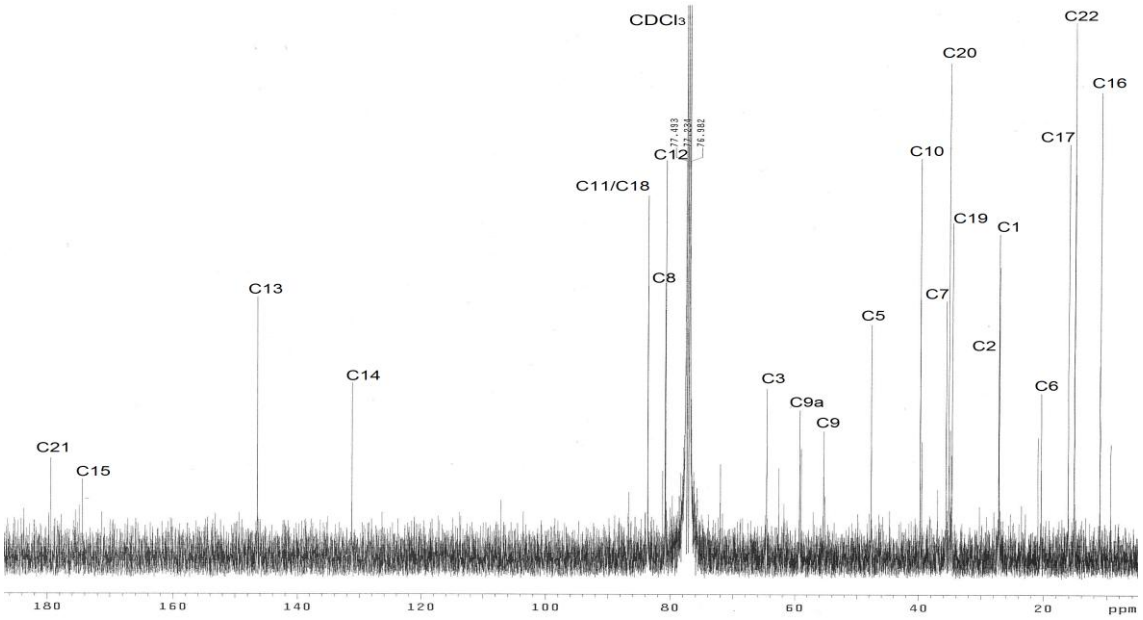

Figure 3.5 ^{13}C NMR spectrum ($CDCl_3$, 125 MHz) of stemocochinine (**46**).

Table 3.3 ^{13}C (125 MHz) and ^{1}H (500 MHz) NMR spectroscopic data of stemocochinine (this work) and stemocochinine (**46**)[10] in $CDCl_3$ solution (δ in ppm).

Data	**Experimental**		**Literature**[10]	
Position	δ_C	δ_H **(mult., *J* (Hz), assign.)**	δ_C	δ_H **(mult., *J* (Hz), assign.)**
1α	27.1	1.82-1.79 (m)	26.9	1.81 (m)
β	-	1.56-1.53 (m)		1.55 (m)
2α	27.2	1.92-189 (m)	27.0	1.91 (m)
β	-	1.38-1.35 (m)		1.37 (m)
3	64.7	3.23 (ddd, *J* 10.0, 7.5, 6.4)	64.3	3.21 (ddd, *J* 10.1, 7.7, 6.4)
5α	47.7	3.45 (ddd, *J* 15.5, 5.5, ~1)	47.4	3.44 (ddd, *J* 15.6, 5.3, ~1)
β	-	2.90 (ddd, *J* 15.5, 11.0, ~1)		2.88 (ddd, *J* 15.6, 11.1, ~1)
6α	20.3	1.61-1.57 (m)	20.2	1.54 (m)
β	-	1.41-1.38 (m)		1.37 (m)
7α	35.6	2.08-2.05 (m)	35.4	2.06 (m)
β	-	1.31-1.28 (m)		1.27 (m)
8	80.8	3.82-3.78 (m)	80.7	3.80 (m)
9	55.2	2.00-1.97 (m)	55.2	2.00 (m)
9a	59.0	3.65 (ddd, *J* 10.0, 5.0, 5.0)	59.0	3.64 (ddd, *J* 9.8, 4.9, 4.9)
10	39.8	2.22-2.19 (m)	39.6	2.20 (m)
11	83.6	3.79-3.76 (m)	83.4	3.77 (m)
12	80.7	4.90 (s)	80.5	4.90 (ddq, *J* 2.7, 2.7)
13	146.4	7.00 (s)	146.2	7.00 (dq, *J* 2.7, 2.7)
14	131.0	-	131.0	-
15	174.5	-	174.4	-
16 (Me)	11.1	1.95 (s)	10.9	1.95 (dd, *J* 2.7, 2.7)
17 (Me)	16.1	1.04 (d, *J* 7.0)	15.9	1.08 (d, *J* 6.6)
18	83.6	4.15 (ddd, *J* 11.0, 8.0, 5.5)	84.0	4.14 (ddd, *J* 11.2, 7.9, 5.3)
19α	34.7	2.37-2.34 (m)	34.4	2.36 (ddd, *J* 12.6, 8.4, 5.3)
β	-	1.53-1.50 (m)		1.52 (ddd, *J* 12.6, 11.5, 11.2)
20	35.0	2.61-2.58 (m)	35.0	2.60 (m)
21	179.6	-	179.6	-
22 (Me)	15.1	1.27 (d, *J* 7.0)	14.9	1.26 (d, *J* 7.1)

3.3.4 Oxystemocurtisine-*N*-oxide (145)

Oxystemocurtisine-*N*-oxide (**145**) was isolated as a yellow gum; ESIMS *m/z* 422 $[M+H]^+$, consistent with molecular $C_{21}H_{31}NO_7$ (MW 421). The ^{1}H NMR spectrum of oxystemocurtisine-*N*-oxide is shown in Figure 3.6. This compound was identified by a comparison of its NMR spectroscopic data with those in the literature.[10] The chemical shifts are in close agreement with those previously reported, as summarized in Table 3.4.

Table 3.4 ^{1}H NMR (500 MHz) spectroscopic data of oxystemocurtisin-*N*-oxide (this work) and oxystemocurtisin-*N*-oxide (**145**)[10] in methanol-d_4 solution (δ in ppm).

Data	**Experimental**	**Literature[10]**
Position	**δ_H (mult., *J* (Hz), assign.)**	**δ_H (mult., *J* (Hz), assign.)**
1	4.32 (br s)	4.38 (br s)
2α	1.99-2.03 (m)	2.02 (m)
β	2.10-2.07 (m)	2.11 (m)
3α	1.99-1.96 (m)	1.98 (m)
β	1.96-1.92 (m)	1.94 (m)
4	3.31 (overlap)	3.31 (ddd, *J* 11.5, 9.0, 2.5)
6α	4.03-4.00 (m)	4.04 (m)
β	3.50 (dd, *J* 12.0, 6.0)	3.55 (ddd, *J* 12.6, 6.5, <1)
7α	2.58-2.55 (m)	2.62 (m)
β	1.91-1.87 (m)	1.96 (m)
8α	2.16-2.12 (m)	2.20 (m)
β	2.07-2.03 (m)	2.10 (m)
9	-	-
10	3.33 (overlap)	3.38 (d, *J* 3.7)
10a	3.90 (br s)	3.93 (br s)
11	3.15 (dq, *J* 6.0, 4.5)	3.18 (dq, *J* 6.8, 4.8)
12	-	-
13	-	-
14	-	-
15	-	-
16	-	-
17 (Me)	2.06 (s)	2.10 (s)
18 (Me)	1.43 (d, *J* 7.0)	1.48 (d, *J* 6.8)
19	4.07-4.04 (m)	4.08 (m)
20a	1.66-1.63 (m)	1.69 (m)
b	1.44-1.40 (m)	1.47 (m)
21 (Me)	1.02 (t, *J* 7.5)	1.04 (t, *J* 7.4)
OMe	4.24 (s)	4.26 (s)

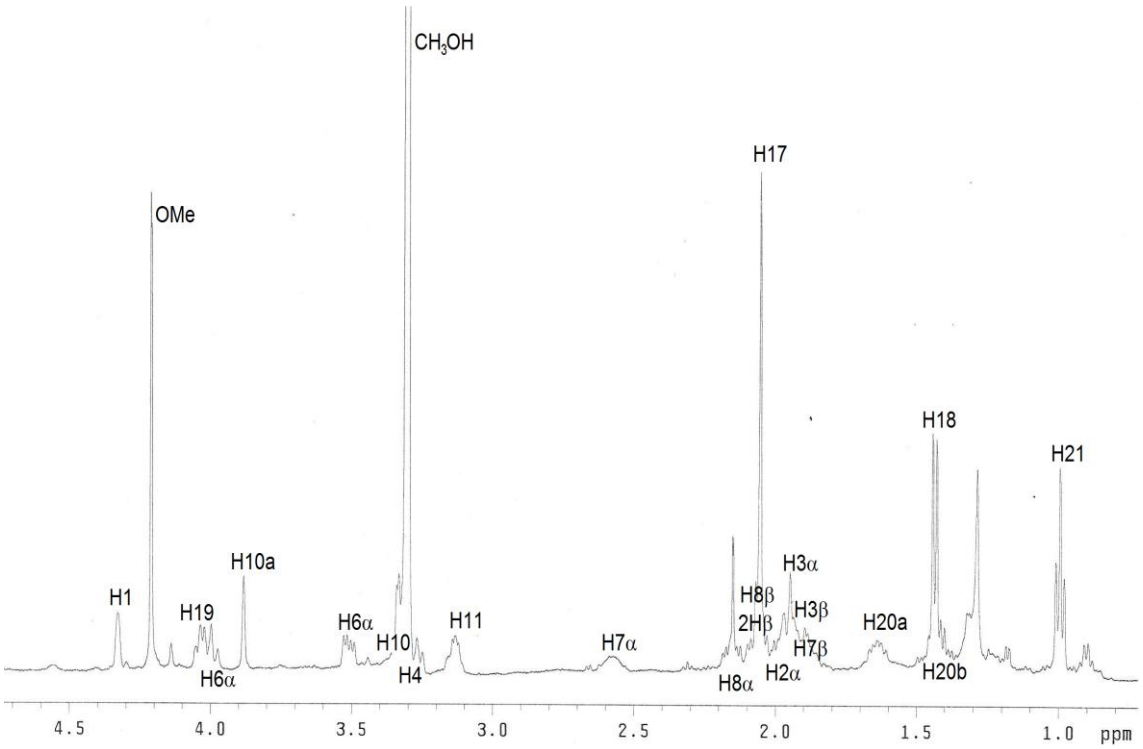

Figure 3.6 ^{1}H NMR spectrum (methanol-d_4, 500 MHz) of oxystemocurtisin-*N*-oxide (**145**).

3.3.5 Stemofoline (111)

Stemofoline (**111**) was isolated as a brown gum; ESIMS *m/z* 388 $[M+H]^+$, consistent with molecular $C_{22}H_{29}NO_5$ (MW 387). The ^{1}H NMR spectrum of stemofoline is shown in Figure 3.7. This compound was identified by a comparison of its NMR spectroscopic data with those in the literature.[15] The chemical shifts are in close agreement with those previously reported, as summarized in Table 3.5.

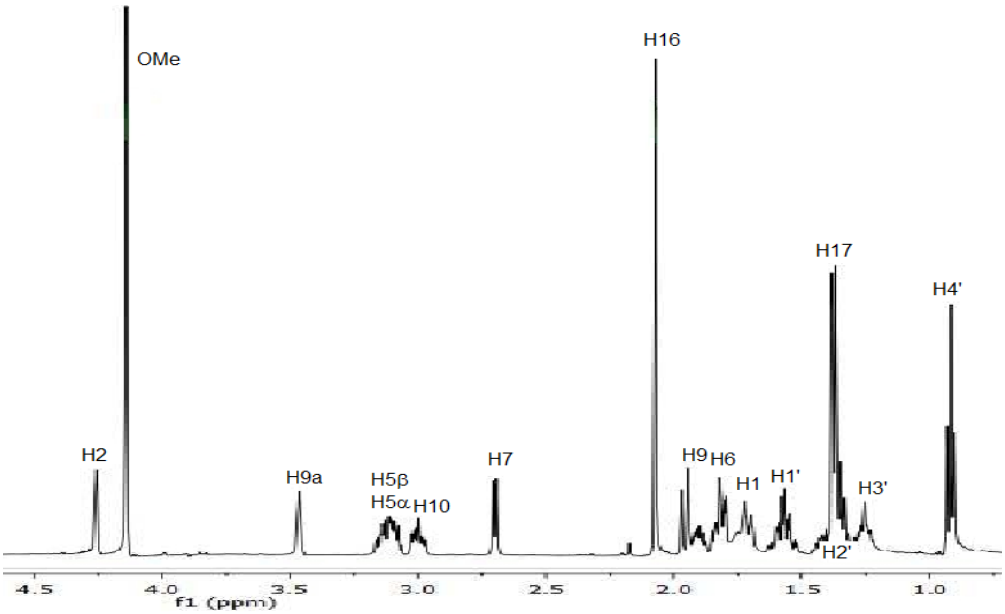

Figure 3.7 ^{1}H NMR spectrum ($CDCl_3$, 500 MHz) of stemofoline (**111**).

Table 3.5 ^{1}H NMR (500 MHz) spectroscopic data of stemofoline (this work) and stemofoline (**111**)[15] in $CDCl_3$ solution (δ in ppm).

Data	**Experimental**	**Literature**[15]
Position	**δ_H (mult., *J* (Hz), assign.)**	**δ_H (mult., *J* (Hz), assign.)**
1	1.85-1.90 (m, 2H)	1.7-2.00 (m)
2	4.26 (br s)	4.25 (br s)
5	3.11-3.08 (m, 2H)	3.20-3.10 (m, 2H)
6	1.92-2.00 (m, 2H)	1.70-2.0 (m, 2H)
7	2.75 (d, *J* 6.4)	2.70 (d, *J* 6.4)
9	1.75-1.80 (m)	1.70-2.00 (m)
9a	3.54 (br s)	3.50 (br s)
10	3.06-3.03 (m)	3.10 (m)
16 (Me)	2.09 (s)	2.07 (s)
17 (Me)	1.40 (d, *J* 6.4)	1.36 (d, *J* 6.4)
1'	1.60-1.65 (m, 2H)	1.50-1.60 (m)
2'	1.35-1.45 (m, 2H)	1.50-1.60 (m)
3'	1.25-1.35 (m, 2H)	1.50-1.60 (m)
4' (Me)	0.94 (t, *J* 7.0)	0.92 (t, *J* 6.8)
OMe	4.17 (s)	4.13 (s)

3.3.6 Isostemofoline (123)

Isotemofoline (**123**) was isolated as a brown gum; ESIMS *m/z* 388 $[M+H]^+$, consistent with molecular $C_{22}H_{29}NO_5$ (MW 387). The ^1H NMR spectrum of isotemofoline is shown in Figure 3.8. This compound was identified by a comparison of its NMR spectroscopic data with those in the literature.[71] The chemical shifts are in close agreement with those previously reported, as summarized in Table 3.6.

Table 3.6 ^1H NMR (500 MHz) spectroscopic data of isotemofoline (this work) and isotemofoline (**123**)[71] in $CDCl_3$ solution (δ in ppm).

Data	**Experimental**	**Literature[71]**
Position	**δ_H (mult., *J* (Hz), assign.)**	**δ_H (mult., *J* (Hz), assign.)**
1	1.90-1.98 (m, 2H)	2.00 (m)
2	4.27 (s)	4.29 (s)
5α	3.15-3.25 (m)	3.20 (m)
β	3.05-3.10 (m)	3.20 (m)
6	1.72 (dd, 2H, *J* 10.8, 3.6)	1.74 (dd, 2H, *J* 10.8, 3.6)
7	2.73 (d, *J* 6.0)	2.73 (d, *J* 5.2)
9	1.85-1.82 (m)	1.84 (m)
9a	3.49 (br s)	3.49 (m)
10	3.02-2.98 (m)	3.03 (m)
16 (Me)	2.04 (s)	2.02 (s)
17 (Me)	1.49 (d, *J* 6.5)	1.46 (d, *J* 6.4)
1'a	1.60-1.57 (m)	1.58 (m)
b	1.31-1.28 (m)	1.28 (m)
2'	1.45-1.49 (m, 2H)	1.58 (m)
3'	1.31-1.27 (m, 2H)	1.36 (q, *J* 6.8)
4' (Me)	0.95 (t, *J* 7.0)	0.92 (t, *J* 6.8)
OMe	4.14 (s)	4.12 (s)

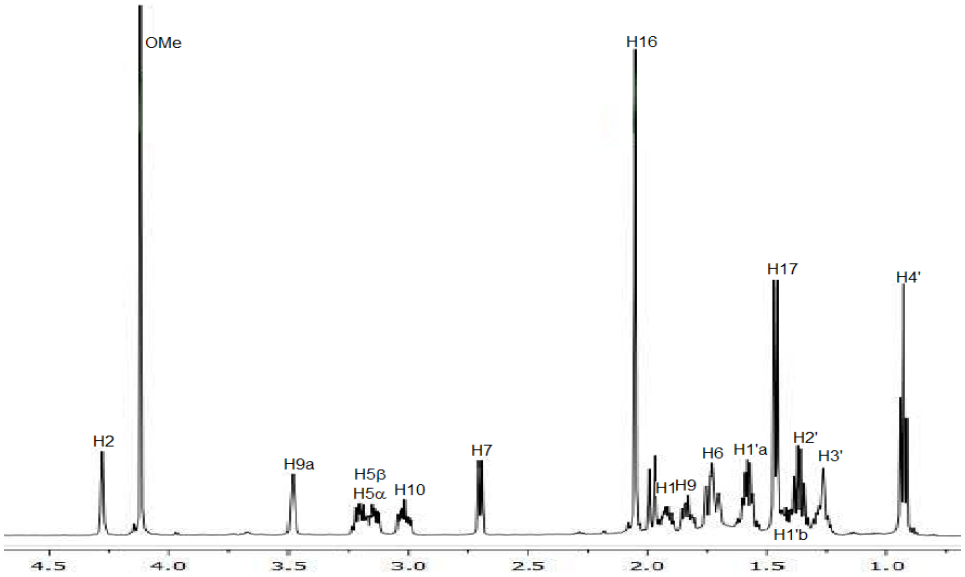

Figure 3.8 ^{1}H NMR spectrum ($CDCl_3$, 500 MHz) of isotemofoline (**123**).

3.4 Conclusions

In a previous study, eleven *Stemona* alkaloids were isolated from *S. curtisii* root extracts from Thailand.[10,11,39,44] Five of these alkaloids, **133**, **134**, **142**, **144**, **148** were pyrrolo[1,2-*a*]azepine alkaloids while compounds **41**, **42**, **43**, **46**, **111**, **114** were pyrido[1,2-*a*]azepine alkaloids. Stemofoline (**111**) was the major alkaloid. In contrast, in this study only one pyrido[1,2-*a*]azepine alkaloid, compound **145**, was isolated from *S. curtisii* growing in Peninsular Malaysia and (2'*S*)-hydroxystemofoline (**114**) was the major alkaloid in the roots from Malaysia. These differences may be due to their different geographical locations (different climates and neutrients), the age of the plants or the season in which the plants were harvested. Additionally, compounds **145** and **123** were never been reported from this species before.

CHAPTER 4

ALKALOIDS FROM ROOTS OF *Stemona javanica* (Kunth) Engl.

4.1 Introduction

In 2011, a phytochemical study on *S. javanica* by Hosoya and co-workers led to the isolation of two *Stemona* alkaloids, stemofoline (**111**) and protostemonine (**40**).[72] The plant material was collected from an undisclosed area in Indonesia. In this study, the roots of *S. javanica* were collected from Alas Purwo, East Java, Indonesia in June and December 2012. Successive purification of the crude MeOH extract (35.2 g) by column chromatography gave pure samples of 13-demethoxy-11(*S**),12(*R**)-dihydroprotostemonine **55** (12 mg), protostemonine **40** (151.3 mg), isoprotostemonine **45** (30 mg), isomaistemonine **95** (2.5 mg), and two new *Stemona* alkaloids, javastemonine A **186** (11.7 mg) and javastemonine B **187** (49.7 mg) (Figure 4.1).

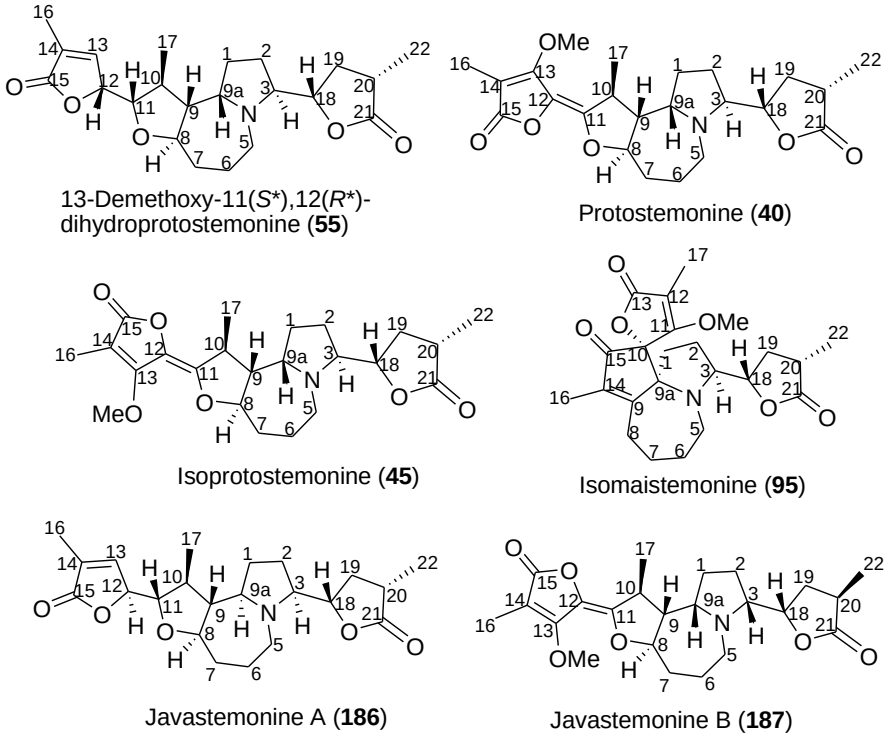

Figure 4.1 Structures of the isolated *Stemona* alkaloids from roots of *S. javanica*.

4.2 Structure elucidation of isolated *Stemona* alkaloids from the roots of *S. javanica*

4.2.1 Javastemonine A (186)

Compound **186** was obtained as a brown gum. Its molecular formula was determined as $C_{22}H_{32}NO_5$ from its HRESIMS (*m/z* 390.2280 $[M+H]^+$, calc. for 390.2291). The IR spectrum of **186** showed characteristic bands at 1771 cm^{-1} and at 1761 and 1657 cm^{-1} for a saturated and an unsaturated γ-lactone, respectively. The ^{13}C/DEPT NMR spectrum (Figure 4.5) displayed resonances for three methyl [δ 15.9 (C-17), 15.1 (C-22) and 11.0 (C-16)], six methylene [δ 48.0 (C-5), 35.3 (C-7), 34.9 (C-19), 26.9 (C-1), 26.8 (C-2), and 19.8 (C-6)], five methine [δ 65.1 (C-3), 59.7 (C-9a), 54.6 (C-9), 39.8 (C-10), and 35.1 (C-20)], four oxymethine [δ 83.5 (C-11), 82.6 (C-18), 80.7 (C-12), and 80.6 (C-8)], two olefinic [δ 146.4 (C-13) and 131.2 (C-14); q C and CH, respectively] and two downfield quaternary [δ 179.5 (C-21) and 174.5 (C-15)] carbons (Table 4.1). The H/H COSY correlations of **186** indicated the partial spin system H-1−H-2−H-3−H-18−H-19−H-20−H-22, typical of the pyrrolidine ring of the *Stemona* alkaloids, with a γ-lactone substituent at C-3 (Figure 4.3). Also observed were the COSY correlations between the vicinal pairs of contiguous protons along the C-5−C-13 and C-9−C-1 backbones and between H-10 and H-17 (Figure 4.3). The ^1H NMR spectrum (Figure 4.6) indicated resonances for two different methyl groups, which were attached to methine carbons, with ^1H NMR resonances at δ 1.26 (d, J = 7.0 Hz, 3H, H-22) and δ 1.10 (d, J = 6.5 Hz, 3H, H-17), and a singlet methyl resonance at δ 1.95 (s, 3H, H-16). Key HMBC correlations for **186** are shown in Figure 4.3, while full details are provided in Table 4.1. HSQC and HMBC experiments identified the protons and carbons (C-18−C-22) of the γ-butyrolactone moiety (Figure 4.3), which was clearly

attached to C-3 from the HMBC correlation between H-3 (δ 3.23, ddd, 6.6, 7.0, 10.0) and C-18 (δ 82.6). HSQC and HMBC experiments further helped to identified the protons and carbons (C-11−C16) associated with the α,β-unsaturated γ-lactone moiety of **186** (Figure 4.3). The ^{1}H NMR spectra of **55**, **186**, and the known alkaloid stemocochinine **46**[10,22] were nearly superimposable, except for small, but noticeable differences in the chemical shifts of some ^{1}H and ^{13}C NMR resonances (Table 4.2).

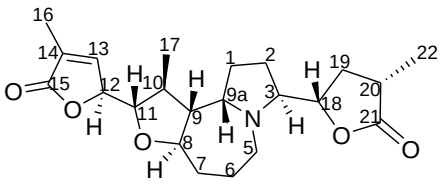

(**46**)

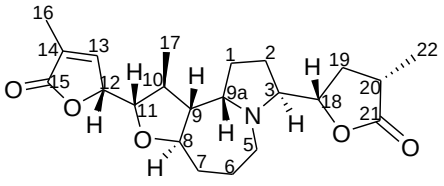

(**55**)

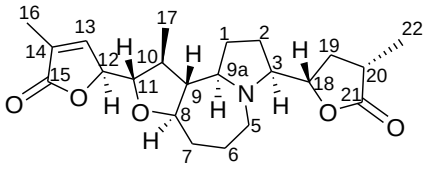

(**186**)

Notably, the ^{1}H NMR chemical shifts of H-9a and H-18 for these three compounds were significantly different [{**55**: H-9a (δ 3.63, ddd, J = 5.0, 5.6, 10.5) and H-18 (δ 4.14, ddd, J = 5.3, 7.5, 11.1)}; {**186**: H-9a (δ 3.77-3.75, overlap) and H-18 (δ 4.31, ddd, J = 5.5, 7.4, 12.8)}and {**46**: H-9a (δ 3.64, ddd, J = 9.8, 4.9, 4.9) and H-18 (δ 4.14, ddd, J = 11.2, 7.9, 5.3)}].[10,22] These differences suggested that **186** was a diastereomer of **55** and **46**. This assumption was also supported by their different chemical shifts for some ^{13}C NMR resonances [{**55**: C-11 (δ 85.0), C-12 (δ 83.1) and C-18 (δ 83.1)}; {**186**: C-11 (δ 83.5), C-12 (δ 80.7) and C-18 (δ 82.6)}and {**46**: C-11 (δ 83.4), C-12 (δ 80.5) and C-18 (δ 84.0)}].[10,22] The relative configuration of **186** was

established from analysis of the ROESY NMR correlations of **186** (Figure 4.7, Table 4.1) and was further supported by molecular modelling experiments [For details of how these molecular modeling studies were undertaken refer to the Experimental section (Chapter 9)]. Compound **186** showed ROESY correlations between H-9a and H-1α, H-2α, H-3 and H-10 (Figure 4.4 and Table 4.1), indicating the mutal *syn*-stereochemical relationships between these five hydrogens. However, no ROESY correlations were observed between H-9a and H-9, or H-9a and H-17. These data suggested the α-configuration of the proton at C-9a, which is opposite to that found in compounds **55** and **46**.

ROESY correlations were also observed between H-1α and H-2α, H-3, H-5α, H-8, and H-10; and H-2α and H-3. These observations indicated the α-configuration of these protons. The ROESY correlations between H-18 and H-19β and H–20; H-19β and H-20; and H-19α and H-22 indicated the relative *syn*-configuration between H-18 and H-20 of the γ-lactone moiety (Figure 4.4). Because of the relatively free rotation around the C-3−C-18 bond in both possible diastereomeric structures for **186** ((3*S*, 18*S*, 20*S*)-**186** or (3*S*, 18*R*, 20*R*)-**186**), it was not possible to confidently assigned the relative configurations of these two vicinal (C-3 and C-18) stereocentres from molecular modelling and ROESY NMR studies. However, we have tentatively assign the 3*S*, 18*S*, 20*S* configuration to **186** since this is the most commonly found absolute configuration of the *Stemona* alkaloids.[12,74] The configurations assigned to C-11 and C-12 in **186** were based on ROESY correlations and the magnitude of $J_{11,12}$ when compared to the known *Stemona* alkaloids 11*S*,12*S*-saxorumamide (**51**) (ROESY correlation between H-12 and H-17, and $J_{11,12}$ = 2.0 Hz) and 11*S*,12*R*-isosaxorumamide (**52**) (ROESY correlation between H-10 and H-13, and $J_{11,12}$ = 6.9 Hz)[25] and related dihydrostemofoline alkaloids

(Figure 4.2).[11] The relative small $J_{11,12}$ value for **186** (1.3 Hz) and the ROESY correlations between H-12 and H-17, as well as the correlation between H-11 and H-17, are consistent with the relative 11*S*,12*S* configuration assigned to compound **186**. Detailed analysis of the ^{1}H and ^{13}C-NMR spectra of **186**, as well as 2D-NMR analyses (COSY, HMBC and ROESY, Table 4.1) established the complete structure and relative configuration of **186**.

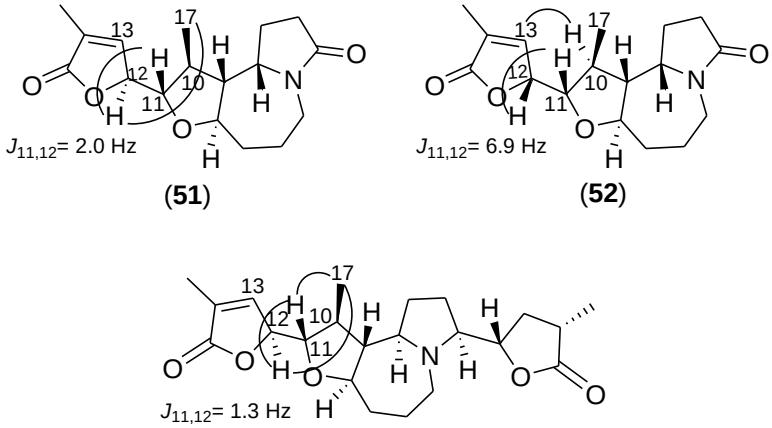

Figure 4.2 The coupling constants (*J*) of H-11 and H-12 in **51**, **52** and **186** together with their ROESY correlations.[11]

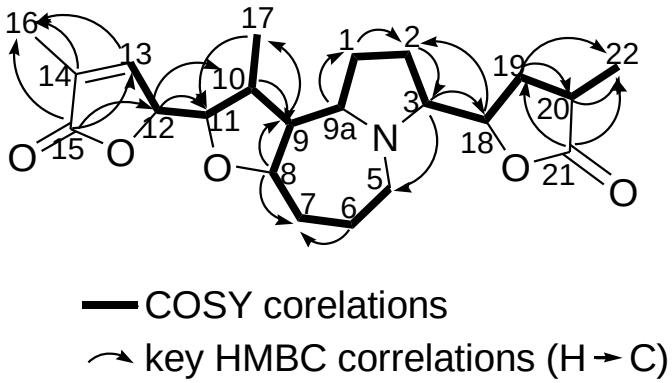

Figure 4.3 Key COSY and HMBC correlations for compound **186**.

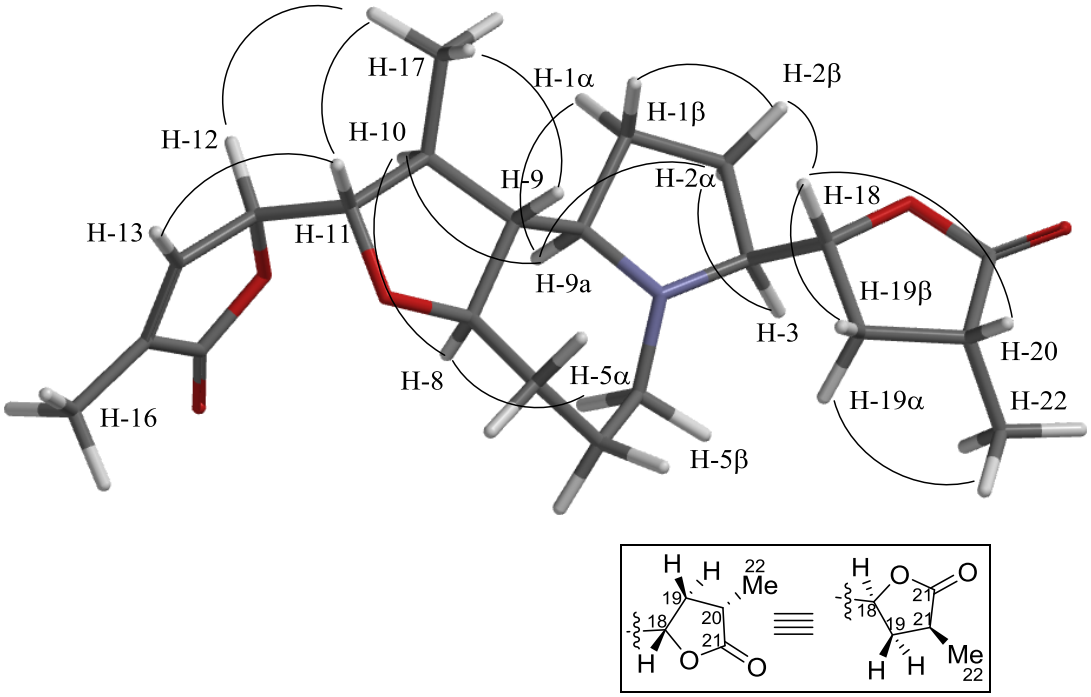

Figure 4.4 Spartan '10 generated lowest energy conformation of **186** showing key ROESY cross-peaks. The details on how this structure was generated are included in the Experimental section (Chapter 9).

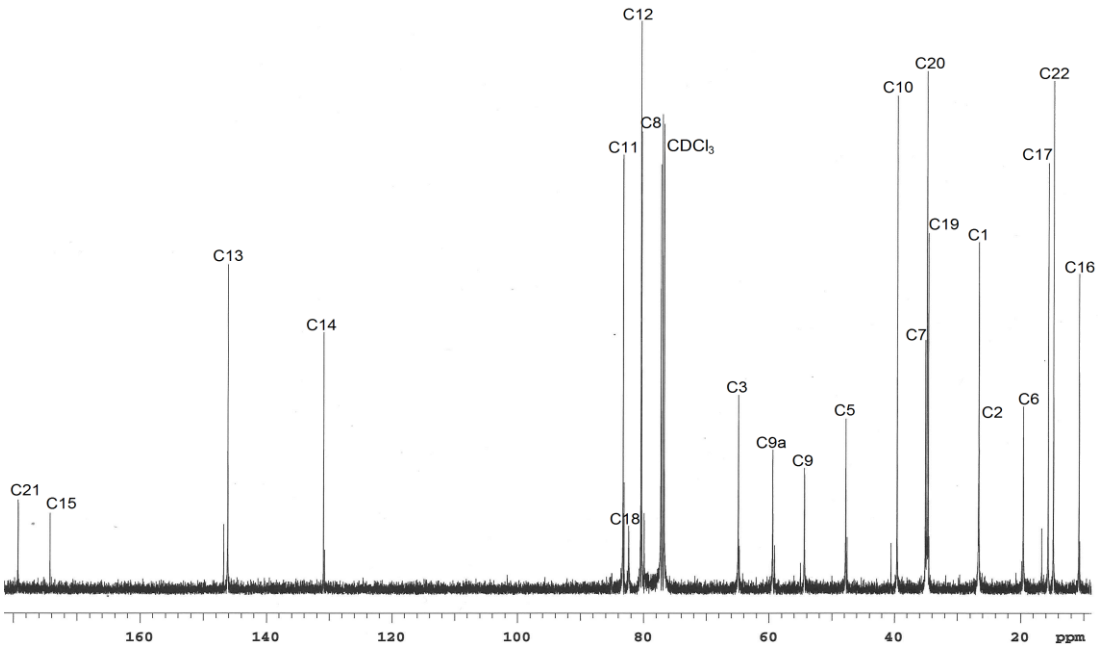

Figure 4.5 ^{13}C NMR spectrum ($CDCl_3$, 500 MHz) of javastemonine A (**186**).

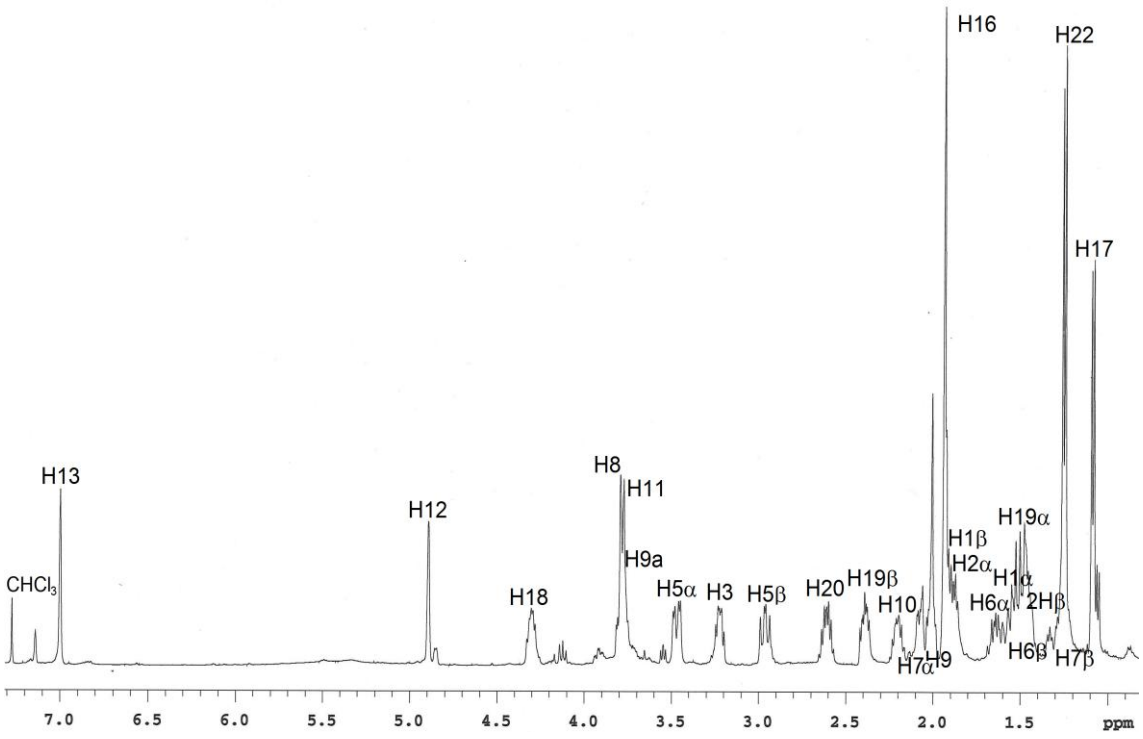

Figure 4.6 ^{1}H NMR spectrum ($CDCl_3$, 500 MHz) of javastemonine A (**186**).

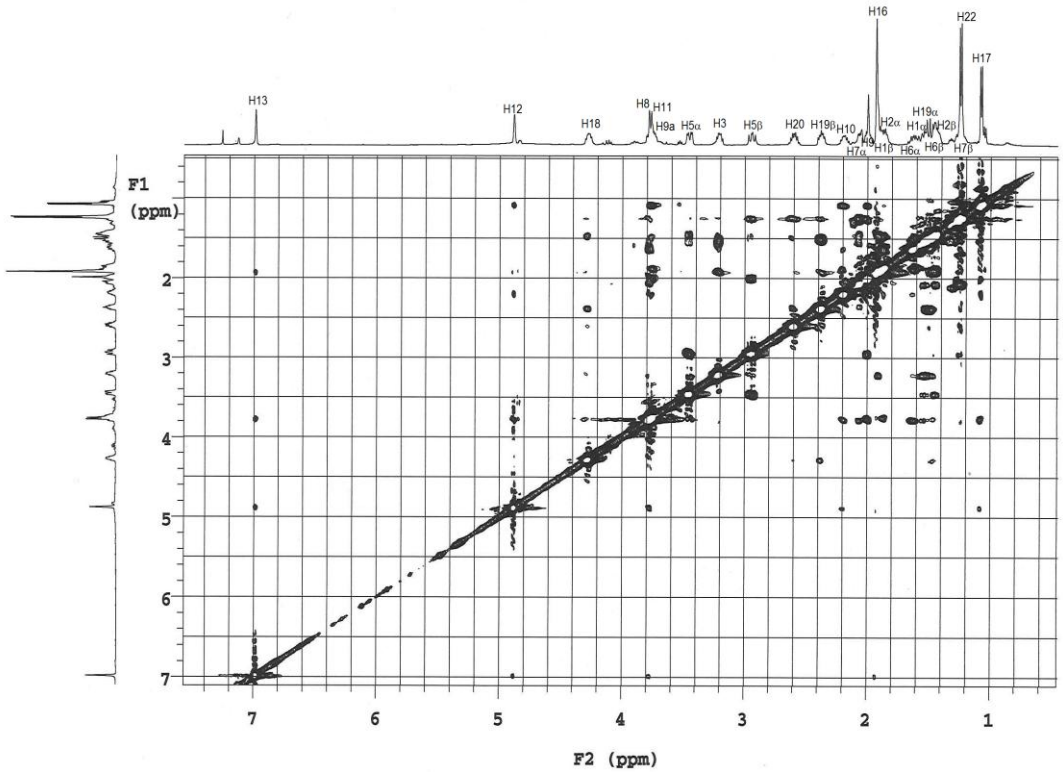

Figure 4.7 ROESY spectrum ($CDCl_3$, 500 MHz) of javastemonine A (**186**).

Table 4.1 ^{13}C NMR (125 Hz), ^{1}H NMR (500 MHz) and 2D spectroscopic data for javastemonine A (**186**) in $CDCl_3$ solution (δ in ppm).

Position	δ_C	δ_H **(mult., J (Hz)**	**HMBC**	**ROESY**	**COSY**
1α	26.9	1.69-1.61 (overlap)	2, 3	2α, 3, 5α, 8, 9a, 10	2, 9a
β		1.94-1.90 (overlap)		2β	
2α	26.8	1.91-185 (overlap)	1, 3	1α, 3, 9a, 10	1, 3
β		1.50-1.42 (overlap)		1β, 18	
3	65.1	3.23 (ddd, *J* 10.0, 7.0, 6.6)	1, 2, 5, 18	1α, 2α, 5β, 9a, 18, 19α	2, 18
5α	48.0	3.47 (dd, *J* 15.3, 5.0)	3	1α, 5β, 8	6
β		2.96 (dd, *J* 15.3, 11.5)		3, 5α, 9	
6α	19.8	1.56-1.51 (overlap)	7	-	5, 7
β		1.50-1.42 (overlap)		-	
7α	35.3	2.08 (dd, *J* 8.7, 3.0)	5, 9	8	6, 8
β		1.38-1.29 (m)		-	
8	80.6	3.83-3.79 (m, overlap)	7, 9a	1α, 5α ,7α, 10	7, 9
9	54.6	2.04-1.99 (m)	1, 17	5β, 11, 17	8, 9a, 10
9a	59.7	3.77-3.75 (overlap)	1, 2, 5	1α, 2α, 3, 10	1, 9
10	39.8	2.25-2.17 (m)	9, 17	1α, 2α, 8, 9a, 12, 17	9, 11, 17
11	83.5	3.82-3.78 (overlap)	7	9, 12, 13, 17	10, 12
12	80.7	4.90 (d, *J* 1.3)	10, 11, 13	10, 11, 13, 17	11, 13
13	146.4	7.00 (br s)	16	11, 12, 16	12
14	131.2	-	16	-	-
15	174.5	-	13, 16	-	-
16 (Me)	11.0	1.95 (s)		13	-
17 (Me)	15.9	1.10 (d, *J* 6.5)	11	9, 10, 11, 12	10
18	82.6	4.31 (ddd, *J* 12.8, 7.4, 5.5)	2, 3, 19	3, 2β, 19β, 20	3, 19
19α	34.9	1.55-1.49 (m)	20, 22	3, 22	18, 20
β		2.40 (ddd, *J* 12.0, 8.3, 5.4)		18, 20	
20	35.1	2.66-2.58 (m)	19, 22	18, 19β, 22	19, 22
21	179.5	-	19, 22	-	-
22 (Me)	15.1	1.26 (d, *J* 7.0)	19, 20	19α, 20	20

Table 4.2 ^{1}H (500 MHz) and ^{13}C NMR (125 MHz) spectroscopic data of 13-demethoxy-(11*S**,12*R**)-dihydroprotostemonine (**55**),[22] javastemonine A (**186**) and stemocochinine (**46**)[10] in $CDCl_3$ solution (δ in ppm).

Position	**δ_C**			**δ_H (mult., *J* (Hz)**		
	55[22]	**186**	**46**[10]	**55**[22]	**186**	**46**[10]
1α	26.8	26.9	26.9	1.81 (m)	1.69-1.61 (overlap)	1.81 (m)
β				1.58 (m)	1.94-1.90 (overlap)	1.55 (m)
2α	26.7	26.8	27.0	1.92 (m)	1.91-185 (overlap)	1.91 (m)
β				1.39 (m)	1.50-1.42 (overlap)	1.37 (m)
3	64.5	65.1	64.3	3.24 (ddd, *J* 9.6, 7.4, 5.6)	3.23 (ddd, *J* 10.0, 7.0, 6.6)	3.21 (ddd, *J* 10.1, 7.7, 6.4)
5α	47.4	48.0	47.4	2.89 (dd, *J* 16.2, 15.6)	3.47 (dd, *J* 15.3, 5.0)	3.44 (ddd, *J* 15.6, 5.3, ~1)
β				3.45 (dd, *J* 16.2, 5.2)	2.96 (dd, *J* 15.3, 11.5)	2.88 (ddd, *J* 15.6, 11.1, ~1)
6α	19.9	19.8	20.2	1.39 (m)	1.56-1.51 (overlap)	1.54 (m)
β				1.39 (m)	1.50-1.42 (overlap)	1.37 (m)
7α	35.1	35.3	35.4	1.28 (m)	2.08 (dd, *J* 8.7, 3.0)	2.06 (m)
β				2.11 (m)	1.38-1.29 (m)	1.27 (m)
8	79.9	80.6	80.7	3.91 (ddd, *J* 10.2, 10.2, 4.0)	3.83-3.79 (m, overlap)	3.80 (m)
9	55.1	54.6	55.2	1.99 (m)	2.04-1.99 (m)	2.00 (m)
9a	59.0	59.7	59.0	3.63 (ddd, *J* 10.5, 5.6, 5.0)	3.77-3.75 (overlap)	3.64 (ddd, *J* 9.8, 4.9, 4.9)
10	40.6	39.8	39.6	1.90 (m)	2.25-2.17 (m)	2.20 (m)
11	85.0	83.5	83.4	3.52 (dd, *J* 7.6, 6.4,)	3.82-3.78 (overlap)	3.77 (m)
12	83.1	80.7	80.5	4.84 (m)	4.90 (d, *J* 1.3)	4.90 (ddq, *J* 2.7, 2.7)
13	146.9	146.4	146.2	7.16 (m)	7.00 (br s)	7.00 (dq, *J* 2.7, 2.7)
14	130.6	131.2	131.0	-	-	-
15	174.1	174.5	174.4	-	-	-
16 (Me)	10.7	11.0	10.9	1.93 (s)	1.95 (s)	1.95 (dd, *J* 2.7, 2.7)
17 (Me)	16.7	15.9	15.9	1.06 (d, *J* 6.2)	1.10 (d, *J* 6.5)	1.08 (d, 6.6)
18	83.1	82.6	84.0	4.14 (ddd, *J* 11.1, 7.5, 5.3)	4.31 (ddd, *J* 12.8, 7.4, 5.5)	4.14 (ddd, *J* 11.2, 7.9, 5.3)
19α	34.4	34.9	34.4	1.53 (m)	1.55-1.49 (m)	2.36 (ddd, *J* 12.6, 8.4, 5.3)
β				2.36 (m)	2.40 (ddd, *J* 12.0, 8.3, 5.4)	1.52 (ddd, *J* 12.6, 11.5, 11.2)
20	34.9	35.1	35.0	2.60 (m)	2.66-2.58 (m)	2.60 (m)
21	179.5	179.5	179.6	-	-	-
22 (Me)	14.8	15.1	14.9	1.26 (m)	1.26 (d, *J* 7.0)	1.26 (d, *J* 7.1)

4.2.2 Javastemonine B (187)

Compound **187** was obtained as a pale yellow gum. The molecular formula of **187** as $C_{23}H_{31}NO_6$ was determined from its HRESIMS (*m/z* 418.2230 $[M+H]^+$, calcd for $C_{23}H_{32}NO_6$ 418.2226). The IR spectrum of **187** showed characteristic bands at 1780 cm^{-1} and at 1745 and 1670 cm^{-1} for a saturated and an unsaturated γ-lactone ring, respectively. The ^{13}C/DEPT NMR spectra of **187** (Figure 4.10) displayed resonances for three methyl [δ 8.7 (C-17), 14.6 (C-22), and 16.6 (C-16)], six methylene [δ 49.5 (C-5), 33.1 (C-7), 35.0 (C-19), 25.9 (C-2), 25.9 (C-1), and 17.8 (C-6)], five methine [δ 67.5 (C-3), 61.8 (C-9a), 50.9 (C-9), 41.7 (C-10), and 34.6 (C-20)], two oxymethine [δ 77.2 (C-18) and 82.7 (C-8)], four olefinic [δ 163.6 (C-13), 98.1 (C-14), 126.1 (C-12), and 149.2 (C-11)] and two quaternary [δ 178.3 (C-21) and 170.6 (C-15) carbons and a methoxy group [δ 59.5 (C-23)] (Table 4.1). The chemical shifts of these ^{13}C NMR signals were similar to these of the known *Stemona* alkaloids, protostemonine (**40**, the 11(*Z*) isomer of **45**) and isoprotostemonine (**45**) (Figure 4.1) which were isolated here and previously from *S. japonica*.[7] The COSY and HMBC spectroscopic analysis of **187** showed analogous correlations to those observed for **186**. The correlations in the COSY spectrum of **187** indicated the spin system H-1−H-2−H-3−H-18−H-19−H-20−H-22, typical of the pyrrolidine ring of the *Stemona* alkaloids with a γ-lactone substituent at C-3 (Figure 4.8). COSY correlations were also observed between the vicinal pairs of contiguous protons along the C-5−C-6−C-7−C-8−C-9−C-9a−C-1 backbone and between H-10 and H-17 (Figure 4.8). The ^1H NMR/COSY spectra indicated resonances for the presence of two methyl groups (δ 1.27 (d, *J* = 7.0 Hz, 3H, H-22), and 1.48 (d, *J* = 7.0 Hz, 3H, H-17), which were attached to methine groups with ^1H NMR resonances at δ 2.70 (ddq, *J* = 11.5, 7.5, 7.0 Hz, 1H, H-20), and δ 3.04 (ddd, *J* = 13.4, 7.1, 7.1, 1H, H-

10), respectively. The HMBC experiment identified another methyl group at δ 2.02 (s, 3H) which was clearly attached to C-14 from the correlation between Me-16 and C-15. Key HMBC correlations are indicated in Figure 4.8, while full details are provided in Table 4.3. While compound **187** had the same molecular formula, and related structure features, to isoprotostemonine **45** and protostemonine (**40**) there were notable differences in their NMR spectroscopic data (Table 4.4).[25] The aforementioned two known alkaloids had very similar ^{13}C NMR chemical shifts, while those of **187** were significantly different, especially those for C-3 (δ 64.4/64.3 vs δ 67.5 for **187**), C-5 (δ 46.6/46.5 vs δ 49.5 for **187**), C-9a (δ 58.4/58.8 vs δ 61.8 for **187**) and C-18 (δ 83.3/83.9 vs δ 77.2 for **187**) (Table 4.4). These chemical shift differences indicated that **187** was diastereomer of these known alkaloids. Compound **187** showed NOESY correlation between H-18 and H-19β; and H-19β and Me-22 (Figure 4.9, Figure 4.12 and Table 4.3), indicating the *syn*-relationship between H-18, H-19β and Me-22. NOESY correlations were also observed between H-9a and H-1β and H-9; H-1β and H-2β; H-2β and H-3; and H-9 and H-17, indicating the *syn*-relationship between these pairs of protons and the relative β-configuration of H-3. Because of the relatively free rotation around the C-3−C-18 bond in both possible diastereomeric structures for **187** [(3*R*, 18*S*, 20*R*)-**187** or (3*R*, 18*R*, 20*S*)-**187**], it was not possible to confidently assign the relative configurations of these two vicinal (C-3 and C-18) stereocentres from molecular modelling and NOESY NMR studies. However, we have tentatively assign the 3*R*, 18*S*, 20*R* configuration to **187** since the 18*S* configuration is the most commonly found absolute configuration of the *Stemona* alkaloids.[2,12,74,75] The lack of a NOESY correlations between the OMe group and the protons on the C-ring was consistent the *E*-configuration of the C-11−C-12 alkene. These NOESY studies indicated that compound

187 was an epimer of **45** at C-3 and C-20 (see Table 4.3). Detailed analysis of the ^{1}H and ^{13}C-NMR spectra of **187**, as well as 2D-NMR analyses (COSY, HMBC and NOESY, Table 4.3) established the complete structure and relative configuration of **187**.

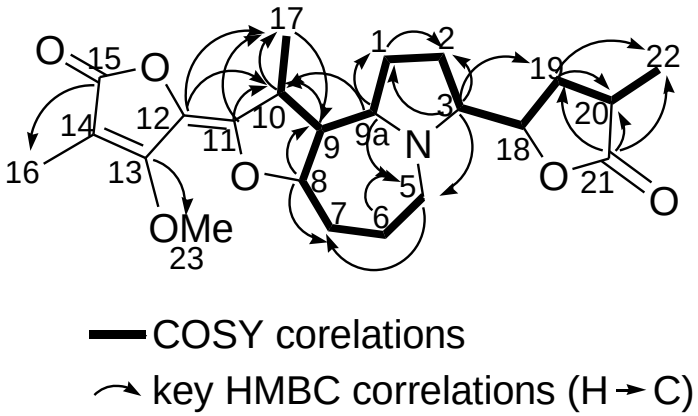

Figure 4.8 Key COSY and HMBC correlations for compound **187**.

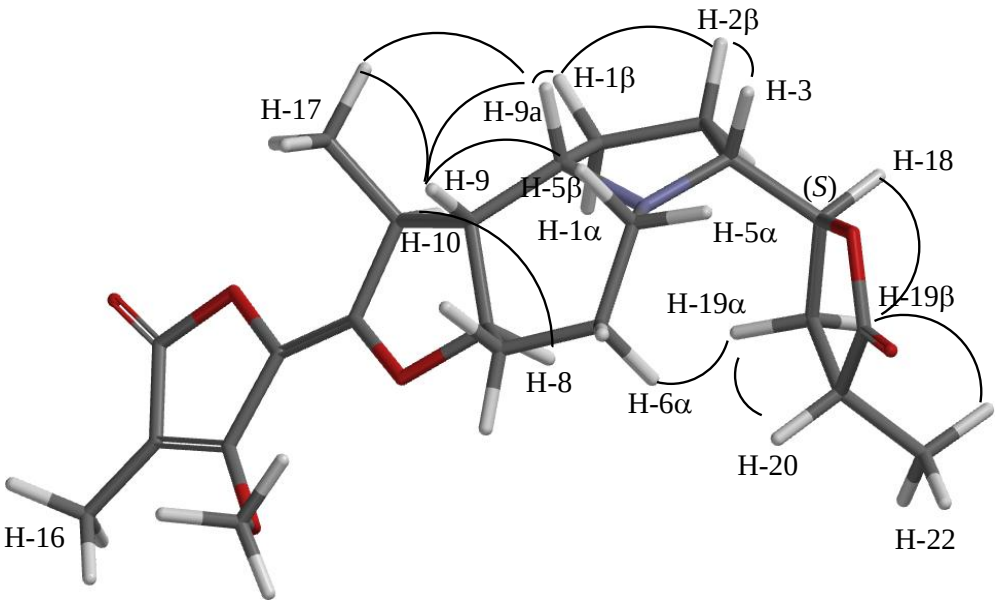

Figure 4.9 Spartan '10 generated lowest energy conformation of **187** showing key NOESY cross-peaks.

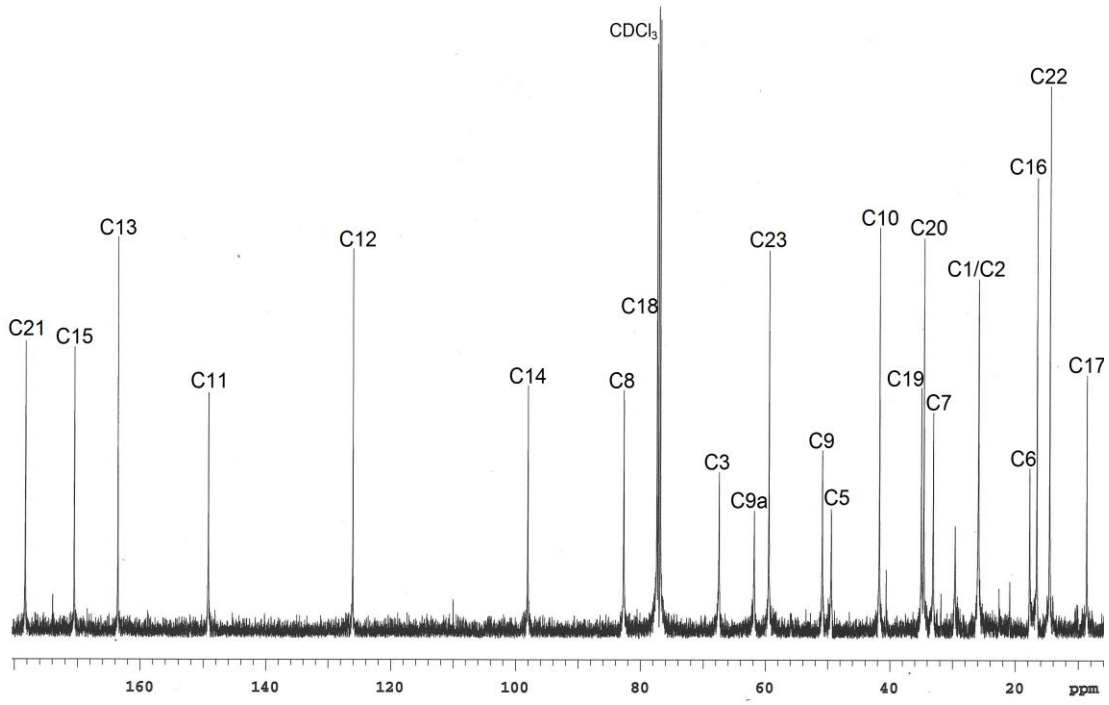

Figure 4.10 ^{13}C NMR spectrum ($CDCl_3$, 500 MHz) of javastemonine B (**187**).

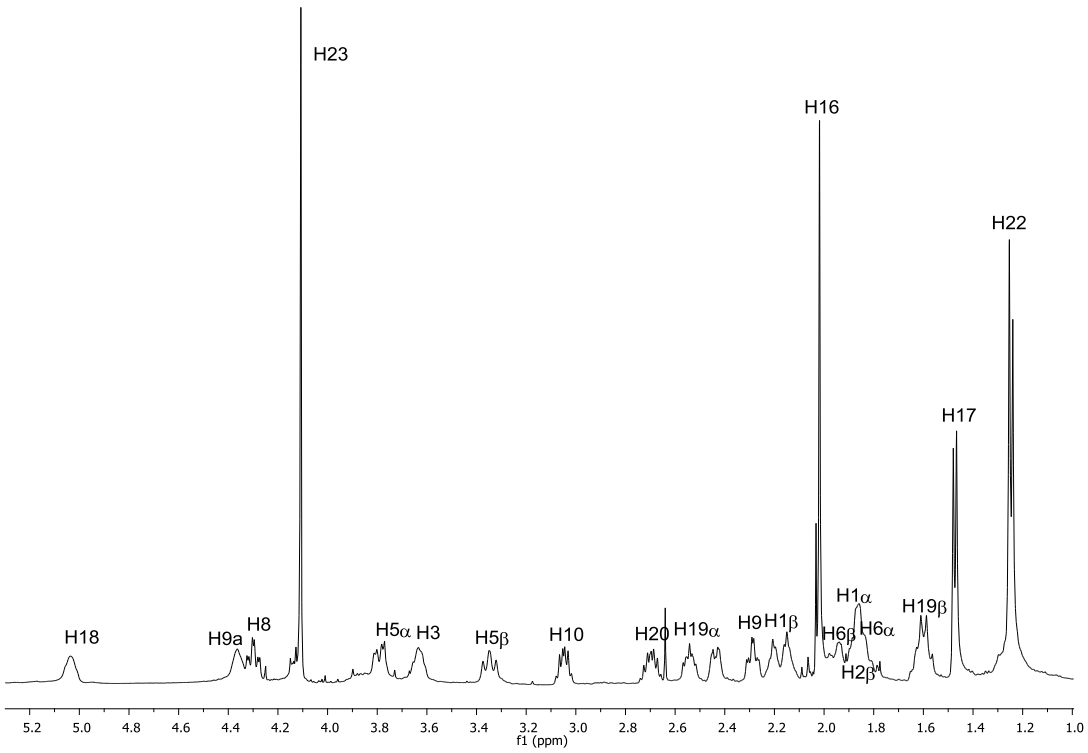

Figure 4.11 ^{1}H NMR spectrum ($CDCl_3$, 500 MHz) of javastemonine B (**187**).

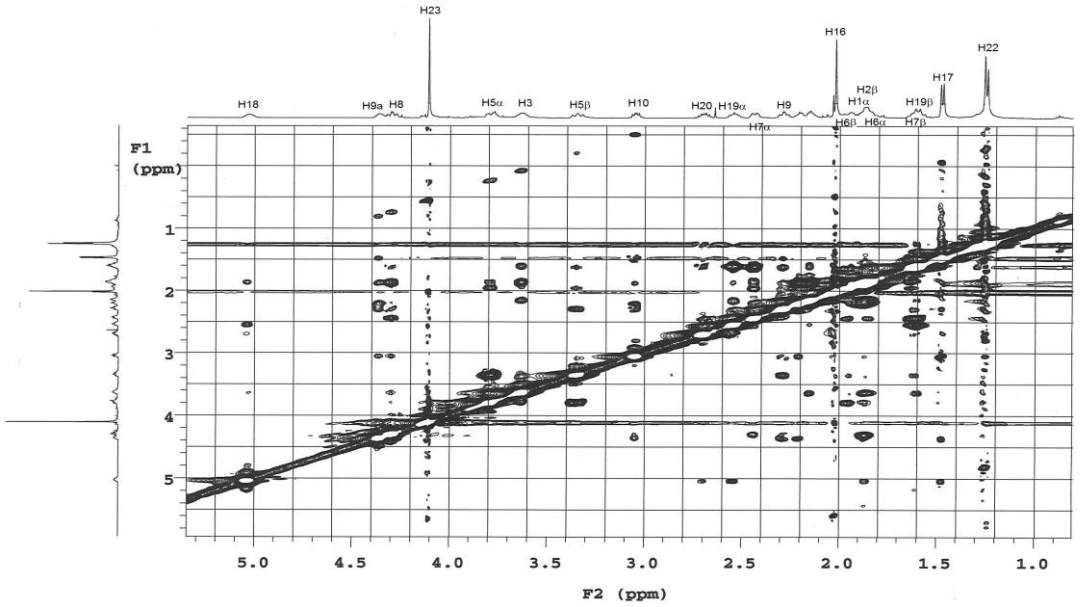

Figure 4.12 NOESY spectrum ($CDCl_3$, 500 MHz) of javastemonine B (**187**).

Table 4.3 ^{13}C NMR (125 Hz), ^{1}H NMR (500 MHz) and 2D spectroscopic data for compound **187** in $CDCl_3$ solution (δ in ppm).

Position	δ_C	δ_H (mult., J (Hz)	HMBC	NOESY	COSY
1α	25.9	1.92-1.86 (overlap)	2	1β, 2α, 8, 19α	2, 9a
β		2.24-2.16 (overlap)		1α, 2β, 9a, 10	
2α	25.9	2.18-2.10 (overlap)	1	1α, 2β, 19α,10	1, 3
β		1.86-1.80 (overlap)		1β, 2α, 3, 9a, 18,	
3	67.5	3.64-3.60 (m)	1, 2, 5, 19	2β, 19β	2, 18
5α	49.5	3.79 (dd, *J* 14.7, 6.0)	7	5β, 6α, 18, 19β	6
β		3.35 (dd, *J* 14.7, 12.5)		5α, 5β, 6α, 6β, 9	
6α	17.8	1.86-1.82 (m)	5	5α, 6β, 7α, 8, 19α	5, 7
β		1.98-1.92 (m)		5β, 6α, 7β	
7α	33.1	2.44 (dd, *J* 12.6, 3.7)	5	6α, 7β, 8	6, 8
β		1.66-1.58 (overlap)		6β, 7α, 9	
8	82.7	4.30 (ddd, *J* 15.0, 11.0, 3.9)	7, 9	1α, 6α, 7α, 10	7, 9
9	50.9	2.29 (ddd, *J* 14.6, 10.7, 4.0)	10	5β, 7β, 9a, 17	8, 9a
9a	61.8	4.36 (ddd, *J* 11.1, 10.9, 6.2)	1, 2, 5, 9, 10	1β, 2β, 9, 17	1, 9
10	41.7	3.04 (ddd, *J* 13.4, 7.1, 7.1)	9, 17	1β, 2α, 8, 17	9, 17
11	149.2	-	10, 17	-	-
12	126.1	-	10, 17	-	-
13	163.6	-	23	-	-
14	98.1	-	16	-	-
15	170.6	-	16	-	-
16 (Me)	16.6	2.02 (s)	-	23	-
17 (Me)	8.7	1.48 (d, *J* 7.0)	9, 10	9, 9a, 10	10
18	77.2	5.03 (ddd, *J* 9.7, 6.4, 6.4)	19	2β, 5α, 19β	3, 19
19α	35.0	2.54 (ddd, *J* 12.6, 8.3, 5.6)	20, 22	1α, 2α, 6α, 19β, 20	18, 20
β		1.64-1.54 (overlap)		3, 5α, 18, 19α, 22	
20	34.6	2.70 (ddq, *J* 11.5, 7.5, 7.0)	19, 22	19α, 22	19, 22
21	178.3	-	19, 20, 22	-	-
22 (Me)	14.6	1.27 (d, *J* 7.0)	19, 20	19β, 20	20
23 (OMe)	59.5	4.11 (s)	-	16	-

Table 4.4 ^{13}C NMR (125 MHz) and ^{1}H NMR (500 MHz) spectroscopic data of protostemonine (**40**),[10] isoprotostemonine (**45**)[7] and javastemonine B (**187**) in $CDCl_3$ solution (δ in ppm).

Position	δ_C			δ_H (mult., J (Hz)		
	40[10]	**45**[7]	**187**	**40**[10]	**45**[7]	**187**
1α	26.5	26.5	25.9	192 (m)	1.89 (ddd) *	1.92-1.86 (overlap)
β				1.48 (m)	1.55 (m)	2.24-2.16 (overlap)
2α	27.2	27.2	25.9	1.90 (m)	1.87 (m)	2.18-2.10 (overlap)
β				1.48 (m)	1.48 (m)	1.86-1.80 (overlap)
3	64.3	64.4	67.5	3.29 (ddd, *J* 8.1, 7.0, 6.8)	3.24 (ddd, *J* 11.5, 7.5, 7.3)	3.64-3.60 (m)
5α	46.5	46.6	49.5	3.48 (ddd, *J* 15.5, 4.6, <1)	3.50 (dd, *J* 14.8, 4.8)	3.79 (dd, *J* 14.7, 6.0)
β				2.93 (m)	2.89 (dd, *J* 14.8, 11.2)	3.35 (dd, *J* 14.7, 12.5)
6α	20.6	20.2	17.8	1.64 (m)	1.50 (m)	1.86-1.82 (m)
β				1.51 (m)	1.65 (m)	1.98-1.92 (m)
7α	33.7	34.3	33.1	2.37 (m)	2.32 (m)	2.44 (dd, *J* 12.6, 3.7)
β				1.50 (m)	1.50 (m)	1.66-1.58 (overlap)
8	82.5	82.5	82.7	4.09 (ddd, *J* 10.6, 10.2, 3.8)	4.18 (ddd)*	4.30 (ddd, *J* 15.0, 11.0, 3.9)
9	55.5	54.2	50.9	2.21 (ddd, *J* 9.6, 8.8, 3.8)	2.12 (ddd, *J* 10.4, 10.3, 5.3)	2.29 (ddd, *J* 14.6, 10.7, 4.0)
9a	58.8	58.4	61.8	3.73 (ddd, *J* 9.6, 5.8, 5.8)	3.69 (ddd, *J* 10.7, 10.6, 5.6,)	4.36 (ddd, *J* 11.1, 10.9, 6.2)
10	39.4	41.7	41.7	2.91 (m)	3.01 (dq, *J* 10.5, 6.7)	3.04 (ddd, *J* 13.4, 7.1, 7.1)
11	148.9	150.8	149.2	-	-	-
12	124.4	125.7	126.1	-	-	-
13	163.1	163.8	163.6	-	-	-
14	96.9	98.3	98.1	-	-	-
15	169.9	168.5	170.6	-	-	-
16 (Me)	20.6	18.1	16.6	2.07 (s)	2.01 (s)	2.02 (s)
17 (Me)	8.9	8.5	8.7	1.34 (d, *J* 6.6)	1.32 (d, *J* 6.7)	1.48 (d, *J* 7.0)
18	83.9	83.9	77.2	4.16 (ddd, *J* 10.9, 7.0, 5.4)	4.14, (ddd)*	5.03 (ddd, *J* 9.7, 6.4, 6.4)
19α	34.2	34.2	35.0	2.35 (ddd, *J* 12.8, 8.1, 5.4)	2.36 (ddd) *	2.54 (ddd, *J* 12.6, 8.3, 5.6)
β				1.53 (m)	1.52 (m)	1.64-1.54 (overlap)
20	34.7	34.8	34.6	2.60 (m)	2.58 (ddq)*	2.70 (ddq, *J* 11.5, 7.5, 7.0)
21	179.1	179.2	178.3	-	-	-
22 (Me)	14.7	14.9	14.6	1.26 (d, *J* 7.1)	1.23 (d, *J* 6.9)	1.27 (d, *J* 7.0)
23 (OMe)	58.8	59.5	59.5	4.13 (s)	4.10 (s)	4.11 (s)

*Coupling constants (*J*) not available from the literature.[7]

4.2.3 13-Demethoxy-11(*S**),12(*R**)-dihydroprotostemonine (55)

13-Demethoxy-11(*S**),12(*R**)-dihydroprotostemonine (**55**) was isolated as a brown gum; ESIMS *m/z* 390 $[M+H]^+$, consistent with molecular $C_{22}H_{31}NO_5$ (MW 389). The ^1H NMR spectrum of 13-demethoxy-11(*S**),12(*R**)-dihydroprotostemonine is shown in Figure 4.13. This compound was identified from a comparison of its NMR spectroscopic data with those in the literature.[22] The ^1H NMR chemical shifts are in agreement with those previously reported, as summarized in Table 4.5.

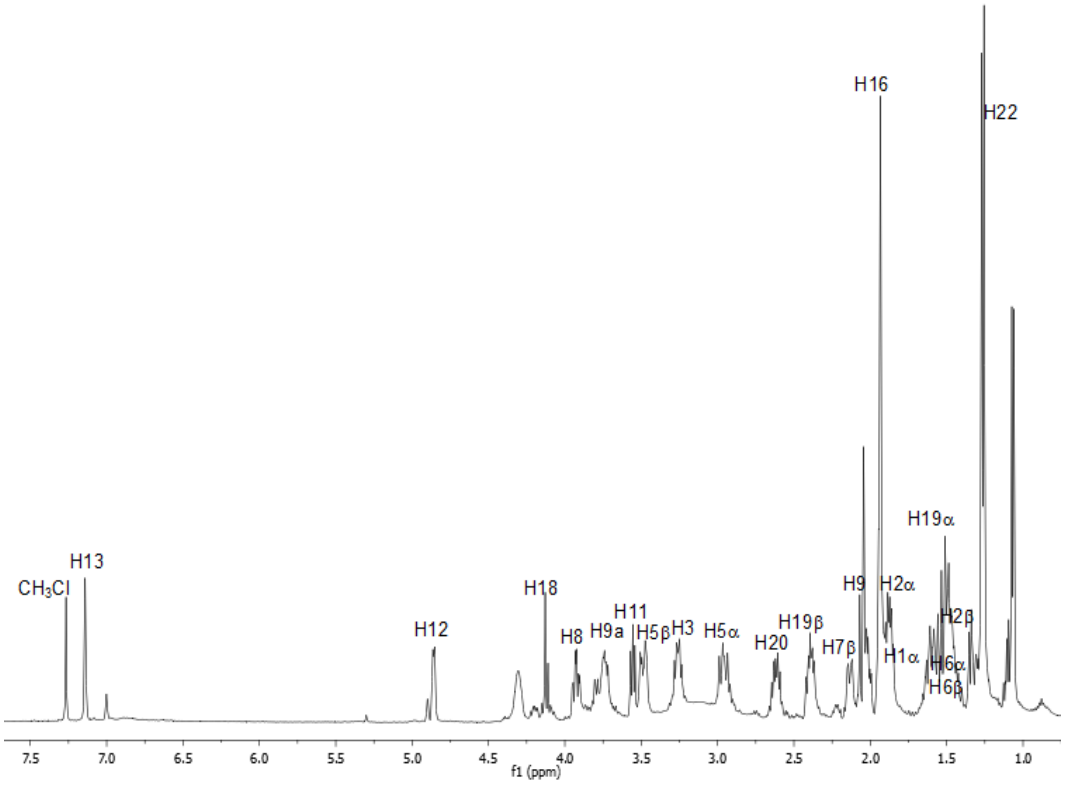

Figure 4.13 ^1H NMR spectrum ($CDCl_3$, 500 MHz) of 13-demethoxy-11(*S**),12(*R**)-dihydroprotostemonine (**55**).

Table 4.5 ^{13}C (125 MHz) and ^{1}H NMR (500 MHz) spectroscopic data of 13-demethoxy-11(*S**),12(*R**)-dihydroprotostemonine (this work) and 13-demethoxy-11(*S**),12(*R**)-dihydroprotostemonine (**55**)[22] in $CDCl_3$ solution (δ in ppm).

Data	**Experimental**	**Literature**[22]
Position	**δ_H (mult., *J* (Hz), assign.)**	**δ_H (mult., *J* (Hz), assign.)**
1α	1.83-1.80 (m)	1.81 (m)
β	1.59-1.55 (m)	1.58 (m)
2α	1.93-1.90 (m)	1.92 (m)
β	1.40-1.36 (m)	1.39 (m)
3	3.24 (ddd, *J* 10.0, 7.0, 5.5)	3.24 (ddd, *J* 9.6, 7.4, 5.6)
5α	2.90 (ddd, *J* 16.0, 15.5)	2.89 (dd, *J* 16.2, 15.6)
β	3.45 (ddd, *J* 16.0, 5.5)	3.45 (dd, *J* 16.2, 5.2)
6α	1.41-1.38 (m)	1.39 (m)
β	1.41-1.38 (m)	1.39 (m)
7α	1.30-1.27 (m)	1.28 (m)
β	2.12-2.09 (m)	2.11 (m)
8	3.92 (ddd, *J* 10.0, 10.0, 4.5)	3.91 (ddd, *J* 10.2, 10.2, 4.0)
9	2.01-1.98 (m)	1.99 (m)
9a	3.65 (ddd, *J* 10.5, 5.5, 5.0)	3.63 (ddd, *J* 10.5, 5.6, 5.0)
10	1.91-1.87 (m)	1.90 (m)
11	3.52 (dd, *J* 7.5, 6.5)	3.52 (dd, *J* 7.6, 6.4)
12	4.85-4.82 (m)	4.84 (m)
13	7.16 (s)	7.16 (m)
14	-	-
15	-	-
16 (Me)	1.93 (s)	1.93 (s)
17 (Me)	1.06 (d, *J* 6.2)	1.06 (d, *J* 6.2)
18	4.18 (ddd, *J* 11.0, 7.0, 5.5)	4.14 (ddd, *J* 11.1, 7.5, 5.3)
19α	1.54-1.50 (m)	1.53 (m)
β	2.38-2.34 (m)	2.36 (m)
20	2.61-2.58 (m)	2.60 (m)
21	-	-
22 (Me)	1.26 (d, *J* 7.0)	1.26 (d, *J* 7.0)

4.2.4 Protostemonine (40)

Protostemonine (**40**) was isolated as brown gum; ESIMS *m/z* 418 $[M+H]^+$, consistent with molecular $C_{23}H_{31}NO_6$ (MW 417). The ^1H and ^{13}C NMR spectra of protostemonine are shown in Figures 4.14 and 4.15, respectively. This compound was identified by a comparison of of its NMR spectroscopic data with those in the literature.[10] The chemical shifts are in close agreement with those previously reported, as summarized in Table 4.6.

Table 4.6 ^{13}C (125 MHz) and ^1H NMR (500 MHz) spectroscopic data of protostemonine (this work) and protostemonine (**40**)[10] in $CDCl_3$ solution (δ in ppm).

Data		**Experimental**	**Literature**[10]	
Position	**δ_C**	**δ_H (mult., *J* (Hz), assign.)**	**δ_C**	**δ_H (mult., *J* (Hz), assign.)**
1α	26.8	1.88 (overlap)	26.5	192 (m)
β		1.48 (overlap)		1.48 (m)
2α	27.6	1.52 (overlap)	27.2	1.48 (m)
β		1.90 (overlap)		1.90 (m)
3	64.4	3.25 (ddd, *J* 8.0, 7.0, 7,0)	64.3	3.29 (ddd, *J* 8.1, 7.0, 6.8)
5α	46.7	3.42 (ddd, *J* 15.5, 4.5, <1)	46.5	3.48 (ddd, *J* 15.5, 4.6, <1)
β		2.88 (overlap)		2.93 (m)
6α	20.2	1.65-1.61 (m)	20.6	1.64 (m)
β		1.51 (overlap)		1.51 (m)
7α	34.4	2.35 (overlap)	33.7	2.37 (m)
β		1.48-1.45 (m)		1.50 (m)
8	84.4	4.07 (overlap)	82.5	4.09 (ddd, *J* 10.6, 10.2, 3.8)
9	55.9	2.18 (ddd, *J* 9.6, 8.5, 4.0)	55.5	2.21 (ddd, *J* 9.6, 8.8, 3.8)
9a	58.8	3.70 (ddd, *J* 9.6, 6.0, 6.0)	58.8	3.73 (ddd, *J* 9.6, 5.8, 5.8)
10	39.7	2.85 (overlap)	39.4	2.91 (m)
11	149.3	-	148.9	-
12	124.3	-	124.4	-
13	163.5	-	163.1	-
14	97.0	-	96.9	-
15	170.1	-	169.9	-
16 (Me)	20.9	2.07 (s)	20.6	2.07 (s)
17 (Me)	9.3	1.34 (d, *J* 7.0)	8.9	1.34 (d, *J* 6.6)
18	83.3	4.18 (ddd, *J* 11.0, 7.0, 5.5)	83.9	4.16 (ddd, *J* 10.9, 7.0, 5.4)
19α	33.9	2.38 (ddd, *J* 12.8, 8.1, 5.4)	34.2	2.35 (ddd, *J* 12.8, 8.1, 5.4)
β		1.55 (overlap)		1.53 (m)
20	35.0	2.63-2.59 (m)	34.7	2.60 (m)
21	179.9	-	179.1	-
22 (Me)	15.0	1.25 (d, *J* 7.0)	14.7	1.26 (d, *J* 7.1)
23	59.0	4.13 (s)	58.8	4.13 (s)

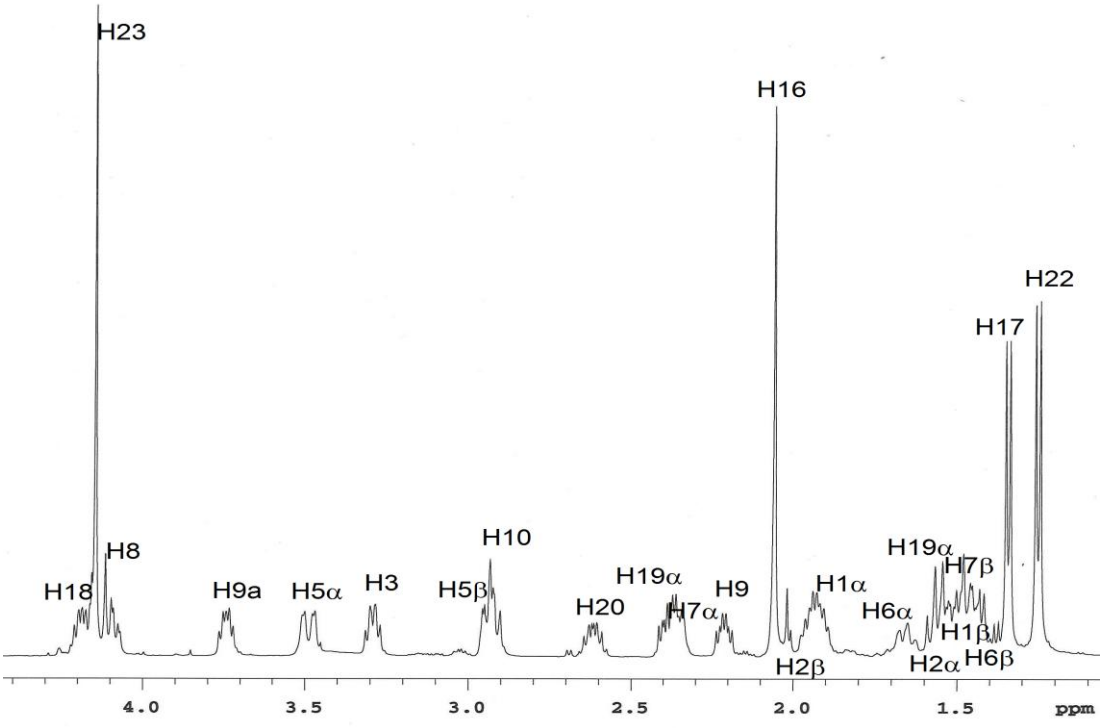

Figure 4.14 ^{1}H NMR spectrum ($CDCl_3$, 500 MHz) of protostemonine (**40**).

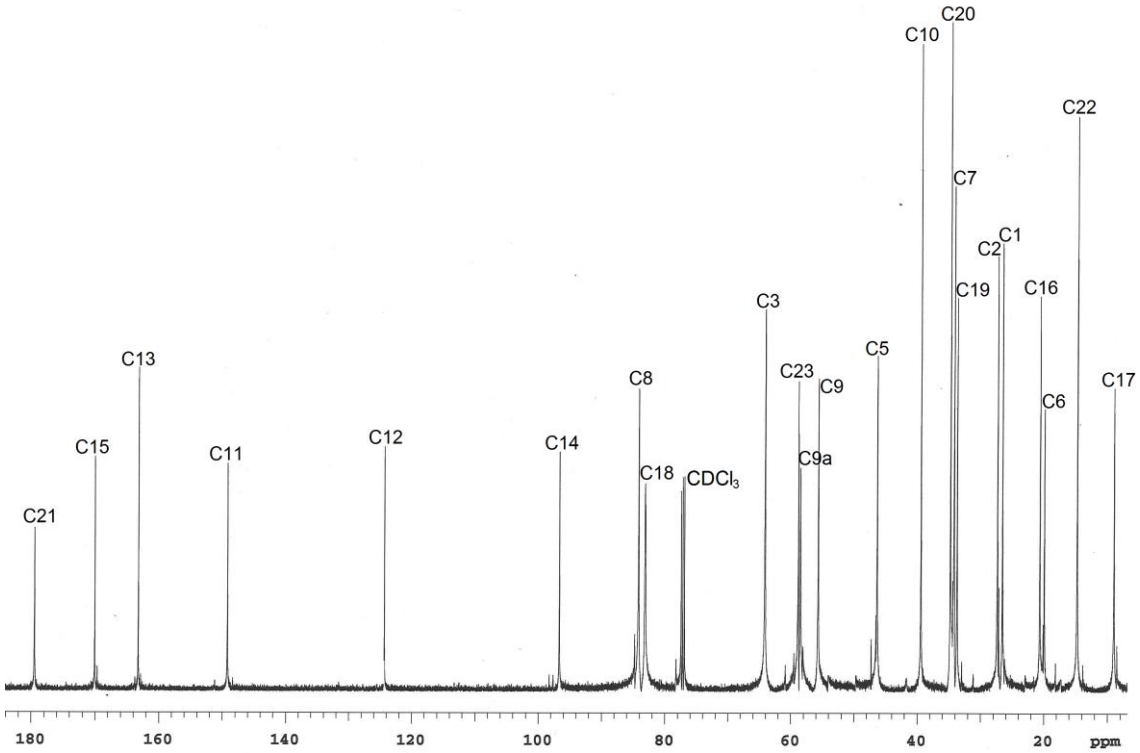

Figure 4.15 ^{13}C NMR spectrum ($CDCl_3$, 125 MHz) of protostemonine (**40**).

4.2.5 Isoprotostemonine (45)

Isoprotostemonine (**45**) was isolated as brown gum; ESIMS *m/z* 418 $[M+H]^+$, consistent with molecular $C_{23}H_{31}NO_6$ (MW 417). The ^1H and ^{13}C NMR spectra of isoprotostemonine are shown in Figure 4.16 and 4.17, respectively. This compound was identified by a comparison of its NMR spectroscopic data with those in the literature.[7] The chemical shifts are in close agreement with those previously reported, as summarized in Table 4.7.

Table 4.7 ^{13}C (125 MHz) and ^1H (500 MHz) NMR spectroscopic data of isoprotostemonine (this work) and isoprotostemonine (**45**)[7] in $CDCl_3$ solution (δ in ppm).

Position	Experimental		Literature[7]	
	δ_C	δ_H (mult., *J* (Hz), assign.)	δ_C	δ_H (mult., *J* (Hz), assign.)
1α	26.8	1.87 (overlap)	26.5	1.89 (ddd)*
β		1.51-1.48 (m)		1.55 (m)
2α	27.5	1.87 (overlap)	27.2	1.87 (m)
β		1.43 (overlap)		1.48 (m)
3	64.4	3.25 (ddd, *J* 11.0, 7.5, 7.5)	64.4	3.24 (ddd, *J* 11.5, 7.5, 7.3)
5α	46.7	3.48 (dd, *J* 15.0, 5.0)	46.6	3.50 (dd, *J* 14.8, 4.8)
β		2.88 (ddd, *J* 15.0, 11.0)		2.89 (dd, *J* 14.8, 11.2)
6α	20.3	1.44-1.40 (m)	20.2	1.50 (m)
β		1.63-1.59 (m)		1.65 (m)
7α	34.6	2.34 (overlap)	34.3	2.32 (m)
β		1.52-1.49 (m)		1.50 (m)
8	85.0	4.15 (overlap)	85.5	4.18 (ddd)*
9	54.4	2.11-2.08 (m)	54.2	2.12 (ddd, *J* 10.4, 10.3, 5.3)
9a	58.3	3.70 (ddd, *J* 11.0, 11.0, 5.5)	58.4	3.69 (ddd, *J* 10.7, 10.6, 5.6)
10	41.9	3.00 (ddd, *J* 11.0, 6.5)	41.7	3.01 (dq, *J* 10.5, 6.7)
11	151.0	-	150.8	-
12	125.8	-	125.7	-
13	163.9	-	163.8	-
14	98.0	-	98.3	-
15	169.9	-	168.5	-
16 (Me)	17.6	2.00 (s)	18.1	2.01 (s)
17 (Me)	8.8	1.40 (d, *J* 7.0)	8.5	1.32 (d, *J* 6.7)
18	83.4	4.15 (overlap)	83.3	4.14, (ddd)*
19α	34.5	2.34 (overlap)	34.3	2.36 (ddd) *
β		1.51-1.48 (m)		1.52 (m)
20	35.1	2.59-2.55 (m)	34.8	2.58 (ddq)*
21	179.7	-	179.2	-
22 (Me)	15.0	1.24 (d, *J* 7.0)	14.9	1.23 (d, *J* 6.9)
23	59.7	4.08 (s)	59.5	4.10 (s)

*Coupling constants (*J*) not available from the literature.[7]

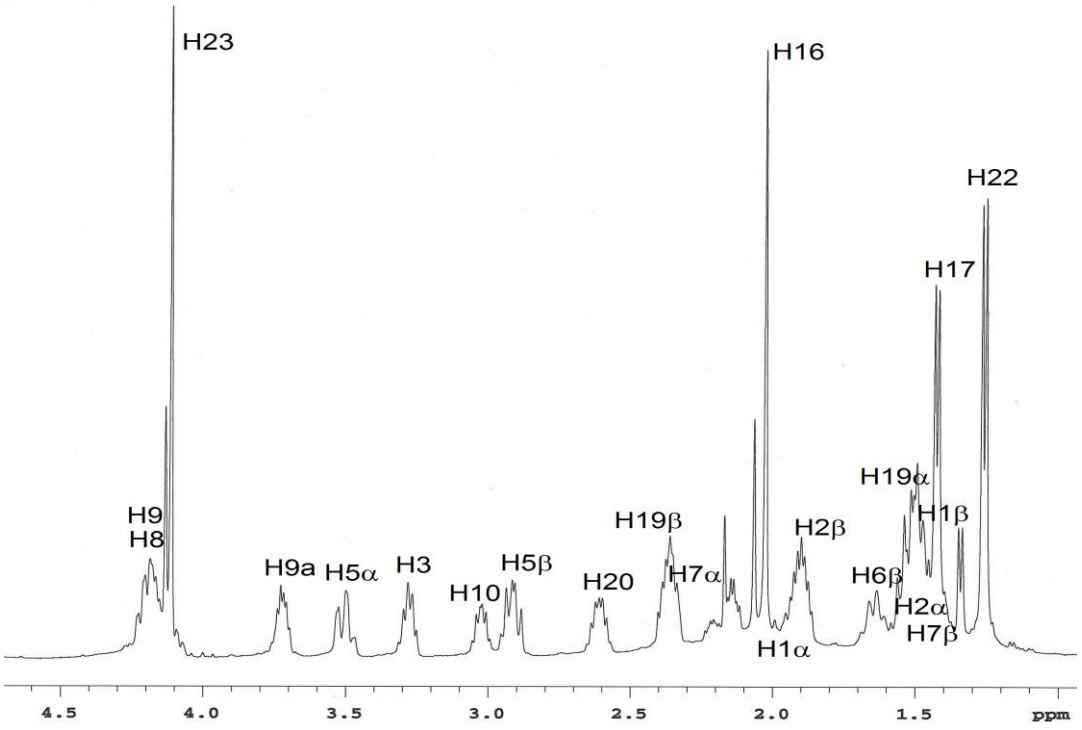

Figure 4.16 ^{1}H NMR spectrum ($CDCl_3$, 500 MHz) of isoprotostemonine (**45**).

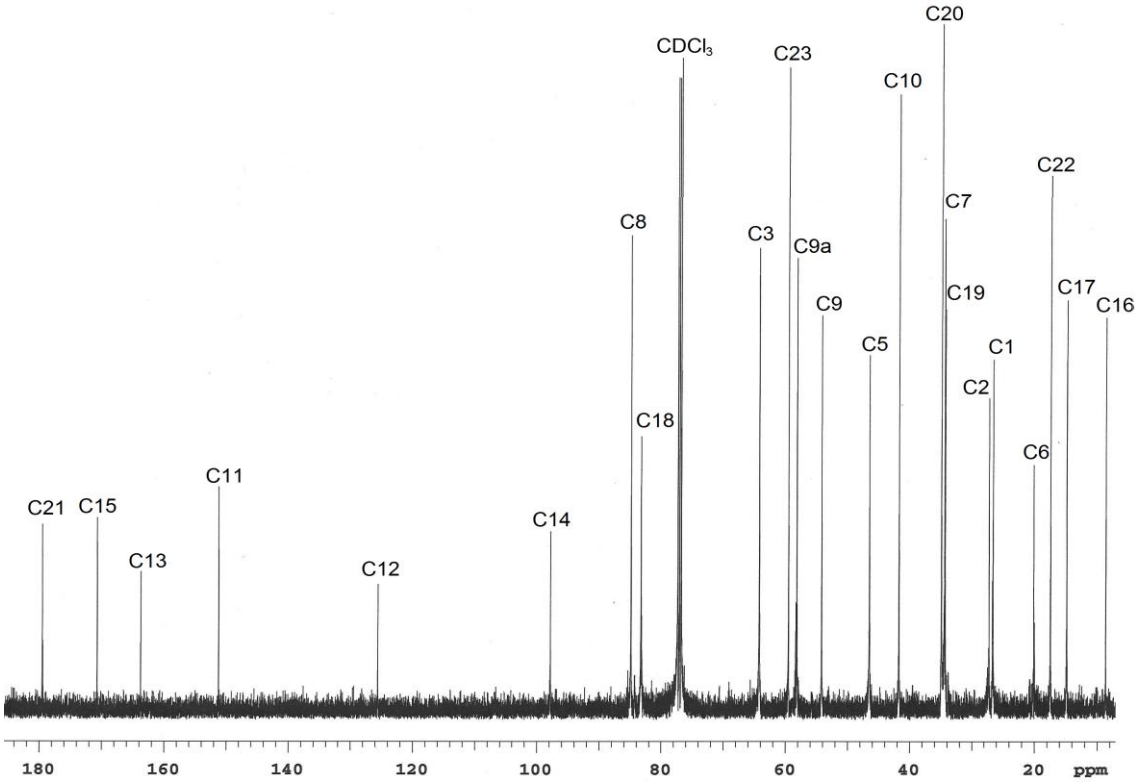

Figure 4.17 ^{13}C NMR spectrum ($CDCl_3$, 125 MHz) of isoprotostemonine (**45**).

4.2.6 Isomaistemonine (95)

Isomaistemonine (**95**) was isolated as brown gum; ESIMS *m/z* 416 $[M+H]^+$, consistent with molecular $C_{23}H_{29}NO_6$ (MW 417)**.** The ^{1}H NMR spectrum of isomaistemonine is shown in Figure 4.18. This compound was identified by a comparison of its NMR spectroscopic data with those in the literature.[73] The ^{1}H NMR chemical shifts are in close agreement with those previously reported, as summarized in Table 4.8.

Table 4.8 ^{1}H NMR (500 MHz) spectroscopic data of isomaistemonine (this work) and isomaistemonine (**45**)[73] in $CDCl_3$ solution (δ in ppm).

Position	**Experimental**	**literature**[73]
	δ_H (mult., *J* (Hz), assign.)	**δ_H (mult., *J* (Hz), assign.)**
1α	2.13-2.07 (m)	2.12-1.98 (m)
β	1.99-1.92 (m)	1.97-1.74 (m)
2α	1.82-1.78 (m)	1.82-1.78 (m)
β	1.52-1.49 (m)	1.52-1.49 (m)
3	3.39-3.35 (m)	3.38 (ddd, *J* 13.0, 6.0, 7.8)
5α	2.90 (overlap)	2.90 (ddd, *J* 15.0, 15.0, 2.5)
β	3.60 (ddd, *J* 15.0, 3.0, 3.0)	3.60 (ddd, *J* 15.0, 3.0, 3.0)
6α	1.87-1.84 (m)	1.87-1.84 (m)
β	1.35-1.32 (m)	1.35-1.32 (m)
7α	1.90-1.84 (m)	1.89-1.85 (m)
β	1.52-1.49 (m)	1.52-1.49 (m)
8α	2.25 (overlap)	2.27 (ddd, *J* 13.8, 12.4, 11.4)
β	2.93 (overlap)	2.93 (ddd, *J* 13.8, 2.0, 1.8)
9	-	-
9a	-	-
10	-	-
11	-	-
12	-	-
13	-	-
14	-	-
15	-	-
16 (Me)	1.79 (s)	1.80 s
17 (Me)	2.01 (s)	2.01 s
18	3.87 (ddd, *J* 12.0, 8.0, 5.5)	3.87 (ddd, *J* 12.0, 7.8, 5.4)
19α	1.48 (ddd, *J* 12.0, 11.5, 11.5)	1.48 ddd, *J* 12.0, 11.5, 11.5)
19β	2.34 (ddd, *J* 12.0, 11.5, 5.5)	2.34 ddd, *J* 12.0, 11.5, 5.4)
20	2.57 (qdd, *J* 11.5, 8.0, 7.0)	2.54 (qdd, *J* 11.5, 7.8, 7.2)
21	-	-
22 (Me)	1.26 (d, *J* 7.0)	1.26 (d, *J* 7.2)
OMe	4.00 (s)	4.00 (s)

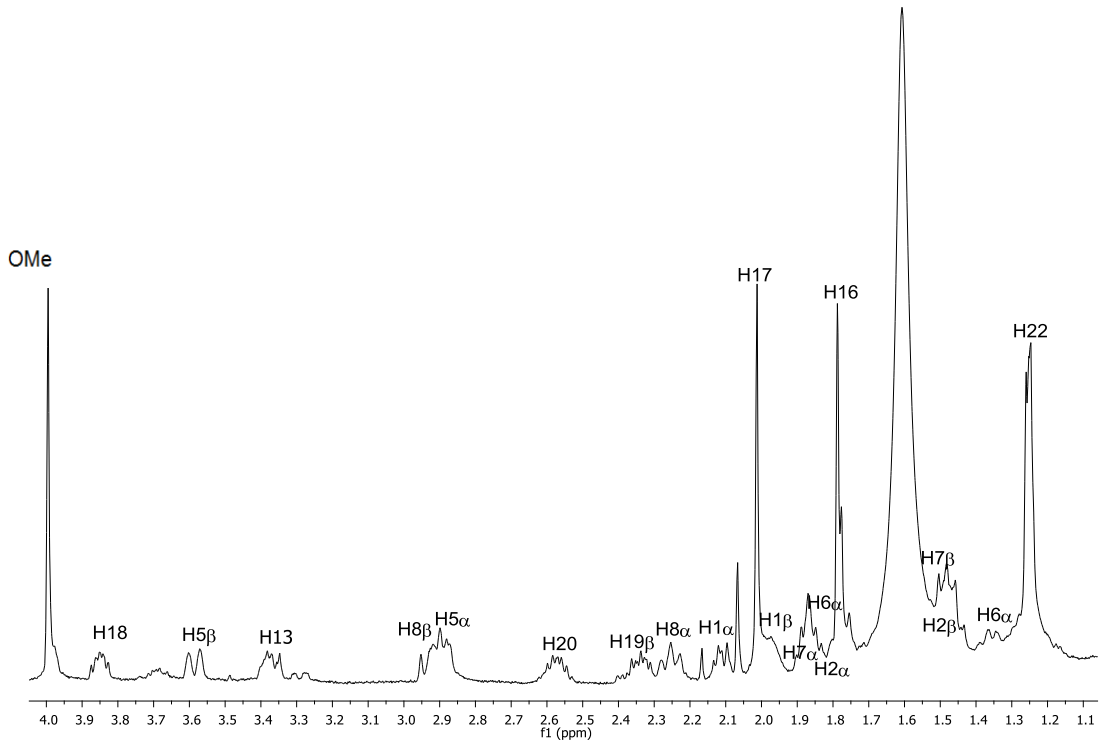

Figure 4.18 ^{1}H NMR spectrum ($CDCl_3$, 500 MHz) of isomaistemonine (**95**).

4.3 Conclusions

In a previous study, two pyrrolo[1,2-*a*]azepine alkaloids, protostemonine (**40**) and stemofoline (**111**) were isolated from *S. javanica* roots extracts from an undisclosed area in Indonesia.[72] Stemofoline (**111**) was the major alkaloid. In contrast, in this study six pyrrolo[1,2-*a*]azepine alkaloids were isolated from *S. javanica* growing in Alas Purwo, East Java, Indonesia but protostemonine (**40**) was the major alkaloid in the roots. As mentioned in Chapter 3 (Section 3.4), these differences may also be due to their different geographical locations (different climates and neutrients), the age of the plants or the season in which the plants were harvested.

CHAPTER 5

PHYTOCHEMICAL STUDY ON THE ROOTS AND LEAVES OF *Stichoneuron halabalensis* HOOK F.

5.1 Introduction

In this chapter, we describe our phytochemical studies of the root and leaf extracts of the hitherto unreported *St. halabalensis* collected from among plants growing in the east part of Peninsular Malaysia.

5.2 Isolation and Purification of Stemona Alkaloids from Ethanol Extract of roots of *St. halabalensis*

The dry ground root (199.2 g) of *St. halabalensis* was extracted with 95% EtOH (4 x 2.5 L) over 4 days at rt. The ethanolic extracts were evaporated to give a dark brown oil (4.4 g). The root extract was chromatographed on silica gel (200 mL) using gradient elution from *n*-hexane/EtOAc (9:1 to 0:10) to EtOAc/MeOH (10:0 to 8:2). A total of 1.5 L eluent was collected in test tubes of 20 mL. These fractions were pooled on the basis of TLC analysis to give non-alkaloid fraction A (180.0 mg) and the alkaloid fractions B (209.0 mg) and C (1.5 g) (Fraction A did not stain with Dragendroff's reagent while fractions B and C did). Further separation of these fractions gave (+)-α-tocopherol (**188**, 4.5 mg), (*R*)-(+)-goniothalamin (**189**, 7.2 mg), bisdehydrostemoninine A (**60**, 6.2 mg), stemoninine (**49**, 41.5 mg), sessilistemoamine C (**98**, 4.2 mg), sessilistemoamine A (**96**, 2.5 mg) and a mixture of stichoneurine C (**190**) and D (**191**) (13.3 mg, **190**:**191** = 5:1). The isolated compounds from the roots of *St. halabalensis* are shown in Figure 5.1.

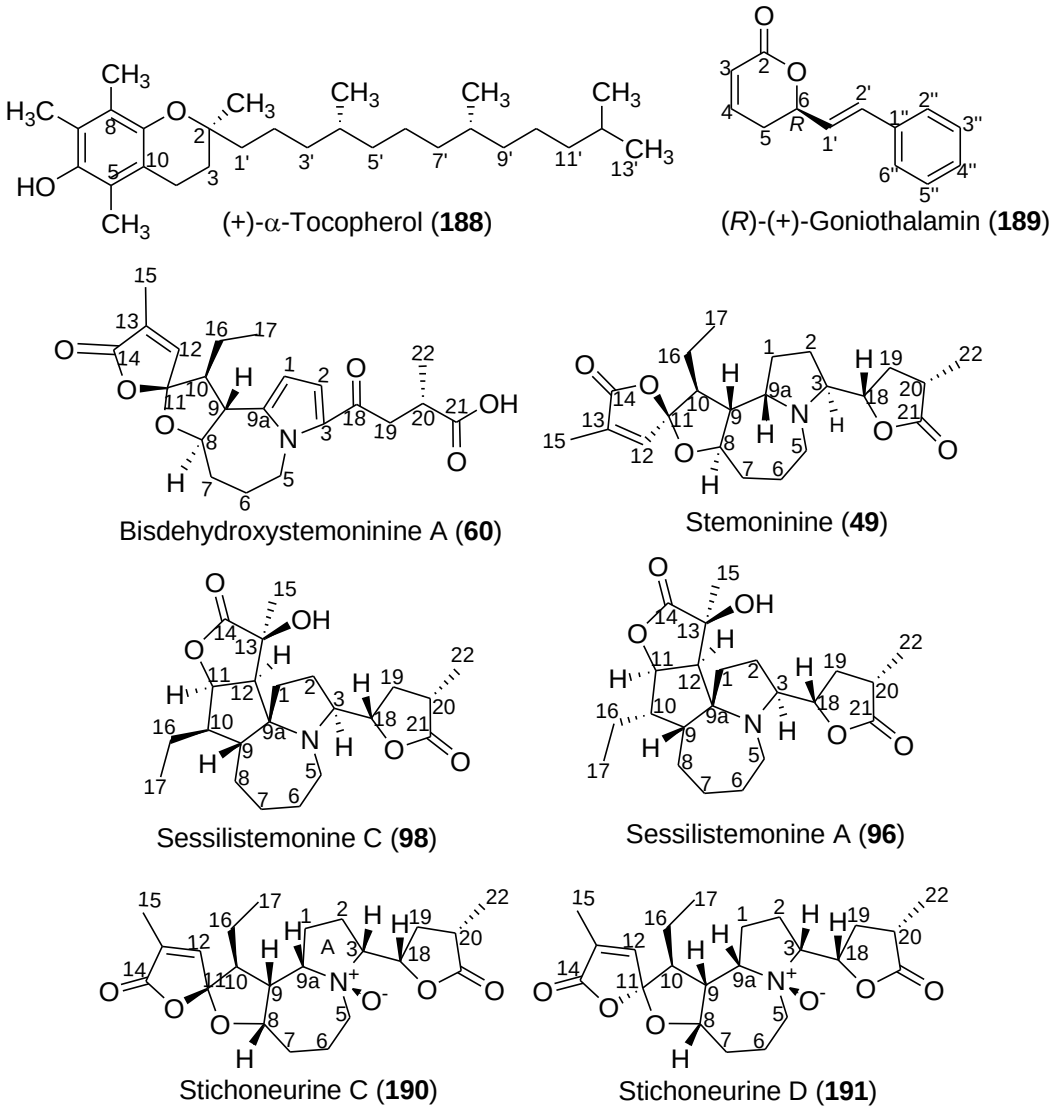

Figure 5.1 Structures of the isolated compounds from the root of *St. halabalensis*.

5.2.1 Structure elucidation of Stichoneurine C (190) and D (191)

The HRMS analysis of the mixture of stichoneurines C and D (ESI, *m/z* $[M+H]^+$, 406.2218, calcd 406.2230) showed both compounds had the molecular formula $C_{22}H_{31}NO_6$, indicating their isomeric structural relationship and that they had one more oxygen than stemoninine (**49**). The IR spectrum of the mixture of stichoneurines C and D showed a strong absorbance at 1776 cm^{-1} consistant with the γ-lactone funtionality. This structural relationship was further supported from their ^{13}C NMR/DEPT, HSQC

and HMBC spectra, which indicated that stemoninine (**49**) and stichoneurine C and D (**190**-**191**) had the same number of carbons and carbon types, with the same relative connectivities and same ring features.

In the ^{13}C NMR spectrum (Figure 5.3) of the mixture of stichoneurine C (**190**) and D (**191**), a complete twofold set of signals with an intensity ratio of approximately 5:1 was observed. In the ^{1}H NMR spectrum (Figure 5.4), the majority of resonances for stichoneurine D (**191**) could also be observed, with eight overlapping with those of stichoneurine C (**190**). Due to the clear intensity differences of the ^{13}C NMR resonances for stichoneurine C (**190**) and D (**191**) (Figure 5.4) and by the use of 2D methods (COSY, HMQC, HMBC, and NOESY) it was possible to assign all ^{13}C NMR resonances of both isomers. Both were characterized by the presence of three methyl groups, seven methylenes, seven methines, two olefinic and three quaternary carbons. The COSY correlations in the COSY spectrum of stichoneurine C (**190**) and D (**191**) indicated the spin system H-1−H-2−H-3−H-18−H-19−H-20−H-22, typical of the pyrrolidine ring of the *Stemona* alkaloids, with a γ-lactone substituent at C-3 (Figure 5.2). COSY correlations were also observed between the vicinal pairs of contiguous protons along the C-5−C-10 backbone, with vicinal correlations also seen between H-10 and H-16; H-16 and H-17 (Figure 5.2). The full ^{1}H and ^{13}C NMR spectral assignments for stichoneurine C and D (**190**-**191**), based on extensive NOESY/ROESY, HSQC and HMBC experiments, are shown in Table 5.1 and Table 5.2.

For stichoneurine C (**190**), the ^{13}C NMR signals included three methyl [δ 10.7 (C-15), 13.0 (C-17) and 14.7 (C-22)], seven methylene [δ 67.7 (C-5), 34.9 (C-1), 24.1 (C-2), 21.3 (C-6), 34.9 (C-7), 35.4 (C-19) and 19.5 (C-16)], seven methine [δ 75.5 (C-3), 85.8 (C-8), 48.7 (C-9), 78.8 (C-9a), 51.5 (C-10), 73.5 (C-18) and 35.3 (C-20)], two

olefinic [δ 143.7 (C-12) and 134.7 (C-13)] and three quaternary carbons [δ 112.4 (C-11), 171.1 (C-14) and 178.3 (C-21)]. The ^{1}H NMR resonances of stichoneurine C at δ 0.85 (t, J = 7.0 Hz), 1.27 (d, J = 7.0 Hz) and 1.95 (d, J = 1.3 Hz) were assigned to the methyl groups C-17, C-22 and C-15, respectively. The olefinic proton resonance at δ 6.61 (apparent d, J = 1.3 Hz) was assigned to H-12. The ^{13}C NMR signals at δ 178.3 and 171.1 indicated two lactone carbonyls, while the signal at δ 112.4 (quartenary carbon) indicated a ketal group such as that present in stemoninine (**49**).[76] The analysis of the 1D and 2D NMR spectra of stichoneurine C (**190**) led to the full assignment of the carbon and proton signals (Table 5.1). The signals resonating at δ 178.3 (C-21) and 171.1 (C-14) showed correlations with those of H-19 and H-22, and with H-12, and H-15, respectively in the HMBC spectrum. The quaternary carbon signal at δ 112.4 (C-11) showed correlations with H-8, H-10, H-12 and H-16, thus indicating the position of the ketal moiety at C-11 and the ethyl group at C-10. Key HMBC correlations for stichoneurine C (**190**) are shown in Figure 5.2, while full NMR spectroscopic details are provided in Table 5.1.

While for stichoneurine D (**191**), the ^{13}C NMR spectrum (Figure 5.3) showed 22 carbon signals including three methyl [δ 10.8 (C-15), 12.2 (C-17) and 14.7 (C-22)], seven methylene [δ 68.1 (C-5), 33.2 (C-1), 24.1 (C-2), 21.0 (C-6), 33.5 (C-7), 35.4 (C-19) and 19.5 (C-16)], seven methine [δ 75.5 (C-3), 86.8 (C-8), 50.7 (C-9), 78.7 (C-9a), 53.0 (C-10), 73.3 (C-18) and 35.2 (C-20)], two olefinic [δ 142.5 (C-12) and 134.1 (C-13)] and three quaternary carbons [δ 113.7 (C-11), 171.3 (C-14) and 178.3 (C-21)]. The ^{1}H NMR resonances of stichoneurine D at δ 0.95 (t, J = 7.5 Hz), 1.27 (overlap) and 1.95 (overlap) were assigned to the methyl groups C-17, C-22 and C-15, respectively. The olefinic proton resonance at δ 6.78 (apparent d, J = 1.3 Hz) was assigned to H-12. Similar to

stichoneurine C, the ^{13}C NMR signals at δ 178.3 and 171.3 correspond to two lactone carbonyls, while the signal at δ 113.7 indicated a ketal group. The signals resonating at δ 178.3 (C-21) and 171.3 (C-14) correlated with those of H-19 and H-20, and with H-15, respectively in the HMBC spectrum. Key HMBC correlations for stichoneurine D (**191**) are shown in Figure 5.2, while full details are provided in Table 5.2.

The ^{1}H and ^{13}C NMR signals of stichoneurine D (**191**) were similar or sometimes the same as those of **190 (**Table 5.2). A comparison of the ^{13}C/DEPT NMR spectra of **190** and **191** with that of stemoninine (**49**)[76] showed that the main differences between them were the ^{13}C NMR chemical shifts of the signals for C-3, C-5, and C-9a. The chemical shifts of these carbons for stemoninine (**49**) were at δ 63.4, 45.6 and 58.3, respectively, whereas the chemical shifts for these carbons for **190 [**{δ 75.5 (C-3), 67.7 (C-5), and 78.7 (C-9a)}] and [**191** {δ 75.5 (C-3), 68.1 (C-5), and 78.7 (C-9a)}] were significantly downfield and consistent with an N-oxide structure, which would result in the deshielding of directly bonded carbons without changing the overall carbon framework of the molecule. The ^{13}C NMR chemical shifts for C-18 in **190** (δ 73.5) and **191** (δ 73.3) were significant shielded compared to C-18 in **49** (δ 82.4) due to the γ-shielded effect on C-18 by the N-oxide oxygen.[77]

The assignment of the relative configurations of stichoneurine C (**190**) and D (**191**) were made from NOESY and molecular modeling experiments, where the structures shown in Figures 5.5 and 5.6 were generated using Spartan ‘10 and conformational searching (MMFF) to find the lowest energy conformers. In **190**, there were strong NOE correlations between H-3 and H-18, as well as between H-8 H-9 and H-9a, which indicated their β configurations. The NOE correlations between H-10 and H-12 in **190** indicated that the configuration of C-11 was the same as that of

stemoninine (**49**). These correlations indicated that stichoneurine C (**190**) was a diastereomer of stemoninine (**49**) at C-3 and C-8. Most of these NOE correlations were also observed in the NOESY spectrum of stichoneurine D (**191**). The difference was that the NOESY correlation between H-10 and H-12 was now absent and a correlation between H-12 and H-16 was now observed (Figure 5.7).

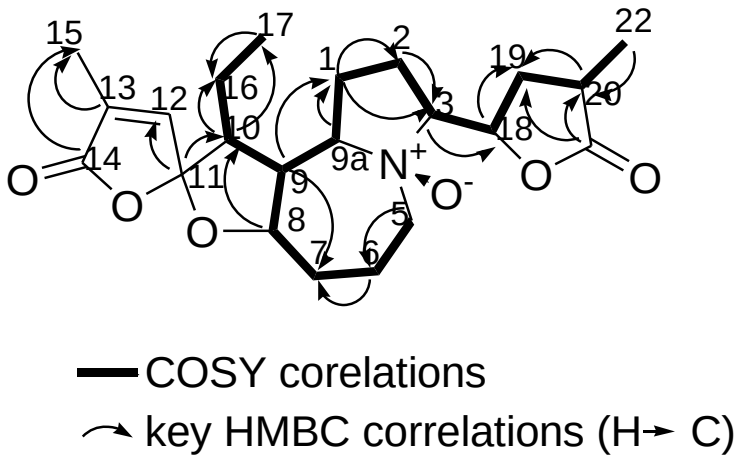

Figure 5.2 Key COSY and HMBC correlations for stichoneurine C and D (**190**-**191**).

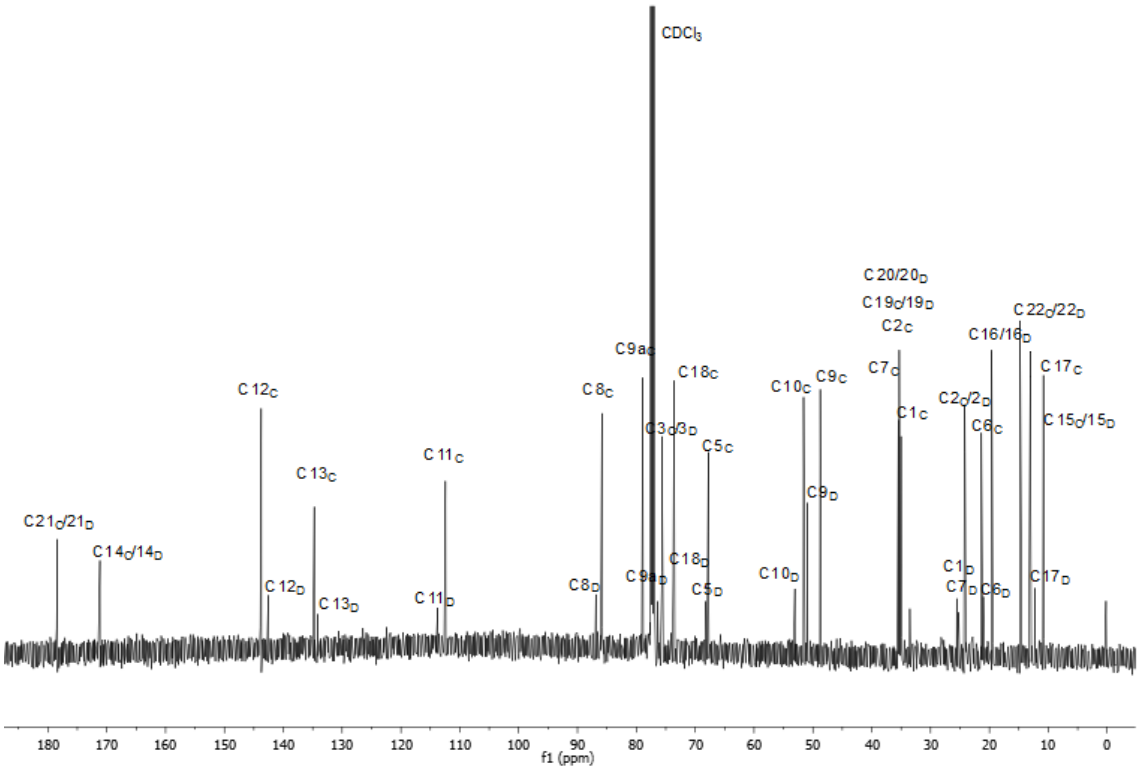

Figure 5.3 ^{13}C NMR spectrum ($CDCl_3$, 125 MHz) of stichoneurine C and D (**190**-**191**).

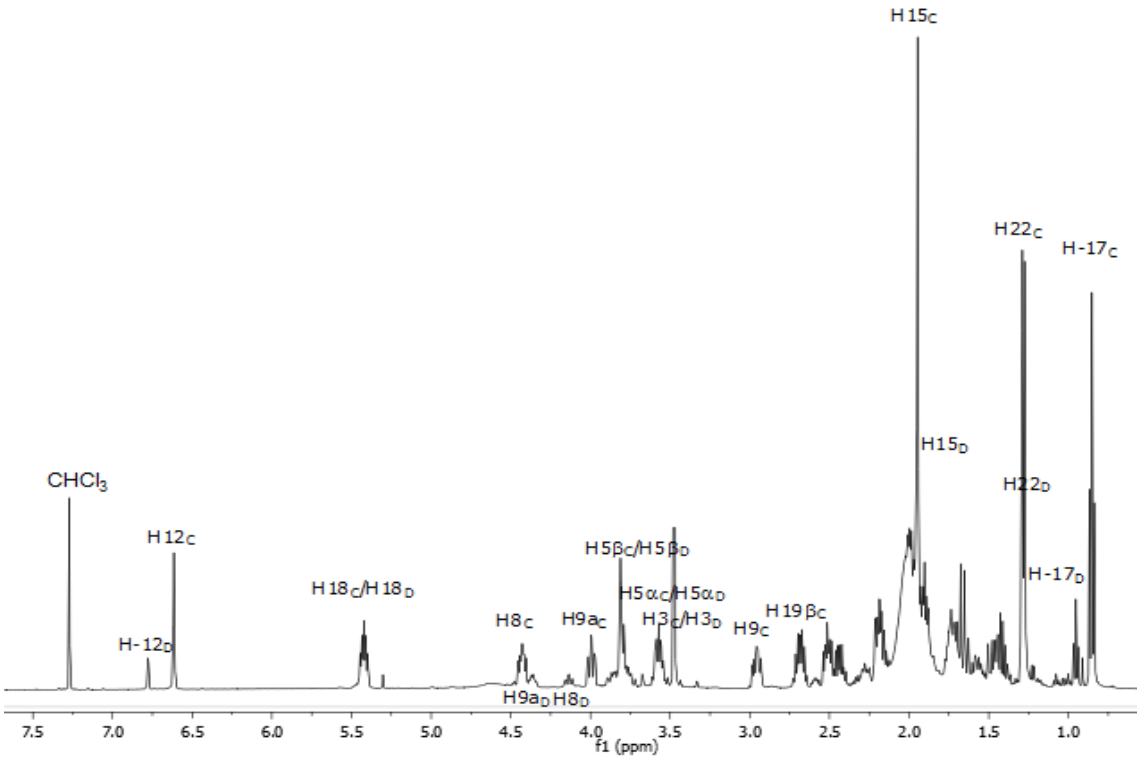

Figure 5.4 ^{1}H NMR spectrum ($CDCl_3$, 500 MHz) of stichoneurine C and D (**190-191**).

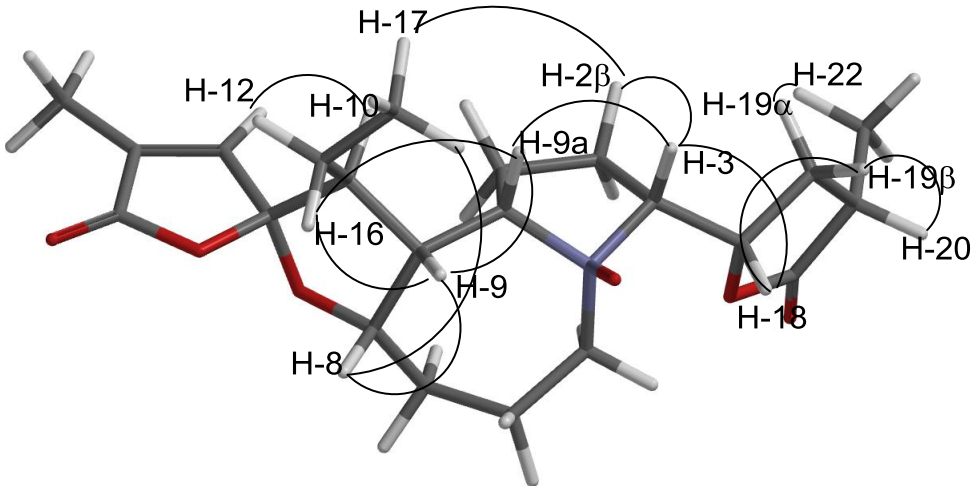

Figure 5.5 Spartan '10 generated AM1 structure of stichoneurine C (**190**) showing key NOESY cross-peaks. The structure was generated using Spartan '10 and conformational searching (MMFF) to find the lowest energy conformers.

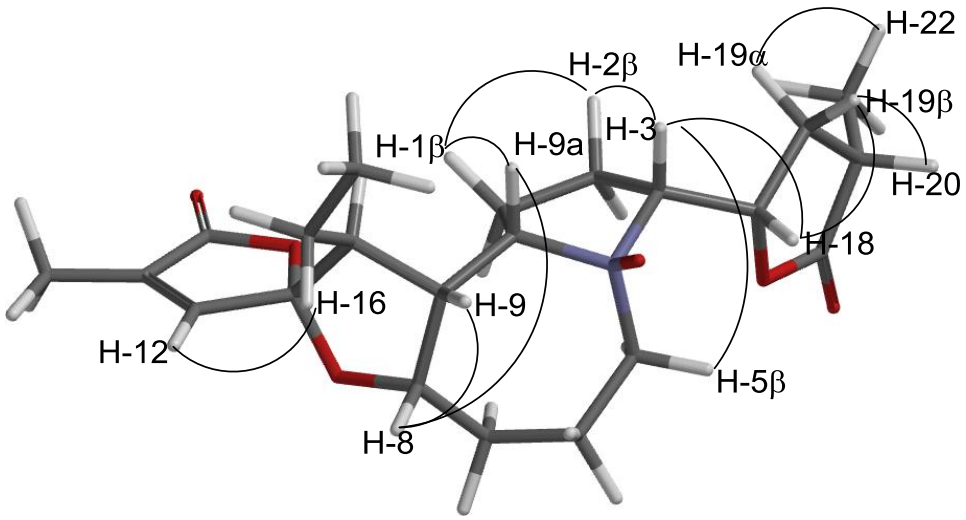

Figure 5.6 Spartan '10 generated AM1 structure of stichoneurine D (**191**) showing key NOESY cross-peaks. The structure was generated using Spartan '10 and conformational searching (MMFF) to find the lowest energy conformers.

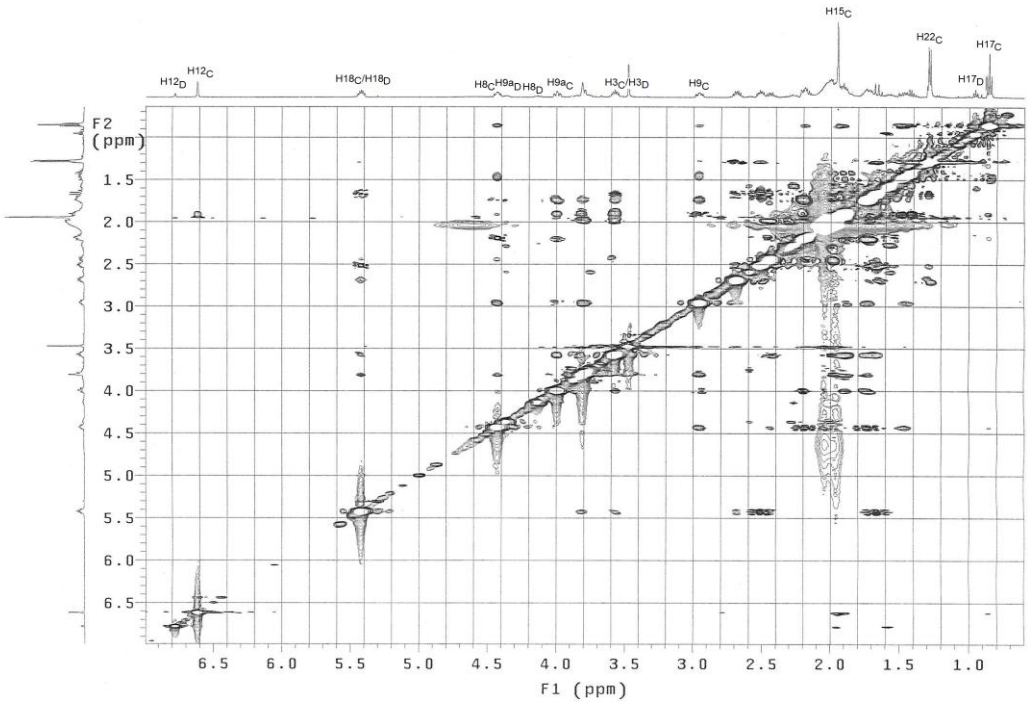

Figure 5.7 NOESY NMR spectrum ($CDCl_3$, 500 MHz) of stichoneurine C and D (**190-191**).

Table 5.1 ^{13}C (125 Hz), ^{1}H (500 MHz) and HMBC NMR spectroscopic data for stichoneurine C (**190**) and a comparison with stemoninine (**49**),[76] in $CDCl_3$ solution (δ in ppm).

Position	δ_C		δ_H (mult., *J* (Hz), assign.)		HMBC of stichoneurine C (190)
	Stemoninine (49)[76]	Stichoneurine C (190)	Stemoninine (49)[76]	Stichoneurine C (190)	
1α	26.3	34.9	1.75 (m)	2.18 (q, *J* 6.5)	2, 3
β	-		1.50 (m)	1.75 (ddd, *J* 6.5, 6.5, 5.2)	-
2α	26.5	24.1	1.80(m)	2.03-1.93 (m)	-
β	-		1.35 (m)	2.44 (dddd, *J* 6.5, 6.5, 6.5)	3
3	63.4	75.5	3.25 (ddd, *J* 10.0, 7.0, 5.5)	3.57 (ddd, *J* 12.0, 6.5, 6.5)	2, 1, 18
5α	45.6	67.7	3.41 (dd, *J* 15.5, 9.0)	3.77-3.68 (m)	-
β	-		2.86 (dd, *J* 15.5, 11.5)	3.89-3.81 (m)	2, 6
6	20.2	21.3	1.57 (m)	2.03-1.86 (m)	7
	-		1.33 (m)	2.03-1.86 (m)	-
7α	35.3	34.9	2.03 (m)	1.75-1.60 (m)	-
β	-		1.43 (m)	2.23-2.15 (m)	-
8	81.1	85.8	3.93 (ddd, *J* 3.5, 9.5, 11.0)	4.43 (dt, *J* 13.7, 5.2, 5.2)	10
9	52.4	48.7	2.43 (ddd, *J* 11.0, 9.5, 5.5)	2.95 (ddd, *J* 13.7, 10.8, 4.9)	1, 7
9a	58.3	78.8	3.68 (dt, *J* 9.5, 6.0, 6.0)	3.99 (dt, *J* 10.8, 10.8, 3.4)	1
10	51.2	51.5	1.93 (ddd, *J* 12.0, 7.0, 5.5)	1.92 (ddd, *J* 12.6, 6.3, 4.9)	16, 17
11	113.5	112.4	-	-	10, 12, 16
12	144.4	143.7	6.56 (d, *J* 2.0)	6.61 (d, *J* 1.3)	15
13	133.5	134.7	-	-	15
14	171.3	171.1	-	-	15
15 (Me)	10.3	10.7	1.85 (d, *J* 2.0)	1.95 (d, *J* 1.3)	-
16	20.0	19.5	a: 1.60 (m)*	1.51-1.39 (m)	10, 17
	-		b: 1.28 (m)*	1.51-1.39 (m)	-
17 (Me)	12.7	13.0	0.77 (t, 7.5)	0.85 (t, *J* 7.5)	16
18	82.4	73.5	4.14 (ddd, *J* 10.0, 7.0, 5.5)	5.42 (dt, *J* 12.1, 6.5, 6.5)	19, 3
19α	34.1	35.4	2.31 (ddd, *J* 12.0, 9.0,5.5)	1.77-1.60 (m)	-
β	-		1.43 (m)	2.51 (ddd, *J* 12.5, 12.0, 6.5)	20
20	34.7	35.3	2.54 (ddq, *J* 12.0, 9.0, 7.0)	2.68 (ddd, *J* 12.5, 12.0, 7.0)	19
21	179.1	178.3	-	-	19, 20
22 (Me)	14.9	14.7	1.17 (d, *J* 7.0)	1.27 (d, *J* 7.0)	19, 20

*a and b represent the two diastereotopic protons at C-16. Their stereochemistries (α and β) were not determined.

Table 5.2 ^{13}C (125 Hz), ^{1}H (500 MHz) and HMBC NMR spectroscopic data for stichoneurine D (**191**) in $CDCl_3$ solution (δ in ppm).

Position	δ_C	δ_H (mult., *J* (Hz), assign.)	HMBC
1α	33.2	1.59-1.52 (m)	-
β		2.31-2.22 (m)	2, 3
2α	24.1	2.03-1.92 (m)	-
β		2.50-2.42 (m)	3
3	75.5	3.57 (overlap)	2, 18
5α	68.1	3.77-3.68 (overlap)	-
β		3.87-3.75 (overlap)	-
6	21.0	1.92-1.88 (m)	-
		1.92-1.88 (m)	-
7α	33.5	2.31-2.22 (m)	-
β		2.31-2.22 (m)	-
8	86.8	4.37 (ddd, *J* 11.0, 8.0, 5.0)	7
9	50.7	2.59 (ddd, *J* 12.5, 10.0, 4.5)	1, 7
9a	78.7	4.13 (ddd, *J* 7.5, 7.5, 3.5)	-
10	53.0	2.21-2.10 (m)	16, 17
11	113.7	-	-
12	142.5	6.78 (d, *J* 1.3)	15
13	134.1	-	15
14	171.3	-	15
15 (Me)	10.8	1.95 (overlap)	-
16	19.5	1.60-1.57 (m)	17
		1.60-1.57 (m)	-
17 (Me)	12.2	0.95 (t, 7.5)	16
18	73.3	5.42 (overlap)	19, 3
19α	35.4	1.77-1.60 (overlap)	-
β		2.51 (overlap)	20
20	35.2	2.68 (overlap)	19
21	178.3	-	19, 20
22 (Me)	14.7	1.27 (overlap)	19, 20

5.2.2 (+)-α-Tocopherol (188)

(+)-α-Tocopherol (**188**) was isolated as a white powder; EIMS *m/z* 430 $[M]^+$, consistent with molecular $C_{29}H_{50}O_2$ (MW 430); $[\alpha]_D^{25}$= +28.4° (*c* 0.075, $CHCl_3$) [literature value: $[\alpha]_D^0$ = +82° (EtOH);[78] $[\alpha]_D^{25}$ = +4.8° (EtOH).[79] These differences in specific rotations are difficult to rationalize. Clearly the specific rotation in EtOH is temperature sensitive and most likely solvent dependent. The ^{1}H NMR spectrum of (+)-

α-tocopherol is shown in Figure 5.8. The structure of (+)-α-tocopherol was confirmed from a comparison of its NMR spectroscopic data with those in the literature.[80] The chemical shifts are in close agreement with those previously reported as summarized in Table 5.3.

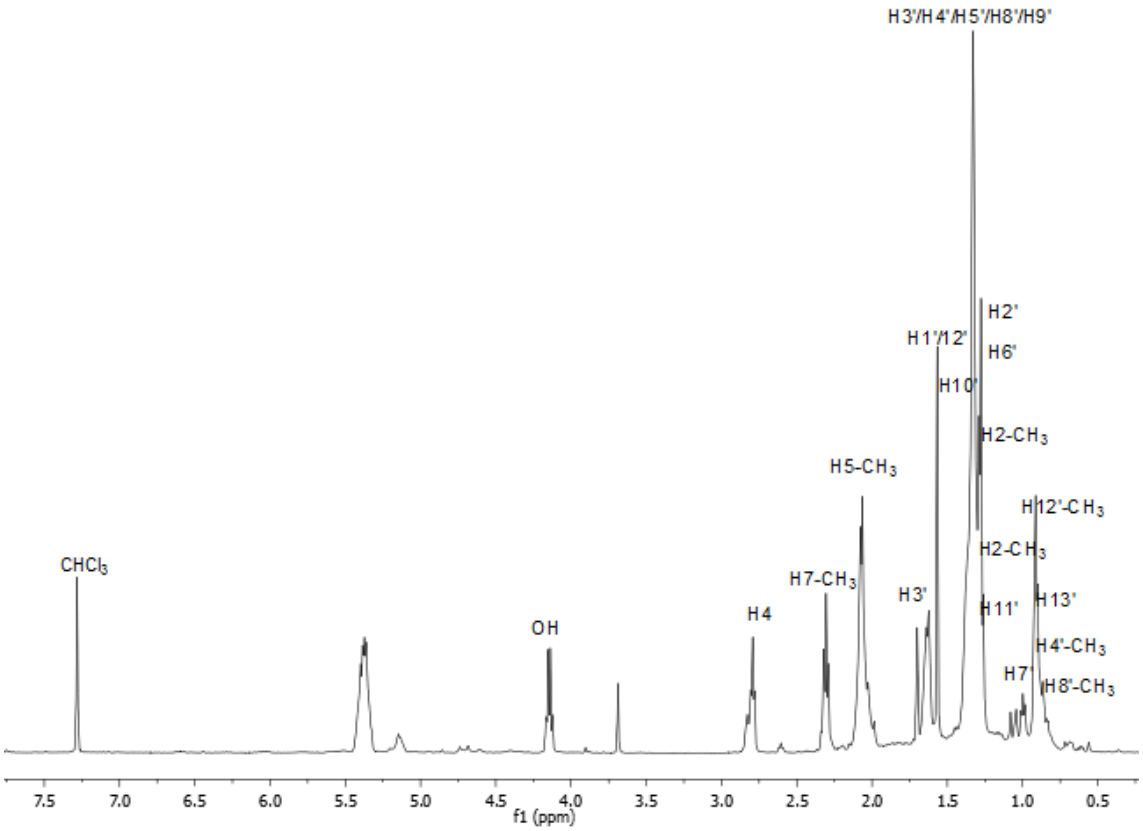

Figure 5.8 ^{1}H NMR spectrum ($CDCl_3$, 500 MHz) of (+)-α-tocopherol (**188**).

Table 5.3 ^{13}C (125 Hz) and ^{1}H NMR (500 MHz) spectroscopic data of (+)-α-tocopherol (this work) and (+)-α-tocopherol (**188**)[80] in $CDCl_3$ solution (δ in ppm).

Data	**Experimental**	**Literature**[80]
Position	**δ_H (mult., *J* (Hz), assign.)**	**δ_H (mult., *J* (Hz), assign.)**
3	1.70 (m)	1.80
4	2.80 (t, *J* 7.5)	2.70
1′	1.56 (s)	1.50
2′	1.29	1.30
3′	1.33	1.40
4′	1.33	1.40
5′	1.33	1.40
6′	1.29	1.30
7′	1.09	1.10
8′	1.33	1.40
9′	1.33	1.40
10′	1.39	1.40
11′	1.26	1.30
12′	1.56 (s)	1.50
2-CH_3	1.28	1.22
5-CH_3	2.08 (t, *J* 6.5)	2.11
7-CH_3	2.31	2.25
8-CH_3	2.08	2.11
4′-CH_3	0.87	0.84
8′-CH_3	0.83	0.83
12′-CH_3	0.91	0.88
13′	0.90	0.85
6-OH	4.15	4.18

5.2.3 (*R*)-(+)-Goniothalamin (189)

(*R*)-(+)-Goniothalamin (**189**) was isolated as a yellow gum; EIMS *m/z* 200 $[M]^+$, consistent with molecular $C_{13}H_{12}O_2$ (MW 200); $[\alpha]_D^{25}$ = +110° (*c* 0.96, $CHCl_3$) [literature value: $[\alpha]_D^{25}$ = +170.3 (*c* 1.38, $CHCl_3$)].[81] The ^{1}H and ^{13}C-APT NMR spectra of (*R*)-(+)-goniothalamin are shown in Figure 5.9 and 5.10. The structure of (*R*)-(+)-goniothalamin was confirmed from a comparison of its NMR spectroscopic data with those in the literature.[82] The chemical shifts are in close agreement with those previously reported as summarized in Table 5.4.

Table 5.4 ^{13}C (125 Hz) and ^{1}H NMR (500 MHz) spectroscopic data of (*R*)-(+)-goniothalamin and (*R*)-(+)-goniothalamin (**189**)[82] in $CDCl_3$ solution (δ in ppm).

Data	**Experimental**		**Literature**[82]	
Position	δ_C	δ_H **(mult., *J* (Hz), assign.)**	δ_C	δ_H **(mult., *J* (Hz), assign.)**
2	163.8	-	163.9	-
3	121.7	6.09 (dt, *J* 10.0, 2.0)	121.5	6.09 (dt, *J* 10.0, 2.0)
4	144.6	6.93 (dt, *J* 9.5, 4.0)	144.7	6.93 (dt, *J* 10.0, 4.0)
5	29.9	2.54 (m)	29.8	2.54 (m)
6	77.9	5.10 (qd, 7.5, 1.0)	77.9	5.10 (qd, 7.0, 1.0)
1'	125.6	6.27 (dd, *J* 15.5, 6.0)	125.6	6.27 (dd, *J* 16.0, 6.0)
2'	133.1	6.73 (d, *J* 15.5)	133.1	6.73 (d, *J* 16.0)
1"	135.7	-	135.7	-
2"/6"	126.9	7.32-7.40 (m)	126.6	7.30 (m)
3"/5"	128.6	7.26-7.40 (m)	128.6	7.30 (m)
4"	128.3	7.27 (t, *J* 7.5)	128.5	7.30 (m)

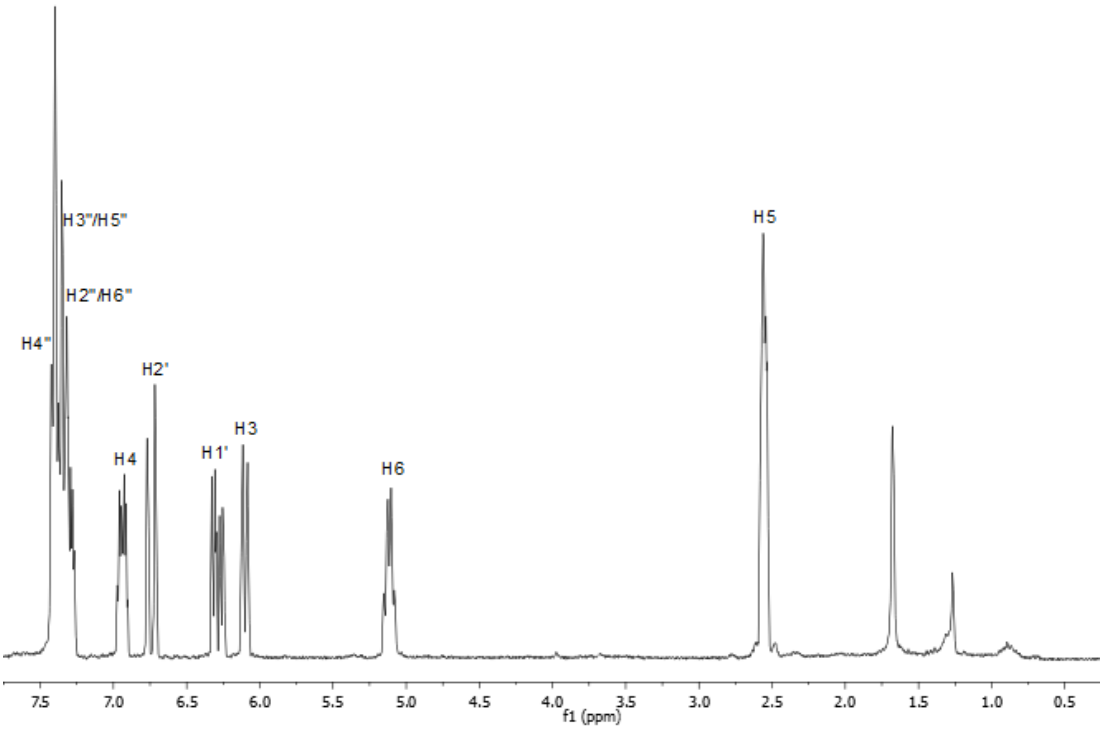

Figure 5.9 ^{1}H NMR spectrum ($CDCl_3$, 500 MHz) of (*R*)-(+)-goniothalamin (**189**).

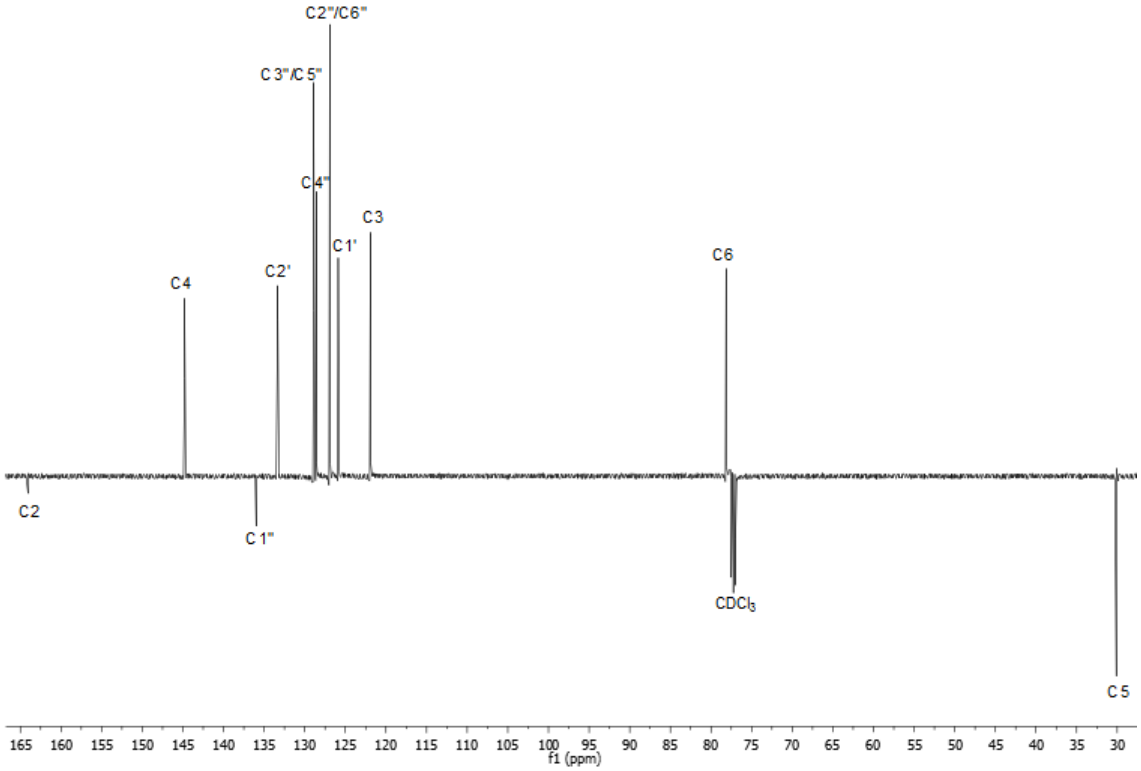

Figure 5.10 ^{13}C-APT NMR spectrum ($CDCl_3$, 125 MHz) of (*R*)-(+)-goniothalamin (**189**).

5.2.4 Stemoninine (49)

Stemoninine (**49**) was isolated as a brown gum; ESIMS *m/z* 390 $[M+H]^+$, consistent with molecular $C_{22}H_{31}NO_5$ (MW 389). The ^{1}H and ^{13}C-APT NMR spectra of stemoninine are shown in Figure 5.11 and 5.12. The structure of stemoninine was confirmed from a comparison of its NMR spectroscopic data with those in the literature.[76] The chemical shifts are in close agreement with those previously reported as summarized in Table 5.5.

Table 5.5 ^{13}C (125 Hz) and ^{1}H NMR (500 MHz) spectroscopic data of stemoninine (this work) and stemoninine (**49**)[76] in $CDCl_3$ solution (δ in ppm).

Data	**Experimental**		**Literature**[76]	
Position	δ_C	δ_H **(mult., *J* (Hz), assign.)**	δ_C	δ_H **(mult., *J* (Hz), assign.)**
1α	26.4	1.81-1.78 (m)	26.3	1.75 (m)
β	-	1.57-1.53 (m)	-	1.50 (m)
2α	26.6	1.83-1.79 (m)	26.5	1.80(m)
β	-	1.44-1.40 (m)	-	1.35 (m)
3	63.2	3.41 (ddd, *J* 9.0, 7.0, 5.5)	63.4	3.25 (ddd, *J* 10.0, 7.0, 5.5)
5α	45.5	3.46 (dd, *J* 15.5, 9.0)	45.6	3.41 (dd, *J* 15.5, 9.0)
β	-	2.93 (dd, *J* 15.5, 11.5)	-	2.86 (dd, *J* 15.5, 11.5)
6	20.1	1.63-1.59 (m)	20.2	1.57 (m)
	-	1.39-1.36 (m)	-	1.33 (m)
7α	35.3	2.16-2.12 (m)	35.3	2.03 (m)
β	-	1.51-1.48 (m)	-	1.43 (m)
8	81.3	4.00 (ddd, *J* 11.0, 9.5, 3.5)	81.1	3.93 (ddd, *J* 11.0, 9.5, 3.5)
9	52.5	2.51 (ddd, *J* 11.0, 9.5, 5.5)	52.4	2.43 (ddd, *J* 11.0, 9.5, 5.5)
9a	58.2	3.75 (dt, *J* 9.5, 5.5, 5.5)	58.3	3.68 (dt, *J* 9.5, 6.0, 6.0)
10	51.2	1.98 (ddd, 12.0, 7.0, 5.5)	51.2	1.93 (ddd, *J* 12.0, 7.0, 5.5)
11	113.5	-	113.5	-
12	144.4	6.64 (d, *J* 2.0)	144.4	6.56 (d, *J* 2.0)
13	133.7	-	133.5	-
14	171.5	-	171.3	-
15 (Me)	10.5	1.94 (d, *J* 2.0)	10.3	1.85 (d, *J* 2.0)
16	20.0	1.65-1.61 (m)	20.0	a: 1.60 (m)
	-	1.39-1.35 (m)	-	b: 1.28 (m)
17 (Me)	12.9	0.85 (t, *J* 7.5)	12.7	0.77 (t, 7.5)
18	82.8	4.20 (ddd)	82.4	4.14 (ddd, *J* 10.0, 7.0, 5.5)
19α	34.2	2.36 (*J* 13.0, 8.5, 5.5)	34.1	2.31 (ddd, *J* 12.0, 9.0,5.5)
β	-	1.51-1.48 (m)	-	1.43 (m)
20	34.8	2.62 (ddq, *J* 12.0, 9.0, 7.0)	34.7	2.54 (ddq, *J* 12.0, 9.0, 7.0)
21	179.5	-	179.1	-
22 (Me)	14.8	1.25 (d, *J* 7.0)	14.98	1.17 (d, *J* 7.0)

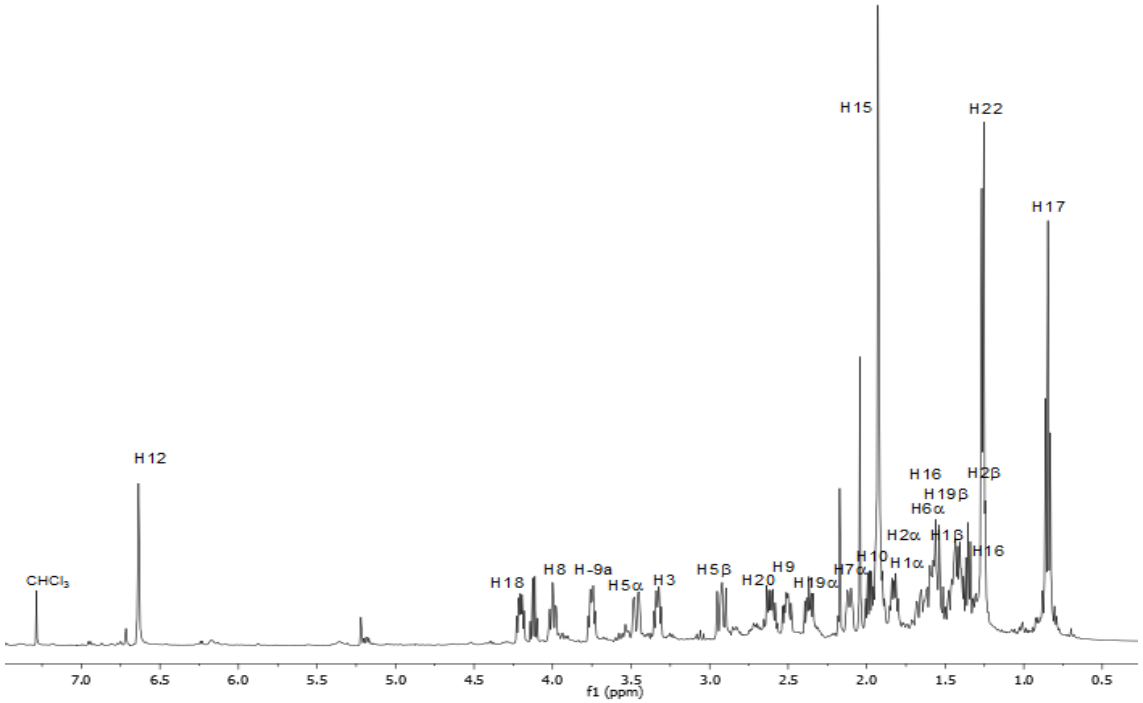

Figure 5.11 ^{1}H NMR spectrum ($CDCl_3$, 500 MHz) of stemoninine (**49**).

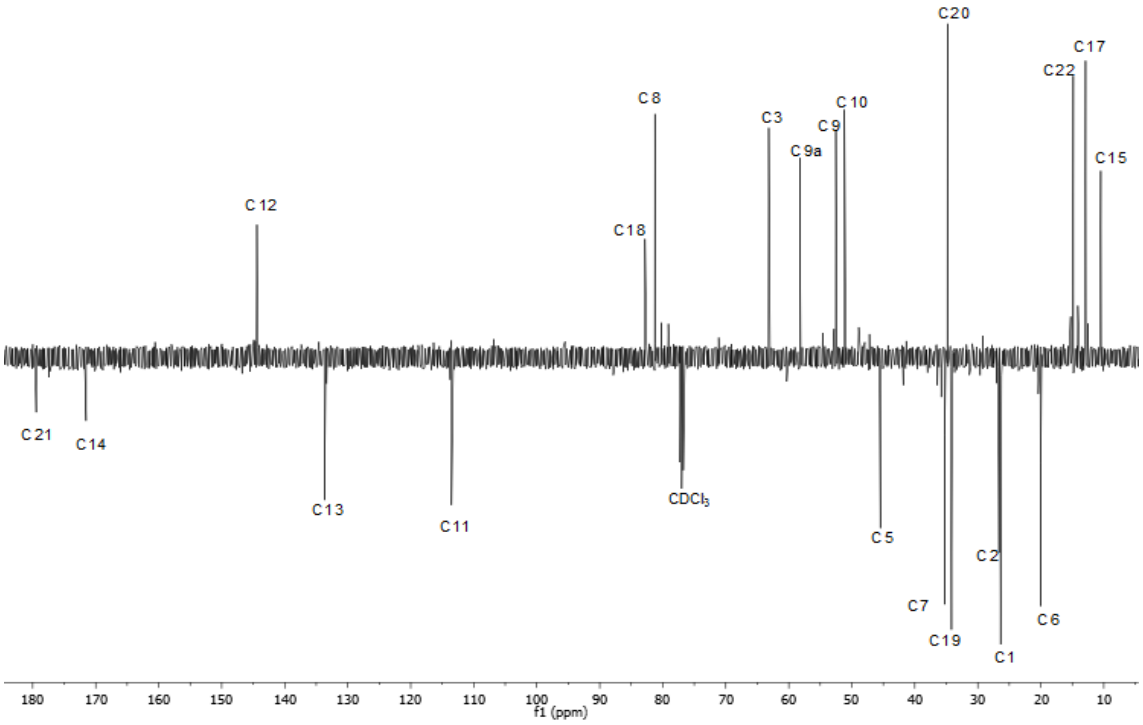

Figure 5.12 ^{13}C-APT NMR spectrum ($CDCl_3$, 125 MHz) of stemoninine (**49**).

5.2.5 Bisdehydrostemoninine A (60)

Bisdehydrostemoninine A (**60**) was isolated as a brown gum; ESIMS *m/z* 402 $[M+H]^+$, consistent with molecular $C_{22}H_{27}NO_6$ (MW 401). The ^1H and ^{13}C NMR spectra of bisdehydrostemoninine A are shown in Figure 5.13 and 5.14. The structure of bisdehydrostemoninine A was confirmed from a comparison of its NMR spectroscopic data with those in the literature.[18] The chemical shifts are in close agreement with those previously reported as summarized in Table 5.6.

Table 5.6 ^{13}C (125 Hz) and ^1H NMR (500 MHz) spectroscopic data of bisdehydrostemoninines A (this work) and bisdehydrostemoninines A (**60**)[18] in $CDCl_3$ solution (δ in ppm).

Data	**Experimental**		**Literature**[18]	
Position	**δ_C**	**δ_H (mult., *J* (Hz), assign.)**	**δ_C**	**δ_H (mult., *J* (Hz), assign.)**
1	105.1	5.94 (d, *J* 4.5)	104.9	5.94 (d, *J* 4.0)
2	119.6	6.96 (d, *J* 4.0)	119.4	6.95 (d, *J* 4.1)
3	140.3	-	140.1	-
5α	45.4	5.81 (dd, *J* 4.5, 14.5)	45.3	5.80 (dd, *J* 14.7, 5.7)
β	-	3.61-3.58 (m)	-	3.68 (dd, *J* 14.3, 2.8)
6α	26.0	2.07-2.04 (m)	25.9	2.08 (m)
β	-	1.64-1.60 (m)	-	1.62 (m)
7α	35.7	2.33-2.30 (m)	35.6	2.31 (m)
β	-	1.86-1.83 (m)	-	1.85 (m)
8	83.7	3.70-3.67 (m)	84.5	3.70 (m)
9	47.3	3.28-3.25 (m)	47.2	3.25 (m)
9a	130.5	-	130.4	-
10	50.7	2.60 (ddd, *J* 12.5, 9.0, 3.5)	50.5	2.58 (ddd, *J* 12.5, 8.9, 3.5)
11	113.2	-	113.0	-
12	145.1	6.76 (d, *J* 1.6)	144.9	6.75 (d, *J* 1.6)
13	133.9	-	133.6	-
14	171.6	-	171.4	-
15 (Me)	10.8	1.96 (s)	10.6	1.98 (d, *J* 1.5)
16a	20.1	1.74-1.70 (m)	19.9	1.72 (m)
b	-	1.66-1.63 (m)	-	1.64 (m)
17 (Me)	13.2	0.91 (t, *J* 7.5)	13.0	0.91 (t, *J* 7.5)
18	188.9	-	188.7	-
19α	42.5	3.28-3.25 (m)	42.3	3.25 (m)
β	-	2.94-2.90 (m)	-	2.92 (m)
20	35.2	3.07-3.03 (m)	35.0	3.12 (dq, *J* 7.3, 2.0)
21	181.2	-	181.3	-
22 (Me)	17.3	1.28 (d, *J* 7.5)	17.1	1.27 (d, *J* 7.2)

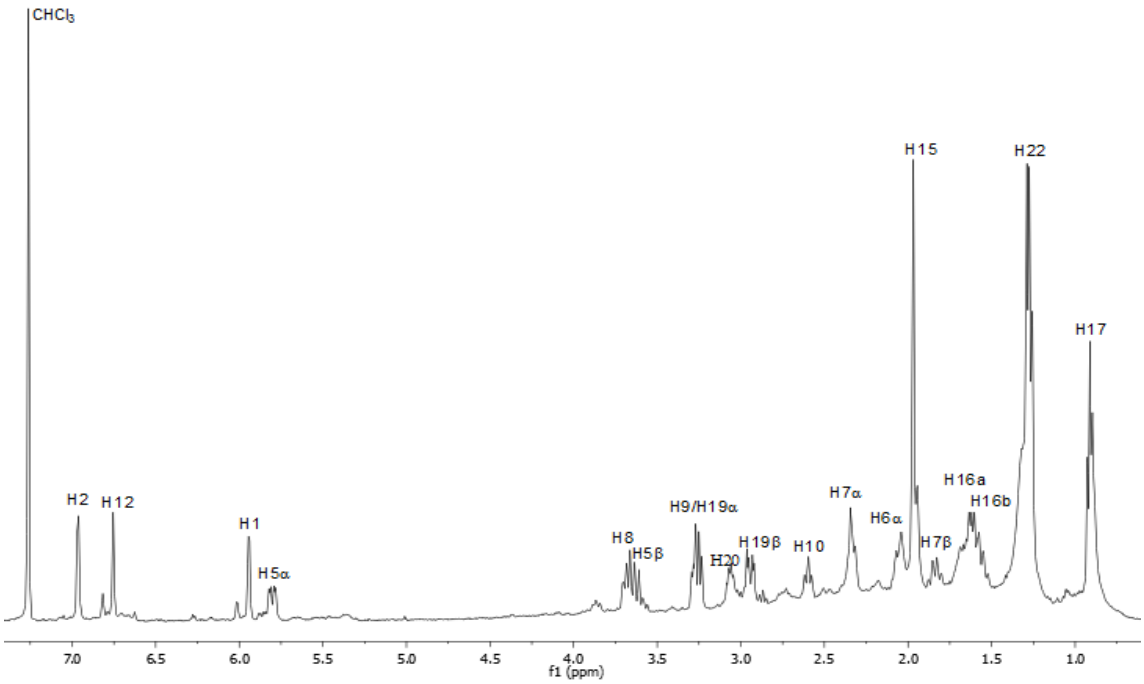

Figure 5.13 ^{1}H NMR spectrum ($CDCl_3$, 500 MHz) of bisdehydrostemoninine A (**60**).

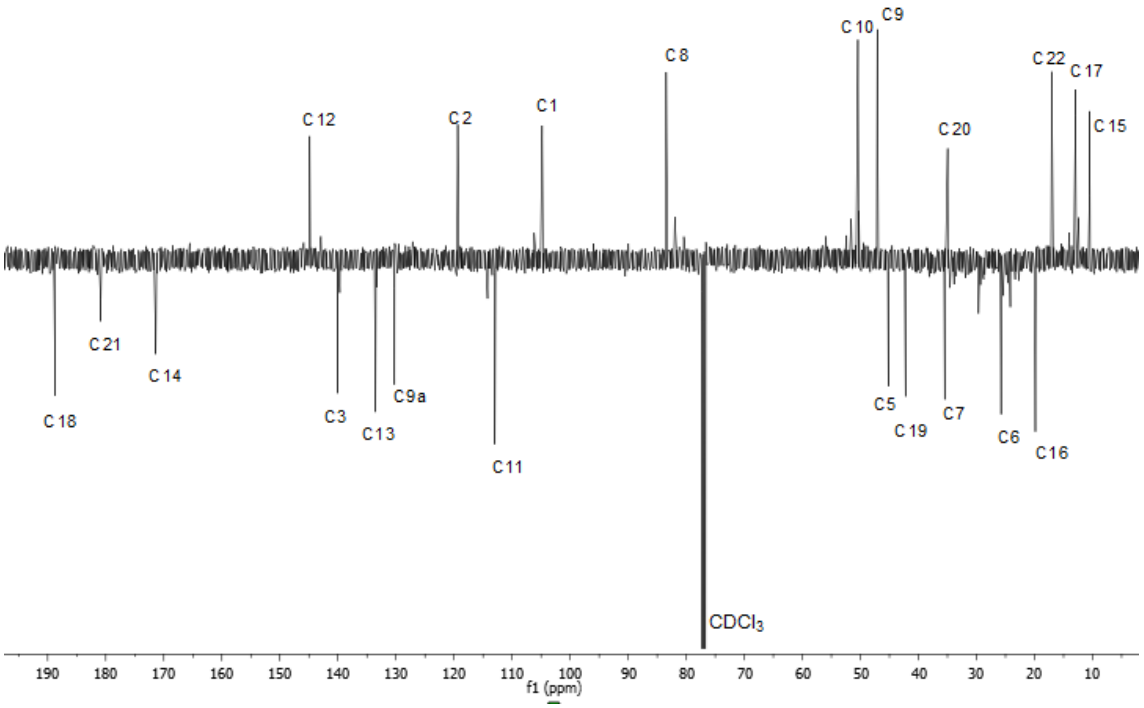

Figure 5.14 ^{13}C-APT NMR spectrum ($CDCl_3$, 125 MHz) of bisdehydrostemoninine A (**60**).

5.2.6 Sessilistemoamine A (96)

Sessilistemoamine A (**96**) was isolated as a yellow gum; ESIMS *m/z* 392 $[M+H]^+$, consistent with molecular $C_{22}H_{33}NO_5$ (MW 391). The ^1H NMR spectrum of sessilistemoamine A is shown in Figure 5.15. The structure of sessilistemoamine A was confirmed from a comparison of its NMR spectroscopic data with those in the literature.[25] The chemical shifts are in close agreement with those previously reported as summarized in Table 5.7.

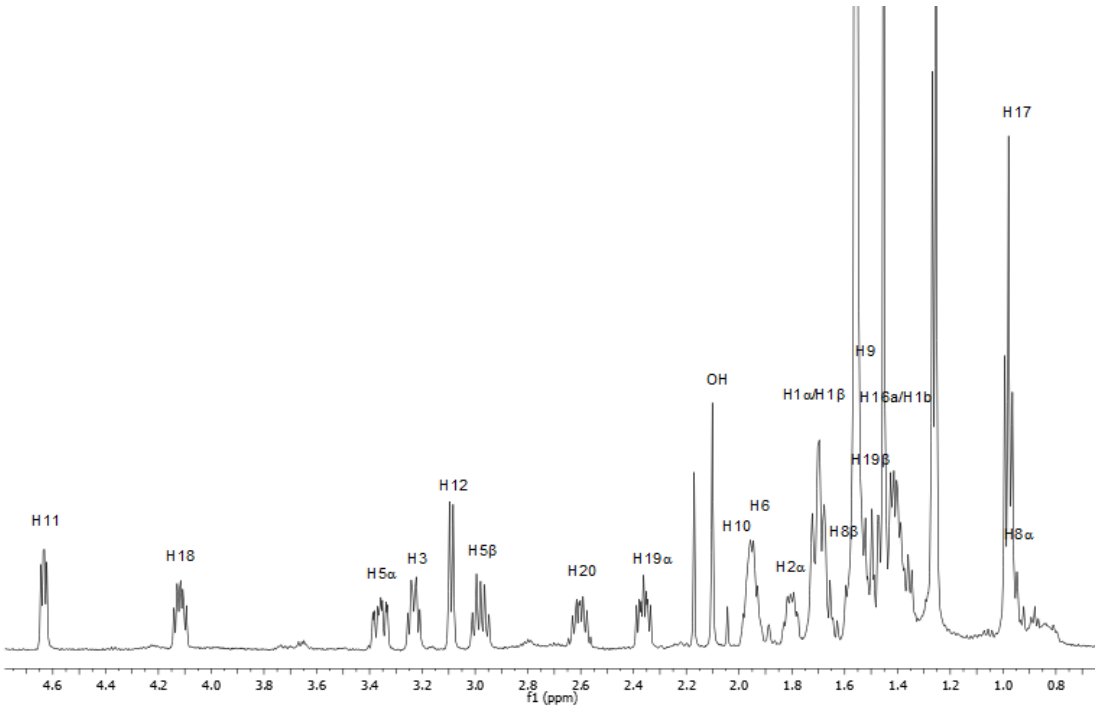

Figure 5.15 ^1H NMR spectrum ($CDCl_3$, 500 MHz) of sessilistemoamine A (**96**).

Table 5.7 ^{1}H NMR (500 MHz) spectroscopic data of sessilistemonamine A (this work) and sessilistemonamone A (**96**)[25] in $CDCl_3$ solution (δ in ppm).

Data	**Experimental**	**Literature**[25]
Position	**δ_H (mult., *J* (Hz), assign.)**	**δ_H (mult., *J* (Hz), assign.)**
1α	1.66-1.72 (m)	1.66-1.71 (m)
β	1.66-1.72 (m)	1.66-1.71 (m)
2α	1.77-1.84 (m)	1.77-1.81 (m)
β	1.46-1.50 (m)	1.46-1.50 (m)
3	3.23 (dt, *J* 9.0, 7.0)	3.23 (dt, *J* 7.0, 9.0)
5α	3.35 (ddd, *J* 15.0, 10.0, 2.5)	3.35 (ddd, *J* 15.5, 9.5, 3.0)
β	2.98 (dt, *J* 16.0, 7.5)	2.97 (dt, *J* 15.5, 8.0)
6α	1.92-1.97 (m)	1.92-1.97 (m)
β	1.37-1.42 (m)	1.37-1.42 (m)
7α	1.66-1.71 (m)	1.66-1.71 (m)
β	1.50-1.55 (m)	1.50-1.55 (m)
8α	0.94-0.97 (m)	0.94-0.97 (m)
β	1.66-1.71 (m)	1.66-1.71 (m)
9	1.54-1.58 (m)	1.54-1.58 (m)
9a	-	-
10	1.92-1.97 (m)	1.92-1.97 (m)
11	4.63 (dd, *J* 6.5, 4.0)	4.63 (dd, *J* 6.5, 4.5)
12	3.09 (d, *J* 6.5)	3.08 (d, *J* 6.5)
13	-	-
14	-	-
15 (Me)	1.45 (s)	1.44 (s)
16a	1.35-1.42 (m)	1.38-1.42 (m)
b	1.35-1.42 (m)	1.38-1.42 (m)
17 (Me)	0.98 (t, *J* 7.5)	0.97 (t, *J* 7.5)
18	4.12 (ddd, *J* 10.0, 7.0, 5.5)	4.11 (ddd, *J* 10.0, 7.0, 5.5)
19α	2.33-2.39 (m)	2.33-2.38 (m)
β	1.47-1.52 (m)	1.47-1.52 (m)
20	2.55-2.64 (m)	2.57-2.63 (m)
21	-	-
22 (Me)	1.25 (d, *J* 7.0)	1.25 (d, *J* 7.0)
13-OH	2.10 (br s)	2.42 (br s)

5.2.7 Sessilistemoamine C (98)

Sessilistemoamine C (**98**) was isolated as a yellow gum; ESIMS *m/z* 392 $[M+H]^+$, consistent with molecular $C_{22}H_{33}NO_5$ (MW 391). The ^1H NMR spectrum of sessilistemoamine C is shown in Figure 5.16. The structure of sessilistemoamine C was confirmed from a comparison of its NMR spectroscopic data with those in the literature.[25] The chemical shifts are in close agreement with those previously reported as summarized in Table 5.8.

Table 5.8 ^1H NMR (500 MHz) spectroscopic data of sessilistemonamonies C (this work) and sessilistemonamonies C (**98**)[25] in $CDCl_3$ solution (δ in ppm).

Data	**Experimental**	**Literature**[25]
Position	**δ_H (mult., *J* (Hz), assign.)**	**δ_H (mult., *J* (Hz), assign.)**
1α	1.83-1.90 (m)	1.83-1.90 (m)
β	1.74-1.81 (m)	1.74-1.81 (m)
2α	1.81-1.89 (m)	1.81-1.89 (m)
β	1.50-1.54 (m)	1.50-1.54 (m)
3	3.16 (dt, *J* 9.0, 7.0)	3.16 (dt, *J* 9.0, 7.0)
5α	2.44-2.40 (m)	2.41 (m)
β	2.84 (ddd, 13.5, 7.0, 2.5)	2.83 (ddd, *J* 13.5, 6.5, 2.5)
6α	1.84-1.91 (m)	1.84-1.91 (m)
β	1.08-1.15 (m)	1.08-1.15 (m)
7α	1.70-1.78 (m)	1.70-1.78 (m)
β	1.57-1.65 (m)	1.57-1.65 (m)
8α	0.86-0.93 (m)	0.87-0.95 (m)
β	1.62-1.66 (m)	1.62-1.66 (m)
9	1.86-1.91 (m)	1.86-1.91 (m)
9a	-	-
10	1.96-1.98 (m)	1.96-1.98 (m)
11	4.97 (t, *J* 6.0)	4.97 (t, *J* 6.0)
12	2.63 (d, *J* 7.0)	2.62 (d, *J* 6.5)
13	-	-
14	-	-
15 (Me)	1.87 (s)	1.87 (s)
16a	1.69-1.73 (m)	1.69-1.73 (m)
b	1.57-1.59 (m)	1.57-1.59 (m)
17 (Me)	0.98 (t, *J* 7.5)	0.98 (t, *J* 7.0)
18	4.44 (dt, *J* 10.5, 5.5)	4.43 (dt, *J* 10.0, 5.0)
19α	1.55-1.62 (m)	1.55-1.62 (m)
β	2.41-2.48 (m)	2.41-2.48 (m)
20	2.64-2.72 (m)	2.64-2.72 (m)
21	-	-
22 (Me)	1.30 (d, *J* 7.0)	1.30 (d, *J* 7.0)

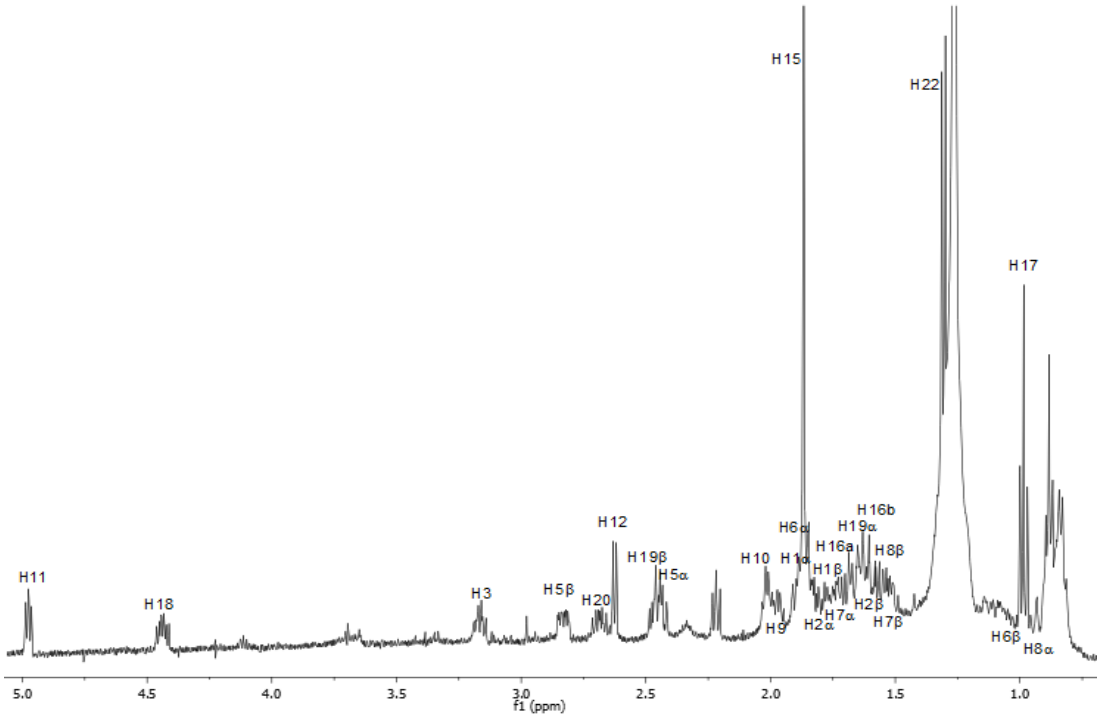

Figure 5.16 ^{1}H NMR spectrum ($CDCl_3$, 500 MHz) of sessilistemoamine C (**98**).

5.3 Isolation and purification of *Stemona* alkaloids from the ethanol extract of the leaves of *St. halabalensis*

The dry ground leaves (248.5 g) of *St. halabalensis* were extracted with 95% EtOH (4 x 1.5 L) over 4 days at rt. The ethanolic extracts were evaporated to give a dark green residue (20.2 g). The ethanol extract of the leaves of *St. halabalensis* was subjected to reversed phase CC using MeOH/H_2O (7.5:2.5) to remove chlorophyll and gave an alkaloid fraction B (953.0 mg). Separation of fraction B by CC (CH_2Cl_2/MeOH, 95:5) gave fraction B1 (120 mg). Further purification of fraction B1 by CC (CH_2Cl_2/MeOH, 95:5) gave stemoninine (**49**, 5.0 mg) and stichoneurine E (**192**, 12.5 mg). The isolated compounds from the leaves of *St. halabalensis* are shown in Figure 5.17.

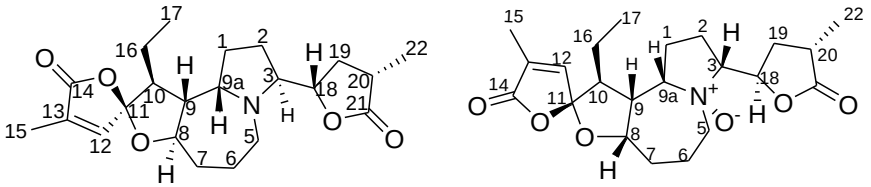

Figure 5.17 Structures of the isolated compounds from the leaf of *St. halabalensis*.

5.3.1 Structure elucidation of Stichoneurine E (192)

Stichoneurine E (**192**) was obtained as a brown gum. Its molecular formula was determined as $C_{22}H_{31}NO_6$ from its HRESIMS (*m/z* 406.2217 $[M+H]^+$, calcd for 406.2230). The IR spectrum of stichoneurine E showed a characteristic γ-lactone carbonyl absorption at 1778 cm^{-1} but not one for the unsaturated γ-lactone. The ^{13}C/DEPT NMR spectrum (Figure 5.18) was similar to that stichoneurine C (**190**) and D (**191**). The ^{13}C NMR signals for stichoneurine E (**192**) corresponded to those of three methyl [δ 10.6 (C-15), 12.8 (C-17) and14.5 (C-22)], seven methylene [δ 19.2 (C-16), 20.8 (C-6), 24.0 (C-2), 24.2 (C-7), 34.4 (C-1), 35.2 (C-19), 66.5 (C-5)], seven methine [δ 34.8 (C-19), 48.1 (C-9), 51.3 (C-10), 72.9 (C-18), 76.1 (C-3), 78.5 (C-9a) and 84.1 (C-8)], two olefinic [δ 143.5 (C-12) and 134.5 (C-13)] and three quaternary carbons [δ 112.2 (C-11), 170.9 (C-14) and 177.9 (C-21)] (Figure 5.18 Table 5.9). The ^1H NMR resonances at δ 0.85 (t, J = 7.5 Hz), 1.27 (d, J = 6.8.0 Hz) and 1.94 (d, J = 1.2 Hz) were assigned to the methyl groups C-17, C-22 and C-15, respectively (Figure 5.19 and Table 5.9). The olefinic proton resonance at δ 6.62 (apparent d, J = 1.3 Hz) was assigned to H-12. The ^{13}C NMR signals at δ 177.9 and 170.9 indicated two lactone carbonyls, while the signal at δ 112.2 indicated a ketal group such as that present in stichoneurine C (**190**) and D (**191**). The COSY and HMBC spectra of stichoneurine E (**192**) showed analogous correlations to those observed in that of stichoneurine C (**190**) and D (**191**).

Key HMBC correlations for stichoneurine E (**192**) are shown in Figure 5.20, while full details are provided in Table 5.9.

The relative stereochemistry assigned to stichoneurine E (**192**) was based on an analysis of its NOESY NMR spectrum (Figure 5.21) and molecular modeling experiments (Figure 5.22). NOESY correlations were observed between H-3 and H-19α and between H-8 and H-9. However, no correlation was observed between H-3 and H-18, which suggested an *anti*-relationship between these protons. NOESY experiments also showed a *syn*-relationship between H-10 and H-12, similar to that found in stichoneurine C (**190**). Thus, stichoneurine E (**192**) is an isomer of stichoneurine C (**190**) at C-3 and C-18.

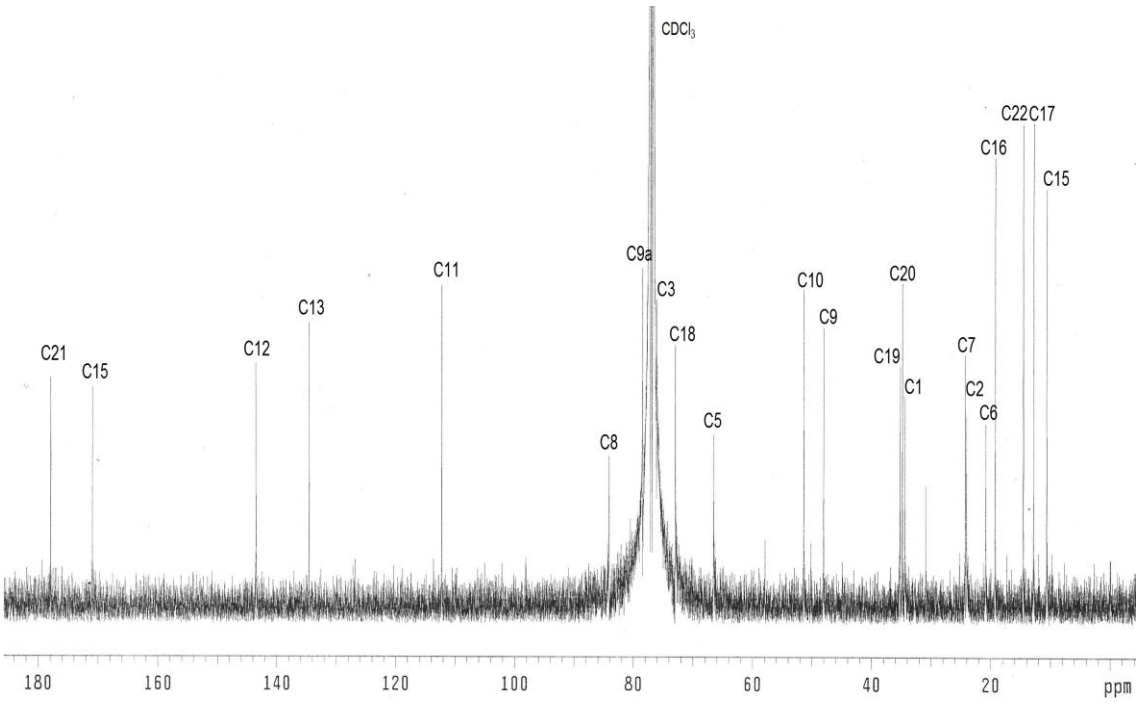

Figure 5.18 ^{13}C NMR spectrum ($CDCl_3$, 125 MHz) of stichoneurine E (**192**).

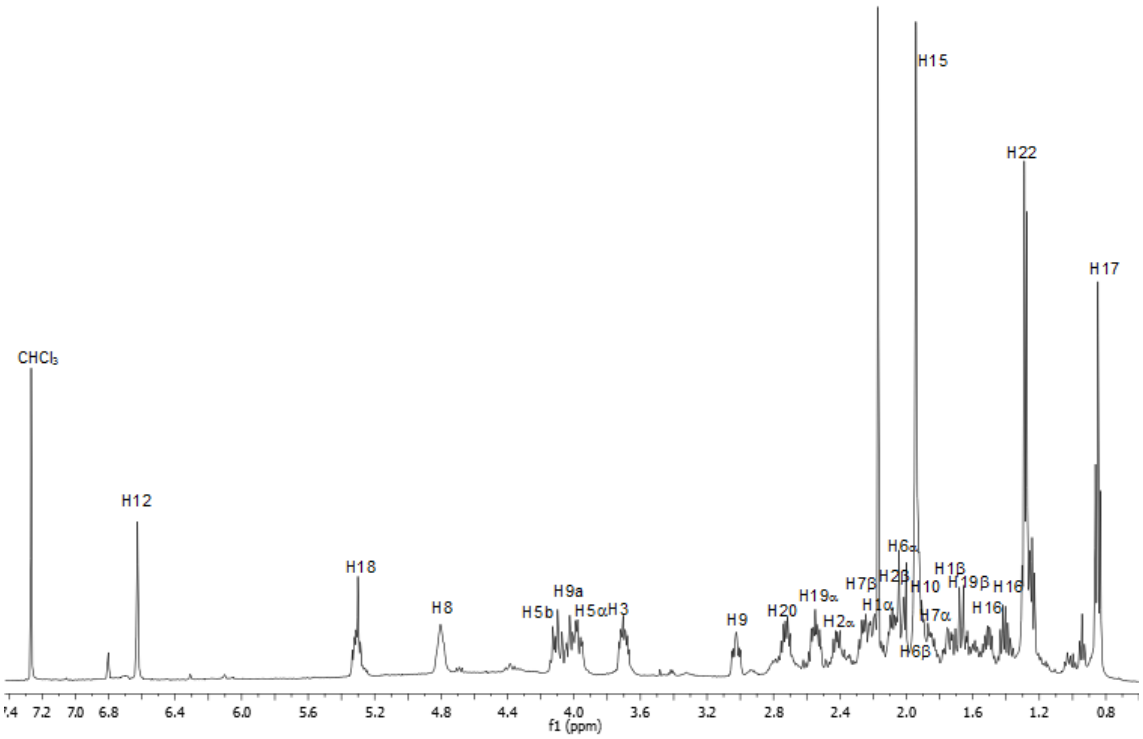

Figure 5.19 ^{1}H NMR spectrum ($CDCl_3$, 500 MHz) of stichoneurine E (**192**).

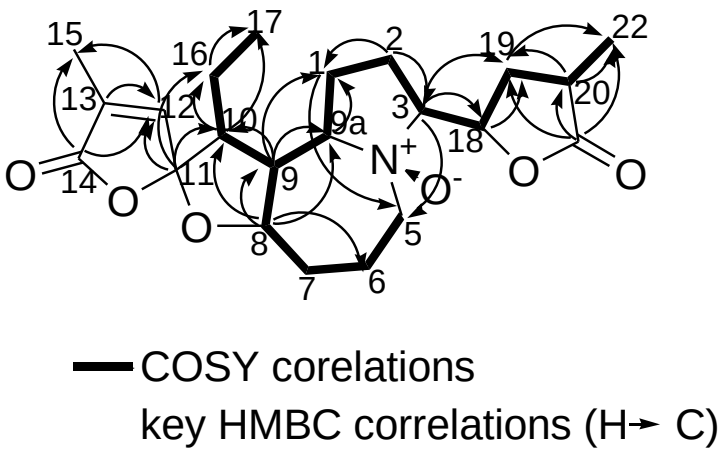

Figure 5.20 Key COSY and HMBC correlations for stichoneurine E (**192**).

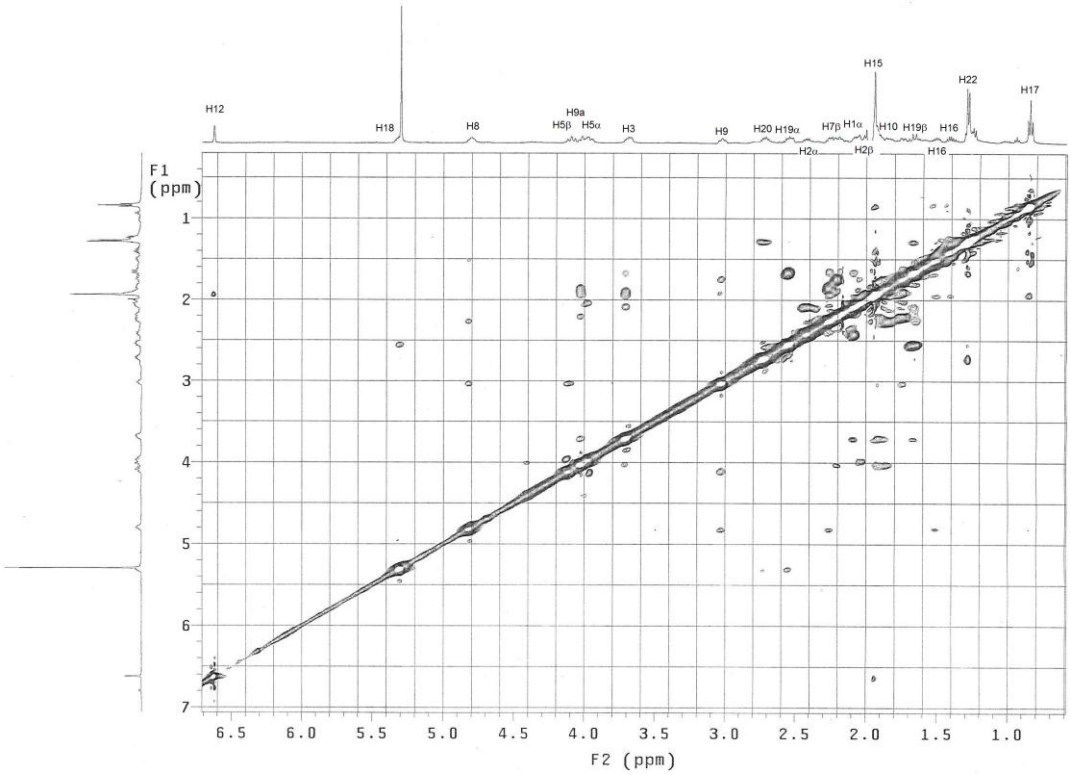

Figure 5.21 ROESY NMR spectrum ($CDCl_3$, 500 MHz) of stichoneurine E (**192**).

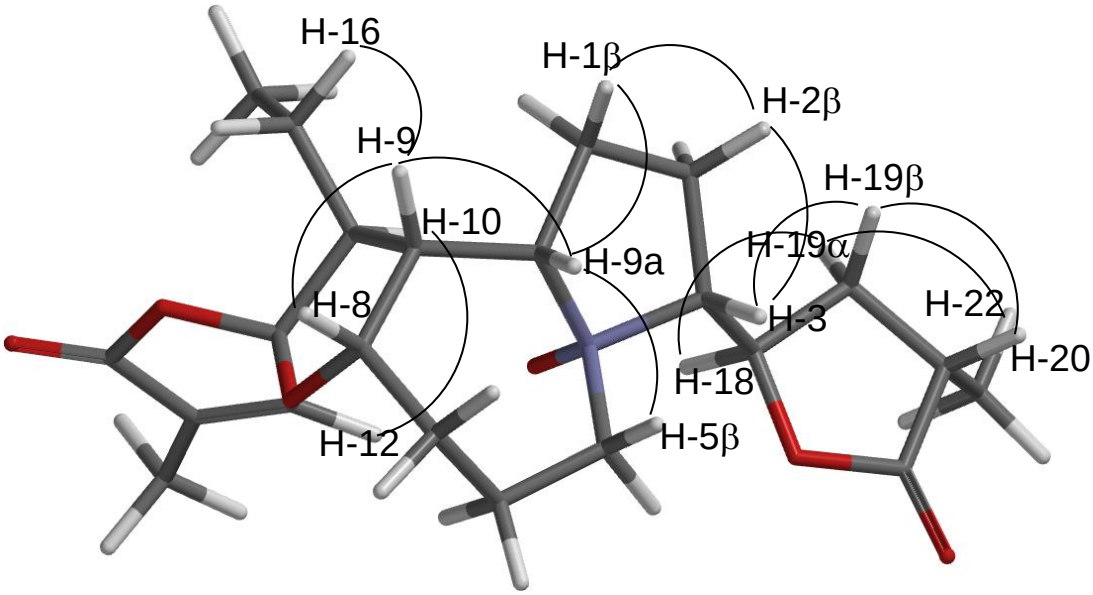

Figure 5.22 Spartan ’10 generated AM1 structure of stichoneurine E (**192**) showing key NOESY cross-peaks.

Table 5.9 ^{13}C (125 Hz), ^{1}H (500 MHz) and HMBC NMR spectroscopic data for stichoneurine E (**192**) in $CDCl_3$ solution (δ in ppm).

Position	δ_C	δ_H **(mult.,** ***J*** **(Hz), assign.)**	**HMBC**
1α	34.4	1.78-1.72 (m)	-
β		2.23-2.19 (m)	5
2α	24.0	2.47-2.39 (m)	-
β		2.14-2.04 (m)	1, 3
3	76.1	3.70 (ddd, *J* 13.6, 7.5, 5.5)	2b, 5b, 18, 19
5α	66.5	4.01-3.93 (m)	-
β		4.15-4.06 (m)	-
6α	20.8	2.06-2.02 (m)	5
β		1.94-1.88 (m)	-
7α	24.2	1.89-1.79 (m)	-
β		2.30-2.22 (m)	-
8	84.1	4.85-4.77 (dt, *J* 18.5, 12.5, 6.0)	2, 6, 9, 9a, 10
9	48.1	3.03 (ddd, *J* 13.6, 9.8, 4.5)	1, 10
9a	78.5	4.06-3.98 (m)	1, 9
10	51.3	1.98-1.89 (m)	9, 16, 17
11	112.2	-	9a, 12, 10, 16
12	143.5	6.62 (d, *J* 1.3)	15
13	134.5	-	10, 12
14	170.9	-	12, 15
15 (Me)	10.6	1.94 (d, *J* 1.2)	12
16	19.2	1.54-1.47 (m)	15, 17
		1.44-1.37 (m)	-
17 (Me)	12.8	0.85 (d, *J* 7.5)	15, 16
18	72.9	5.36-5.26 (m)	3, 19b
19α	35.2	1.72-1.61 (m)	-
β		2.59-2.53 (m)	22
20	34.8	2.76-2.67 (m)	19, 20, 22
21	177.9	-	20, 19, 22
22 (Me)	14.5	1.27 (d, *J* 6.8)	19, 20

5.4 Conclusions

This study of the hitherto unreported *St. halabalensis* led to the characterization of the known compounds (+)-α-tocopherol (**188**) and (*R*)-(+)-goniothalamin (**189**) and seven pyrrolo[1,2-*a*]azepine type alkaloids including four known *Stemona* alkaloids, bisdehydoxystemoninine A (**60**), stemoninine (**49**), sessilistemonamine C (**98**) and sessilistemonamine A (**96**) and three new alkaloids, stichoneurines C (**190**), D (**191**) and E (**192**). Compounds **188**, **189**, **60**, **49**, **98**, **96**, **190** and **191** were isolated from the roots, while only two alkaloids **49** and **192** were isolated from the leaves. Interestingly, the three new alkaloids, stichoneurines C-E (**190**-**192**) are diastereoisomers and have a N-oxide structure. It is possible that **190**-**192** are artifacts are formed by oxidation during the purification procedure, however this seems unlikely since no other alkaloids were isolated as their N-oxides. It would be interesting if further studies can be carrying out to investigate the enzymes or other factors that were involved in their occurrences.

CHAPTER 6

ALKALOIDS FROM THE ROOTS *Stichoneuron caudatum* RIDLEY

6.1 Introduction

This chapter reports on the phytochemical study of the roots extracts of *St. caudatum* collected at Dungun, Terengganu in Malaysia. In 2005, Schinner and co-workers isolated two pyrrolo[1,2-*a*]azepine type alkaloids, stichoneurines A and B (**108** and **109**) from the lipophilic root extracts of *St. caudatum* collected from Than To waterfall, between Yala and Betong, in southern Thailand.[4] The isolation of pyrrolo[1,2-*a*]azepine alkaloids from *Stichoneuron* supported the affiliation of this genus to the family Stemonaceae.

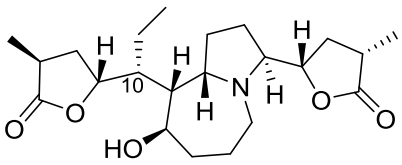

Stichoneurine A (**108**)

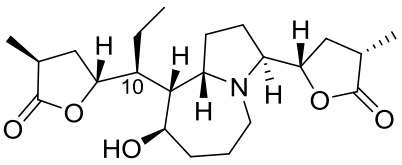

Stichoneurine B (**109**)

6.2 Isolation and purification of *Stemona* alkaloids from ethanol extract of the roots of *St. caudatum*

The dry, ground roots of *S. caudatum* (1.3 kg) were extracted with 95% MeOH (4 × 1000 mL) over 3 days at room temperature. The MeOH solution was evaporated to give a dark residue (56.0 g). The residue was chromatographed on silica gel (200 mL) using gradient elution from *n*-hexane/EtOAc (2:8−0:10) to CH_2Cl_2/EtOAc (2:8−0:10). A total of 5 L of eluent was collected in test tubes of 200 mL. These fractions were pooled on the basis of TLC analysis to give three alkaloid fractions; A (1.5 g), B (150

mg) and C (3.5 g). Further separation and purification of these fractions gave stichoneurine F (**193**, 100.5 mg), sessilistemonamine E (**195**, 3.5 mg), stichoneurine G (**194,** 49.2 mg) and sessilistemonamine F (**196,** 50.2 mg). Figure 6.1 shows the isolated *Stemona* alkaloids from roots of *St. caudatum*.

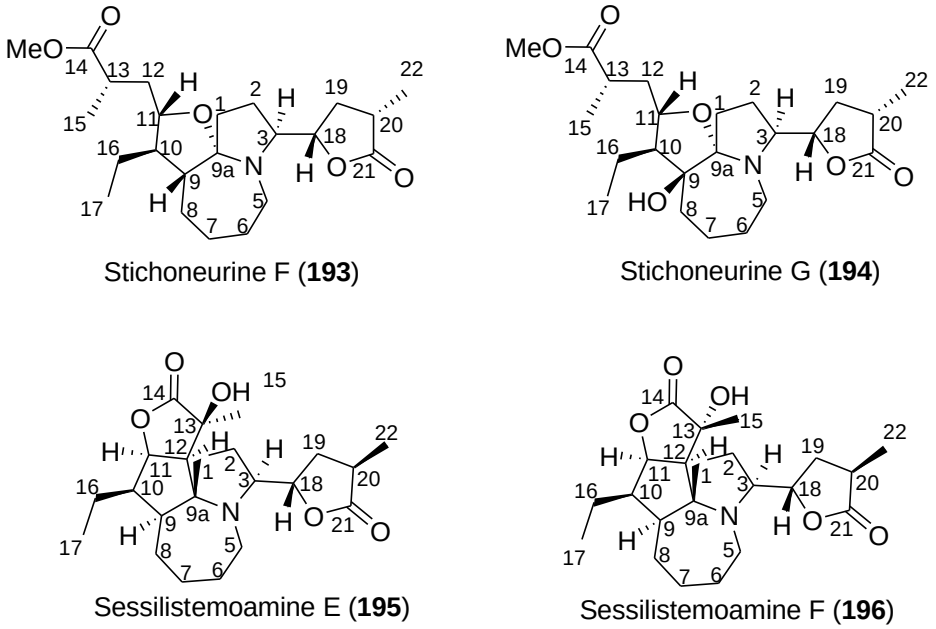

Figure 6.1 Isolated *Stemona* alkaloids from *St. caudatum*.

6.3 Structure elucidation of the isolated *Stemona* alkaloids from the ethanol extract of the roots of *St. caudatum*

6.3.1 Stichoneurine F (193)

Stichoneurine F (**193**) was obtained as a pale yellow gum. Its molecular formula was determined as $C_{23}H_{37}NO_5$ from its HRESIMS (*m/z* 408.2750 $[M+H]^+$, calc. for 408.2753). The IR spectrum of stichoneurine F showed characteristic ester and γ-lactone carbonyl absorptions at 1734 and 1771 cm^{-1}, respectively. The ^{13}C/DEPT NMR spectrum (Figure 6.4) displayed signals for three methyl [δ 10.4 (C-17), 13.6 (C-22) and 16.6 (C-15)], nine methylene [δ 45.0 (C-5), 37.2 (C-12), 32.8 (C-19), 31.1 (C-7), 30.7

(C-1), 26.3 (C-8), 23.3 (C-16), 23.3 (C-2) and 23.0 (C-6)], five methine [δ 66.4 (C-3), 49.4 (C-9), 46.3 (C-10), 36.7 (C-13) and 34.7 (C-20)], two oxymethines [δ 82.1 (C-18) and 76.6 (C-11)] and three quaternary [δ 180.2 (C-21), 176.9 (C-14) and 104.5 (C-9a)] carbons and a methoxy group [δ 50.3] (Table 1). The correlations in the COSY spectrum indicated the spin system H-1−H-2−H-3−H-18−H-19−H-20−H-22, typical of the pyrrolidine ring of the *Stemona* alkaloids, with a γ-lactone substituent at C-3 (Figure 6.2). However, unlike many of these alkaloids, C-9a in **193** was a quaternary carbon, and not a methine, since H-1 showed only a COSY correlation to H-2.[2,12,74,75] COSY correlations were also observed between the vicinal pairs of contiguous protons along the C-5−C-13 backbone, with vicinal correlations also seen between H-10 and H-16; H-16 and H-17; and H-13 and H-15 (Figure 6.2). The ^{1}H NMR/COSY spectra (Table 6.1) indicated the presence of two different methyl groups from the signals at δ 1.16 (d, J = 6.5 Hz, 3H, H-22) and δ 1.12 (d, J = 7.0 Hz, 3H, H-15), that are attached to methines with resonances at δ 2.73-2.63 (m, 1H, H-20) and δ 2.72-2.63 (m, 1H, H-13), and a methyl group at δ 0.90 (t, J = 7.5 Hz, 3H, H-17) which is vicinally coupled to the methylene resonance at δ 1.46−1.26 (m, 2H, H-16). Key HMBC correlations for stichoneurine F (**193**) are shown in Figure 6.2, while full details are provided in Table 6.1.

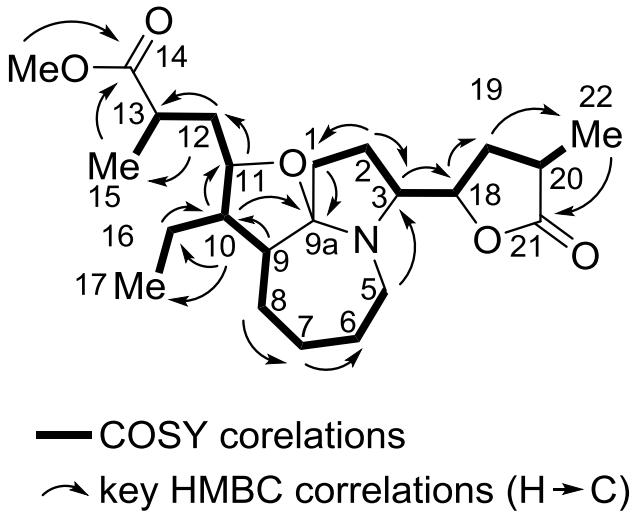

Figure 6.2 Key COSY and HMBC correlations for stichoneurine E (**193)**.

HSQC and HMBC experiments identified the protons and carbons (C-18−C-22) of the γ-butyrolactone moiety (Figure 6.2), which was clearly attached to C-3 from the HMBC correlation between H-3 [δ 3.06 (app t, J = 7.0 Hz, 1H)] and C-18 (δ 82.1). The carbonyl carbon resonance at δ 176.9 (C-14) and the methoxy ^{1}H NMR signal at δ 3.63 suggested a methyl ester. This was confirmed from their correlation in the HMBC spectrum. The HMBC correlation between C-14 and the Me-15 protons (δ 1.12 (d, J = 7.0 Hz, 3H) indicated that the C-15 methyl group was in a position α to the ester group. The HMBC correlations from H-1 and H-10 to the quaternary carbon signal at δ 104.5 identified this signal as corresponding to that of C-9a. The downfield ^{13}C NMR chemical shift of C-9a indicated that this carbon was substituted by two heteroatoms; in this case a nitrogen and an oxygen atom. The HMBC correlations of H-9 to C-10 and of H-10 to C-9a, C-11, C-16 and C-17 identified the connectivity and position of the C-10 ethyl substituent in the tetrahydrofuran ring of **193**. The HMBC spectrum showed that C-12 (δ 37.2) correlated to H-11 (δ 3.17) and H-13 (δ 2.72−2.63); C-14 (δ 176.9) correlated to H-12 (δ 2.05−1.97) and H-15 (δ 1.12); and C-11 (δ 76.6) correlated to H-

12 (δ 2.05-1.97). These data and correlations indicated that a methyl 2-methylpropanoate moiety (C-12−C-14) was attached via C-12 to C-11 of the tetrahydrofuran ring. The relative configuration of stichoneurine F was determined from ROESY and molecular modelling experiments. The ROESY spectrum (Figure 6.6) showed correlations between H-9 and H-11; H-11 and H-1α and H-16; H-1α and H-2α; and H-2α and H-3. These correlations, along with molecular modelling studies (Figure 6.3) indicated that the tetrahydrofuran ring in **193** was *cis*-fused to the azepine ring at C-9 and C-9a and that the C-3 proton was on the opposite face of the pyrrolo[1,2-*a*]azepine nucleus to H-9, H-11 and H-16, which had a mutual *syn*-stereochemical relationship. Figure 6.3 shows the lowest energy conformer of stichoneurine F (**193**), other low energy conformers (the next 20 higher energy ones, ranging from *ca* 1-12 kcal /mol higher in energy) were also examined, however in these conformers the conformation of the basic tricyclic structure remained essentially the same. The relative configurations proposed for the pyrrolo[1,2-*a*]azepine and tetrahydrofuran rings in this structure are consistent with the calculated inter proton distances (all less than 3 Å) for the aforementioned correlated protons. Since the majority of *Stemona* alkaloids have the 3*S* configuration, including stichoneurines A (**108**) and B (**109**), we have tentatively assigned this absolute configuration at C-3 for compound stichoneurine F (**190**). The ROESY correlations between: H-18 and H-19β; H-19β and H-20; and H-19α and H-22 indicated the relative *syn*-configuration between H-18 and H-20 of the γ-lactone moiety (Figure 6.3). Because of the relatively free rotation around the C-3−C-18 bond in both possible diastereomeric structures for stichoneurine F ((3*S*, 18*S*, 20*S*)- stichoneurine F or (3*S*, 18*R*, 20*R*)- stichoneurine F), it was not possible to confidently assign the relative configurations of these two vicinal (C-3 and C-18) stereocentres from molecular

modelling and ROESY NMR studies. However we have tentatively assigned the 3*S*, 18*S*, 20*S* configuration to stichoneurine F (**193**) since this is the most commonly found absolute configuration of the *Stemona* alkaloids.[2,12,74,75] For similar conformational reasons we cannot unambiguously assign the configuration at C-13 relative to that of C-11, however, we have assigned C-13 the *S*-configuration, based on this configuration in stichoneurines A (**108**) and B (**109**). Indeed it is conceivable that stichoneurine F (**193**) arises biosynthetically from stichoneurine A (**108**), via cyclization of the free C-11 hydroxyl group onto an N-4-C-9a iminium ion intermediate **A** to produce the tetrahydrofuran ring of stichoneurine F (path A, Scheme 6.1). Detailed analysis of the ^{1}H and ^{13}C-NMR spectra, as well as 2D-NMR analyses (COSY, HMBC and ROESY) (Table 6.1) established the planar structure and relative configuration of stichoneurine F (**193**).

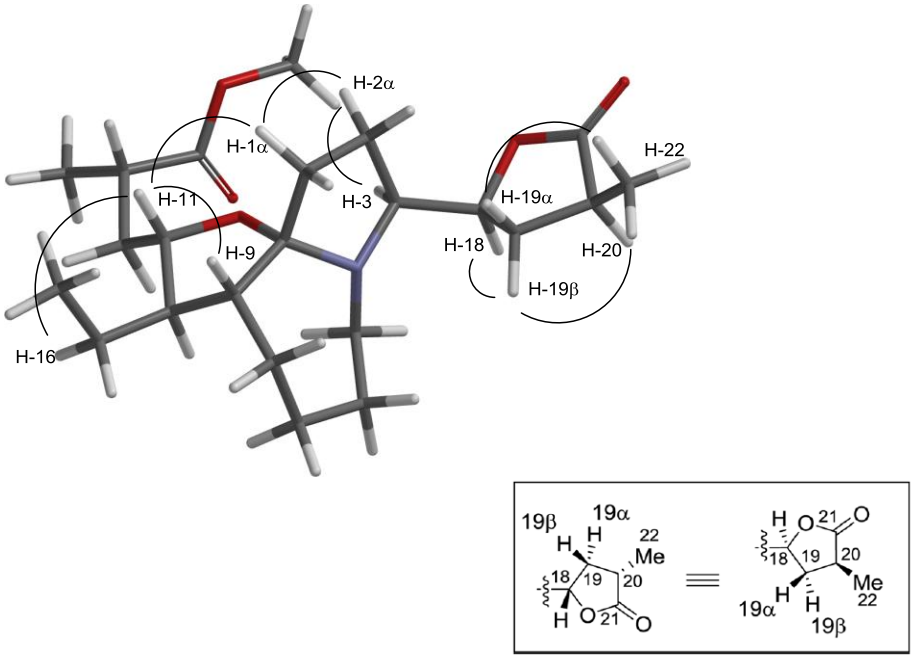

Figure 6.3 Spartan ’10 generated lowest energy conformation of stichoneurine F (**193**) showing key ROESY cross-peaks. The structure shown were generated using Spartan ‘10 and conformational searching (MMFF) to find the lowest energy conformers).

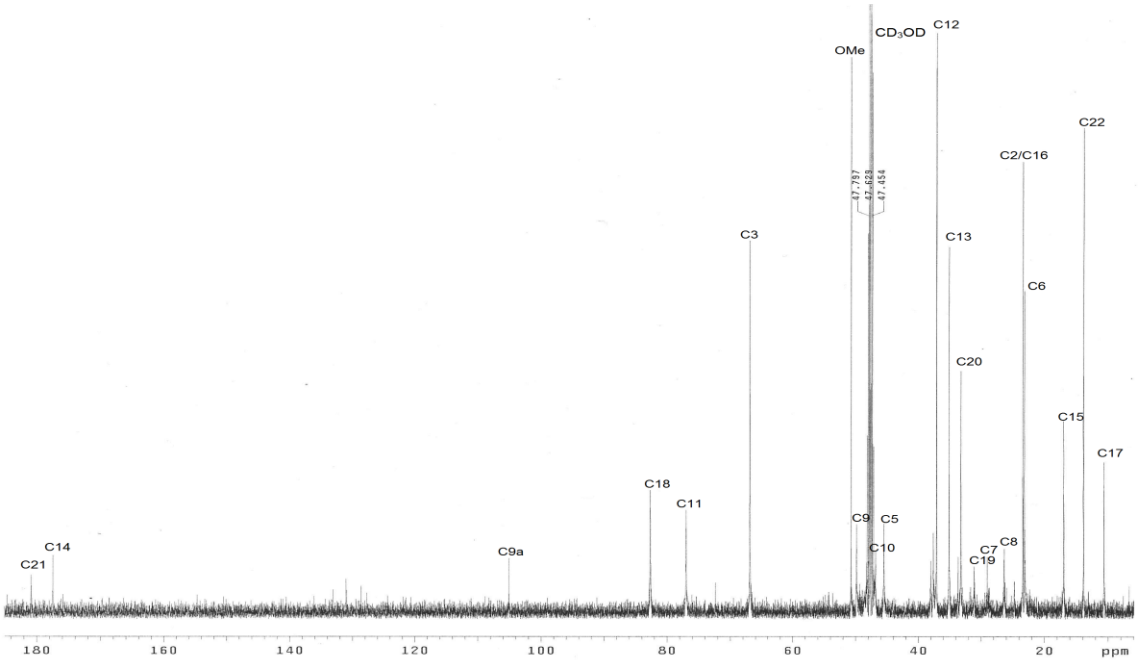

Figure 6.4 ^{13}C NMR spectrum (methanol-d_4, 125 MHz) of stichoneurine F (**193**).

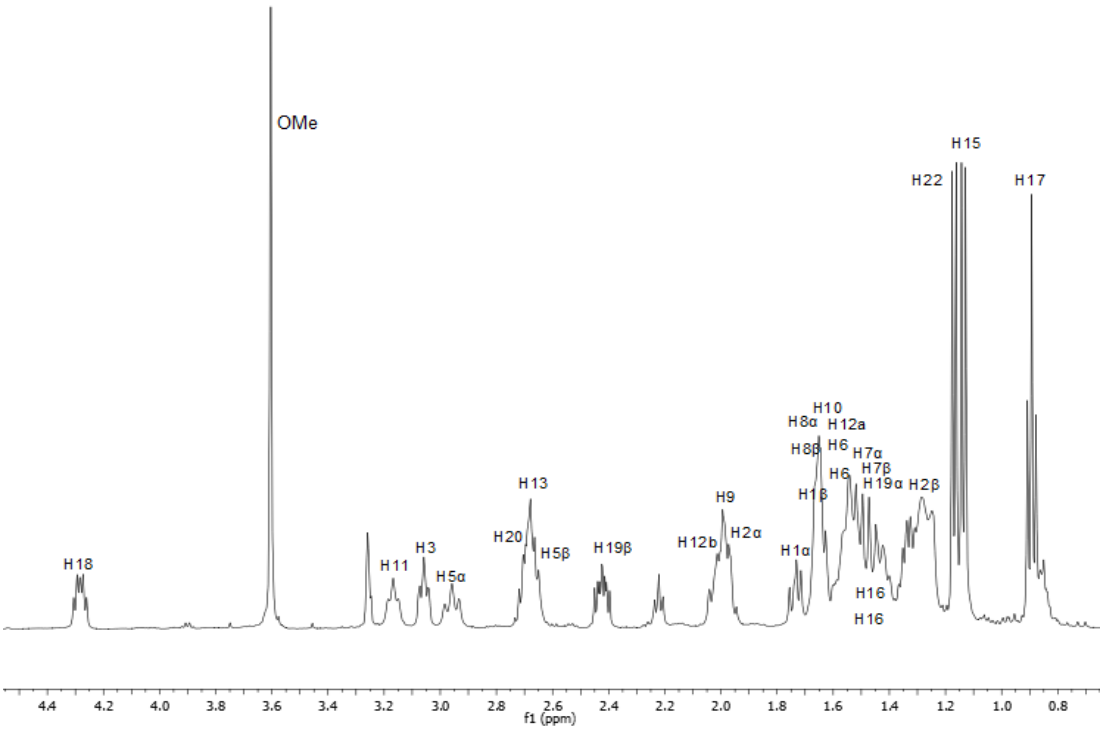

Figure 6.5 ^{1}H NMR spectrum (methanol-d_4, 500 MHz) of stichoneurine F (**193**).

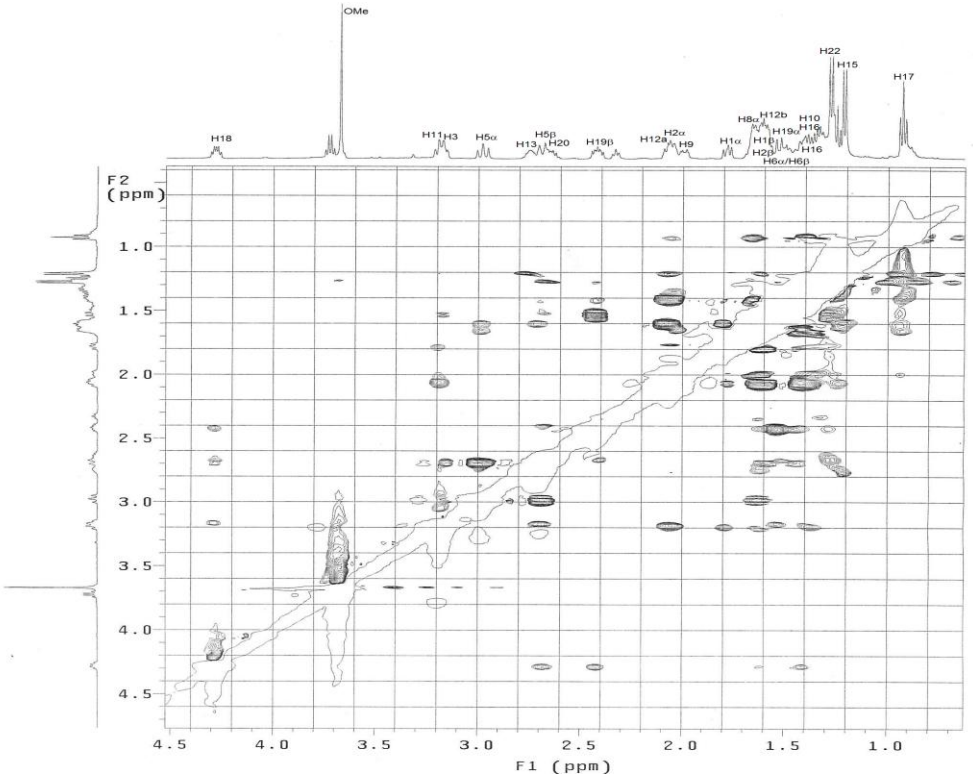

Figure 6.6 ROESY spectrum (methanol-d_4, 500 MHz) of stichoneurine F (**193**).

Table 6.1 ^{13}C (125 Hz), ^{1}H (500 MHz) and 2D NMR spectroscopic data for stichoneurine F (**193**) in methanol-d_4 solution (δ in ppm).

Position	δ_C	δ_H (mult., *J* (Hz), assign.)	HMBC	ROESY	COSY
1α	30.7	1.77-1.68 (m)	2, 3	1β, 2α, 3, 11	2
β		1.67-1.59 (m)		1α, 2β	
2α	23.3	2.03-1.93 (m)	1, 18	1α, 2β, 3, 11, 15, 18	1, 3
β		1.36-1.26 (m)		1β, 2α, 15	
3	66.4	3.06 (app t, *J* 7.0)	1, 5, 18, 19	1α, 2α, 5β, 10, 18, 19α	2, 18
5α	45.0	2.96 (app t, *J* 13.0)	3, 7	5β, 7α, 8α, 12a	6
β		2.69-2.61 (m)		3, 5α, 18, 19α, 22	
6	23.0	1.57-1.37 (m)	7		5, 7
		1.57-1.37 (m)		18, 19β	
7α	31.1	1.55-1.47 (m)	5, 6	5α	6, 8
β		1.47-1.40 (m)			
8α	26.3	1.69-1.60 (m)	7	5α, 9, 16a	7, 9
β		1.69-1.60 (m)			
9	49.4	2.01-1.93 (m)	10	8α, 11	8, 10
9a	104.5	-	1, 2, 5, 10	-	
10	46.3	1.69-1.60 (m)	8, 16, 17	3, 12a, 16a, 16b	9, 11
11	76.6	3.17 (t, *J* 8.5)	10, 12, 16	1α, 2α, 9, 12b, 13, 15, 16b	10, 12
12a	37.2	1.60-1.52 (m)	15, 16	5α, 10, 12b, 15, 16b	11, 13
b		2.05-1.97 (m)		11, 12a, 13, 15, 17	
13	36.7	2.72-2.63 (m)	12	11, 12b, 15, 17	12
14	176.9	-	12, 15, OMe		
15 (Me)	16.6	1.12 (d, *J* 7.0)	12, OMe	2α, 2β, 11, 12a, 12b, 13	13
16	23.3	1.46-1.26 (m)	11, 17	10, 8α	10, 17
		1.46-1.26 (m)		10, 11, 12a, 17	
17 (Me)	10.4	0.90 (t, *J* 7.5)	16	12b, 13, 16b	16
18	82.1	4.29-4.26 (m)	2, 3, 19β, 20	2α, 3, 5β, 6β, 19β	3, 19
19α	32.8	1.53-1.42 (m)	20, 22	3, 5β, 19β, 22	18, 20
β		2.46-2.37 (m)		6β, 18, 19α, 20	
20	34.7	2.73-2.63 (m)	19, 22,	19β, 22	19, 22
21	180.2	-	19, 20, 22,	-	
22 (Me)	13.6	1.16 (d, *J* 6.5)	19, 20	5β, 19α, 20	20
OMe	50.3	3.63 (s)	-	-	

In some cases, the ^{13}C NMR signals of **193** were determined from the HSQC and HMBC spectra.

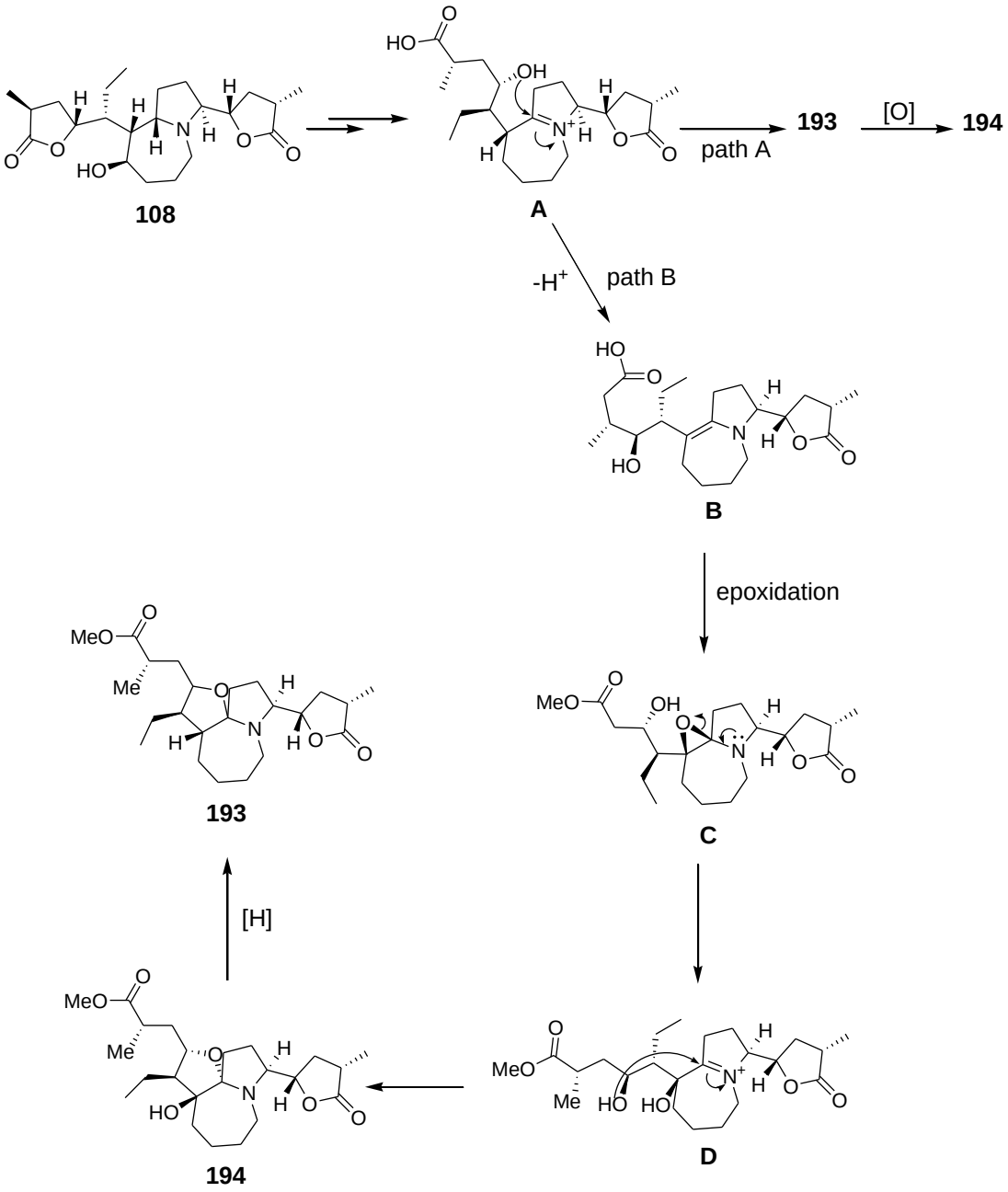

Scheme 6.1 Proposed biosynthesis of stichoneurine F and G (**193** and **194**).

6.3.2 Stichoneurine G (194)

Stichoneurine G (**194**) was obtained as a pale yellow gum. The molecular formula of stichoneurine G (**194**) as $C_{23}H_{37}NO_6$ was determined from its HRESIMS (*m*/*z* 424.2699 $[M+H]^+$, calc. for 424.2682). This data indicated that stichoneurine G (**194**) had one more oxygen atom than stichoneurine F (**193**). The IR spectrum of stichoneurine G (**194**) showed characteristic alcohol, ester and γ-lactone carbonyl absorptions at 3520, 1730 and 1761 cm^{-1}, respectively. The ^{13}C/DEPT NMR spectrum of stichoneurine G (**194**) (Figure 6.7) was similar to that of stichoneurine F (**193**) except for the number of methine and quaternary carbons, which were both four, indicating that one methine carbon in stichoneurine F (**193**) had become a quaternary carbon in stichoneurine G (**194**). The signal for the new quaternary carbon at δ 83.7 (C-9) suggested that this carbon was substituted by the hydroxyl group that was observed in the IR spectrum. There were ^{13}C/DEPT NMR signals for three methyl [δ 12.3 (C-17), 13.6 (C-22) and 17.1 (C-15)], nine methylene [δ 45.6 (C-5), 38.1 (C-12), 33.5 (C-19), 36.2 (C-7), 33.8 (C-1), 30.6 (C-8), 23.9 (C-6), 22.5 (C-2) and 17.9 (C-16)], four methine [δ 67.9 (C-3), 51.1 (C-10), 37.2 (C-20) and 35.4 (C-13)], two oxymethine [δ 82.9 (C-18) and 76.1 (C-11)] and four quaternary carbons [δ 181.2 (C-21), 177.8 (C-14), 109.1 (C-9a) and 83.7 (C-9)] and a methoxy group [δ 50.9]. The COSY and HMBC spectra of stichoneurine G (**194**) showed analogous correlations to those observed in that of stichoneurine F (**193**), except that the correlations observed from H-9 in the spectrum of stichoneurine F (**193**) were now absent. The ROESY spectrum of stichoneurine G (**194**) (Figure 6.9) showed correlations between H-11 and H-1α and H-16; H-1α and H-2α; and H-2α and H-3, which were also found in the ROESY spectrum of structure stichoneurine F (**193**) (Figure 6.6), and correlations between H-18 and H-19β; H-19β

and H-20; and H-19α and H-22 which indicated the relative *syn*-configuration between H-18 and H-20 of the γ-lactone moiety. This data was thus consistent with stichoneurine G (**194**) being the C-9 hydroxy derivative of stichoneurine F (**193**). A possible biosynthesis of **194** is outline in Scheme 6.1. Stichoneurine G (**194**) could arise from oxidation of **193** at C-9 (Scheme 6.1, path A) or from conversion of the iminium ion intermediate **A** to the enamine **B** (Scheme 6.1, path B), which upon epoxidation could give the epoxide **C**. Ring opening of **C** could give the iminium ion **D** which could cyclise to **194** (Scheme 6.1).

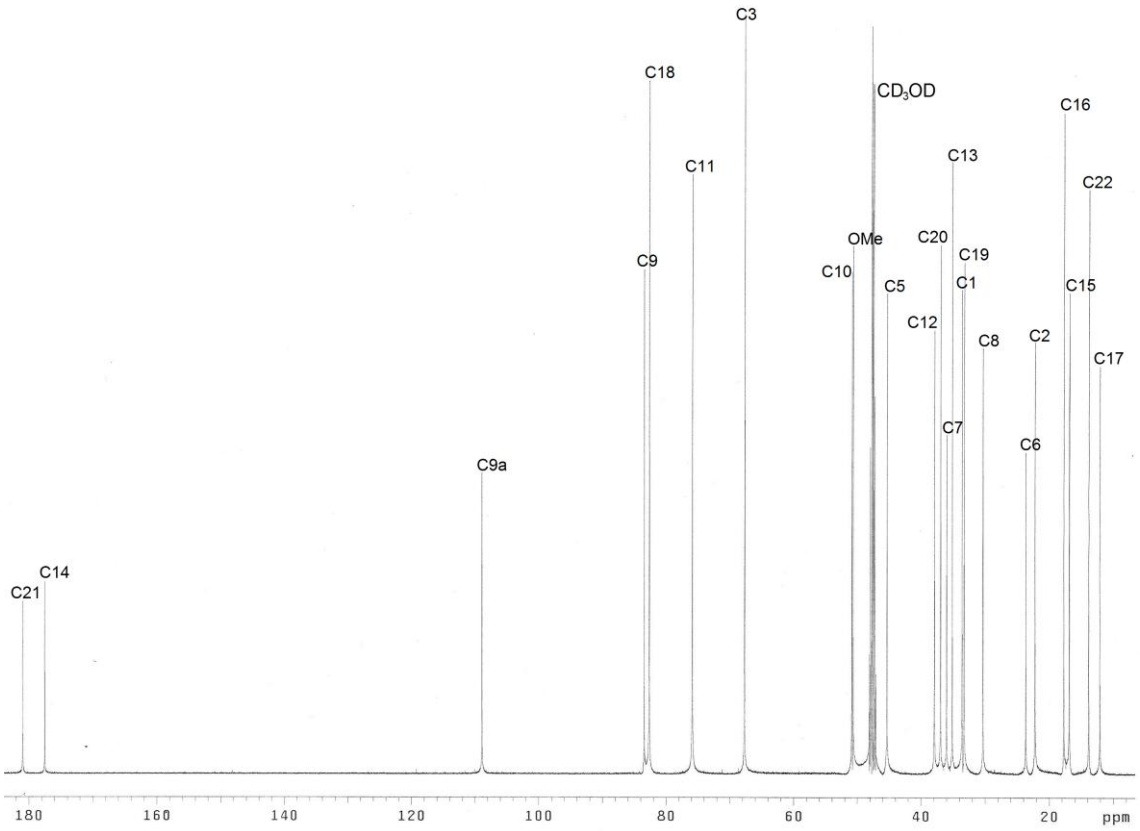

Figure 6.7 ^{13}C NMR spectrum (methanol-d_4, 125 MHz) of stichoneurine G (**194**).

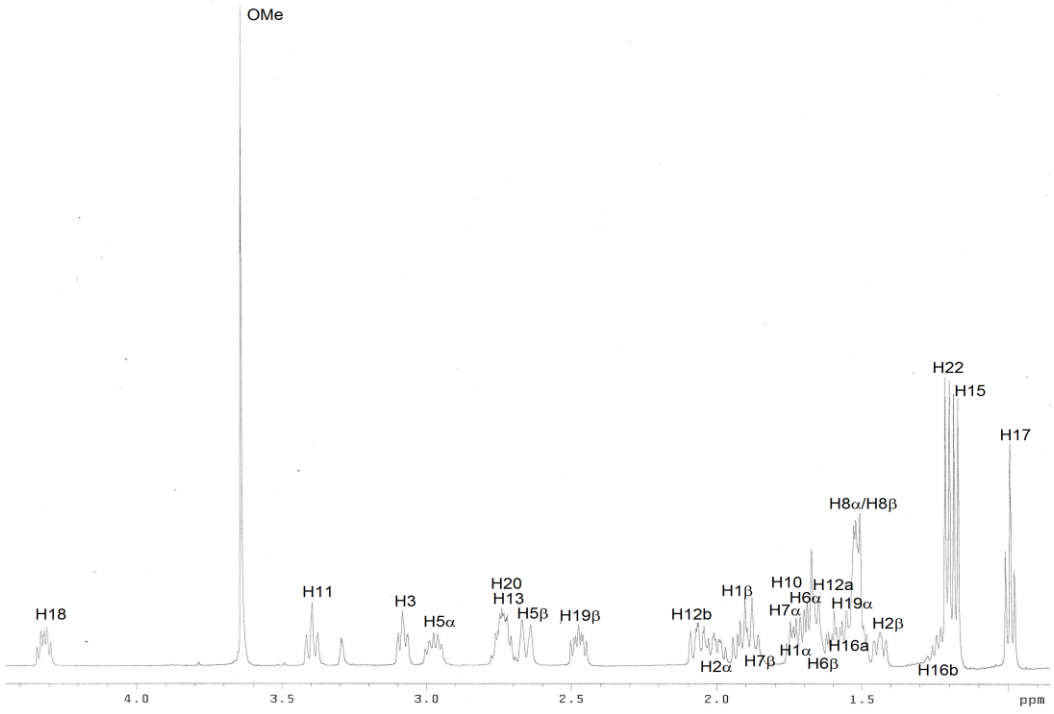

Figure 6.8 ^{1}H NMR spectrum (methanol-d_4, 500 MHz) of stichoneurine G (**194**).

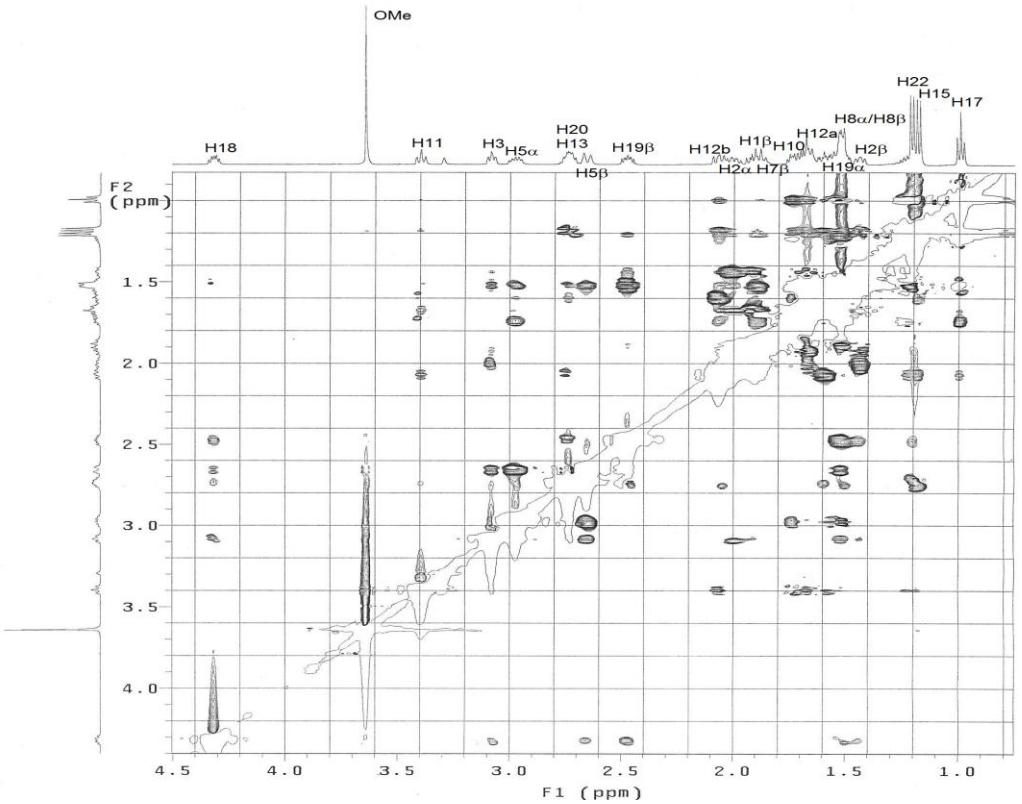

Figure 6.9 ROESY spectrum (methanol-d_4, 500 MHz) of stichoneurine G (**194**).

Table 6.2 ^{13}C (125 Hz), ^{1}H (500 MHz) and 2D NMR spectroscopic data for stichoneurine G (**194**) methanol-d_4 solution (δ in ppm).

Position	**δ_C**	**δ_H (mult., *J* (Hz), assign.)**	**HMBC**	**ROESY**	**COSY**
1α	33.8	1.70-1.64 (m)	2	1β, 2α, 11	2
β		1.95-1.89 (m)		1α, 2β	
2α	22.5	2.05-1.98 (m)	1, 3, 18	1α, 3, 2β, 15	1, 3
β		1.47-1.41 (m)		1β, 2α, 15, 18, 19β	
3	67.9	3.08 (app t, *J* 9.5)	1, 2, 5, 18, 19	2α, 5α, 5β, 18, 19α	2, 18
5α	45.6	3.00-2.95 (m)	6	3, 5β, 7α, 8α, 12a	6
β		2.67 (br d, *J* 15.0)		3, 5α, 18, 19α, 22	
6	23.9	1.71-1.62 (m)	7	19α	5, 7
		1.60-1.51 (m)			
7α	36.2	1.72-1.66 (m)	5, 8	5α	6, 8
β		1.91-1.85 (m)			
8α	30.6	1.55-1.49 (m)	5α, 7, 10	5α	7
β		1.55-1.49 (m)			
9	83.7	-	1, 8, 10, 11, 16	-	
9a	109.1	-	1, 2, 5		
10	51.1	1.77-1.71 (m)	7, 8, 11, 16, 17	12a, 16a, 16b, 17	11
11	76.1	3.40 (br t, *J* 9.5)	1, 10, 12, 13, 16	1α, 12b, 13, 15	10, 12
12a	38.1	1.63-1.56 (m)	10, 11	5α, 10, 12b, 15, 16b	11, 13
b		2.11-2.03 (m)		11, 12a, 13, 15, 17	
13	35.4	2.78-2.70 (m)	10, 12	11, 12b, 15	12
14	177.8	-	12, 15, OMe		
15 (Me)	17.1	1.18 (d, *J* 7.0)	11, 12	2α, 2β, 11, 12a, 12b, 13	13
16	17.9	1.58-1.49 (m)	10, 17	10	10, 17
		1.28-1.19 (m)		10, 12a, 17	
17 (Me)	12.3	0.99 (t, *J* 7.5)	10, 16	10, 12b, 16b	16
18	82.9	4.34-4.30 (m)	2, 3	2β, 3, 5β, 19β, 20	3, 19
19α	33.5	1.57-1.50 (m)	20	3, 6α, 5β, 19β, 22	18, 20
β		2.52-2.44, (m)		2β, 18, 19α, 20	
20	37.2	2.78-2.71 (m)	19, 22	18, 19β, 22	19, 22
21	181.2	-	19, 20, 22		
22 (Me)	14.1	1.22 (d, *J* 7.0)	19, 20	5β, 19α, 20	20
OMe	50.9	3.65 (s)	13		

6.3.3 Sessilistemonamine E (195)

Sessilistemonamine E (**195**) was obtained as a pale yellow gum. The molecular formula of sessilistemonamine E (**195**) as $C_{22}H_{33}NO_5$ was determined by HRESIMS (*m*/*z* 392.2436 $[M + H]^+$, calcd for $C_{22}H_{34}NO_5$ 392.2376). The IR spectrum of sessilistemonamine E (**195**) showed characteristic hydroxyl and γ-lactone carbonyl absorptions at 3348 and 1761 cm^{-1}, respectively. The ^{13}C/DEPT spectrum of sessilistemonamine E (**195**) (Figure 6.12) displayed signals for three methyls [δ 20.5 (C-15), 15.2 (C-22) and 12.7 (C-17)], eight methylene [δ 48.5 (C-5), 43.2 (C-1), 36.7 (C-19), 32.1 (C-7), 31.0 (C-6), 27.3 (C-8), 24.9 (C-2) and 20.0 (C-16)], two oxymethine [δ 79.6 (C-18) and 85.5 (C-11)], five methine [δ 69.5 (C-3), 60.2 (C-12), 53.9 (C-9), 48.9 (C-10) and 36.6 (C-20)] and four quaternary carbons [δ 182.2 (C-21), 180.5 (C-14), 81.9 (C-9a) and 77.8 (C-13)]. The quaternary carbon signals at δ 180.5 (C-14) and 182.2 (C-21) and the oxymethine carbon signals at δ 85.5 (C-11) and 79.6 (C-18), with their corresponding downfield ^1H NMR resonances at δ 4.95 (dd, J = 5.0, 6.3, 1H, H-11) and δ 4.54 (ddd, J = 5.5, 10.0, 10.0, 1H, H-18), respectively, indicated the presence of two γ-butyrolactone rings. The correlations in the COSY spectrum of sessilistemonamine E (**195**) indicated the spin system H-1−H-2−H-3−H-18−H-19−H-20−H-22, typical of the pyrrolidine ring of the *Stemona* alkaloids with a γ-lactone substituent at C-3 (Figure 6.10). Similar to stichoneurine F (**193**) and G (**194**), C-9a in sessilistemonamine E (**195**) was a quaternary carbon since H-1 showed only a COSY correlation to H-2. COSY correlations were also observed between the vicinal pairs of contiguous protons along the C-5−C-12 backbone, with correlations indicating the vicinal relationships between H-10 and H-16; and H-16 and H-17 (Figure 6.10). The ^1H NMR/COSY spectra indicated the presence of a methyl group (δ 1.76 (s, 3H, H-15)) attached to a quaternary

carbon (C-13), a methyl group (δ 1.21 (d, J = 7.0 Hz, 3H, H-22)) attached to methine [δ 2.81-2.72 (m, 1H, H-20)] and a methyl group (δ 0.98 (t, J = 7.0 Hz, 3H, H-17)) which was vicinally coupled to the methylene resonance at δ 1.56−1.46 (m, 2H, H-16).

Key HMBC correlations are shown in Figure 6.10, while full details are provided in Table 6.3. HSQC and HMBC experiments identified the protons and carbons (C-18−C-23) of the appended γ-butyrolactone moiety (Figure 6.10), which was clearly attached to C-3 from the HMBC correlation between H-3 (δ 3.21 (ddd, J = 8.5, 8.5, 8.5 Hz, 1H)) and C-18 (δ 79.6). While HSQC and HMBC experiments helped to further identified the protons and carbons (C-11−C15) associated with the fused γ-butyrolactone moiety of sessilistemonamine E (**195**) (Figure 6.10). These data suggested that sessilistemonamine E (**195**) was a diastereoisomer of the sessilistemonamines A−C (**96**-**98**) which were isolated from the root extracts of *Stemona sessilifolia*.[25]

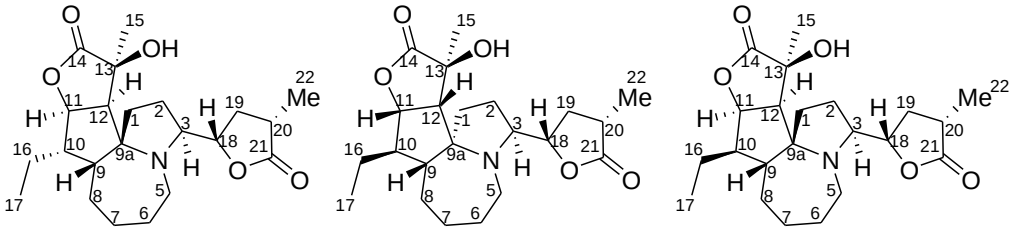

Sessilistemoamine A (**96**) Sessilistemoamine B (**97**) Sessilistemoamine C (**98**)

Sessilistemonamine E (**195**) showed ROESY correlations between H-9 and H-10; H-10 and H-11; H-11 and H-12; and H-12 and 15-Me (Figure 6.11 and Table 6.3), indicating the mutal *syn*-stereochemical relationships between all these hydrogens and that sessilistemonamine E was a different stereoisomer to sessilistemonamines A−C (**96**-**98**). ROSEY correlations were also observed between H-1α and H-3; H-2α and H-3; H-3 and 15-Me; H-2β and H-18; H-18 and H-5β and H-19β; H-5α and H-9; and H-

19β and 22-Me (Figure 6.11 and Figure 6.14). These data were consistent with the structure assigned to sessilistemonamine E (**195**) which has the opposite configuration at C-9, C-13 and C-20 to sessilistemonamines A−C (**96**-**98**) and the opposite configuration at C-10 to sessilistemonamine A (**96**) and at C-9a to sessilistemonamine B (**97**).

For conformational mobility reasons the relative configurations between the rigid tetracyclic framework and that of the appended *γ*-butyrolactone in sessilistemonamine E (**195**) could not be confidently assigned, although the ROESY correlations observed were consistent with the structure and the relative configuration proposed for sessilistemonamine E (**195**) (Figure 6.11).

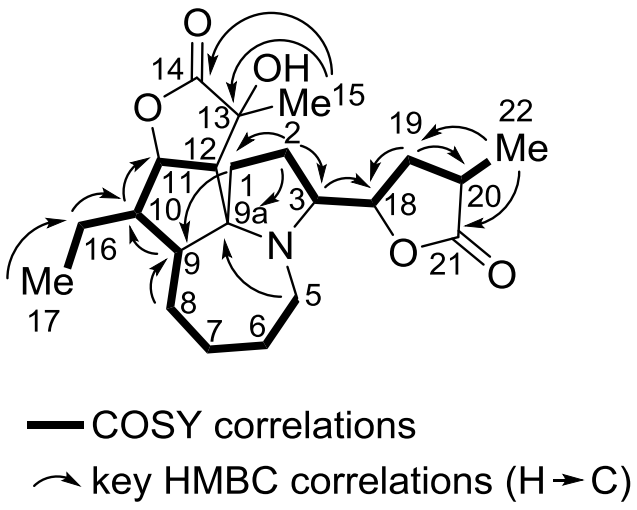

Figure 6.10 Key COSY and HMBC correlations for sessilistemonamine E (**195**).

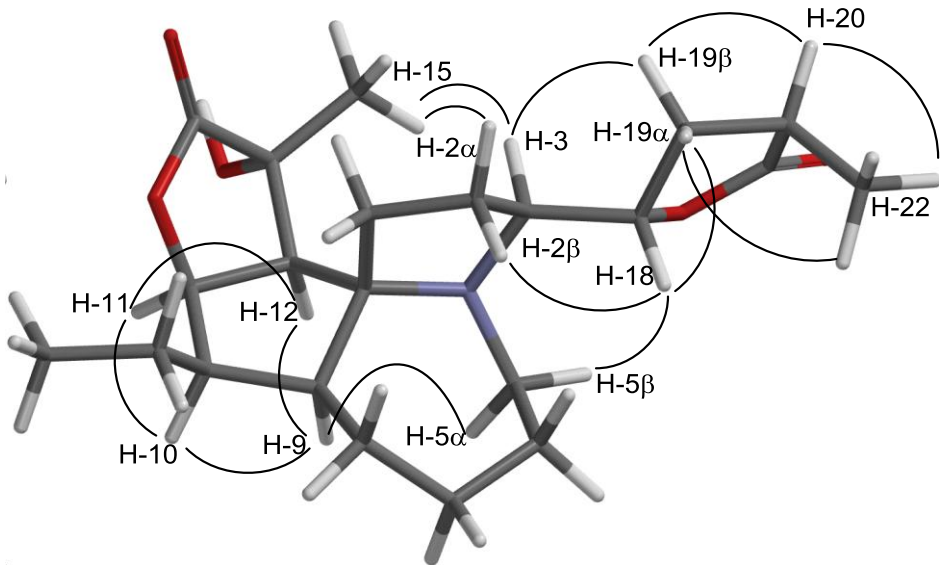

Figure 6.11 Spartan '10 generated lowest energy conformation of sessilistemonamine E (**195**) showing key ROESY cross-peaks. The structure shown were generated using Spartan '10 and conformational searching (MMFF) to find the lowest energy conformers).

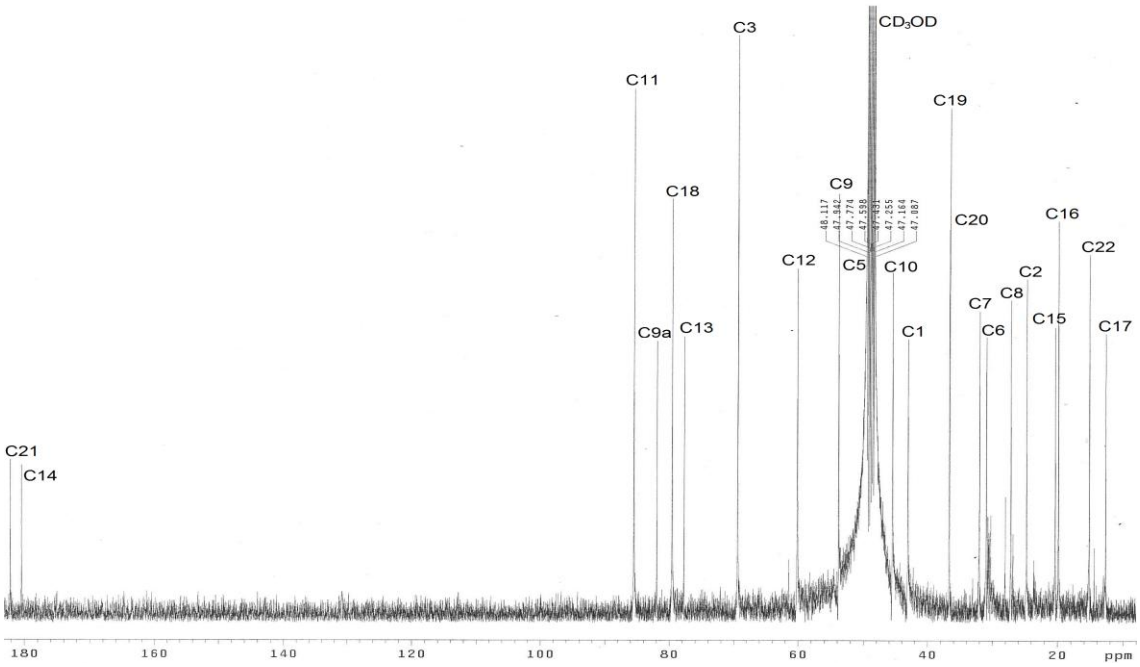

Figure 6.12 ^{13}C NMR spectrum (methanol-d_4, 125 MHz) of sessilistemonamine E (**195**).

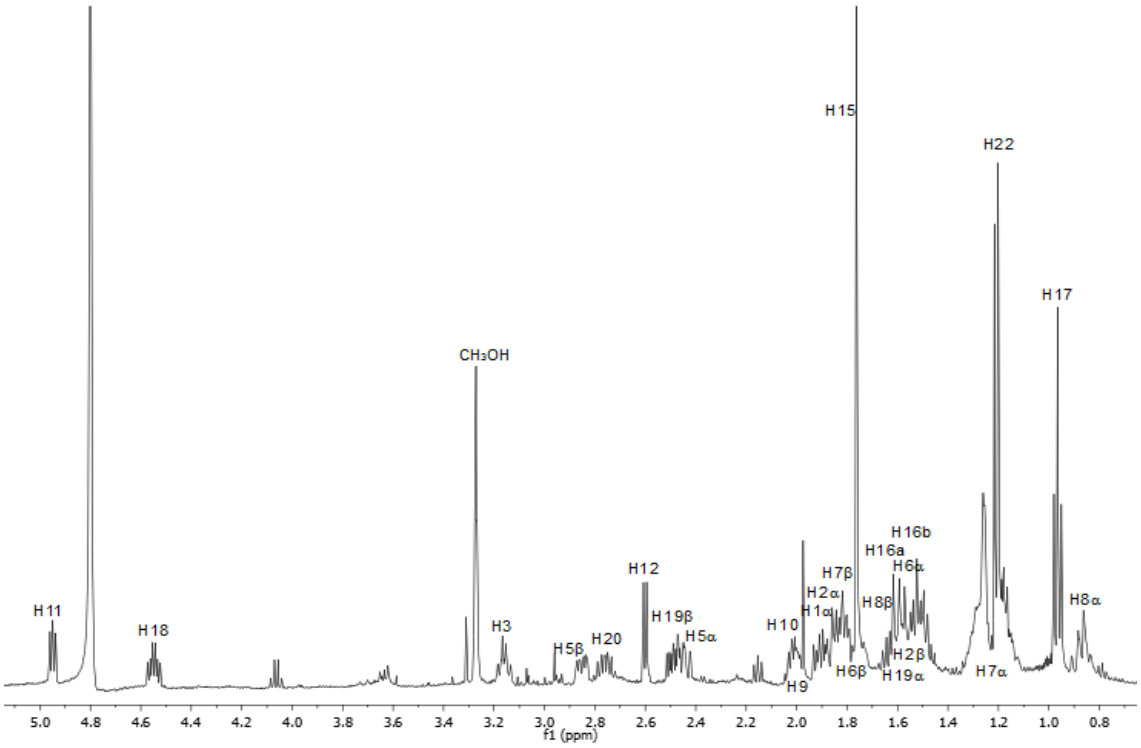

Figure 6.13 ^{1}H NMR spectrum (methanol-d_4, 500 MHz) of sessilistemonamine E (**195**).

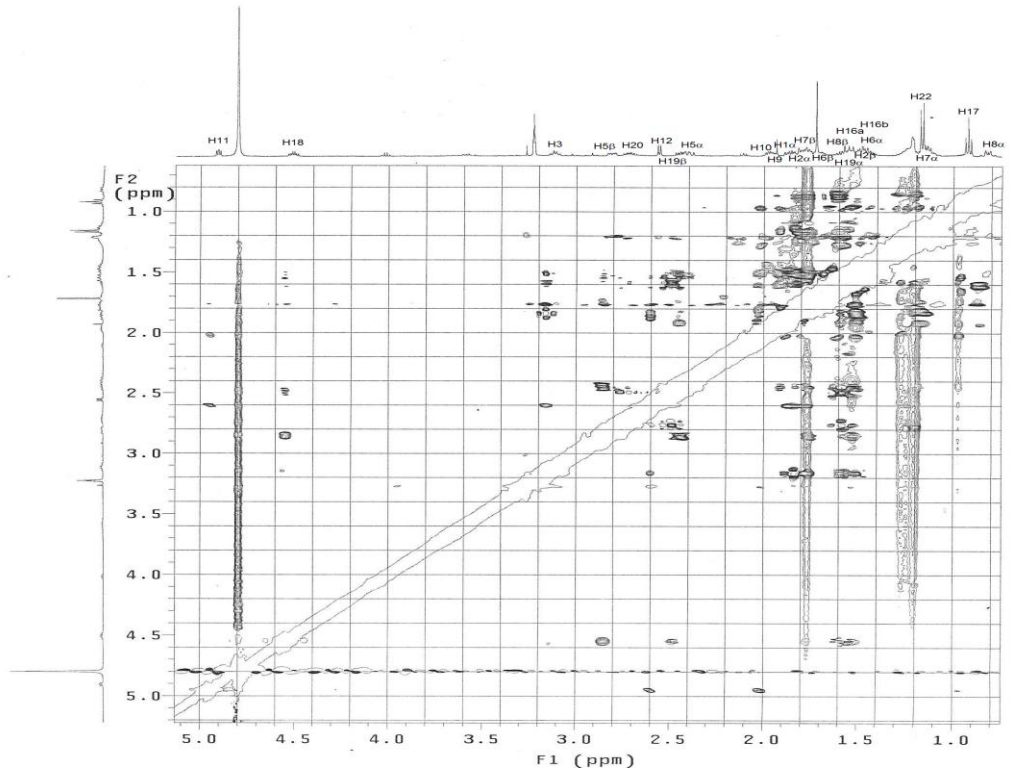

Figure 6.14 ROESY spectrum (methanol-d_4, 500 MHz) of sessilistemonamine E (**195**).

Table 6.3 ^{13}C (125 Hz), ^{1}H (500 MHz) and 2D NMR spectroscopic data for sessilistemonamine E (**195**) in methanol-d_4 solution (δ in ppm).

Position	**δ_C**	**δ_H (mult., *J* (Hz), assign.)**	**HMBC**	**ROESY**	**COSY**
1α	43.2	1.91-1.77 (m)	9, 12	1β, 2α, 3, 12, 16a, 19α	2
β		1.91-1.77 (m)		1α, 16b, 19β	
2α	24.9	1.90-1.80, (m)	1	1α, 2β, 3, 18, 19β	1
β		1.56-1.47 (m)		2α, 19β	
3	69.5	3.18-3.12 (m)	2	1α, 2α, 12, 15, 19α	2
5α	48.5	2.48-2.41 (m)	-	5β, 9	6
β		2.88-2.83 (m)		5α, 6β, 18	
6	31.0	1.57-1.48 (m)	8		5
		1.78-1.71 (m)		5β	
7α	32.1	1.21-1.13 (m)	5, 9	9	6, 8
β		1.86-1.79 (m)			
8α	27.3	0.91-0.81 (m)	9, 10		7, 9
β		1.64-1.59 (m)			
9	53.9	2.04-1.99 (m)	1, 8, 10, 12	5α, 7α, 10, 12	8, 10
9a	81.9	-	1, 2, 9, 5		-
10	48.6	2.04-1.98 (m)	9, 12, 16, 17	9, 11, 17	
11	85.5	4.95 (dd, *J* 6.3, 5.0)	10, 16	10, 12	10, 12
12	60.2	2.60 (d, *J* 6.3)	1, 9	1α , 3, 9, 11, 15	11
13	77.8	-	12, 15		-
14	180.5	-	12, 15		-
15 (Me)	20.5	1.76 (s)	-	3, 12	10, 17
16a	20.0	1.68-1.58 (m)	10, 17	1α	
b		1.56-1.46 (m)		1β	16
17 (Me)	12.7	0.98 (t, *J* 7.0)	16	10	3, 19
18	79.6	4.54 (ddd, *J* 10.0, 10.0, 5.5)	3, 19	2α, 5β, 19β	18, 20
19α	36.7	1.61-1.56 (m)	22	1α, 3, 5α, 19β, 20	
β		2.53-2.46 (m)		1β, 2α, 18, 19α, 22	19, 22
20	36.6	2.79-2.71 (m)	19, 22	19α, 22	-
21	182.2	-	19, 20, 22		20
22 (Me)	15.2	1.21 (d, *J* 7.0)	19, 20	19β, 20	2

6.3.4 Sessilistemonamine F (196)

Sessilistemonamine F (**196**) was obtained as a pale yellow gum. The molecular formula of sessilistemonamine F (**196**) as $C_{22}H_{33}NO_5$ was determined by HRESIMS (*m*/*z* 392.2437 $[M + H]^+$, calcd for $C_{22}H_{34}NO_5$ 392.2476). The IR spectrum of sessilistemonamine F (**196**) showed characteristic hydroxyl and γ-lactone carbonyl absorptions at 3454 and 1764 cm^{-1}, respectively. The ^{13}C/DEPT spectrum (Figure 4.15) of **196** displayed signals for three methyl [δ 20.4 (C-15), δ 13.8 (C-22) and δ 11.3 (C-17)], eight methylene [δ 51.2 (C-5), δ 34.6 (C-1), δ 33.8 (C-19), δ 29.3 (C-8), δ 26.5 (C-7), δ 26.1 (C-6), δ 23.9 (C-2) and δ 20.7 (C-16)], two oxymethine [δ 85.1 (C-11) and δ 81.4 (C-18)], five methine [δ 67.0 (C-3), δ 58.1 (C-12), δ 48.0 (C-9), δ 47.3 (C-10) and δ 35.0 (C-20)] and four quaternary carbons [δ 181.0 (C-14), δ 180.9 (C-21), δ 76.9 (C-9a) and δ 75.5 (C-13)]. The quaternary carbon signals at δ 180.9 (C-21) and 181.0 (C-14) and the methine signals at δ 85.1 (C-11) and 81.4 (C-18), with their corresponding downfield ^1H NMR resonances at δ 4.95 (dd, J = 5.0, 6.3, 1H, H-11) and δ 4.54 (ddd, J = 5.5, 10.0, 10.0, 1H, H-18), respectively, indicated the presence of two γ-butyrolactone rings. These data suggested that sessilistemonamine F (**196**) was a stereoisomer of sessilistemonamine E (**195**) and sessilistemonamines A−C (**96**-**98**).[25] The ROESY spectrum of sessilistemonamine F (**196**) (Figure 6.17) showed correlations between, H-1α and H-3; H-2α and H-3; H-3 and H-15; H-9 and H-16; H-11 and H-12; H-11 and H-16; and H-12 and H-15. These correlations indicated that sessilistemonamine F (**196**) had the same configuration at C-9, C-9a and C-11-13 to that of sessilistemonamine E (**195**). However the lack of ROESY correlations between H-9 and H-10 and H-10 and H-11, as were observed in the ROESY spectrum of sessilistemonamine E (**195**), and the new correlations between H-16 and H-9 and H-10, indicated that sessilistemonamine F

(**196**) had the opposite configuration at C-10 to compound sessilistemonamine E (**195**). Compound **196** had similar ROESY correlations between the pyrrolidine ring protons and those on the C-3 γ-lactone ring to those observed in sessilistemonamine E (**195**), specifically between H-3 and H-19α; H-2β and H-18; H-18 to H-19β; and H-19β and 22-Me (Table 6.4). These ROESY correlations indicated that sessilistemonamine E (**195**) and F (**196**) were epimeric only at C-10 (see Tables 6.3 and 6.4).

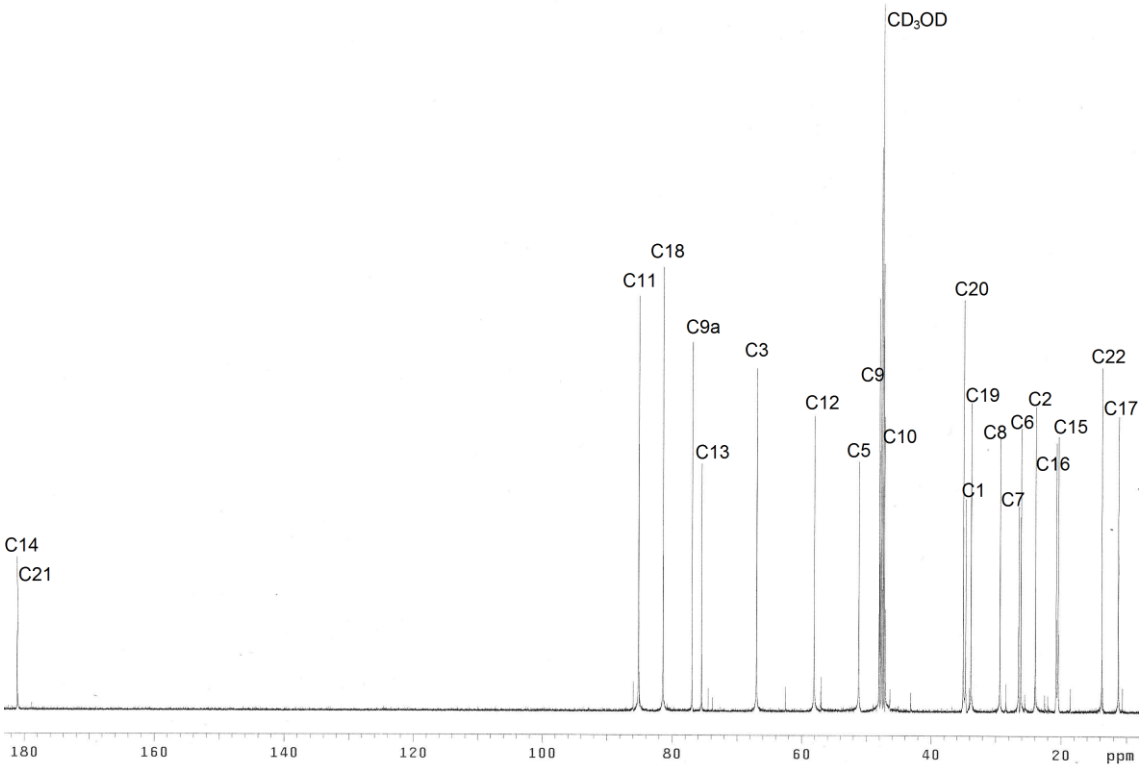

Figure 6.15 ^{13}C NMR spectrum (methanol-d_4, 125 MHz) of sessilistemonamine F (**196**).

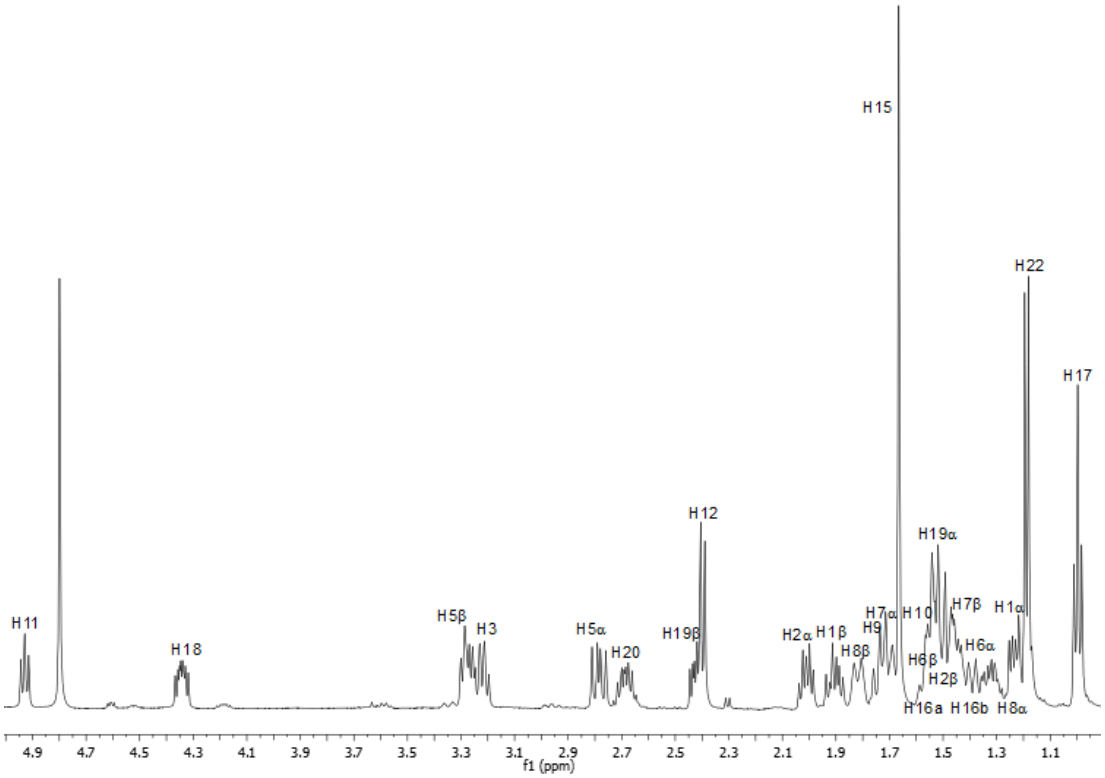

Figure 6.16 ^{1}H NMR spectrum (methanol-d_4, 500 MHz) of sessilistemonamine F (**196**).

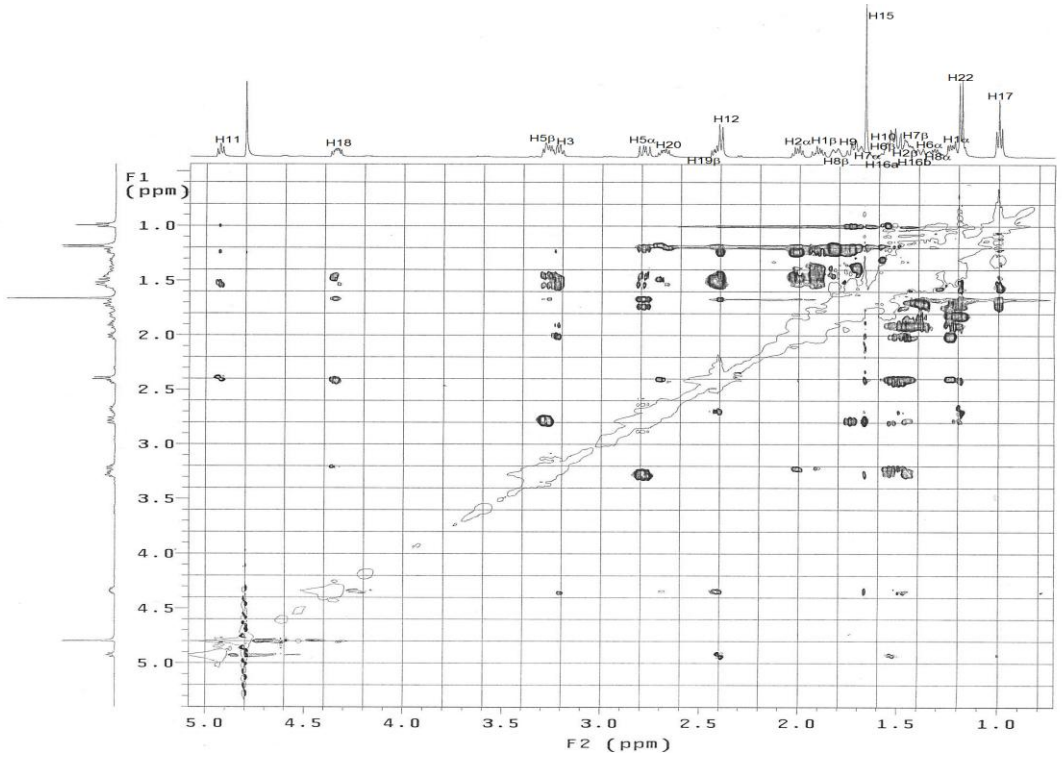

Figure 6.17 ROESY spectrum (methanol-d_4, 500 MHz) of sessilistemonamine F (**196**).

Table 6.4 ^{13}C (125 Hz), ^{1}H (500 MHz) and 2D NMR spectroscopic data for sessilistemonamine F (**196**) in methanol-d_4 solution (δ in ppm).

Position	δ_C	δ_H (mult., *J* (Hz), assign.)	HMBC	ROESY	COSY
1α	34.6	1.27-1.17 (m)		1β, 2α, 3, 12, 19α	2
β		1.95-1.83 (m)		1α, 2β, 10	
2α	23.9	2.06-1.94 (dt, *J* 13.0, 7.0)	1, 3	1α, 2β, 3, 12, 18	1
β		1.51-1.35 (m)		1β, 2α, 5β, 19β	
3	67.0	3.21 (ddd, *J* 8.5, 8.5, 8.5)	1, 2, 5, 8, 19	1α, 2α, 15, 19α	2
5α	51.2	2.81-2.76 (dd, *J* 16.0, 10.5)	3	5β, 9	6
β		3.32-3.20 (m)		2β, 5α, 7β, 8β, 19β	
6α	26.1	1.40-1.31 (m)			5
β		1.60-1.50 (m)			
7α	26.5	1.74-1.65 (m)			6, 8
β		1.49-1.41 (m)		5β, 17	
8α	29.3	1.26-1.14 (m)	2, 5, 7, 12		7, 9
β		1.86-1.76 (m)		5β	
9	48.0	1.77-1.65 (m)	8, 12	5α, 16a	8, 10
9a	76.9	-	1, 2, 5, 7, 8, 9, 15		-
10	47.3	1.57-1.45 (m)	9, 11, 12, 16, 17	1β	
11	85.1	4.93 (t, *J* 7.3)	10, 12, 16	12, 16a, 17	10, 12
12	58.1	2.40 (d, *J* 7.3)	1, 8, 15	1α, 2α, 11, 15, 16	11
13	75.5	-	15, 11		-
14	181.0	-			-
15 (Me)	20.4	1.66, s	12	3, 12, 19α	10, 17
16a	20.7	1.58-1.49 (m)	17	9, 11, 12	
b		1.36-1.49 (m)			16
17 (Me)	11.3	1.00, t (7.0)	10, 16	7β, 11	3, 19
18	81.4	4.33 (ddd, *J* 11.0, 8.5, 5.5)	3, 19	2α, 19β	18, 20
19α	33.8	1.56-1.41 (m)	20, 22	1α, 3, 5α, 15, 20	
β		2.47-2.32 (m)		2β, 5β, 18, 22	19, 22
20	35.0	2.73-2.65 (m)	19, 22	19α, 22	-
21	180.9	-	22, 19	-	20
22 (Me)	13.8	1.19 (d, *J* 7.0)	20, 19	19β, 20	2

A possible scheme for the biosynthesis of **193**-**196** from the hypothetical intermediate **E** is outlined in Scheme 6.2. Reduction of the ketone group of **E** and the oxidation at C-8 could give stichoneurine B (**109**), which could be the precursor of **193** and **194** (Schemes 6.1 and 6.2). Intermediate **A** could form the enol- or enolate-iminium ion intermediate **B** which could under an intramolecular Mannich reaction then ketone reduction and cyclization to the lactone **E** (Scheme 6.2). Hydroxylation of the lactone ring of **E** would give sessilistemoamines E (**195**) and F (**196**) (Scheme 6.2).

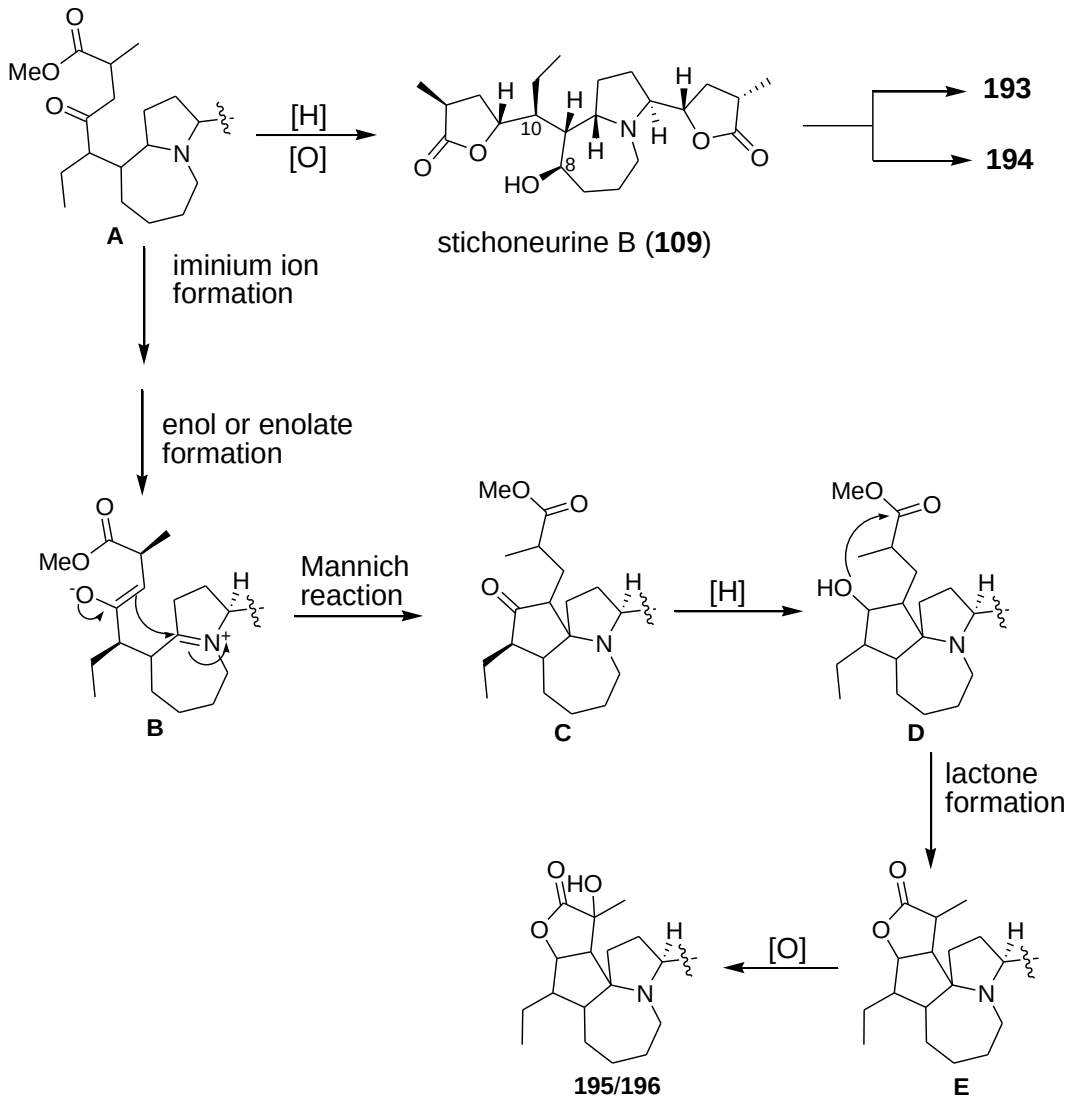

Scheme 6.2 Proposed biosynthesis of sessilistemoamine E and F (**195** and **196**).

6.4 Conclusions

In the previous study, two pyrrolo[1,2-*a*]azepine alkaloids stichoneurines A and B (**108** and **109**) were isolated from the roots of *St. caudatum* collected from Thailand.[4] In contrast, four new pyrrolo[1,2-*a*]azepine alkaloids were isolated from the roots of *St. caudatum* collected from Malaysia, stichoneurines F and D (**193** and **194**) and sessilistemoamine E and F (**195** and **196**). These differences may be due to their different geographical locations (different climates and neutrients), the age of the plants or the season in which the plants were harvested. A possible biosynthesis of these new alkaloids has been proposed starting from stichoneurine B, involving an intramolecular Mannich reaction to form the cyclopentane ring (Schemes 6.1 and 6.2). Further studies should be carried out in order to understand the mechanisms of their formation. In addition, I believe that the synthesis studies of these new alkaloids would be interesting and new findings would be reported.

CHAPTER 7

THE BIOLOGICAL ACTIVITIES OF THE ISOLATED CHEMICAL COMPONENTS

7.1 Acetylcholinestrase (AChE) inhibitory activities

The original methodology and principal for the AChE inhibitory assay were described by Ellman (1961).[83] This assay uses the thiol ester acetylcholine (ATCh) which is hydrolysed by AChE to produce thiocholine (Scheme 7.1 (a)). The enzyme activity is determined by the amount of the yellow coloured 5-thio-nitrobenzoic acid dianion (TNB) that is produce from the reaction between thiocholine and dithiobisnitrobenzoate (DTNB) (Scheme 7.1 (b)). The colour intensity (absorbance) of TNB dianion is measured at λ 412 nm at 25 ^{o}C. This intensity is proportional to the enzyme activity. The inhibition of AChE prevents the hydrolysis of ATCh to thiocholine which terminates the formation of the yellow coloured TNB dianion. The AChE inhibitory activities were analysed with the software package GraphPad Prism® and were determined as IC_{50} values which are the concentration of tested compounds that inhibited AChE by 50%. IC_{50} values are means ± SD of three individual determinations each performed in triplicate. The R^2 (coefficient of determination) must be >0.9 which indicates that the model fits the data better.

This assay was performed using enzymes from two different sources, electric eel AChE (eeAChE) and human AChE (hAChE) (Table 7.1 and Table 7.2). The latter enzyme being more relavant to human AD. Galanthamine, the standard therapeutic drug to treat AD, was used as the reference compound in our assays, with IC_{50} values of 0.55μM and 0.82 μM against hAChE and eeAChE, respectively (Table 7.8, entry 22).

Compound **49** was the most active *Stemona* alkaloid against hAChE with an IC_{50} of 3.74 $\pm$ 0.09 µM, about seven times less active than galanthamine. Compound **192** showed the best activity against eeAChE with an IC_{50} value of 5.90 $\pm$ 0.08 µM (Table 7.1). Compounds **60**, **189**, **195**, **46** also showed significant inhibitory activities, while compounds **188**, **192**, **41** and **193** showed moderate activities against hAChE (Table 7.1). The ethanol roots extract of *S. curtisii* and the methanol crude extracts of *St. halabalensis* and *St. caudatum* showed moderate activities against hAChE, while the crude extract of *S. javanica* was not active (Table 7.2). Consistent with these finding was the fact that the alkaloids from *S. javanica* were also inactive against AChE (IC_{50} > 100 µM).

(a)

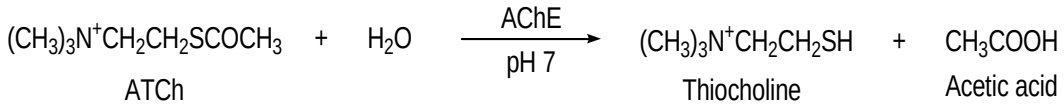

(b)

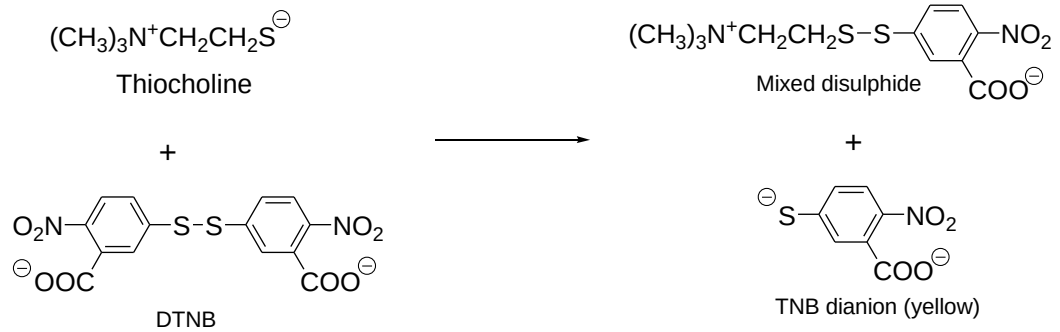

Scheme 7.1 Principle of the Ellman method.[83]

Table 7.1 AChE inhibitory activities of isolated compounds.

Entry	Compounds	IC_{50} values µM (R^2)	
		hAChE	**eeAChE**
1	Stemoninine (**49**)	3.74 ± 0.09 (0.91)	>100
2	Bisdehydoxystemoninine A (**60**)	5.52 ± 0.13 (0.94)	>100
3	(*R*)-(+)-Goniothalamin (**189**)	7.24 ± 0.52 (0.91)	>100
4	Sessilistemoamine E (**195**)	9.1 ± 0.15 (0.94)	-
5	Stemocochinine (**46**)	10.88 ± 0.66 (0.91)	-
6	(+)-α-Tocopherol (**188**)	27.82 ± 0.04 (0.94)	>100
7	Stichoneurine E (**192**)	34.63 ± 0.81 (0.98)	5.90±0.08 (0.99)
8	1-Hydroxyprotostemonine (**41**)	37.45 ± 0.70 (0.90)	-
9	Stichoneurine F (**193**)	71.5 ± 0.10 (0.90)	-
10	Stemofoline (**111**)	>100	-
11	Stichoneurine G (**194**)	>100	-
12	Sessilistemoamine F (**196**)	>100	-
13	Isoprotostemonine (**45**)	>100	-
14	Protostemonine (**40**)	>100	-
15	Isomaistemonine (**95**)	>100	-
16	13-Demethoxy-(11*S**,12*R**)-dihydroprotostemonine (**55**)	>100	-
17	Javastemonine A (**186**)	>100	-
18	Javastemonine B (**187**)	>100	-
19	(2'*S*)-Hydroxystemofoline (**114**)	>100	-
20	Oxystemocurtisinol-*N*-oxide (**145**)	>100	-
21	Isostemofoline **(123)**	>100	-
22	Galanthamine*	0.55 ± 0.03 (0.95)	0.82±0.25 (0.97)

*reference drug for acetylcholinesterase activity

Table 7.2 AChE inhibitory activities of crude extracts.

Entry	Crude extracts	IC_{50} values µg/mL (R^2)	
		hAChE	**eeAChE**
1	Ethanol root extract of *S. curtisii*	17.12 ± 0.40 (0.99)	-
2	Ethanol root extract of *St. halabalensis*	32.94 ± 0.88 (0.90)	>100
3	Methanol root extract of *St. caudatum*	41.8 ± 0.05 (0.98)	-
4	Methanol root extract *S. javanica*	>100	-

7.2 Modulation of drug resistance by *Stemona* alkaloids on multi drug resistant (MDR) cancer cell lines

Of the approximately 1.3 million new cases of cancer which have been described to each year in North America, a significant number are drug resistant.[84,85] This is often due to the fact that these cancers either are inherently untreatable or are resistant to a wide variety of anticancer drugs or their combinations. MDR is a term used to describe the phenomenon characterized by the ability of drug resistant tumour to exhibit simultaneous resistance to a number of structurally and functionally unrelated chemotherapeutic agents.[86] A number of mechanisms have been described to explain the phenomenon of MDR in mammalian cells. They have been broadly classified into cellular and non-cellular mechanisms.[87]

7.2.1 Mechanisms contributing to drug resistant cancer cells

Cancer drug resistance is clinically manifested as either a lack in the reduction of tumour size following chemotherapy or a clinical recurrence or 'relapse' of a tumour after an initial positive response to therapy.[88] Cancer cells effectively evade chemotherapy by a number of different mechanisms. These pathways can either occur simultaneously or sequentially at various times during the course of treatment. Physiological determinants contributing to the availability of the drug to the target site include biopharmaceutical and pharmacokinetic determinants, the tumour microenvironment (including extent of vascularization, hypoxia, tumour geometry and mass), nuclear receptors and localization at pharmacological sanctuary sites.[89–91] Detoxification mechanisms arising from genetic and epigenetic alterations following drug exposure also contribute to the overall resistance phenotype observed clinically.

These include (1) processes limiting anticancer drug concentrations at the molecular target (i.e. increased active drug efflux, decreased drug influx, vesicular sequestration and enhanced drug metabolism,[90–94] (2) mechanisms involving altered molecular targets[91] and (3) mechanisms preventing drug induced cell death (such as increased DNA repair mechanisms[91] and alteration of the cellular death apparatus) (Figure 7.1).[95]

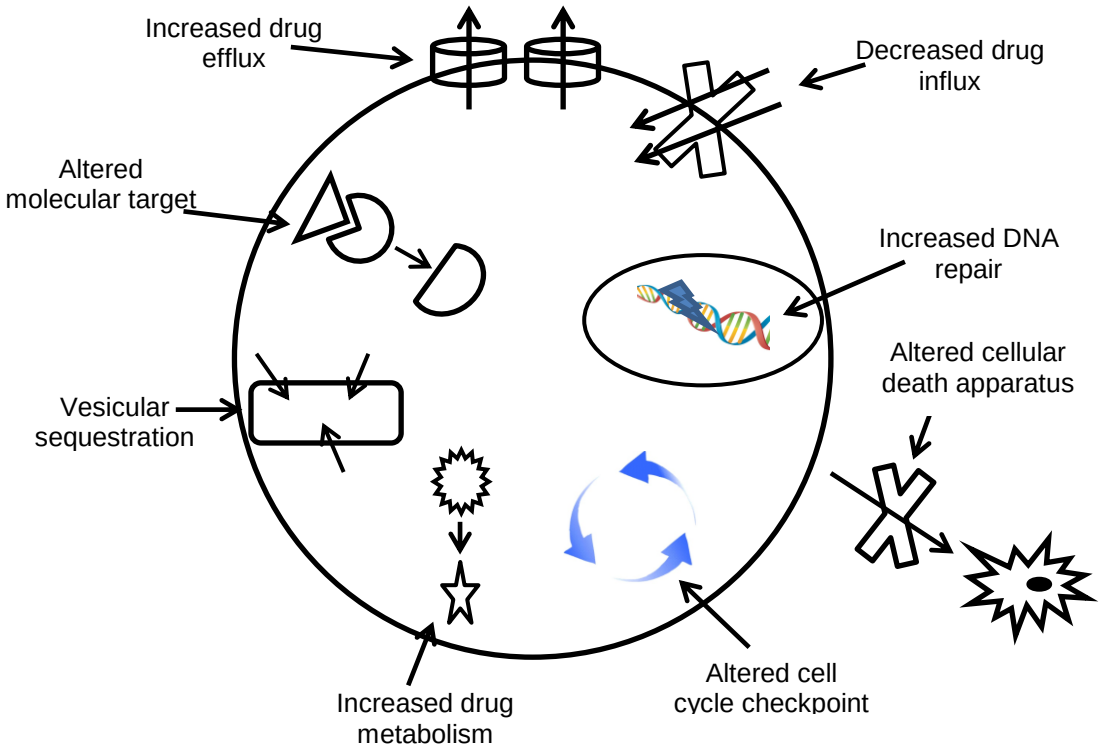

Figure 7.1 Mechanisms of drug resistance in cancer cells. Cancer cells can evade chemotherapeutic treatment by increasing active drug efflux, decreasing drug influx, increasing DNA repair mechanisms, altering apoptotic machinery, altering cell cycle checkpoints, enhancing drug metabolism, increasing vesicular sequestration or altering molecular drug targets.[95]

7.2.2 Modulation of P-glycoprotein in drug resistance in cancer cell lines

Chemotherapy is the treatment of choice in many malignant tumours. Cancer cells may develop a multidrug resistant (MDR) phenotype after prolonged treatment. Multidrug resistance is a significant reason for failure in the treatment of cancer patients. It is often related to the over expression of a 170 kDa plasma membrane glycoprotein (P-gp). P-gp belongs to the superfamily of transporter proteins containing an ATP-binding cassette. It is thought to function as a broad substrate, ATP-dependent pump which can reduce intracellular drug concentrations below a cell-killing threshold.[26–28] Overexpression of P-gp causes cancer cells to be resistant to a variety of structurally and functionally dissimilar anticancer drugs, such as vinblastine, doxorubicin and paclitaxel.

P-Glycoprotein (P-gp)

P-gp, a member of a superfamily of ATP-dependent membrane transport proteins, is a plasma membrane protein that was first characterized in multidrug resistant Chinese hamster ovary cells by Ling and co-workers.[96–99] It has been shown to pump substrates out of tumour cells through an ATP dependent mechanism in a unidirectional fashion. In tumour cells over expressing P-gp, this results in reduced intracellular drug concentrations which decreases the cytotoxicity of a broad spectrum of antitumour drugs including anthracyclines (e.g. doxorubicin), vinca alkaloids (e.g. vincristine) podophyllotoxins (e.g. etoposide) and taxanes (e.g. taxol). Several mechanisms have been put forward to explain this transport function of P-gp. The model of Higgins postulates[86] that P-gp encounters xenobiotics in the inner leaflet of the

plasma membrane and flips the agents to the outer leaflet, where they diffuse into the extracellular region (Figure 7.2).

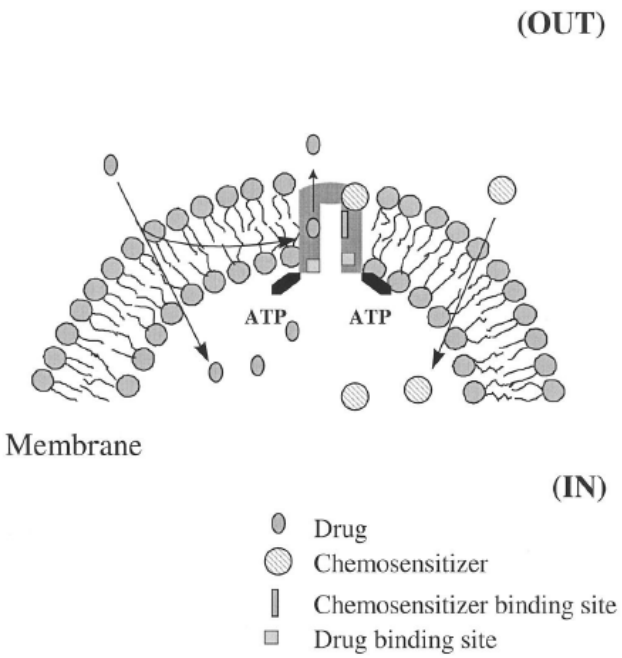

Figure 7.2 Function of the P-gp pump. The model illustrates a protein which uses ATP energy to actively efflux drug substrate across the plasma membrane. The MDR modulator (chemosensitiser) may act as a competitive inhibitor by occupying drug binding sites or as a non-competitive inhibitor at chemosensitiser binding sites.[86]

The calcium channel blocker, verapamil, was the first compound able to enhance intracellular accumulation of many anticancer drugs.[100] However, it suffered as a therapeutic drug due to its intrinsic toxicity at the doses required to inhibit P-gp function.[101] The agents used to enhance drug accumulation and cause no potentiation of drug cytotoxicity in sensitive cells are classified as chemosensitisers or resistance modifiers. In 2011, stemofoline (**9**) was the first *Stemona* alkaloid to be reported as a chemosensitisers for the anticancer drugs, vinblastine, paclitaxel and doxorubicin, in a dose and time-dependent manner in KB-V1 cells, which are MDR human cervical

carcinoma cells with P-gp expression.[29] In this study we focused on the MDR-reversing properties of the *Stemona* alkaloids isolated from *Stemona curtisii* and *Stichoneuron halabalensis* against K562 and K562/Adr.

7. 3 Modulation of resistance to anticancer drug by isolated *Stemona* alkaloids

These alkaloids were chosen because they were available in relatively larger amounts and had not decomposed after isolation and characterization. In collaboration with the Department of Biochemistry, Faculty of Medicine, Chiang Mai University, Thailand, some of the isolated *Stemona* alkaloids were selected to be tested for inhibitory activity against P-glycoprotein (P-gp). The cytotoxicity of eight selected *Stemona* alkaloids (**41**, **46**, **49**, **60**, **114**, **118**, **123** and (11*E*)-1′,2′-didehydrostemofoline) (Figure 7.3) were for the first time investigated against a human leukemic (K562-Adr) cell line, which overexpresses P-gp, and a drug-sensitive cell line (K562) using the tetrazolium-based colorimeteric MTT assay (by treatment with the alkaloids at 0-50 μM for 48 h). Cytotoxicity assays showed that the eight *Stemona* alkaloids were not cytotoxic to K562-Adr or K562 cells at 5μM (>90% cell survival). Thus the alkaloid compounds were applied in all subsequent experiments at a final concentration of 5 μM. These cell lines were then treated with selected *Stemona* alkaloids at 5 μM and various concentrations of doxorubicin (DOX) or paclitaxel (PTX) (0-40 μM DOX for K562-Adr and 0-500 nM for K562) or (0-1.5 μM PTX for K562-Adr and 0-20 nM for K562). The cells were incubated for 48 h at 37 ^{o}C, and then cell growth was assessed by means of an MTT colorimeteric assay. Verapamil (20 μM) was used as a positive control. The relative resistance (RR) was calculated as the ratio of the IC_{50} value of the K562-Adr cells (resistant cells) to the IC_{50} value of the K562 cells (drug sensitive cells). The fold-

reversal activity (FR) was calculated as the ratio of the RR for cells with the anticancer agent but without selected *Stemona* alkaloids to the RR for cells with the anticancer agent and the alkaloid compounds. The results for modulation of resistance to doxorubicin or paclitaxel in K562 and K562-Adr cells after 48 h treatment are shown in Tables 7.3 and 7.4, respectively.

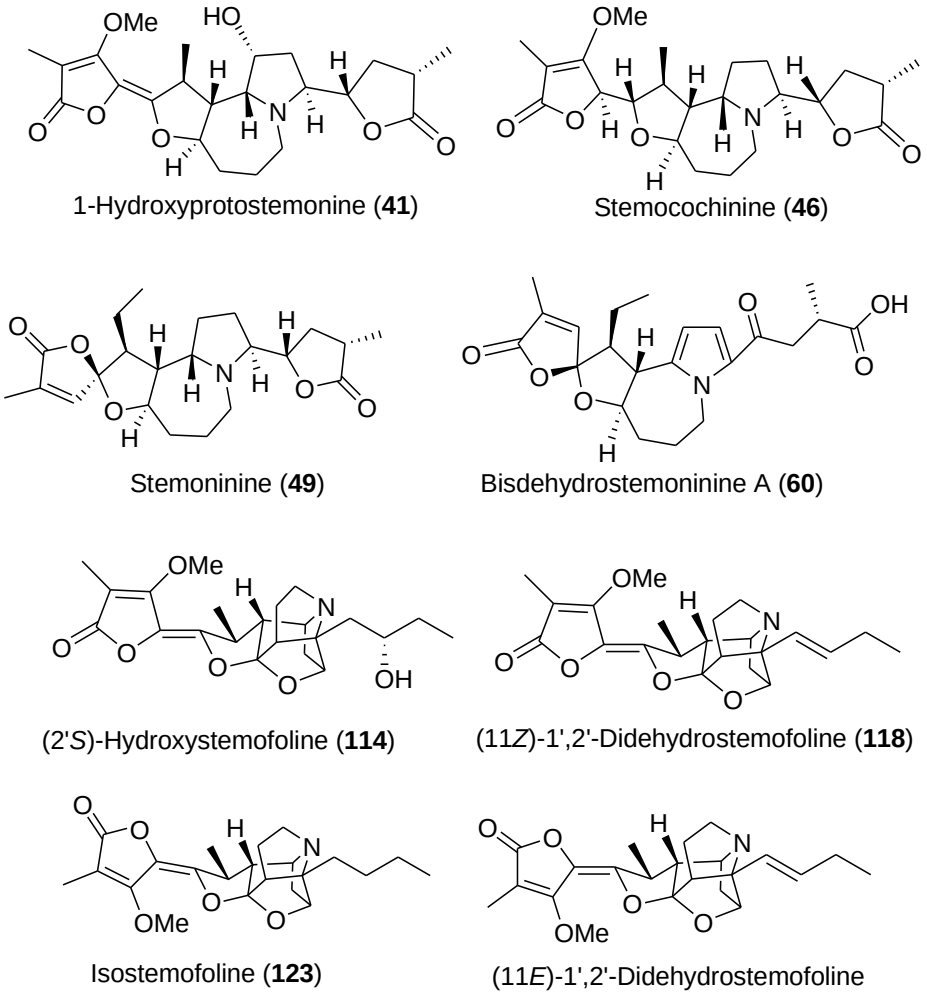

Figure 7.3 *Stemona* alkaloids which were tested for inhibitory activity against P-gp.

Table 7.3 Modulation of resistance to doxorubicin K562-Adr cells by *Stemona* alkaloids (5 μM) after 48 h treatment.

	IC_{50} of doxorubicin (μM)[a]	**Relative resistance (RR)[b]**	**Fold reversal activity (FR)[c]**
Doxorubicin Treatment			
K562	0.448 ± 0.16	1.00 ± 0.00	1.00 ± 0.00
K562-Adr	22.33 ± 2.08	49.75 ± 3.13	1.00 ± 0.00
***Stemona* alkaloids**			
K562-Adr + 5 μM of **46**	22.33 ± 1.15	49.80 ± 0.87*	1.00 ± 0.05
K562-Adr + 5 μM of **114**	15.83 ± 0.76***	35.38 ± 2.89***	1.42 ± 1.18
K562-Adr + 5 μM of **41**	19.67 ± 0.58	43.87 ± 0.36*	1.13 ± 0.07
K562-Adr + 5 μM of **123**	2.52 ± 0.03***	5.62 ± 0.27***	8.88 ± 0.92***
K562-Adr + 5 μM of **49**	19.33 ± 1.15	43.10 ± 1.10*	1.15 ± 0.04
K562-Adr + 5 μM of **118**	6.00 ± 0.00***	13.39 ± 0.49***	3.72 ± 0.35***
K562-Adr + 5 μM of 11*E*-didehydrostemofoline	4.83 ± 0.29***	10.80 ± 0.87***	4.64 ± 0.67***
K562-Adr + 5 μM of **60**	24.00 ± 4.09	53.36 ± 7.35	0.90 ± 0.16

[a]Determined by the MTT assay, and the values are means ± SD of three independent experiments.

[b]IC_{50} of K562-Adr/IC_{50} of K562. Each point represents the mean (±SD) of three independent experiments performed in triplicate.

[c]RR of K562-Adr without *Stemona* alkaloids/RR of K562-Adr with stichoneuron alkaloids. Each point represents the mean (±SD) of three independent experiments performed in triplicate. $^{*}P<0.05$, $^{**}P<0.01$ and $^{***}P<0.001$, vs control treated without *Stemona* alkaloids.

Table 7.4 Modulation of resistance to paclitaxel in K562-Adr cells by *Stemona* alkaloids (5μM) after 48 h treatment.

	IC_{50} of paclitaxel (μM)[a]	**Relative resistance (RR)[b]**	**Fold reversal activity (FR)[c]**
Paclitaxel Treatment			
K562	18.10 ± 0.17	1.00 ± 0.00	1.00 ± 0.00
K562-Adr	1.48 ± 0.01 μM	81.96 ± 1.37	1.00 ± 0.00
***Stemona* alkaloids**			
K562-Adr + 5 μM of **46**	1.33 ± 0.04	73.50 ± 2.66	1.12 ± 0.03
K562-Adr + 5 μM of **114**	1.26 ± 0.23*	69.75 ± 12.43	1.20 ± 0.24
K562-Adr + 5 μM of **41**	1.50 ± 0.00	82.88 ± 0.79	0.99 ± 0.01
K562-Adr + 5 μM of **123**	0.23 ± 0.01 ***	12.61 ± 0.46	6.51 ± 0.34***
K562-Adr + 5 μM of **49**	1.47 ± 0.04	81.12 ± 1.45	1.01 ± 0.02
K562-Adr + 5 μM of **118**	0.47 ± 0.01***	25.97 ± 0.42***	3.16 ± 0.05***
K562-Adr + 5 μM of 11*E*-didehydrostemofoline	0.38 ± 0.01 ***	21.09 ± 0.24***	3.89 ± 0.09***
K562-Adr + 5 μM of **60**	1.46 ± 0.03	80.75 ± 1.06	1.02 ± 0.03

[a]Determined by the MTT assay, and the values are means ± SD of three independent experiments.

[b]IC_{50} of K562-Adr/IC_{50} of K562. Each point represents the mean (±SD) of three independent experiments performed in triplicate.

[c]RR of K562-Adr without *Stemona* alkaloids/RR of K562-Adr with *Stemona* alkaloids. Each point represents the mean (±SD) of three independent experiments performed in triplicate. $^{*}P<0.05$, $^{**}P<0.01$ and $^{***}P<0.001$, vs control treated without *Stemona* alkaloids.

The MDR-reversing properties of the selected the *Stemona* alkaloids on doxorubicin cytotoxicity are shown in Table 7.3. The efficiency of this modulating effect is indicated by a lowering of the RR value from 81.96 and an increase in the FR value from 1.00. Among the tested compounds, isostemofoline (**123**) showed the highest modulating effect on the resistance K562-Adr cells by decreasing the IC_{50} of doxorubicin from 22.33 ± 2.08 μM (Table 7.3) to 2.52 ± 0.03 μM (Table 7.3). It showed the lowest RR of 5.62 ± 0.27 and the highest FR of 8.88 ± 0.92 (Table 7.3). The other compounds that showed MDR-reversing properties were **118,** and 11*E*-didehydrostemofoline. In the present of these compounds, doxorubicin had IC_{50} values 6.00 ± 0.00 and 4.83 ± 0.29 μM respectively (Table 7.3). Compounds **118** and 11*E*-didehydrostemofoline increased sensitivity of K562-Adr cells to doxorubicin, as measured by their FR values by 3.72 ± 0.35 and 4.64 ± 0.67 fold, respectively, while the other compounds showed no modulating effect.

The MDR-reversing properties of the selected the *Stemona* alkaloids on paclitaxel cytotoxicity are shown in Table 7.4. Among the tested compounds, isostemofoline (**123**) showed the highest modulating effect on the resistant K562-Adr cells by decreasing the IC_{50} of paclitaxel from 1.48 ± 0.01 μM to 0.23 ± 0.01 μM (Table 7.4). It showed the lowest RR of 12.61 ± 0.46 and the highest FR of 6.51 ± 0.34 (Table 7.4). The other compounds that showed MDR-reversing properties were **118** and 11*E*-didehydrostemofoline. In the present of these compounds, paclitaxel had IC_{50} values of 0.47 ± 0.01 and 0.38 ± 0.01 μM, respectively (Table 7.4). 11*E*- didehydrostemofoline and compound **118** increased sensitivity of K562-Adr cells to paclitaxel as measured by their FR values of 3.89 ± 0.09 and 3.16 ± 0.05 fold, respectively, while the other compounds showed no modulating effects.

In comparison, stemofoline-type alkaloids **123**, **118** and 11*E*-didehydrostemofoline, which had a non-polar side chain, were observed to be good modulators for both doxorubicin and paclitaxel on K562-Adr cells. Stemofoline-type alkaloids with an alcohol side chain and stemoamide-type alkaloids showed no modulating effects.

7.4 Antimalarial activity of isolated *Stemona* alkaloids against *P. falpacirum*

Thirteen isolated *Stemona* alkaloids were examined for their antiplasmodial (Table 7.5). Compounds **55**, **45**, **40**, **196**, **193**, and **41** demonstrated moderate *in vitro* antiplasmodial activity against the *P. falciparum* strains, TM4 (a wild type chloroquine and antifolate sensitive strain) with IC_{50} values of 17.7 µg/mL, 16.8 µg/mL, 16.0 µg/mL, 18.5 µg/mL, 20.2 µg/mL, and 27.1 µg/mL, respectively, and K1 (multidrug resistant strain) with IC_{50} values of 16.8 µg/mL, 14.1 µg/mL, 11.9 µg/mL, 17.7 µg/mL, 16.5 µg/mL, 20.6 µg/mL, respectively. Stichoneurine G (**194**) only showed moderate antiplasmodial activity against TM4 with an IC_{50} value of 26.8 µg/mL. The other compounds did not show antiplasmodial activity, even at the highest tested concentration of 38.9-42.3 µg/mL.

Table 7.5 Antimalarial activity (IC_{50}) of isolated *Stemona* alkaloids against *P. falpacirum*.

Entry	Compounds	Antimalarial activity against *P. falciparum* (IC_{50}) (µg/mL)	
		TM4	K1
1	Isoprotostemonine (**45**)	16.0 ± 4.2	11.9 ± 3.3
2	Protostemonine (**40**)	16.8 ± 5.4	14.1 ± 3.7
3	13-Demethoxy-(11*S**,12*R**)-dihydroprotostemonine (**55**)	17.7 ± 3.7	16.8 ± 3.1
4	Sessilistemoamine F (**196**)	18.5 ± 3.8	17.7 ± 4.8
5	Stichoneurine F (**193**)	20.2 ± 3.0	16.5 ± 2.2
6	1-Hydroxyprotostemonine (**41**)	27.1 ± 4.5	20.6 ± 4.6
7	Stichoneurine G (**194**)	26.8 ± 3.8	> 42.3
8	Isostemofoline (**123**)	> 38.7	21.4 ± 6.2
9	(2′*S*)-Hydroxystemofoline (**114**)	> 40.3	34.3 ± 8.8
10	Stichoneurine E (**192**)	> 40.5	> 40.5
11	Stemofoline (**111**)	> 38.7	> 38.7
12	Javastemonine A (**186**)	> 38.9	> 38.9
13	Javastemonine B (**187**)	> 41.7	> 41.7
14	Cycloguanil*	0.009	0.810
15	Pyrimethamine*	0.020	7.700

*reference drugs for antiplasmodial activity.

7.5 Cytotoxicity activity of isolated *Stemona* alkaloids againt mammalian cells

Thirteen isolated *Stemona* alkaloids were also examined for their cytotoxicity activity (Table 7.6). However, none of these isolated alkaloids showed toxicity against mammalian cell lines, KB (human mouth epidermal carcinoma cells) and Vero (kidney epithelial cells from an African green monkey), even at the highest tested concentration of 38.9-42.3 µg/mL.

Table 7.6 Cytotoxicity activity (IC_{50}) of isolated *Stemona* alkaloids against mammalian cells (VERO and KB cells).

Entry	Compounds	Cytotoxicity activity against mammalian cells (IC_{50}) (μg/mL)	
		VERO	KB
1	Stemofoline (**111**)	> 38.7	> 38.7
2	1-Hydroxyprotostemonine (**41**)	> 43.3	> 43.3
3	Isostemofoline (**123**)	> 38.7	> 38.7
4	(2′*S*)-Hydroxystemofoline (**114**)	> 40.3	> 40.3
5	Stichoneurine E (**192**)	> 40.5	> 40.5
6	Stichoneurine F (**193**)	> 40.7	> 40.7
7	Stichoneurine G (**194**)	> 42.3	> 42.3
8	Sessilistemoamine F (**196**)	> 39.1	> 39.1
9	13-Demethoxy-(11*S**,12*R**)-dihydroprotostemonine (**55**)	> 38.9	> 38.9
10	Protostemonine (**40**)	> 41.7	> 41.7
11	Isoprotostemonine (**45**)	> 41.7	>41.7
12	Javastemonine A (**186**)	> 38.9	> 38.9
13	Javastemonine B (**187**)	> 41.7	> 41.7
14	Ellipticine*	0.093	-
15	Doxorubicin*	-	0.56

*reference drugs for cytotoxicity activity.

7.6 Conclusions

In this study, some of the isolated alkaloids and a synthesised derivative were tested for four biological activities (AChE inhibitory, MDR-reversing properties, anti-malarial and cytotoxic activities). Some of isolated compounds in this study were not tested due to their limited amounts or because they had decomposed after their characterization. Stemoninine and bisdehydoxystemoninine A had the highest inhibitory activities against human AChE (hAChE) while stichoneurine E showed the highest activity against electric eel AChE (eeAChE). Compounds 13-demethoxy-11(S^*),12(R^*)-dihydroprotostemonine, isoprotostemonine, protostemonine, sessilistemoamine F, stichoneurine F, and 1-hydroxyprotostemonine demonstrated moderate *in vitro* antiplasmodial activity against the *P. falciparum* strains, TM4 and K1.

Stichoneurine G showed only moderate antiplasmodial activity against TM4 while the other compounds did not show antiplasmodial activity. Clearly, in stichoneurines F and G, the occurance of the hydroxyl group in stichoneurine G resulted in higher antiplasmodial activity against TM4. The pyrrolo[1,2-*a*]azepine type alkaloids showed better activities in AChE inhibitory and anti-malarial activities compared to the pyrido[1,2-*a*]azepine type alkaloids. In contrast, the pyrido[1,2-*a*]azepine type alkaloids isostemofoline, (11*Z*)-1′,2′-didehydrostemofoline, and (11*E*)-didehydrostemofoline showed the highest modulating effect on drug resistant K562/Adr cells by decreasing the IC_{50} values of doxorubicin and paclitaxel. None of the tested alkaloids showed toxicity against mammalian cell lines, KB and Vero cells. Further studies should be carried out to synthetic derivatives of these compounds to better understand the structural factors that affect the biological activites of these alkaloids.

CHAPTER 8

CONCLUSIONS

In this project, one *Stemona* spp., *Stemona* curtisii Hook F., and two *Stichoneuron* spp. i.e *Stichoneuron halabalensis* Hook F. and *Stichoneuron caudatum* Ridley were collected from different sites in Malaysia while *Stemona javanica* (Kunth) Engl. was collected in Indonesia. These plants were studied in order to discover new chemical constituents especially *Stemona* alkaloids and to explore the biological activities of these compounds including their i) acetylcholinesterase (AChE) inhibitory activities against human AChE and electric eel acetylcholinesterase (eeAChE), ii) P-glycoprotein (P-gp) modulator activities for the potential treatment of multidrug resistant (MDR) cancers, iii) antiplasmodial activities against the *Plasmodium falciparum* strains, TM4 (a wild type chloroquine and antifolate sensitive strain) and K1 (multidrug resistant strain) and iv) cytotoxicity activity against mammalian cell lines, KB (human mouth epidermal carcinoma cells) and Vero (kidney epithelial cells from an African green monkey) cells.

The phytochemical study on the roots extract of *S. curtisii* led to the isolation six of known alkaloids, (2'*S*)-hydroxystemofoline (**114**), stemocochinine (**46**), 1-hydroxyprotostemonine (**41**), oxystemokerrin-*N*-oxide (**145**), isostemofoline (**123**) and stemofoline (**111**). Phytochemical investigations on *S. curtisii* from Thailand have been carried out since 2003 with the latest finding of new alkaloid **148** reported in 2013. The differences of alkaloids distribution from Malaysia (as found in this study) and Thailand may be due to their different geographical locations (different climates and neutrients), the age of the plants or the season in which the plants were harvested.

Two new protostemonine-type alkaloids, javastemonine A and B (**186** and **187**) (Figure 8.1) were isolated from the root extracts of *Stemona javanica* together with four known *Stemona* alkaloids, 13-demethoxy-11(*S**),12(*R**)-dihydroprotostemonine (**55**) protostemonine (**40**), isoprotostemonine (**45**) and isomaistemonine (**95**). Protostemonine (**40**) was the major alkaloid. Javastemonine A (**186**) was a diastereomer of **55** and **46** while javastemonine B (**187**) was an epimer of **45**. Importantly, noticeable differences in the chemical shifts of some ^{1}H and ^{13}C NMR resonances of these diastereomers were observed.

A study of the hitherto unreported *Stichoneuron halabalensis* led to the characterization of the known compounds (+)-α-tocopherol (**188**), (*R*)-(+)-goniothalamin (**189**), seven pyrrolo[1,2-*a*]azepine type alkaloids including four known alkaloids bisdehydrostemoninine A (**60**), stemoninine (**49**), sessilistemoamine C (**98**), sessilistemoamine A (**96)**; and three new alkaloids, stichoneurines C (**190**), D (**191**) and E (**192**) (Figure 8.1). Stichoneurines C-E (**190**-**192**) are diastereoisomers and have a N-xide structure. The occurances of (+)-α-tocopherol (**188**) and (*R*)-(+)-goniothalamin (**189**) from the family Stemonaceae have never before been reported.

Four novel stichoneurine-type alkaloids, stichoneurines F and G (**193** and **194**) and sessilistemonamines E and F (**195** and **196**) (Figure 8.1) were isolated from the root extracts of *Stichoneuron caudatum* Ridley. Stichoneurines F (**193**) was the major alkaloids. The biosynthesis of stichoneurines F and D (**193** and **194**) and sessilistemoamine E and F (**195** and **196**) were proposed in Schemes 6.1 and 6.2 respectively. This proposed biosynthesis starts from stichoneurine B and involved an intramolecular Mannich reaction to form the cyclopentane.

The isolation and purification of these chemical constituents were performed using various chromatography techniques. The structures of the known compounds were determined on the basis of their spectroscopic data and from comparisons made with literature data. The structures and relative configurations of the new alkaloids have been determined by 1D and 2D NMR spectroscopic, MS and IR methods and molecular modeling experiments. Molecular modeling was an important method to help interpret the NOESY and ROESY NMR experiments and assign the relative configurations of the new alkaloids.

The AChE inhibitory activities of the isolated compounds and crude extracts were performed using a spectrophotometric-based method known as Ellman's method. Stemoninine (**49**) and bisdehydoxystemoninine A (**60**) showed the highest inhibitory activities against hAChE but were far less active againts eeAChE. In contrast, stichoneurine E (**192**) showed highest activity against eeAChE when compared to hAChE. While the crude extracts of *St. caudatum*, *St. halabalensis* and *S. curtisii* showed significant inhibitory activities against hAChE. The highest modulating activity was observed with isostemofoline (**123**) which had a simple non-polar side chain. Other stemofoline-type alkaloids, **118** and (11*E*)-didehydrostemofoline, also exhibited better activities than the stemoamide alkaloids as modulators of resistance to anticancer drugs. Thirteen isolated *Stemona* alkaloids were examined for their antiplasmodial activities. The pyrrolo[1,2-*a*]azapine alkloids **41**, **40**, **45**, **55**, **193** and **196** demonstrated moderate *in vitro* antiplasmodial activity against the *P. falciparum* strains, TM4 and K1, while alkaloid **194** only showed moderate antiplasmodial activity against TM4. The other compounds, are pyrido[1,2-*a*]azapine alkaloids, except alkaloids **186** and **187**, which

did not show antiplasmodial activity. None of these alkaloids showed toxicity against KB and Vero cell lines.

Some isolated alkaloids that were isolated in relatively large amount would make useful starting materials for the synthesis other minor alkaloids or analogues for further biological testing. Instead of using commercial chemicals, using stable isolated alkaloids might save money and time and provide a ‘short cut’ for the synthesis of other alkaloids with potentially useful biological activities. Further study using isotopically labeled molecules should be carried out in order to understand their biosynthesis and to test the biosynthetic pathways proposed in this thesis. Phytocemical studies on Stemonaceae plants should be developed further to include studies of plants in other locations, including well studies species which may have produced new chemical components due to their different geographical locations and levels of nutrients and climate.

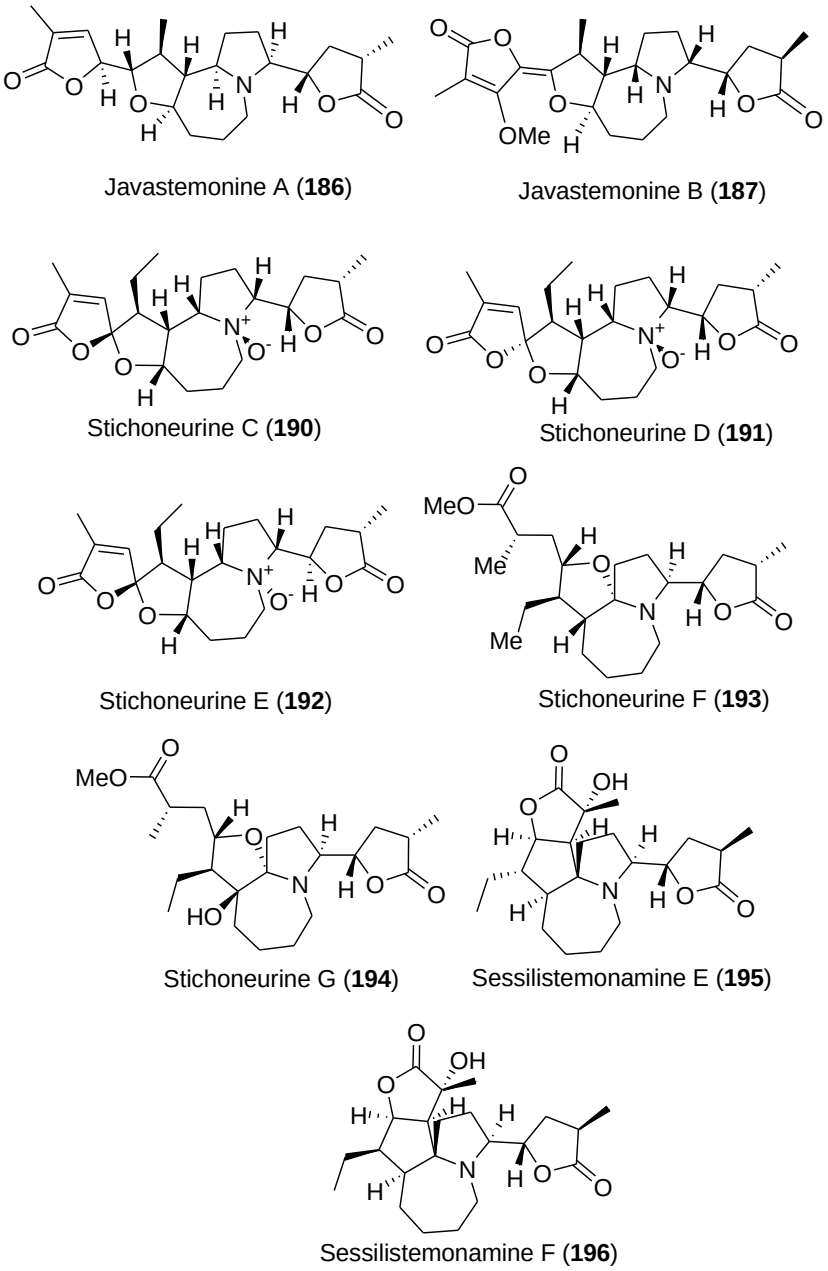

Figure 8.1 New alkaloids isolated from this work.

CHAPTER 9

EXPERIMENTAL

9.1 General Experimental

9.1.1 Chromatography

Thin Layer Chromatography (TLC) was performed using aluminium-backed Merck sorbent silica gel (0.1 mm thickness). Compounds were detected by staining with Dregendroff reagent. Preparative TLC (PTLC) was performed using commercial glass-backed plates (20 x 20 cm) with Merck 60 PF 254 silica gel (1 mm thickness). Compounds were detected under a 254 nm ultraviolet lamp.

The Dragendroff's reagent was prepared from a mixture of two stock solutions. Stock solution A contained H_2O (10 mL), concentrated HCl (2 mL) and bismuth subnitrate (0.6 g). Stock solution B contained H_2O (10 mL) and KI (6.0 g). These two stock solutions were combined and diluted with H_2O (15 mL) and concentrated HCl (7 mL). The mixture was then made up to 400 mL with H_2O. The TLC spots were dipped in the Dragendroff's reagent in order to see the alkaloid spots.

Purification of compounds by column chromatography was performed using Merck GF 254 flash silica gel (40-63 μm). Small-scale separations (< 2.0 g) were performed using either a 10 or 20 mm diameter column, and large scale separations (> 2.0 g) were performed using either 30 or 50 mm diameter column, each with the stated solvent system. Most columns were developed using gradient elution using the solvent mixtures defined in the experimental section.

9.1.2 Polarimeter

Optical rotations were measured using a 1 cm cell, in a Jasco DIP-370 digital polarimeter or a 10 cm cell, in a Jasco P-2000 polarimeter. Ten measurements were taken and the average was used to calculate the specific rotation.

9.1.3 Mass spectrometer

Low resolution mass spectra were obtained either on a Shimadzu GC mass spectrometer (EI and Cl) or a Waters LCZ single quadropole (ESI). High-resolution mass spectra were obtained either on a VG Autospec mass spectrometer (EI and Cl) or a Waters QTOF (ESI). HRMS (exact masses) were used in lieu of elemental analysis and TLC analysis and ^{1}H and ^{13}C NMR spectroscopy were used as criteria for purity. In most case compounds were purified to 90-95% purityas judged by ^{1}H NMR analysis.

9.1.4 Infrared spectroscopy

Infrared spectra were obtained as neat samples on a Smart Omni-Sampler Avator ESP Nicolet spectrometer.

9.1.5 Nuclear magnetic resonance spectroscopy

^{1}H and ^{13}C NMR spectra were recorded on a Varian Inova-500 spectrometer (500 MHz, ^{1}H and 125 MHz, ^{13}C) in deuterochloroform ($CDCl_3$), unless otherwise specified. NMR assignments were based on gCOSY, gHSQC, gHMBC, ROESY, NOESY, TOCSY and DEPT or APT experiments. These experiments were performed using the standard Varian pulse sequences and mixing times. NMR solvents used in the experiments and their associated referencing data are displayed in Table 9.1. Unless

otherwise stated, the applied NMR frequency was 500 MHz for ^{1}H NMR experiments and 125 MHz for ^{13}C NMR experiments, with samples dissolved in $CDCl_3$.

Table 9.1 The references used for ^{1}H and ^{13}C NMR spectroscopy.

Solvent	^{1}H NMR		^{13}C NMR
	Internal standard	**Other**	**Other**
$CDCl_3$	TMS, s, 0.00 ppm	Residual $CHCl_3$, s, 7.26 ppm	$CDCl_3$, 77.0 ppm
CD_3OD	TMS, s, 0.00 ppm	Residual MeOH, s, 3.31 ppm	CD_3OD, 49.0 ppm

9.1.6 Molecular modeling

Molecular modeling was performed using Spartan'10 for Window, Version 1.0.1, January 4th 2011. To find the lowest energy structure, a conformational library was generated using molecular mechanics (MMFF force field in Spartan). The lowest energy conformation was then geometry optimized using Semi-Empirical calculations at the AM1 level. These calculations showed that conformers within 5 kcal/mol in energy of the lowest energy conformer had essentially the same skeleton structure and these conformers only differed in the dihedral angle about the rotatable C-3 to C-18 bond. The molecular modelling was consistent with the NOESY/ROSY correlations observed where protons less than 3A [please use angstrom symbol] apart would be expected to show a correlation.

9.2 Experimental for Chapter 3

Plant material. The roots of *Stemona curtisii* were collected at Dungun, Terengganu, Malaysia in May 2011. The plant material was identified by Mr. Sani. A voucher

specimen, UKMB29952 was deposited at Department of Biology, National University of Malaysia.

Extraction of crude from roots of *Stemona curtisii*. The roots (2205.30 g) were dried in an oven at 50 ^{o}C until the dry weight became constant. The dried roots of *S. curtisii* (558.26 g) were ground into a powder and extracted with 95% ethanol. The ethanolic extracts were evaporated to give a dark brown gum (7.2 g).

Isolation of compounds from the roots of *Stemona curtisii*. The root extract (7.2 g) was chromatographed by column chromatography (CC) on a silica gel using gradient elution CH_2Cl_2/EtOAc (3:7 to 0:10) to EtOAc/MeOH (10:0 to 8:2). A total of 2.5 L eluent was collected in test tubes of 20 mL. These fractions were pooled on the basis of TLC analysis to give fractions A (97.4 mg), B (40.3 mg), C (50 mg) and D (5.7 g). Fraction A (97.4 mg) was further purified on a silica gel column using CH_2Cl_2/MeOH/NH_3 (99:1:1) to give (2'*S*)-hydroxystemofoline **114** (21.1 mg, 21.7%). Separation of fraction B by CC using CH_2Cl_2/MeOH/NH_3 (99:1:1) gave fraction B1 (15 mg) and stemocochinine **46** (5.9 mg, 14.6%). Further purification of fraction B1 on a small column using CH_2Cl_2/NH_3 (99:1) gave 1-hydroxyprotostemonine **41** (7.6 mg, 50.6%). Separation of fraction C by CC (CH_2Cl_2/MeOH/NH_3, 95:4:1) and then CC (diethyl ether/acetone, 7:3) gave oxystemokerrin-*N*-oxide **145** (2.9 mg, 5.8%). A portion of fraction D (1.2 g) was subjected to CC using (CH_2Cl_2/EtOAc, 3:7) then CC (*n*-hexane/EtOAc, 9:1) to give fraction D1 (520 mg). Further purification of fraction D1 by CC (EtOAc/MeOH 9:1) gave isostemofoline **123** (27.4 mg, 5.3%) and stemofoline **111** (6.9 mg, 1.3%).

1-Hydroxyprotostemonine (41)

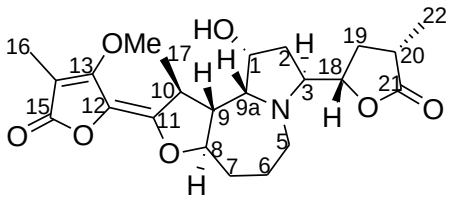

Isolated as a yellow gum.

ESIMS *m/z* 408 $[M+H]^+$; $[C_{22}H_{31}NO_7 + H]^+$.

^{1}H NMR (500 MHz, methanol-*d*4) refer to Table 3.1 for specific details.

The ^{1}H NMR spectroscopic data agreed with those previously reported.[39]

(2′*S*)-Hydroxystemofoline (114)

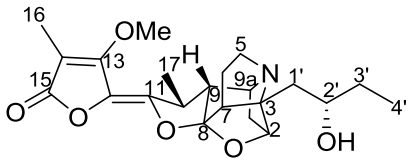

Isolated as a yellow gum.

ESIMS *m/z* 404 $[M+H]^+$; $[C_{22}H_{29}NO_6 + H]^+$.

^{1}H NMR (500 MHz, $CDCl_3$) refer to Table 3.2 for specific details.

^{13}C NMR (125 MHz, $CDCl_3$) refer to Table 3.2 for specific details.

The ^{1}H and ^{13}C NMR spectroscopic data agreed with those previously reported.[46]

Stemocochinine (46)

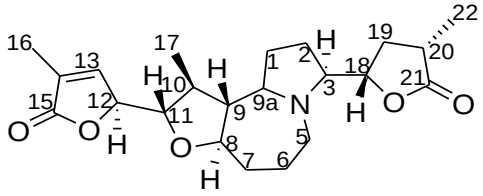

Isolated as a yellow gum.

ESIMS *m/z* 390 $[M+H]^+$; $[C_{22}H_{31}NO_5 + H]^+$.

^{1}H NMR (500 MHz, $CDCl_3$) refer to Table 3.3 for specific details.

^{13}C NMR (125 MHz, $CDCl_3$) refer to Table 3.3 for specific details.

The ^{1}H and ^{13}C NMR spectroscopic data agreed with those previously reported.[10]

Oxystemocurtisin-*N*-oxide (145)

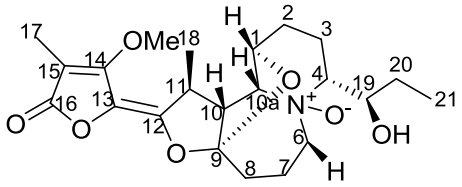

Isolated as a yellow gum.

ESIMS *m/z* 422 $[M+H]^+$; $[C_{21}H_{31}NO_7 + H]^+$.

^{1}H NMR (500 MHz, methanol-*d*4) refer to Table 3.4 for specific details.

The ^{1}H NMR spectroscopic data agreed with those previously reported.[10]

Stemofoline (111)

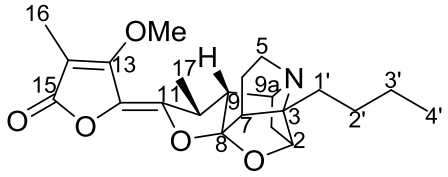

Isolated as a brown gum.

ESIMS *m/z* 388 $[M+H]^+$; $[C_{22}H_{29}NO_5 + H]^+$.

^{1}H NMR (500 MHz, $CDCl_3$) refer to Table 3.5 for specific details.

The ^{1}H NMR spectroscopic data agreed with those previously reported.[15]

Isostemofoline (123)

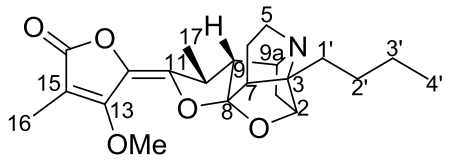

Isolated as a brown gum.

ESIMS *m/z* 388 $[M+H]^+$; $[C_{22}H_{29}NO_5 + H]^+$.

^{1}H NMR (500 MHz, $CDCl_3$) refer to Table 3.6 for specific details.

The ^{1}H NMR spectroscopic data agreed with those previously reported.[71]

9.3 Experimental for Chapter 4

Plant material. The roots of *S. javanica* were collected from Alas Purwo, East of Java, Indonesia in June and December 2012. The material was identified at the Conservation Institute of Purwodadi Botanical Garden, Pasuruan, East of Java, Indonesia, where a voucher specimen (No. IV.D.IV.7) was deposited.

Extraction of crude from roots of *Stemona javanica*. The dry, ground roots of *S. javanica* (1.3 kg) were extracted with 95% MeOH (4 × 1000 mL) over 3 days at room temperature. The MeOH solution was evaporated to give a dark residue (35.2 g).

Isolation of compounds from the roots of *Stemona javanica*. The residue was chromatographed on silica gel (200 mL) using gradient elution from CH_2Cl_2/MeOH (0:10) to CH_2Cl_2/MeOH (8:2). A total of 4 L of eluent was collected in test tubes of 200 mL. These fractions were pooled on the basis of TLC analysis to give three alkaloid fractions; A (2.2 g), B (5.2 g) and C (1.2 g). A portion of fraction A (100 mg) was further separated by preparative thin layer chromatography (PTLC) using *n*-

hexane/EtOAc (1:9) as the eluent to give isomaistemonine **95** (2.5 mg, 2.5%) and protostemonine **40** (55.3 mg, 55.3%). Fraction B (2.5 g) was then separated by column chromatography using isocratic eluent (CH_2Cl_2/MeOH; 8:2) to give fraction B1 (507 g) and B2 (700 mg). A portion of fraction B1 (240 mg) was further purified by PTLC (*n*-hexane/EtOAc (9:1)) and gave 13-demethoxy-(11*S**,12*R**)-dihydroprotostemonine **55** (8.3 mg, 3.5%) and javastemonine A **186** (11.7 mg, 4.9%). Fraction B2 (700 mg) was chromatographed on silica gel (*n*-hexane/EtOAc (9:1)) to give isoprotostemonine **45** (30 mg, 4.3%). A portion of fraction C (130 mg) was further chromatographed by PTLC (*n*-hexane/EtOAc (9:1)) to give javastemonine B **187** (49.7 mg, 38.2%).

Javastemonine A (186)

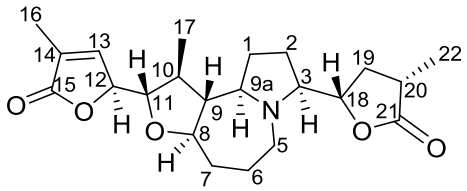

Isolated as a brown gum.

$[\alpha]_D^{25}$ = +36° (*c* 0.09, $CHCl_3$).

HRESIMS *m*/*z* 390. 2280 $[M + H]^+$ (calcd for $C_{22}H_{32}NO_5$ 390.2291).

IR film *v*max 3436, 2963, 2874, 1771, 1761, 1657, 1455, 1159, 1044, 726 cm^{-1}.

^1H NMR (500 MHz, $CDCl_3$) refer to Table 4.1 for specific details.

^{13}C NMR (125 MHz, $CDCl_3$) refer to Table 4.1 for specific details.

Javastemonine B (187)

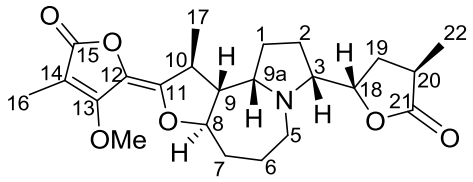

Isolated as a brown gum.

$[\alpha]_D^{25}$ = -45° (*c* 0.01, $CHCl_3$).

HRESIMS *m/z* 418.2230 $[M + H]^+$ (calcd for $C_{23}H_{32}NO_6$ 418.2226).

IR film *v*max 2940, 1780, 1745, 1670, 1610, 1455, 1399, 1195, 1165, 1000 cm^{-1};

^1H NMR (500 MHz, $CDCl_3$) refer to Table 4.3 for specific details.

^{13}C NMR (125 MHz, $CDCl_3$) refer to Table 4.3 for specific details.

13-Demethoxy-11(*S),12(*R**)-dihydroprotostemonine (55)**

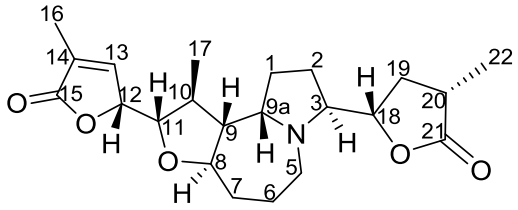

Isolated as a brown gum.

ESIMS *m/z* 390 $[M+H^+]$; $[C_{22}H_{31}NO_5 + H]^+$.

^1H NMR (500 MHz, $CDCl_3$) refer to Table 4.5 for specific details.

The ^1H NMR spectroscopic data agreed with those previously reported.[22]

Protostemonine (40)

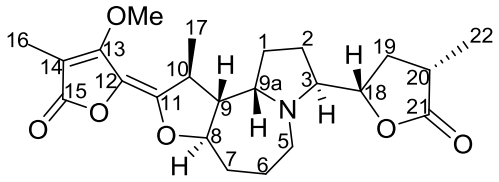

Isolated as a brown gum.

ESIMS *m/z* 418 $[M+H]^+$; $[C_{23}H_{31}NO_6 + H]^+$.

^{1}H NMR (500 MHz, $CDCl_3$) refer to Table 4.6 for specific details.

^{13}C NMR (125 MHz, $CDCl_3$) refer to Table 4.6 for specific details.

The ^{1}H and ^{13}C NMR spectroscopic data agreed with those previously reported.[10]

Isoprotostemonine (**45)**

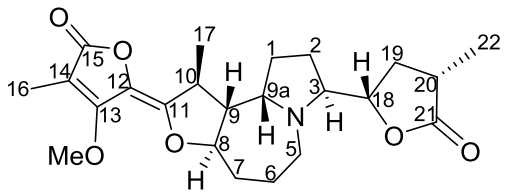

Isolated as a brown gum.

ESIMS *m/z* 418 $[M+H]^+$; $[C_{23}H_{31}NO_6 + H]^+$.

^{1}H NMR (500 MHz, $CDCl_3$) refer to Table 4.7 for specific details.

^{13}C NMR (125 MHz, $CDCl_3$) refer to Table 4.7 for specific details.

The ^{1}H and ^{13}C NMR spectroscopic data agreed with those previously reported.[7]

Isomaistemonine (95)

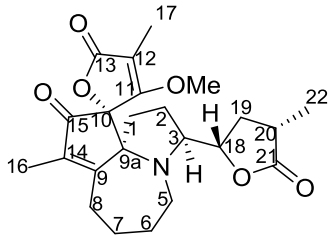

Isolated as a brown gum.

ESIMS *m/z* 416 $[M+H]^+$; $[C_{23}H_{29}NO_6 + H]^+$.

^{1}H NMR (500 MHz, $CDCl_3$) refer to Table 4.8 for specific details.

The ^{1}H NMR spectroscopic data agreed with those previously reported.[73]

9.4 Experimental for Chapter 5

Plant material. The roots of *Stichoneuron halabalensis* were collected at Endau-Rompin National Park, Pahang, Malaysia in April 2010. The plant material was identified by Prof. Latiff Mohammad. A voucher specimen, UKM29953 was deposited at Department of Biology, National University of Malaysia.

Extraction of crude from roots of *St. halabalensis*. The dry ground root (199.2 g) of *St. halabalensis* was extracted with 95% EtOH (4 x 2.5 L) over 4 days at rt. The ethanolic extracts were evaporated to give a dark brown (4.4 g).

Isolation and purification of chemical constituents from ethanol extract of roots of *St. halabalensis*. The root extract was chromatographed on silica gel (200 mL) using gradient elution from *n*-hexane/EtOAc (9:1 to 0:10) to EtOAc/MeOH (10:0 to 8:2). A total of 1.5 L eluent was collected in test tubes of 20 mL. These fractions were pooled on the basis of TLC analysis to give non-alkaloid fraction A (180.0 mg) and the alkaloid fractions B (209.0 mg) and C (1.5 g). Separation of fraction A by column

chromatography (CC) (light petrol/EtOAc, 8:2) gave (+)-α-tocopherol **188** (4.5 mg, 2.5%) and fraction A2 (30 mg). Further purification of fraction A2 by preparative TLC gave (*R*)-(+)-goniothalamin **189** (7.2 mg, 24%). Fraction B was purified by CC (CH_2Cl_2/EtOAc, 1:1) to give bisdehydrostemoninine A **60** (6.2 mg, 3.0%) and stemoninine **49** (41.5 mg, 19.9%). Separation of fraction C by CC (CH_2Cl_2/MeOH, 98:2) then preparative TLC (light petrol/EtOAc, 8:2) gave fractions C1 (66.7 mg) and C2 (180 mg). A portion of fraction C1 (12.4 mg) was subjected to preparative TLC (CH_2Cl_2/EtOAc, 7:3), which gave sessilistemoamine C **98** (1.0 mg, 8.1%). This technique was repeated for fraction C2 (32 mg) to gain more sessilistemoamine C **98** (3.2 mg, 10%). Further purification by preparative TLC (CH_2Cl_2/EtOAc, 1:1) of fraction C3 (30 mg) gave sessilistemoamine A **96** (2.5 mg, 8.3%). An inseparable mixture of stichoneurine C **190** and D **191** (13.3 mg, **190**:**191** = 5:1, 44.4%) was isolated from fraction C3 (30 mg) by using repeated (x 2) preparative TLC (CH_2Cl_2/MeOH, 9.5:0.5).

Stichoneurine C (190)

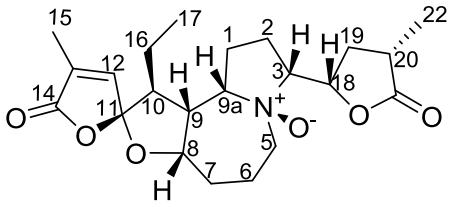

Isolated as a yellow gum.

R_f = 0.13 in CH_2Cl_2/MeOH, (95:5).

ESIMS *m/z* 406 $[M+H]^+$.

HRESIMS *m/z* $[M+H]^+$ 406.2218 (calcd for $C_{22}H_{32}NO_6$, 406.2230).

^{1}H NMR (500 MHz, $CDCl_3$) refer to Table 5.1 for specific details.

^{13}C NMR (125 MHz, $CDCl_3$) refer to Table 5.1 for specific details.

Stichoneurine D (191)

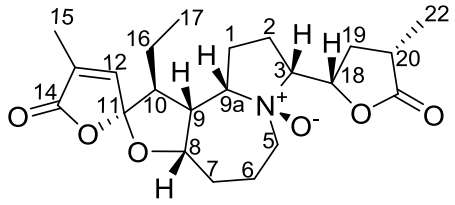

Isolated as a yellow gum.

R_f = 0.13 in CH_2Cl_2/MeOH, (95:5).

ESIMS *m/z* 406 $[M+H]^+$.

HRESIMS *m/z* $[M+H]^+$ 406.2218 (calcd for $C_{22}H_{32}NO_6$, 406.2230).

^{1}H NMR (500 MHz, $CDCl_3$) refer to Table 5.1 for specific details.

^{13}C NMR (125 MHz, $CDCl_3$) refer to Table 5.1 for specific details.

(+)-α-Tocopherol (188).

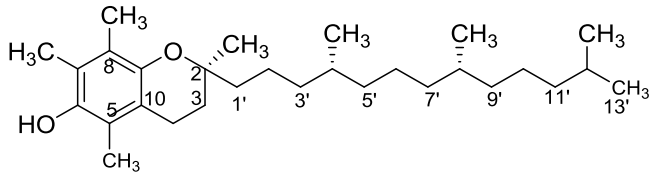

Isolated as a white powder. $[\alpha]_D^{25}$ = +28° (*c* 0.075, $CHCl_3$) [(Literature value: $[\alpha]_D^0$ = +82° (EtOH);[78] $[\alpha]_D^{25}$ = +4.8° (EtOH)[79]]

EIMS *m/z* 430 $[M^+]$; $[C_{29}H_{50}O_2^+]$

^{1}H NMR (500 MHz, $CDCl_3$) refer to Table 5.3 for specific details.

The ^{1}H NMR spectroscopic data agreed with those previously reported.[80]

(*R*)-(+)-Goniothalamin (189).

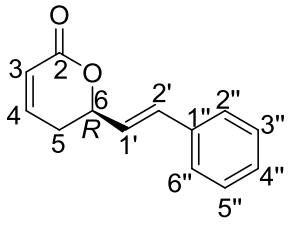

Isolated as a yellow gum.

$[\alpha]_D^{25}$ = +110° (*c* 0.96, $CHCl_3$); Literature value: $[\alpha]_D^{25}$ = +170 (*c* 1.38, $CHCl_3$).[81]

EIMS *m/z* 200 [M^+]; [$C_{13}H_{12}O_2^+$]

^{1}H NMR (500 MHz, $CDCl_3$) refer to Table 5.4 for specific details.

^{13}C NMR (125 MHz, $CDCl_3$) refer to Table 5.4 for specific details.

The ^{1}H and ^{13}C NMR spectroscopic data agreed with those previously reported.[82]

Stemoninine (49)

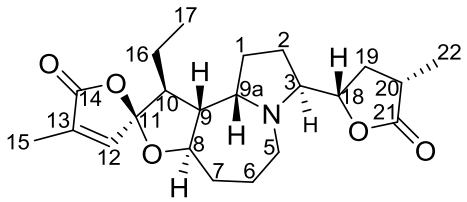

Isolated as a brown gum.

ESIMS *m/z* 390 [M+H]$^+$; [$C_{22}H_{31}NO_5$+H]$^+$

^{1}H NMR (500 MHz, $CDCl_3$) refer to Table 5.5 for specific details.

^{13}C NMR (125 MHz, $CDCl_3$) refer to Table 5.5 for specific details.

The ^{1}H and ^{13}C NMR spectroscopic data agreed with those previously reported.[76]

Bisdehydoxystemoninine A (60)

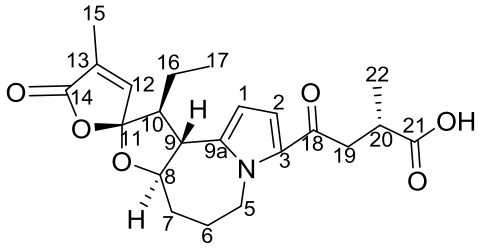

Isolated as a brown gum.

ESIMS *m/z* 402 $[M+H^+]$; $[C_{22}H_{27}NO_6+H]^+$

^{1}H NMR (500 MHz, $CDCl_3$) refer to Table 5.6 for specific details.

^{13}C NMR (125 MHz, $CDCl_3$) refer to Table 5.6 for specific details.

The ^{1}H and ^{13}C NMR spectroscopic data agreed with those previously reported.[18]

Sessilistemoamine A (96)

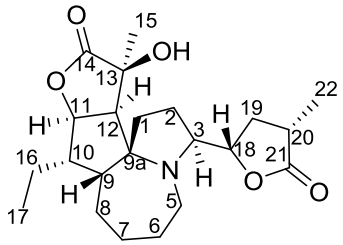

Isolated as a yellow gum.

ESIMS *m/z* 392 $[M+H^+]$; $[C_{22}H_{33}NO_5+H]^+$

^{1}H NMR (500 MHz, $CDCl_3$) refer to Table 5.7 for specific details.

The ^{1}H NMR spectroscopic data agreed with those previously reported.[25]

Sessilistemonamine C (98)

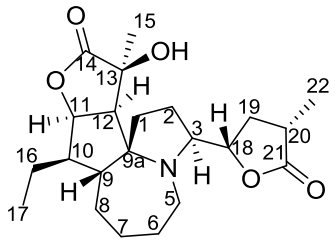

Isolated as a yellow gum.

ESIMS *m/z* 392 $[M+H^+]$; $[C_{22}H_{33}NO_5+H]^+$

^{1}H NMR (500 MHz, $CDCl_3$) refer to Table 5.8 for specific details.

The ^{1}H NMR spectroscopic data agreed with those previously reported.[25]

Extraction of crude from leaves of *St. halabalensis*. The dry ground leaves (248.5 g) of *St. halabalensis* was extracted with 95% EtOH (4 x 1.5 L) over 4 days at rt. The ethanolic extracts were evaporated to give a dark green residue (20.2 g).

Isolation and purification of *Stemona* alkaloids from ethanol extract of leaves of *St. halabalensis*. The ethanol extract of the leaves of *St. halabalensis* was subjected to reverse phase CC using MeOH/H_2O (7.5:2.5) to remove chlorophyll and gave an alkaloid fraction B (953.0 mg). Separation of fraction B by CC (CH_2Cl_2/MeOH, 95:5) gave fraction B1 (120 mg). Further purification of fraction B1 by CC (CH_2Cl_2/MeOH, 95:5) gave stemoninine **49** (5.0 mg, 4.2%) and stichoneurine E **192** (12.5 mg, 10.4%).

Stichoneurine E (192)

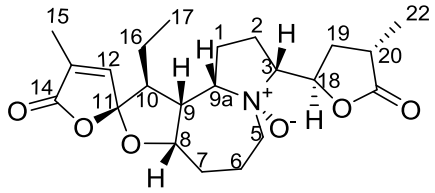

Isolated as a brown gum.

R_f = 0.08 in CH_2Cl_2/MeOH, (95:5).

$[\alpha]_D^{25}$ = -43° (*c* 0.33, $CHCl_3$)

ES-IMS *m/z* 406 $[M+H]^+$.

HRESIMS *m/z* $[M+H]^+$ 406.2217, calcd for $C_{22}H_{32}NO_6$, 406.2230.

^{1}H NMR (500 MHz, $CDCl_3$) refer to Table 5.9 for specific details.

^{13}C NMR (125 MHz, $CDCl_3$) refer to Table 5.8 for specific details.

9.5 Experimental for Chapter 6

Plant material. The roots of *Stichoneuron caudatum* were collected at Lojing River, Gua Musang, Kelantan, Malaysia in December 2011. The plant material was identified by Prof. Latiff Mohammad. A voucher specimen, UKM29978, was deposited at Department of Biology, National University of Malaysia.

Extraction of crude from roots of *Stichoneuron caudatum*. The dry, ground roots of *St. caudatum* (1.3 kg) were extracted with 95% MeOH (4 × 1000 mL) over 3 days at room temperature. The MeOH solution was evaporated to give a dark residue (56.0 g).

Isolation of compounds from the roots of *Stichoneuron caudatum*. The residue was chromatographed on silica gel (200 mL) using gradient elution from *n*-hexane/EtOAc (2:8−0:10) to CH_2Cl_2/EtOAc (2:8−0:10). A total of 5 L of eluent was collected in test

tubes of 200 mL. These fractions were pooled on the basis of TLC analysis to give three alkaloid fractions; A (1.5 g), B (150 mg) and C (3.5 g). Fraction A (1.5 g) was further separated by column chromatography (CC) using *n*-hexane/EtOAc (2:8) as the eluent to give fraction A1 (500 mg) and fraction A2 (320 mg). Fraction A1 (500 mg) was then separated by reverse phase CC ($MeOH/H_2O$; 9:1) to give fraction A11 (205 mg). Fraction A11 (205 mg) was further purified by silica gel CC using isocratic eluent (*n*-hexane/EtOAc (4:6)) to give stichoneurine F **193** (100.5 mg, 49%). Fraction A2 (320 mg) was subjected to reverse phase CC ($MeOH/H_2O$ (7.5:2.5), 100 mL of eluent) to give fraction A21 (23.1 mg). Fractions A21 (23.1 mg) was purified by silica gel CC using petrol/acetone (2:8) to give sessilistemonamine E **195** (3.5 mg, 15.2%). Fraction B (150 mg) was separated by silica gel CC (petrol/acetone (2:8) to give fraction B2 (70.5 mg) which was purified again by the same procedure to give stichoneurine G **194** (49.2 mg, 69.8%). A portion of fraction C (2.0 g) was separated by silica gel CC (petrol/acetone (3:7) to give fraction C1 (364.9 mg). This fraction was chromatographed on silica gel (*n*-hexane/acetone (3:7) to give fraction C12 (137.2 mg). This purification procedure was repeated on fraction C12 (137.2 mg) to give pure sessilistemonamine F **196** (50.2 mg, 36.6%).

Stichoneurine F (193)

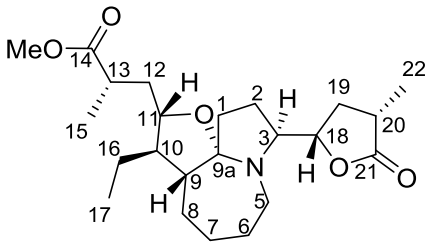

Isolated as a pale yellow gum.

R_f = 0.77 in CH_2Cl_2/MeOH, (9.5:0.5).

$[\alpha]_D^{25}$ = -31° (*c* 0.10, $CHCl_3$).

HRESIMS *m/z* 408.2750 $[M+H]^+$ (calcd for $C_{23}H_{38}NO_5$ 408.2753).

IR film *v*max 2927, 2857, 1771, 1734, 1457, 1191, 1163, 1014, 922 cm^{-1}.

^{1}H NMR (500 MHz, methanol-d_4) refer to Table 6.1 for specific details.

^{13}C NMR (125 MHz, methanol-d_4) refer to Table 6.1 for specific details.

Stichoneurine G (194)

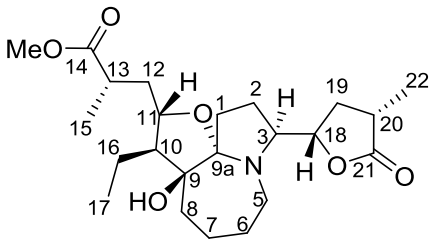

Isolated as a white amorphous solid.

R_f = 0.50 in petroleum spirit/acetone (6.5:3.5).

$[\alpha]_D^{25}$ = -21° (*c* 0.1, $CHCl_3$).

HRESIMS *m/z* 424.2699 $[M + H]^+$ (calcd for $C_{23}H_{38}NO_6$ 424.2682).

IR film *v*max 3520, 2934, 2871, 1761, 1730, 1457, 1377, 1193, 1011, 923 cm^{-1}.

^{1}H NMR (500 MHz, methanol-d_4) refer to Table 6.2 for specific details.

^{13}C NMR (125 MHz, methanol-d_4) refer to Table 6.2 for specific details.

Sessilistemonamine E (195)

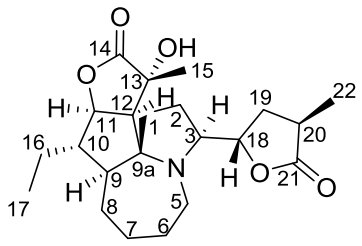

Isolated as a pale yellow gum.

R_f = 0.66 in petroleum spirit/acetone (6.5:3.5).

$[\alpha]_D^{25}$ = +11° (*c* 0.03, $CHCl_3$).

HRESIMS *m/z* 392.2436 $[M + H]^+$ (calcd for $C_{22}H_{34}NO_5$ 392.2376).

IR film *v*max 3348, 2925, 2884, 1761, 1649, 1461, 1375, 1196, 1024, 978 cm^{-1}.

^1H NMR (500 MHz, methanol-d_4) refer to Table 6.3 for specific details.

^{13}C NMR (125 MHz, methanol-d_4) refer to Table 6.3 for specific details.

Sessilistemonamine F (196)

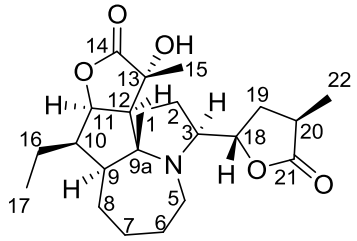

Isolated as a white amorphous solid.

R_f = 0.41 in petroleum spirit/acetone (6.5:3.5).

$[\alpha]_D^{25}$ = +46 (*c* 0.06, $CHCl_3$).

HRESIMS *m/z* 392.2437 $[M + H]^+$ (calcd for $C_{22}H_{34}NO_5$ 392.2476).

IR film *v*max 3454, 2930, 2873, 1764, 1458, 1366, 1193, 1150, 1015, 916 cm^{-1}.

^1H NMR (500 MHz, methanol-d_4) refer to Table 6.4 for specific details.

^{13}C NMR (125 MHz, methanol-d_4) refer to Table 6.4 for specific details.

9.6 Experimental for Chapter 7

9.6.1 AChE inhibitory activity

General methodology. AChE inhibitory assays were performed according to Sastraruji.[102] Acetylthiocholine iodide (ATChI) was used as a substrate while 5,5′-dithiobis[2-nitrobenzoic acid] (DTNB) was used as a reagent. Two stock solutions were used in this assay, buffer solution and substrate solution. The pH 7.0 phosphate buffer solution was prepared from a mixture of 37.2 mM $NaH_2PO_4 \cdot H_2O$ and 62.7 mM $Na_2HPO_4 \cdot 2H_2O$, in Milli Q H_2O. The substrate solution was prepared as a 4.73 mM ATChI solution in phosphate buffer pH 7.0. The reagent solution was prepared as a 3.15 mM DTNB solution in phosphate buffer pH 7.0. The assay was performed in 96-well plates. In each well, 120 µL of phosphate buffer pH 7.0 was mixed with 20 µL of reagent and 20 µL of substrate, then 20 µL of AChE (0.75 U/mL) in phosphate buffer pH 7.0 was added with 20 µL of the sample (which was prepared in concentrations of 0.01-0.2 µM in DMSO). The final concentrations of each compound 1000, 500, 250, 125, 62.5, 31.250, 15.625, 7.813, 3.906, 1.953, 0.977, 0.488, 0.244 µM were prepared by using the two-fold dilution technique, using the phosphate buffer to dilute the solutions. Then the well plate was directly put into the microplate reader which was thermostated at 25 °C. The absorbances were read using a SPECTRAmax® PLUS384 microplate thermostated spectrophotometer (California, USA) at 412 nm. Enzyme activity was calculated as a percentage compared to an assay using a buffer without any inhibitor. Galanthamine was used as a reference compounds. The AChE inhibitory data were analyzed with the software package GraphPad Prism® (Graph Pad Inc., San Diego, USA). IC_{50} values are means ± SD of three individual determinations each performed in triplicate.

9.6.2 Antiplasmodial assay

These assays were performed by Dr. Roonglawan Rattanajak from the Medical Molecular Biology Research Unit, National Center for Genetic Engineering and Biotechnology, National Science and Technology Development Agency, Thailand. A few isolated compounds were tested *in vitro* against a multidrug resistant K1CB1 strain and a wild type chloroquine and antifolate sensitive TM4/8.2 strain of *Plasmodium falciparum*. The method described by Trager and Jensen[103] was used for maintaining the parasites in human red blood cells in RPMI 1640 medium supplemented with 25 mM of HEPES, 0.2% of 12 sodium bicarbonate, and 8% human serum in a 3% carbon dioxide gas incubator maintained at 37 ^{o}C. The test samples were made up in DMSO solution and the in vitro antiplasmodial activity testing was carried out using the Microdilution Radioisotope Technique.[104] The test sample (25 µL, in the culture medium) was placed in triplicate in a 96-well plate where parasitised erythrocytes (200 µL) with a cell suspension (1.5%) of parasitemia (0.5-1%) were then added to the wells. Generally, the ranges of the final concentrations of the samples varied from 2 x 10-5 to 1 x 10-7 M or up to 1 x 10-4 g/mL with 0.1% of the organic solvent. Due to the poor solubility of some samples, only about 10-5 g/mL final concentration could be tested. The plates were then cultured under standard conditions for 24 h after which 3H-hypoxanthine (25 µL, 0.5 µCi) was added to the culture medium. The culture was incubated (18-20 h) after which the DNA from the parasite was harvested from the culture onto glass fibre filters and a liquid scintillation counter was used to determine the amount of 3H-hypoxanthine incorporation.[105-106] The inhibitory concentration of the sample was determined from its dose-response curves or by calculation. The assay was performed in at least three replicates. Chloroquine (Sigma Company), pyrimethamine (Sigma

Company) and cycloguanil were used as positive controls for both plasmodial strains (Table 2). DMSO (0.1%) and distilled water were used as controls to rule out the solvent effects on the bioassay results of the test samples. All the experiments were performed three times in duplicate (3x2).

9.6.3 Cytotoxicity assay and chemosensitivity testing

These assays were performed in Assoc. Prof. Pornngarm Limtrakul's laboratory at the Department of Biochemistry, Faculty of Medicine, Chiang Mai University, Thailand.

Chemicals and reagents.

Doxorubicin (Dox), Verapamil (Ver), Paclitaxel (PTX), 3-(4,5-dimethylthiazol-2-yl)-2,5-diphenyltetrazolium bromide (MTT) were obtained from Sigma Chemical Company (St. Louis, MO, U.S.A.). Dulbecco's modified Eagle's medium (DMEM) and Roswell Park Memorial Institute 1640 medium (RPMI1640) were purchased from Gibco BRL (Grand Island, NY, U.S.A.).

Cell lines and culture conditions

The MDR leukemic cell line (K562/Adr) was purchased from RIKEN Cell Bank (Tsukuba, Ibaraki, Japan). A drug-sensitive leukemic cell line (K562) was purchased from The American type Culture Collection (ATCC, Manassas, VA, U.S.A.). Both cell lines were cultured in RPMI1640 with 10% fetal bovine serum (FBS), 5 mm l-glutamine, 50 IU/mL penicillin and 50 g/mL streptomycin; 700 nm of DOX was added only to the K562/Adr culture medium. These cell lines were maintained in a humidified

incubator with an atmosphere comprising 95% air and 5% CO_2 at 37°C.When the cells reached 70–80% confluence, they were harvested and plated either for subsequent passages or for drug treatments.

Cytotoxicity assay and chemosensitivity testing

K562 and K562/Adr cells were plated at 2.5×10^3 cells per well in 96-well plates. 24 hours after plating increasing concentrations of isolated *Stemona* alkaloids (5, 10, 20, 40, 50 μM) were added and the cells were then further incubated for 48 h at 37°C. Overall cell number/viability was assessed by MTT assay. In each experiment, determinations were carried out in triplicate. For measurement of DOX, and PTX cytotoxicity, K562/Adr and K562 cells were plated at 2.5×10^3 cells per well in 96-well plates. After 24 hours, 5 mM of the S*temona* alkaloids and various concentrations of DOX or PTX were added. The cells were incubated for 48 h at 37°C, and then cell growth was assessed by means of an MTT colorimetric assay. In each experiment, determinations were carried out in triplicate. Relative resistance was calculated as the ratio of the IC_{50} value of the K562/Adr cells to the IC_{50} value of the K562 cells.

Statistical Analysis

The results are presented as means ±S.D. from triplicate samples of three independent experiments. Differences between the means were analyzed by one-way ANOVA. Statistical significance was considered when $p<0.05$, or $p<0.01$, or $p<0.001$.

9.6.4 Cytotoxicity assay against Vero and KB cells

This assay was performed by Roonglawan Rattanajak from Medical Molecular Biology Research Unit, National Center for Genetic Engineering and Biotechnology, National Science and Technology Development Agency, Thailand. Normal Vero cells from kidney of African green monkey, *Cecopithecus aethiops* and human oral carcinoma KB cells were maintained and cultured in powdered GE Healthcare HyClone Minimal Essential Medium with Earle's (MEM/EBSS) supplemented with heated-inactivated fetal bovine serum (10%), $NaHCO_3$ (2.2 g/L) and of sodium pyruvate (1%). KB cell lines were cultured in DMEM/low glucose supplemented with heated inactivated fetal bovine serum (10%), $NaHCO_3$ (3.7 g/L) and non-essential amino acids (1%). Cytotoxicity was evaluated by the sulforhodamine B (SRB) assay (OD510 nm).[107] Doxorubicin and ellipticine were used as positive control drugs for cytotoxicity activities.

REFERENCES

1. Inthachub, P.; Vajrodaya, S.; Duyfjes, B. E. E. *Edinburgh J. Bot.* **2009**, *66*, 213–228.
2. Pilli, R. A.; Rosso, G. B.; De Olievera, M. D. C.; *The Stemona Alkaloids*, in *The Alkaloids*: *Chemistry and Biology*; Cordell, G. A., Editor; Academic Press: San Diego, **2005**; Vol. 62, Chapter 2, pp 77–173.
3. Majumdar, K.; Datta, B. K. *Modern Phytomorphology* **2013**, *3*, 39–44.
4. Schinner, J.; Kaltenegger, E.; Pacher, T.; Vajrodaya, S.; Hofer, O.; Greger; H. *Montash. Chem.* **2005**, *136*, 1671–1680.
5. Greger, H.; Schinner, J.; Vajrodaya, S.; Brecker, L.; Hofer, O. *J. Nat. Prod.* **2009**, *72*, 1708–1711.
6. Xu, R.-S.; Lu, Y.-J.; Chu, J.-H. *Tetrahedron* **1982**, *38*, 2667–2670.
7. Ye, Y.; Qin, G.-W.; Xu, R.-S. *Phytochemistry*. **1994**, *37*, 1201–1203.
8. Sakata, K.; Aoki, K.; Chang, C.-F.; Sakurai, A.; Mura-koshi. *J. Agri. Biol. Chem.* **1978**, *42*, 457–463.
9. Chung, H.-S.; Hon, P.-M., Lin, G.; But, P. P,-H., Dong, H. *Planta Med.* **2003**, 914–920.
10. Kaltenegger, E.; Brem, B.; Mereiter, K.; Kalchhauser, H.; Kahlig, H. Hofer, O.; Vajrodaya, S.; Greger, H. *Phytochemistry* **2003**, *63*, 803–816.
11. Mungkornasawakul, P.; Pyne, S. G.; Jatisatienr, A.; Supyen, D. Jatisatienr, C.; Lie, W.; Ung, A. T.; Skelton, B. W.; White, A. H. *J. Nat. Prod.* **2004**, *67*, 675–677.
12. Greger, H. *Planta Med.* **2006**, *72*, 99–113.

13. Mungkornasawakul, P.; Pyne, S. G.; Jatisatienr, A.; Supyen, D.; Lie, W; Ung, A. T.; Skelton, B. W.; White, A. H. *J. Nat. Prod.* **2003**, *66*, 980–982.

14. Pili, R. A.; Rosso, G. B.; De Oliveira, M. D. C. F. *Nat. Prod. Rep.* **2010**, *27*, 1908–1937

15. Jiwajinda, S.; Hirai, N.; Watanabe, K.; Santisopasri, V.; Cheungsamarnyart, N.; Koshimizu, K.; Ohigashi, H. *Phytochemistry* **2001**, *56*, 693–695.

16. Ramachandran, P. V.; Srivastava, A.; Hazra, D. *Org. Lett.* **2006**, *9*, 157–160.

17. Lin, L.-G.; Li, K. M.; Tang, C.-P.; Ke, C.-Q.; Rudd, J. A.; Lin, G.; Ye, Y. *J. Nat. Prod.* **2008**, *71*, 1107–1110.

18. Lin, L.-G.; Zhong, Q.-X.; Cheng, T.-Y.; Tang, C.-P.; Ke, C.-Q; Lin, G.; Ye, Y. *J. Nat. Prod.* **2006**, *69*, 1051–1054.

19. Pilli, R. A.; De Oliveira, M. D. C. F. *Nat. Prod. Rep.* **2000**, *17*, 117–127.

20. Shinozaki, H.; Ishida, M. *Brain Res.* **1985**, *334*, 33–40.

21. Thany, S. T.; Tricoire-Leignel, H.; Lapied, B.; *Identification of Cholinergic Synaptic Transmission in the Insect Nervous System*, in *Illustrates the finding that the insect central nervous system is extremely rich in acetylcholine receptors which have a predominantly nicotinic pharmacology*; Thany. S. H., Editor; Landes Bioscience and Springer Science and Business Media: France, **2010**; Vol. 583, Chapter 1, pp 1–10.

22. Tang, C.-P.; Chen, T.; Velten, R.; Jeschke, P.; Ebbinghaus-Kintscher, U.; Geibel, S.; Ye, Y. *J. Nat. Prod.* **2008**, *71*, 112–116.

23. Sussman, *J. Science* **1991**, *253*, 872–879.

24. Williams, P.; Sorribas, A.; Howes, M.-J. R. *Nat. Prod. Rep.* **2011**, *28*, 48–77.

25. Wang, P.; Liu, A. L; An. Z.; Li, Z. H.; Du, G. H.; Qin, H. L. *Chem. Biodiv.* **2007**, *4*, 523–530.

26. Gottesman, M. M.; Pastan, I.; Ambudkar, S.V. *Current Opinion in Genetic & Development* **1996**, *6*, 610–617.

27. Litman, T.; Druley, T. E.; Stein, W. D.; Bates, S. E. *Cell. Mol. Life Sci.* **2001**, *58*, 931–959.

28. Ambudkar, S.V.; Kimchi-Sarfaty, C.; Sauna, Z.E.; Gottesman, M. M. *Oncogene* **2003**, *22*, 7468–7485.

29. Chanmahasathien, W.; Ampasavate, C.; Greger, H.; Limtrakul, P. *Phytomed.* **2011**, *18*, 199–204.

30. Manohar, A. *Braz. Arch. Biol. Technol.* **2013**, *56*, 21–25.

31. Lin, W.-H.; Cai, M.-S.; Ying, B.-P.; Feng, R. *Acta Pharm. Sin.* (Yaoxue Xuebao) **1993**, *28*, 202–206.

32. Hitotsuyanagi, Y.; Takeda, E.; Fukaya, H.; Takeya, K. *Tetrahedron Lett.* **2008**, *49*, 7376–7379.

33. Ueo, S.; Irie, H.; Harada, H. *Chem. Pharma. Bull.* **1967**, *15*, 768–70.

34. Hitotsuyanagi, Y.; Uemura, G.; Takeya, K. *Tetrahedron Lett.* **2010**, *51*, 5694–5696.

35. Hitotsuyanagi, Y.; Fukaya, H.; Takeda, E.; Matsuda, S.; Saishu, Y.; Zhu, S.; Komatsu, K.; Takeya, K. *Tetrahedron* **2013**, *69*, 6297–6304.

36. Hitotsuyanagi, Y.; Genta S.; Haruhiko F.; Maho, H.; Shu, Z.; Katsuko, K.; Koichi, T. *Tetraherdron Lett.* **2013**, *54*, 6995–6998.

37. Lai, D.-H.; Yang, Z.-D.; Xui, W.-W; Sheng, J.; Shi, Y.; Yao, X.-J. *Fitoterapia* **2013**, *89*, 257–264.

38. Yu, G.; Jun, W.; Zhang, C.-F; Xu, X.-H.; Miang, Z.; Kong, L.-Y. *Tetrahedron* **2014**, *70*, 967-974.

39. Chaiyong, S.; Jatisatienr, A.; Mungkornasawakul, P.; Sastraruji, T.; Pyne, S. G.; Ung, A. T., Urathamakul, T.; Lie, W. *J. Nat. Prod.* **2010**, *73*, 1833–1838.

40. Pudjiastuti, P.; Pyne, S. G.; Sugiyanto; Lie, W. *Phytochemistry Lett.* **2012**, *5*, 358–360.

41. Guo, J.; He, H.; Li, S.; Hua, H.; Hao, X. *Acta Botanica Yunnan*. **2010**, *32*, 463–465.

42. Sastraruji, T.; Chaiyong, S.; Jatisatienr, A.; Pyne, S. G.; Ung, A. T.; Lie, W. *J. Nat. Prod.* **2011**, *74*, 60-64.

43. Sastraruji, T.; Jatisatienr, A.; Issakul, K.; Pyne, S. G.; Ung, A. T.; Lie, W.; Williams, M. C. *Nat. Prod. Commun.* **2006**, *1*, 813-818.

44. Mungkornasawakul, P.; Pyne, S. G.; Wilis, A. C.; Jatisatienr, A.; Phuthsuk, D.; Lie, W. *Phytochemistry Lett.* **2013**, *6*, 602–605.

45. Hitotsuyanagi, Y.; Hikita, M.; Uemura, G.; Fukaya, H.; Takeya, K. *Tetrahedron* **2011**, *67*, 455–461.

46. Seger, C.; Mereiter, K.; Kaltenegger, E.; Pacher, T.; Greger, H; Hofer, O. *Chem. Biodiv.* **2004**, *1*, 265–279.

47. Mungkornasawakul, P.; Matthews, H.; Ung, A. T.; Pyne, S. G.; Jatisatienr, A.; Lie, W.; Skelton, B. W.; White, A. H. *ACGC Chem. Res. Comm.* **2005**, *19*, 30–33.

48. Lin, L.-G.; Tang, C.-P.; Dien, P.-H.; Xu, R.-S.; Ye, Y. *Tetrahedron Lett.* **2007**, *48*, 1559–1561.

49. Takayama, H,; Ichikawa, T.; Kitajima, M.; Aimi, N.; Lopez, D.; Nonato, M. G. *Tetrahedron Lett.* **2001**, *42*, 2995–2996.

50. Takayama, H,; Ichikawa, T.; Kuwajima, M.; Kitajima, M; Seki, H.; Aimi, N.; Nonato, M. G. *J. Am. Chem. Soc.* **2000**, *122*, 8635–8639.

51. Duyfjes, B. E. E. *Fl. Malesiana* **1993**, *11*, 404–405.

52. Tsi, Z. H., Duyfjes, B. E. E. *Stemonaceae*, Wu, Z. Y., Raven, P., Editor; Flora of China, *Science Press: Beijing*, **2000**, *24*, 70–72.

53. Kostecki, K.; Engelmeier, D.; Pacher, T.; Hofer, O.; Vajrodaya, S.; Greger, H. *Phytochemistry* **2004**, *65*, 99–106.

54. http://users.skynet.be/fhoes/rsasucculents/stemona_sesselifolia_flowers.htm (September 2014)

55. http://www.bihrmann.com/caudiciforms/subs/ste-col-sub.asp (September 2014)

56. https://www.geocities.jp/caposaldo/bkbbyakubu.jpg (September 2014)

57. https://www.flickr.com/photos/17457752@N00/7959902042 (September 2014)

58. https://www.google.com.au/maps/place/Dungun,+Terengganu,+Malaysia/@3.0002712,97.8747087,5z/data=!4m2!3m1!1s0x31c805887d316621:0xab269c5406262890) (September 2014)

59. Murugan, C. *Rheedea* **2010**, *20*, 77–79.

60. Thirapasakun, L.; Phanurai, P. *Bull. Med. Sci*. (Mahidol University) **1977**, *19*, 145-155.

61. http://www.kew.org/index.htm (September 2014)

62. Telford, I. R. *Fl. Australia* **1986**, *46*, 180.

63. http://commons.wikimedia.org/wiki/File:Stichoneuron_membranaceum_IP.png (September 2014)

64. https://www.google.com.au/maps/preview?q=taman+negara+endau+rompin+pahang&ie=UTF-8&ei=c6TpU9O3ONXi8AW8_IGIAQ&ved=0CAkQ_AUoAg (September 2014)

65. Pili, R. A.; Rosso, G. B.; De Olievera, M. D. C.; *The Stemona Alkaloids,* in *The Alkaloids*: *Chemistry and Biology*; Cordell, G. A., Editor; Academic Press: San Diego, **2005**; Vol. 62, Chapter 2, pp 77–173.

66. Bouman, F.; *Seed structure and systematics in Dioscoreales*, In: Rudall, P. J., Editor; Cribb, P. J.; Cutler, D. F.; Humphries, C. J. (eds) Monocotyledons: Systematics and Evolution: Royal Botanic Gardens, **1995**; pp 139–156.

67. Ridley. H. N. *J. Straits Branch Roy. Asiat. Soc.* **1911**, *57*, 107.

68. Said, I. M.; Din, L. B.; Samsudin, M. W.; Zakaria, Z.; Yusoff, N. I.; Suki, U.; Manap, A.; Ibrahim, A. Z.; Latiff, A. *Malayan Nature Journal* **1990**, *43*,260–266.

69. Inthachub, P.; Taxonomic Revision on the Family Stemonaceae in Thailand. Master's thesis, **2008**. Kasetsart University, Bangkok, Thailand.

70. https://www.google.com.au/maps/place/Moonriver+Lodge/@2.4142552,106.2624157,7z/data=!4m2!3m1!1s0x31ca676565a2d71b:0x779a90d111c7239e (September 2014)

71. Kende, A. S.; Smalley, T. L.; Jr.; Huang, H. *J. Am. Chem. Soc.* **1999**, *121*, 7431–7432.

72. Hosoya, T.; Yamasaki ,F.; Nakata, A.; Rahman, A.; Kusumawati, I.; Zaini, N. C.; Morita, H. *Planta Med.* **2011**, *77*, 256–258.

73. Guo, A.; Jin, L.; Cai, S.; Guo, S.; Lin, W. *Chem. Biodiv.* **2008**, *5*, 598–605.

74. Kongkiatpaiboon, S.; Schinnerl, J.; Felsinge, S.; Keeratinijakal, V.; Vajrodaya, S.; Gritsanapan, W.; Brecker, L.; Greger, H. *J. Nat. Prod.* **2011**, *74*, 1931−1938.

75. Pilli, R. A.; Rosso, G. B.; de Oliveira, M. C. F. *Nat. Prod. Rep.* **2010**, *27*, 1908–1937.

76. Cheng, D.; Guo, J.; Chu, T. T. *J. Nat. Prod.* **1988**, *51*, 202–211.

77. Sastraruji, T.; Jatistienr, A.; Pyne, S. G.; Ung, A. T.; Lie, W.; Williams, M. C. *J. Nat. Prod.* **2005**, *68*, 1763–1767.

78. Mayer, H.; Schudel, P.; Ruegg, R.; Isler, O. *Helv. Chim. Acta* **1963**, *46*, 963–982.

79. Moss, A. R.; Drummond, J. C. *Biochem. J.* **1938**, *32*, 1953–1956.

80. Baker, J. K.; Myers, C. W. *Pharm. Res.* **1991**, *8*, 763–770.

81. Jewers, K.; Blunden, G.; Wetchapinan, S.; Dougan, J.; Manchada, A. H.; Davis, J. B.; Kyi, A. *Phytochemistry* **1972**, *11*, 2025.

82. Cavalheiroa, A. J.; Yoshida, M. *Phytochemistry* **2000**, *53*, 811-819.

83. Ellman, G. L; Courtney, K. D.; Andres, V. J.; Featherstone, R. M. *Biochem. Pharmacol.* **1961**, *7*, 88–95.

84. Landis, S. H.; Murray, T.; Bolden, S.; Wingo, P. A. *Cancer J. Clin.* **1998**, *48*, 6–29.

85. Gottesman, M. M. *Cancer Res.* **1993**, *53*, 747–754.

86. Krishna, R.; Mayer, L. D. *Eur. J. Pharm. Sci. 11* **2000**, 265–283.

87. Fan, D.; Beltran, P. J.; O'Brien, C. A.; *Reversal of multidrug Resistance*, In *Reversal of Multidrug Resistance in Cancer*; Kellen, J. A.; Editor; CRC Press: Boca Raton, FL, **1994** pp 93–124.

88. Gong, J.; Jaiswal, R.; Mathys, J. -M.; Combes, V.; Grau, G. E.R.; Bebawy, M. *Cancer Treat. Rev.* **2012**, *38*, 226–234.

89. Callaghan, R.; Crowley, E.; Potter, S.; Kerr, I. D. *J. Clin. Pharmacol.* **2008**, *48*, 365–378.

90. Gottesman, M. M. *Annu. Rev. Med.* **2002**, *53*, 615–627.

91. Lehnert, M. *Eur. J. Cancer* **1996**, *32*, 912–920.

92. Lage, H. *Cell. Mol. Life Sci.* **2008**, *65*, 3145–3167.

93. Hilton, J. *Cancer Res.* **1984**, *44*, 5156–5160.

94. Andersson, B. S.; Mroue, M.; Britten, R. A.; Murray, D. *Cancer Res.* **1994**, *54*, 5394–5400.

95. Simon, S. M.; Schindler, M. *Proc. Nat. Acad. Sci. USA* **1994**, *91*, 3497-3504.

96. Ling, V.; Thompson, L. H.; *J. Cell. Physiol.* **1974**, *83*, 103–116.

97. Juliano, R. L.; Ling, V. *Biochim. Biophys. Acta* **1976**, *455*, 152–162.

98. Riordan, J. R.; Ling, V. *J. Biol. Chem.* **1979**, *254*, 12701–12705.

99. Kartner, N.; Riordan, J. R.; Ling, V. *Science* **1983**, *221*, 1285–1288.

100. Nobili, S.; Landini, I.; Giglioni, B.; Mini, E. *Curr. Drug Targets* **2006**, *7*, 861–879.

101. Zhou, T.; Shi, Q.; Bastow, K.; Lee, K. -H. *J. Med. Chem.* **2010**, *53*, 8700–8708.

102. Sastraruji, K.; Sastraruji, T.; Ung, A. T.; Griffith, R.; Jatisatienr, A.; Pyne, S. G. *Tetrahedron* **2012**, *68*, 7103–7115.

103. Trager, W., Jensen, J. B. *Science* **1976**, *193*, 673–675.

104. Wangchuk, P.; Keller, P.A.; Pyne, S.G.; Taweechotipatr, M.; Tonsomboon, A.; Rattanajak, R.; Kamchonwongpaisan, S. *J. Ethnopharm.* **2011**, *137*, 730–742.

105. Desjardins, R.E.; Canfield, C.J.; Haynes, J.D.; Chulay, J.D. *Antimicrob. Agents Chemother.* **1979**, *16*, 710–718.

106. Kamchonwongpaisan, S.; Quarell, R.; Charoensetakul, N.; Ponsinet, R.; Vilaivan, T.; Vanichtanankul, J.; Tarnchompoo, B.; Sirawaraporn, W.; Lowe, G.; Yuthavong, Y. *J. Med. Chem.* **2004**, *47*, 673–680.

107. Wangchuk, P.; Keller, P.A.; Pyne, S.G.; Sastraruji, T.; Taweechotipatr, M.; Tonsomboon, A.; Rattanajak, R.; Kamchonwongpaisan, S. *Nat. Prod. Commun.* **2012**, *7*, 575–580.